

WATER TABLE MANIPULATIONS AND PEATLAND
EVAPOTRANSPIRATION

THE EFFECTS OF LONG-TERM WATER TABLE MANIPULATIONS ON
PEATLAND EVAPOTRANSPIRATION, SOIL PHYSICAL PROPERTIES, AND
MOISTURE STRESS

By PAUL MOORE, B.A., M.Sc.

A Thesis Submitted to the School of Graduate Studies in Partial Fulfilment of the
Requirements for the Degree Doctor of Philosophy

McMaster University © Copyright by Paul Moore, July 2013

McMaster University DOCTOR OF PHILOSOPHY (2013) Hamilton, Ontario

(School of Geography and Earth Sciences)

TITLE: The effects of long-term water table manipulations on peatland
evapotranspiration, soil physical properties, and moisture stress.

AUTHOR: Paul Moore

SUPERVISOR: Dr. J.M. Waddington

OF PAGES: 251

ABSTRACT

Northern boreal peatlands represent a globally significant carbon pool that are at risk of drying through land-use change and projected future climate change. The current ecohydrological conceptualization of peatland response to persistent water table (WT) drawdown is largely based on short-term manipulation experiments, but where the long-term response may be mediated by vegetation and microtopography dynamics. The objective of this thesis is to examine the changes to peatland evapotranspiration, soil physical properties, and moisture stress in response to a long-term WT manipulation. The energy balance, hydrology, vegetation, and soil properties were examined at three adjacent peatland sites in the southern sub-boreal region which were subjected to WT manipulations on the order of ± 10 cm at two treatment sites (WET, and DRY) compared to the reference site (INT) as a result of berm construction in the 1950s.

Sites with an increasing depth to WT were found to have greater microtopographic variation and proportion of the surface covered by raised hummocks. While total abundance of the major plant functional groups was altered, species composition and dominant species of vascular and non-vascular species within microforms was unaltered. Changes in vegetation and microtopography lead to differences in albedo, surface roughness, and surface moisture variability. However, total ET was only significantly different at the WET site. Transpiration losses accounted for the majority of ET, where LAI best explained differences in total ET between sites. Surface moisture availability did not appear to be limiting on moss evaporation, where lab results showed similar moisture retention capacity between microforms and sites, and

where low surface bulk density was shown to be a strong controlling factor. Modelling results further suggested that, despite dry surface conditions, surface moisture availability for evaporation was often not limited based on several different parameterizations of peat hydraulic structure with depth.

ACKNOWLEDGEMENTS

I would first like to thank my supervisor, Dr. Mike Waddington for introducing me to the fascinating and exciting research field of peatland ecohydrology. His supervision and encouragement to pursue my own interests has greatly helped develop my skills as a researcher. His dedication to his graduate students is exemplary, and his contribution to this thesis cannot be understated.

The valuable insight and discussion with members of the McMaster Ecohydrology Lab, both past and present, has helped to develop some of the ideas and analysis of this thesis. The great collaborative spirit of the group, and friendships developed over the years have made this a thoroughly enjoyable experience. I would like to give a special thanks to my one and only field assistant, Reyna Matties. Although there were equipment failures, illness, denial of entry into the US, a minor car accident, and a loss of many, many hours of data collection, it has been said that anyone who has never made a mistake has never tried anything new, and the progress of science is defined by trying something new.

I would like to thank my family and friends for their support through these past several years. Last, but certainly not least, I would like to give a heartfelt thanks to my wife and best friend, Erin. Her love and support has given me the opportunity to pursue a path that few have the privilege to enjoy. Her hard work and dedication to everything she does is an example I can only dream to live up to.

TABLE OF CONTENTS

LIST OF FIGURES	ix
LIST OF TABLES	xv
DECLARATION OF ACADEMIC ACHIEVEMENT	xvi
CHAPTER 1: INTRODUCTION	1
1.1 Northern peatlands, climate change, and water table drawdown	1
1.2 Ecohydrology of northern peatlands	6
1.2.1 Surface energy balance	6
1.2.2 Energy partitioning	8
1.2.3 Peat hydrophysical properties	10
1.3 Study objectives.....	13
1.4 References	15
CHAPTER 2: EFFECT OF LONG-TERM WATER TABLE MANIPULATIONS ON PEATLAND EVAPOTRANSPIRATION	23
2.1 Abstract.....	23
2.2 Introduction	24
2.3 Methods	28
2.3.1 Study site.....	28
2.3.2 Instrumentation	31
2.3.3 High-frequency data processing and corrections.....	33
2.3.4 Quality assurance and gap filling.....	34
2.3.5 Calculations.....	35
2.4 Results	38
2.4.1 Meteorological and hydrological conditions	38
2.4.2 Surface Energy Exchange	40
2.4.3 Controls on Evaporation	46
2.5 Discussion.....	50
2.5.1 Evapotranspiration	50
2.5.2 Albedo and Surface Temperature	51
2.5.3 Energy Partitioning	53
2.5.4 Aerodynamic and Surface Resistance.....	55
2.5.5 Evapotranspiration and Water Table Position	56
2.6 Conclusions	58
2.7 Acknowledgements	60
2.8 References	60
2.9 Tables	68

2.10 Figures	69
CHAPTER 3: MICROTOPOGRAPHIC AND VEGETATION CONTROLS ON PEATLAND EVAPOTRANSPIRATION ACROSS A LONG-TERM WATER TABLE MANIPULATION GRADIENT	79
3.1 Abstract.....	79
3.2 Introduction	80
3.3 Methods	84
3.3.1 Study site.....	84
3.3.2 Evapotranspiration and supporting measurements	86
3.3.3 Supplementary measurements	89
3.3.4 Modelling and supporting calculations	90
3.4 Results and Discussion.....	94
3.4.1 Microtopography, vegetation, and moisture availability	94
3.4.2 Evapotranspiration partitioning	98
3.5 Implications and Conclusions.....	106
3.6 Acknowledgements	110
3.7 References	111
3.8 Tables	116
3.9 Figures	117
CHAPTER 4: MULTI-DECADAL WATER TABLE MANIPULATION ALTERS PEATLAND HYDRAULIC STRUCTURE AND MOISTURE RETENTION	128
4.1 Abstract.....	128
4.2 Introduction	129
4.3 Methods	132
4.3.1 Study site.....	132
4.3.2 Lab measurements	134
4.3.3 Field measurements	136
4.3.4 Calculations and statistics	138
4.4 Results	139
4.4.1 General hydrology	139
4.4.2 Bulk density	141
4.4.3 Lab and field moisture-retention.....	142
4.4.4 Van Genuchten vs. logistic	144
4.4.5 Empirical relations for moisture-retention parameters	146
4.5 Discussion.....	148
4.5.1 General hydrology	148
4.5.2 Bulk density	149
4.5.3 Moisture retention.....	151
4.5.4 VG vs. logistic	152
4.5.5 Empirical relations for moisture-retention parameters	154
4.6 Conclusions	155
4.7 References	157

4.8 Tables	162
4.9 Figures	163
CHAPTER 5: MODELLING <i>SPHAGNUM</i> MOISTURE STRESS IN RESPONSE TO 21 ST CENTURY CLIMATE CHANGE	174
5.1 Abstract.....	174
5.2 Introduction	175
5.3 Methods	178
5.3.1 Model overview and study area	178
5.3.2 Model description	180
5.3.4 Moisture stress	183
5.3.5 Soil parameterization	185
5.3.6 Model validation	187
5.3.7 Rainfall simulations	188
5.3.8 Climate change scenario	189
5.3.9 Model simulations.....	190
5.4 Results	190
5.4.1 Model sensitivity analysis & non-equilibrium behaviour.....	190
5.4.2 Stochastic rainfall and evaporation.....	192
5.4.3 Simulations of peatland moisture status and stress.....	193
5.5 Discussion.....	198
5.5.1 Peat hydrology and moisture-retention.....	198
5.5.2 Sphagnum stress.....	200
5.5.3 Model limitations and sensitivity.....	203
5.6 Conclusions	205
5.7 Acknowledgements	207
5.8 References	207
5.9 Tables	214
5.10 Figures	216
CHAPTER 6: SUMMARY AND CONCLUSIONS	226
6.1 Summary and conclusions.....	226
6.2 References	233

LIST OF FIGURES

Figure 2 - 1: Daily total rainfall (bars) and water table levels (a and c) for the WET (solid), INT (dash-dot), and DRY (dot) sites. Volumetric water content (three day average shown for clarity) at all three sites (b and d) measured at 0.05 m depth in a representative hummock (grey) and hollow (black) over the 2010 (top) and 2011 (bottom) growing seasons.	69
Figure 2 - 2: Daily total gap-filled evapotranspiration at all three study sites over the 2010 and 2011 growing seasons. INT and DRY traces represent the difference in daily evapotranspiration relative to the WET site.....	70
Figure 2 - 3: Cumulative sum of all common half-hourly evapotranspiration measurements (thick black lines) for WET (solid), INT (dash-dot), and WET (dashed) sites where quality control flagging system indicated high quality data based on integral turbulence characteristics, wind direction, stationarity, and a u_* threshold of 0.1 m s^{-1} . Significant differences between sites (thin grey lines) are relative to the INT site and are based on an assumption of purely random error (Moncrieff <i>et al.</i> , 1996).	71
Figure 2 - 4: Empirical cumulative distribution functions of residual half-hourly R_n values between all sites from DOY = 120 – 300, for 2010 and 2011. Vertical bars represent the 2.5 th and 97.5 th percentiles.	72
Figure 2 - 5: 7-day running average midday albedo across all study sites during the 2011 growing season.....	73
Figure 2 - 6: Correlation of daily average long-wave radiation against the DRY site for 2010 and 2011 growing season data combined. The linear relation between sites is represented by the solid (WET v. DRY) and dashed (INT v. DRY) lines. For clarity, the relation between WET and INT has been omitted due to the close correspondence between INT and DRY.	74
Figure 2 - 7: Boxplots comparing daytime ground heat flux for both 2010 (black) and 2011 (grey). Standard error estimate of the median is represented by the solid dots, and outliers by the crosses. Letters bellow each boxplot indicate where there are significant differences in the median.	75

Figure 2 - 8: Daily Bowen ratio for all three sites over the 2010 and 2011 growing seasons. Lines represent the 7-day running average Bowen ratio for WET (solid), INT (dash-dot), and DRY (dashed) sites. 76

Figure 2 - 9: Median half-hourly daytime ($K_{dwn} > 100 \text{ W m}^{-2}$) bulk surface resistance for 2010 (a) and 2011 (b) binned based on vapour pressure deficit with 100 values per bin. Error bars represent the standard error estimate of the median. The grey line represents the cumulative distribution of D 77

Figure 2 - 10: Relation between normalized ET and bin-averaged WTD for 2010 and 2011 growing seasons. Grey curves represent the relative frequency distribution of WTD. 78

Figure 3 - 1: Seney National Wildlife Refuge (SNWR) study area in the Upper Peninsula of Michigan (46.20° N, 86.02° W, elev. ~205 m a.s.l.) showing the three primary sampling locations. The top-left panel shows the study area prior to berm construction (SNWR airphoto BWD-5K-147) and general flow direction (white arrow), while the top-right panel shows the location of the berm (white dashed line) and impact on surface ponding (Google Earth – imagery date: 31/05/2005 – USDA Farm Service Agency). Daily total rainfall (bars) and water table levels for the WET (solid), INT (dash-dot), and DRY (dot) sites are shown for the 2010 (bottom-left) and 2011 (bottom-right) growing seasons. 117

Figure 3 - 2: Temporal variability in near-surface θ ($\theta_{0.10}$) at all three sites in a representative hummock (grey) and hollow (black) over the 2010 (a) and 2011 (b) growing seasons. Boxplot comparison of plot-measured surface θ (θ_{surf}) where dots are the confidence interval on the median, crosses represent outliers, and letters represent significant differences ($\alpha = 0.05$) using Tukey’s hsd (c). Spatio-temporal variability in θ_{surf} within 0.6 x 0.6 m plots ($n = 4$) for hummock (solid) and hollows (open) at the WET (Δ), INT (\square), and DRY (\circ) sites (d). Gaussian fit (solid line) parameters: $scale = 36.7$; $mean = 48.0$; and $std = 27.0$ 118

Figure 3 - 3: Relative abundance from vegetation survey using a 10 x 10 grid-intercept method for a 1 m² area centered on each of the chamber collars. 119

Figure 3 - 4: One-sided leaf area from destructive sampling plots (top) and mean leaf area and standard deviation (error bars) for live vascular vegetation based on four 0.25 m² plots (bottom). 120

Figure 3 - 5: Distribution of stomatal resistance (r_{leaf}) values from daytime porometry measurements for the dominant vascular species.	121
Figure 3 - 6: Chamber ET response (ET_{ch}) to vapour pressure deficit D , for PPFD > 1000 $\mu\text{mol m}^{-2} \text{s}^{-1}$	122
Figure 3 - 7: Daily modeled surface conductance (g_{surf}) / resistance (r_{surf}) for a hummock (a) and hollow (b) at each site, determined using a modified three-source model derived from Kim and Verma (1996).	123
Figure 3 - 8: Response of $r_{bulk} r_a^{-1}$ to $\theta_{0.10}$ at the WET (blue), INT (green), and DRY (red) sites over the 2010 growing season.	124
Figure 3 - 9: Jarvis-style component functions describing the relative control of PPFD (squares) and D (circles) on bulk surface resistance (r_b) for the WET (black), INT (grey), and DRY (white) sites. PPFD data points are bin averages of 50 daytime half-hour measurements where D is relatively constant, and vice versa for D data points. The best fit parameters for PPFD (see Eq. 2.13) and D (see Eq. 2.14) curves are: $a_2 = 1.9\text{E-}03 / 2.0\text{E-}03 / 1.6\text{E-}03$, $a_3 = 0.25 / 0.39 / 0.40$, and $a_4 = 0.85 / 0.58 / 0.68$ for WET (solid) / INT (dashed) / DRY (dotted) respectively.	125
Figure 3 - 10: Green index (dots) during 2010 based on changes in the spectral characteristics of the lower left portion of daily images taken at SNWR at 12:00. A summation of several Gaussian curves was used to fit measured data (black line).	126
Figure 3 - 11: Comparison of canopy LE estimated from the phenomenological model (x-axis) and the residual of the measured LE and estimated surface LE (y-axis) for the WET (blue), INT (green) and DRY (red) sites. Open circles represent ‘early’ growing season values up to DOY 141.	127
Figure 4 - 1: Seney National Wildlife Refuge (SNWR) study area in the Upper Peninsula of Michigan (46.20° N, 86.02° W, elev. ~205 m a.s.l.) showing the three primary sampling locations. The left panel shows the study area prior to berm construction (SNWR airphoto BWD-5K-147), while the right panel shows the location of the berm (white dashed line) and impact on surface ponding (Google Earth – imagery date: 31/05/2005 – USDA Farm Service Agency).	163

Figure 4 - 2: Estimated WT probability distribution from early May to mid-Oct. using a normal kernel function. Reported WT is relative to the local hollow surface at all three sites for the 2010 (solid lines) and 2011 (dashed lines) growing seasons. 164

Figure 4 - 3: Boxplots of the depth dependence of the rainfall-water table response (top panel) for the WET (blue), INT (green), and DRY (red) sites. Dots represent the 95% confidence interval on the median. Lower panel shows estimated differences in mean (symbols) specific yield by site, separated into hummocks (solid symbols) and hollows (empty symbols). Error bars show standard error..... 165

Figure 4 - 4: Relation between lab-measured saturated hydraulic conductivity (K_s) and bulk density for samples from the top 25 cm of the peat profile (a). Depth-dependence of the geometric mean (symbols) and standard deviation (error bars) of K_s in the saturated zone (b). 166

Figure 4 - 5: Boxplots of the depth dependence of peat sample bulk density with all sites lumped together. Black dots represent the 95% confidence interval on the median. 167

Figure 4 - 6: Comparison of lab-based moisture retention for 0.05 m thick peat samples lumped over 0 – 0.1 m (a) and 0.15 – 0.25 m (b) depth intervals. The mean (symbols) and standard error (bars) are reported for both hummocks (filled symbols) and hollows (open symbols). Lines represent the non-linear least-square fit of the Van Genuchten equation. 168

Figure 4 - 7: Field-measured pore water pressure versus relative water table position (top panel). Solid 1:1 line represents an equilibrium ψ profile, with dashed lines representing tensicorder measurement error (± 5 cm). Field-based moisture content as a function of relative water table position (bottom panel). Van Genuchten fit (solid grey) and 95% confidence interval on the curve shown (dashed grey)..... 169

Figure 4 - 8: Uncertainty analysis of Van Genuchten (a) and logistic (b) parameters using a non-linear least squares fit for field-based moisture-retention data. 170

Figure 4 - 9: Empirical relations for moisture retention parameters using the Van Genuchten equation. The grey bars in (a) represent the empirical probability distributions of the Van Genuchten n (VG- n) parameter and bulk density (ρ_b). The log-linear robust fit using a Cauchy weight function (solid line) and 95% confidence interval on the curve (dashed lines) are shown for the relation between α and $\square - \theta\psi = -5$ cm (b). A robust linear fit (solid line) is shown for the relation between the Van Genuchten residual water content (θ_r) and bulk density (ρ_b) (c). 171

Figure 4 - 10: Empirical relations for moisture retention parameters using a logistic fit. The coefficients for the power functions used in (a) and (b) are $p_1=13$, $p_2=0.62$, and $p_1=19$, $p_2=1.52$ respectively. The coefficients of determination are 0.59, 0.83, and 0.84 based on a robust fit (outliers down-weighted)..... 172

Figure 4 - 11: Sample relation between moisture content at a pore water pressure of -200 mb normalized by porosity ($\theta_{\psi=-200}$ cm/ \square), and bulk density (ρ_b) for hummock (open) and hollow (filled) samples (a). A sigmoid fit (solid line) and the 95% confidence interval on the curve (dashed line) are shown. The relation between the initial slope of the sigmoid curve ($asig$) and pore water pressure (ψ) are shown with the explained variance of the relation over the range of measured ψ (b). A log-linear fit (solid line) and the 95% confidence interval on the curve (dashed line) are shown. 173

Figure 5 - 1: (a) E_{max} (triangle), $E_{seas,i}$ (solid line), and sample $E_{daily,i}$ (circles with dashed line) based the occurrence of rainfall and random c_i values from the distributions in (b); (b) empirical cumulative distributions of the ratio of measured daily K_d to modelled K_{ex} for the 2010 growing season at SNWR during days with (dashed black line) and without (solid black line) rain; and (c) hourly fraction of $E_{daily,i}$ based on DOY, where black lines represent the summer solstice and the end of the growing season. 216

Figure 5 - 2: Cumulative frequency distribution of rainfall depths (a) and return period (b) based on 50 years of MJJAS daily rainfall data. Growing season (MJJAS) stochastic rainfall parameters (rainfall depth – top; return period – bottom) using a Weibull fit based on daily rainfall data from the Sault Ste. Marie, ON weather station (Environment Canada). 217

Figure 5 - 3: Comparison between modelled and observed WT position at Seney National Wildlife Refuge for two consecutive growing seasons. The model used the hollow hydrophysical properties listed in Table 1, an EXP profile, and initial WT level equal to the measured value..... 218

Figure 5 - 4: Deviation of the surface soil water pressure for a hummock and hollow over 100 simulated growing seasons using an EXP soil profile, relative to a soil water pressure profile in equilibrium with the water table level..... 219

Figure 5 - 5: Sample traces of θ in the surface layer for a simulated growing season with high (top), average (middle) and low (bottom) precipitation. 220

Figure 5 - 6: Cumulative distribution of volumetric water content (left) and soil-water pressure (left) for hummock (heavy lines) and hollow (thin lines) simulations under current climate conditions based on 100 growing seasons. θ^* thresholds are based on an optimal GWC of 10 g g^{-1} and high, mid and low measured ρ_b for surface samples from SNWR where 90% of all surface (0 – 0.05 m) samples fell between 10 and 30 kg m^{-3} . ψ^* thresholds are based on $\theta_{\rho_b, med}^*$ using hummock and hollow surface moisture retention parameters. 221

Figure 5 - 7: Empirical probability distributions of water table level based on 100 simulated growing seasons. WT simulations under future climate scenario are based solely on EXP soil profiles. 222

Figure 5 - 8: Comparison of cumulative frequency distribution of surface soil water pressure based on an EXP soil profile. 223

Figure 5 - 9: Average static (top - left panel) and dynamic (top - right panel) stress over a range of stress parameters for the hummock simulations given an EXP profile. Comparisons of time of simulated stress (lower – left panel) and seasonal stress periods (lower – right panel) between hummock (thick lines) and hollow (thin lines) simulations for all three profile types. 224

Figure 5 - 10: Comparison of average static and dynamic stress between hummocks (thick lines) and hollows (thin lines) across profile types (a & b) and between EXP-profile simulations under contemporary (black) and future (grey) climate conditions (c & d). Stress values are shown for $q = 1$ and $k = 0.2$ 225

LIST OF TABLES

Table 2 - 1: Summary of microtopography and vegetation characteristics across study sites.	68
Table 2 - 2: Summary of average climatological and flux variables for the study area. ..	68
Table 3 - 1: Summary of microtopography and vegetation characteristics across study sites.	116
Table 3 - 2: Summary of the ET components from EC and three-source model (Eq. 2.3-8) over the 2010 growing season.....	116
Table 4 - 1: Summary of mean hummock (HUM) and hollow (HOL) Van Genuchten parameters (std) for moisture-tension relations for the WET, INT, and DRY sites at SNWR. (* - Reported values are medians).....	162
Table 5 - 1: Key parameters used in the model for the <i>Sphagnum</i> hummock and hollow, and at depth for all profile types.	214
Table 5 - 2: Sensitivity analysis of peat surface ψ using hummock parameters (Table 1) and an EXP soil profile.	215

DECLARATION OF ACADEMIC ACHIEVEMENT

This dissertation takes the form of a series of manuscripts in publication or to be submitted to peer-reviewed academic journals. There is some degree of repetition in the site description and methods. Latter chapters do in some degree build on the previous ones, but only by utilizing some minor data. Each of the chapters can be read as a stand-alone document. The reference style in the text has been standardized for the purposes of this dissertation.

In addition to the work presented here, I contributed to one other publication currently in review relevant to this dissertation during the course of my graduate studies. I contributed primarily to data analysis of eddy covariance data and writing of the associated methods.

Pypker TG, Moore PA, Waddington JM, Hribljan JA, Chimner RC. 2013. Shifting environmental controls on CH₄ fluxes in a sub-boreal peatland. *Biogeosciences Discuss.*, **10**: 11757-11784.

The work presented in this thesis is the result of collaborative research, and the contributions of the candidate are listed below.

Chapter 2

Title: Effect of long-term water table manipulation on peatland evapotranspiration

Authorship: P.A. Moore, T.G. Pypker, and J.M. Waddington

Status: Published in *Agricultural and Forest Meteorology*, **178-179**: 106-119. DOI: 10.1016/j.agrformet.2013.04.013

Candidate's contribution: All data collection and analysis was done by the candidate. The draft manuscript was prepared by the candidate, with edits and feedback from both co-authors. All authors contributed to the experimental design, with funding secured by T.G. Pypker and J.M. Waddington.

Chapter 3

Title: Microtopographic and vegetation controls on peatland evapotranspiration across a long-term water table manipulation gradient.

Authorship: P.A. Moore, T.G. Pypker, J.A. Hribljan, R.A. Chimner, and J.M. Waddington

Status: Manuscript to be submitted to *Journal of Geophysical Research: Biogeosciences*

Candidate's contribution: All data collection, except for the vegetation survey and chamber measurements, and analysis was done by the candidate. The draft manuscript was prepared by the candidate, with edits and feedback from J.M. Waddington. All authors contributed to the experimental design, with funding secured by J.M. Waddington, T.G. Pypker, and R.A. Chimner.

Chapter 4

Title: Multi-decadal water table manipulation alters peatland hydraulic structure and moisture retention.

Authorship: P.A. Moore, P.J. Morris, and J.M. Waddington

Status: Manuscript to be submitted to *Hydrological Processes*

Candidate's contribution: All data collection and analysis except for field hydraulic conductivity was done by the candidate. The draft manuscript was prepared by the candidate, with edits and feedback from J.M. Waddington. All authors contributed to the experimental design, with funding secured by J.M. Waddington.

Chapter 5

Title: Modelling *Sphagnum* moisture stress in response to 21st century climate change

Authorship: P.A. Moore, N. Kettridge, P.J. Morris, and J.M. Waddington

Status: Manuscript to be submitted to *Ecohydrology*

Candidate's contribution: All data collection, model coding, and analysis were done by the candidate. The draft manuscript was prepared by the candidate, with edits and feedback from J.M. Waddington, N. Kettridge, and P.J. Morris. All authors contributed to the model design, with funding secured by J.M. Waddington.

CHAPTER 1: INTRODUCTION

1.1 Northern peatlands, climate change, and water table drawdown

Northern peatlands are estimated to cover 3.5×10^6 km² of the land surface, with 1.7×10^6 km² located in North America alone (Gorham, 1991; and O'Neill, 2000), and provide valuable ecosystem services (Vitt *et al.*, 2000) including the maintenance of biodiversity (Rydin *et al.*, 2006) and conservation of water resources (Devito *et al.*, 2013). These peatlands, primarily located between 50°N and 70°N latitude, are estimated to contain 455 Pg of soil organic carbon (Gorham, 1991), or approximately one-third of the global total (Bird *et al.* 2001).

Despite having a much lower productivity rate compared to other ecosystems (Thormann and Bayley, 1997), accumulation of carbon stores in northern peatlands has occurred slowly over several thousand years (*cf.* Clymo, 1984) as a result of slow rates of decomposition (Moore, 2002) due to a perennially shallow water table (WT), relatively cool temperatures, and the recalcitrance of *Sphagnum* species, particularly hummock forming species (Johnson and Damman, 1991; Turetsky *et al.*, 2008). Reconstruction of peatland carbon dynamics during the Holocene suggest that carbon accumulation rates have been decreasing over the past several thousand years (Yu *et al.*, 2011), where both biological and hydrological limits to growth are suggested (Belyea and Baird, 2006). Since peatlands are at a thermodynamic boundary governed by a shallow WT with relatively small seasonal and interannual fluctuations, it has been suggested that they may

be sensitive to disturbances which affect their hydrological structure and water balance (Frolking *et al.*, 2011).

As a result of future climate change, where temperatures in the boreal region are estimated to rise between 2 – 8°C (Christensen, 2007), peatlands in the continental interior are predicted to experience WT drawdown due to increased evaporative loss in excess of the predicted increase in precipitation (Roulet *et al.*, 1992). Since WT position has been shown to have a significant impact on peatland carbon balances (Hilbert *et al.*, 2001; Ise *et al.*, 2008), species composition and distribution (Talbot *et al.*, 2010; Bubier *et al.*, 2006), and hydraulic structure (Whittington and Price, 2006), understanding the spatio-temporal effect of climate or land-use change on peatland hydrology is of great importance (Holden, 2005).

Vegetation distribution, microtopography (*i.e.* raised dry hummocks and low-lying wet hollows), and the spatio-temporal variability in surface moisture are intricately linked in peatlands, but where the temporal scale of the response to disturbance varies. Both short-term field experiments (*e.g.* Chivers *et al.*, 2009; Strack and Waddington, 2007) and multi-decadal vegetation impact studies (*e.g.* Gunnarsson *et al.*, 2002; Talbot *et al.*, 2010) have shown a decrease in *Sphagnum* cover and a concomitant increase in shrub and tree cover (*e.g.* Pellerin and Lavoie, 2003; Weltzin *et al.*, 2003) in response to drainage or surface drying in peatlands. Increasing vascular cover has been associated with higher ET in peatlands (Takagi *et al.*, 1999), while a lower WT will likely increase fine root production (Weltzin *et al.*, 2000) and nutrient availability (Macrae *et al.*, 2013) which may further affect leaf area and transpiration capacity (Schulze *et al.*, 1994). Over

longer timeframes, stratigraphy studies suggest hummocks are stable features, resilient to changes in saturated water storage, while hollows are unstable features (Belyea and Clymo, 2001). This suggests that, in addition to changes in *Sphagnum* and vascular cover, WT drawdown may initiate microform succession towards a greater abundance of hummocks, the effects of which are not captured by short-term manipulation experiments. With changes in surface vegetation, microtopography, and moisture availability that result from persistent WT alterations, there would be a concomitant change in surface radiative and aerodynamic properties, thus fundamentally affecting energy partitioning between latent and sensible heat, as well as sourcing from the moss surface and canopy.

Studies of global and regional climate have identified that understanding of the mass and energy exchange between land surfaces and the atmosphere are of critical importance for the accuracy of climate change predictions (Garratt, 1993). Climate models are sensitive to changes in surface properties in terms of the partitioning of available energy at the surface into latent and sensible heat. These properties cannot be assumed to be constant with time, but rather vary depending on spatio-temporal variability in surface moisture conditions and transpiration capacity of vascular vegetation. Therefore, the inclusion of microtopography for peatland classifications in land surface schemes (*e.g.* Wu *et al.*, 2011) is needed in order to accurately represent the effect of spatial variability in moisture on flux partitioning; and plant functional groups are needed to better capture different rooting strategies (Luken *et al.*, 1985), resource allocation (Bubier *et al.*, 2006; Murphy and Moore, 2010), and physiological control on

water loss (Korner *et al.*, 1979). The problem herein is threefold: (1) a physically-based understanding of controls on evaporative loss for *Sphagnum* is limited (Kettridge and Waddington, 2013) where simple empirical functions using WT (*e.g.* Hilbert *et al.*, 2000) or surface moisture (*e.g.* Lawrence *et al.*, 2011) are often used; (2) there is a lack of a strong physical understanding of moisture and vegetation controls on peatland ET, though conceptual models have been proposed (*cf.* Kim and Verma, 1996; Comer *et al.*, 2000; and Lafleur *et al.*, 2005); and (3) there is limited data on how moisture retention properties vary between microforms, how it responds to WT drawdown, and how this feeds back into surface moisture availability and evaporative losses. In order to improve parameterization of peatlands in any land surface scheme, a better understanding of moss evaporation, as well as the feedbacks between microform succession, vascular vegetation, and surface moisture variability is needed.

The response of peatland ET to changes in moisture availability has been characterized using interannual variability at a site (Lafleur *et al.*, 2005; Liljedahl *et al.*, 2011), climatic gradients between sites (Humphreys *et al.*, 2006), and through field or laboratory manipulations (Price and Whittington, 2010; Bond-Lamberty *et al.*, 2011; Kettridge and Waddington, 2013). Measurements in years with different weather conditions can be used to quantify short-term, direct impacts on surface energy partitioning that result from warmer/colder or wetter/drier conditions (Teklemariam *et al.*, 2010), but often both moisture availability, temperature, and other weather variables vary simultaneously so specific impact attribution can be difficult to elicit. Comparisons between sites along climatic gradients are often used to represent long-term impacts of

climate (*e.g.* Chapin *et al.*, 2000; Eugster *et al.*, 2000), where plant community composition is assumed to be in quasi-equilibrium with the local climate. However, attribution of change can be confounded by other overlapping gradients (*e.g.* nitrogen deposition, Lund *et al.*, 2009). Manipulation studies, which are predominantly focused on carbon fluxes (*e.g.* Oechel *et al.*, 1998; Weltzin *et al.*, 2003; Strack and Waddington, 2007; Chivers *et al.*, 2009; and Huemmrich *et al.*, 2010), use warming or draining to control for different anticipated climate change effects, but are often limited to a few years and thus are potentially measuring the response of a system in disequilibrium. As such, there is a need to characterize peatland ET following a persistent change in moisture availability, where sufficient time has elapsed for both peat hydrophysical properties and the vegetation community to come into a quasi-equilibrium with the new hydrological conditions.

Despite the need for an improved understanding of long-term peatland response to climate change, research is limited on the effects of multi-decadal hydrological alterations on peatland vegetation dynamics (Miller 2011). Moreover, most long-term WT drawdown studies are from peatlands drained for forestry and agriculture by ditching which results in WT drawdowns greater than 0.30 m (Wells and Williams 1996; Sundström *et al.* 2000; Laiho *et al.* 2008) and is in excess of the 0.14 cm WT drawdown predicted for northern peatlands under a future climate change scenario (Roulet *et al.* 1992). Consequently research is lacking on more subtle (*i.e.* ± 0.15 m) long-term WT alteration effects on vegetation composition, surface morphology, and associated energy

balance dynamics that more realistically reflect the conditions predicted for northern regions in the next century.

1.2 Ecohydrology of northern peatlands

1.2.1 Surface energy balance

ET is a significant component of a peatland's energy and water balance (Lafleur *et al.*, 2005), where along with precipitation, they represent the major water fluxes in many peatlands (Kim and Verma, 1996). Despite the patchiness of peatlands within their local landscape, they must be investigated separately from the surrounding upland regions since peatlands are shown to have distinct energy and water balances, where midday ET and water storage tends to be greater (Sellers *et al.*, 1995). Differences in albedo (Thompson, 2012), aerodynamic roughness (Kettridge and Baird, 2006), soil moisture, and bulk surface resistance (Humphreys *et al.*, 2006) between peatlands can affect their energy and water balance. Seasonal leaf development in peatlands, for example, decreases net radiation as a function of incoming solar radiation (Lafleur *et al.*, 1997). This can be the result of increasing albedo or longwave loss as the surface dries and surface temperatures increase. The dependence of the energy balance on plant phenology implies that there will be differences in flux partitioning in peatlands with different vegetation communities or relative abundance of plant functional types.

Mer Bleue bog represents one of very few North American continental peatlands for which multi-year annual ET has been measured (Lafleur *et al.* 2005). Despite differences in the summer water balance and depth to WT, ET as a function of its

potential value was fairly conservative across years, with differences only discernable in the driest year. Despite having the lowest WT of reviewed Canadian peatlands (Humphreys *et al.*, 2006), energy partitioning and controls at Mer Bleue bog are similar to other bogs (Admiral *et al.*, 2006). This would suggest that, in the absence of microform or vegetation succession, a difference in flux partitioning at the ecosystem scale would only be expected in response to a large WT drawdown.

In peatlands with an abundance of vascular plant cover, there is evidence that ET is strongly controlled by the stomatal response to vapour pressure deficit (D). By contrast, clear-day ET is more strongly controlled by the amount of solar radiation in moss-dominated peatlands (Price, 1991). However, the response of ET and water use efficiency to varying environmental conditions across peatland types with different WT depths is still not clear (Humphreys *et al.*, 2006) as a continuum of both total leaf area and the relative proportion of different plant functional types exists.

In general, peatlands have been shown to evaporate at or near the equilibrium level, similar to high productivity broadleaf forests in the boreal region, but less than what would be predicted for an extensive, well-watered surface (Baldocchi *et al.*, 2000; Humphreys *et al.*, 2006). Nevertheless, large canopy resistance measured in a southern bog resulted in uncharacteristically low evaporation despite the WT being near the surface (Campbell and Williamson, 1997). The departure from a regular peatland evaporative regime is thought to be the result of a dense canopy limiting vapour diffusion from the moss surface. The importance of capturing this trade-off between canopy and

surface evaporative losses and their differing physical controls is highlighted by the variable performance of ET models across peatland types (Comer *et al.*, 2000).

In assessing the controls on ET, bulk surface resistance has been shown to be better correlated with D compared to surface moisture (Kellner, 2001). However, the strength of the relation has been shown to deteriorate under drying conditions (Admiral *et al.*, 2006). Early in the growing season, water tends to be freely available, with minimal stomatal control as observed from the ecosystem scale due to the relatively low LAI of vascular vegetation. As the vascular canopy develops and reaches full leaf-out, stomatal closure decouples ET from D . Finally, as leaves begin to senesce, mosses can no longer meet atmospheric moisture demand due to low a WT and moisture content, particularly in hummocks (Admiral and Lafleur, 2007). Nonetheless, D and the stomatal response of vascular vegetation tend to control the diurnal course of ET over a range WT depths, where a change in the ET regime is only detected at very low WT depths (Lafleur *et al.*, 2005).

1.2.2 Energy partitioning

Forest micrometeorological studies have recognized the importance of the understory contribution to ecosystem scale ET (Baldochi *et al.*, 1997; Baldochi *et al.*, 2000; Blanken *et al.*, 1997a; and Kelliher *et al.*, 1990), where controls on ET can be out of phase in the case where plant functional type of the dominant canopy and understory species differ (Baldochi *et al.*, 2004). For peatlands, this may suggest that differences in phenology between vegetation types will lead to different sourcing of water vapour throughout the season

Few peatland studies have used field measurements to determine the variation in evaporative flux due to vegetation composition, so it is unclear to what degree vascular vegetation controls ecosystem scale ET. A fairly even contribution of moss and vascular shrubs to early season conductance values is shown at an eastern Canadian bog, while vascular conductance dominates as LAI increases and WT drops (Admiral and Lafleur, 2007). Therefore, where long-term WT manipulations have an effect on LAI and the relative abundance of plant functional types, we would expect a measurable impact on the magnitude and seasonality of ET.

A three-source ET model for an eastern Canadian bog with a relatively low LAI of 1.3 showed that the canopy contributed the majority of evaporative losses, with between 10% to 30% sourcing from the moss surface. Using field measurements and modelling, Bond-Lamberty *et al.* (2011) showed that bryophytes contribute 49% - 69% of total ET in a poorly-drained forested peatland. Furthermore, laboratory measurements suggested there was no difference in the relation between moss evaporation and water content for hummocks and hollows (Bond-Lamberty *et al.*, 2011), but where moisture status differed between microforms in the field. Conversely, Brown *et al.* (2010) showed no difference in ET between microform in *Sphagnum* dominated plots throughout the growing season, but where the vascular canopy was both sparse and heterogeneous. With increasing LAI, shading of the moss surface reduces the energy balance at the surface, thus limiting potential evaporative losses. The architecture and density of the vascular canopy also affects the magnitude of turbulent mixing near the surface, providing additional resistance to evaporative loss from the surface. Moreover, sourcing of ET has

been argued to be influenced by microadvection, either between the surface and the vascular canopy (Kim and Verma, 1996), or between hummocks and hollows (Kellner, 2001). In both cases, a dry moss surface would partition more available energy to sensible heat, with the potential to increase the energy balance of the vascular canopy or of wet hollows adjacent to dry hummocks. Furthermore, where microtopography is pronounced and plant functional type differs (*e.g.* sedges versus shrubs), shelter and edge effects may further enhance spatial variability in evaporative losses.

The sheltering effect of vascular vegetation on the moss surface must be balanced against the net effect of increased transpiration on the water balance and interception losses on surface moisture content. Farrick and Price (2009) showed that 66% of precipitation inputs were lost through transpiration and interception losses in a shrub dominated bog (Farrick and Price, 2009). By limiting water inputs at the surface, the moisture retention properties and hydraulic structure of the underlying peat become increasingly important for *Sphagnum* to be able to meet evaporative demand and avoid desiccation. The link between surface moisture status and evaporative losses from *Sphagnum* have been shown to be highly non-linear (Bond-Lamberty *et al.*, 2011; Kettridge and Waddington, 2013), where differences in the moisture retention properties of *Sphagnum* species and the hydraulic structure of peat from contrasting microforms may serve to limit the impact of WT drawdown.

1.2.3 Peat hydrophysical properties

Sphagnum, which passively transports and evaporates water, cannot control water loss due to a lack of conducting vascular tissue and stomata. However, there are

characteristic *Sphagnum* species which tend to grow at different heights above the WT (Andrus *et al.*, 1983). Differences in peat hydrophysical properties between species growing in perennially wet versus dry locations (Whittington and Price, 2006), and differences in the relation between *Sphagnum* moisture content and productivity (Rydin and McDonald, 1985) help to explain the vertical zonation of *Sphagnum* species. The physical structure of hummock species and their close packing results in a smaller pore size distribution (Hayward and Clymo, 1982), resulting in greater water retention. This has important implications for moss evaporation (Kellner and Halldin, 2002), where greater moisture content at an equivalent soil water potential is likely to support higher rates of evaporation. Furthermore, based on theory of capillary rise in a tube, the small pore size distribution implies hummocks would be able to support evaporation at greater WT depths (Hayward and Clymo, 1982).

Peat moisture retention and the associated pF curves/Van Genuchten parameters, hydraulic conductivity (K_s), bulk density (ρ_b), and botanical origin has been widely studied (*e.g.* Paivanen, 1973; Schwarzel *et al.*, 2002; Naasz *et al.*, 2005; Gnatowski *et al.*, 2010; McCarter and Price, 2012). Boelter (1969) has shown that the moisture-tension (θ - ψ) relations of peat are primarily controlled by ρ_b , but where a broad categorization of the level of decomposition also plays an important secondary role. Several studies have looked at the combined effect of drainage and harvesting on peat hydrophysical properties in relation to restoration work (*e.g.* Schlotzhauer and Price, 1999; Price and Whitehead, 2001; Cagampan and Waddington, 2008; Waddington *et al.*, 2011) but applicability to natural WT drawdown is limited due to the removal of high porosity, low

ρ_b surface peat and *Sphagnum* during peat harvesting. Within the literature, Thompson and Waddington (2013) are one of the few to report on the differences between hummock and hollow θ - ψ relations, though they focus on the effect of wildfire.

In addition to moisture retention, the hydraulic structure of peat differs between microforms, where WT drawdown has been shown to have a variable effect on ρ_b , K_s , specific yield, and WT variability between microforms (Whittington and Price, 2006). WT drawdown often results in surface subsidence due to both short-term changes in shear stress (Kennedy and Price, 2005) and long term consolidation through oxidation loss (Waddington *et al.*, 2002). This in turn can increase ρ_b , lower porosity, specific yield, and K_s . As a result of lower specific yield and K_s , water in the system may be conserved but at the expense of greater WT variability. Waddington *et al.* (2010) showed that peat volume changes are greater in low-lying microforms in response to WT variability, suggesting a feedback mechanism for reducing fluctuations in surface moisture availability. Nevertheless, increased WT variability will favour *Sphagnum* species which have greater moisture retention and a community structure which limits evaporative losses.

While WT has previously been used in modelling peatland energy balances and ET (Moore *et al.*, 2002), the physical basis is limited since surface moisture availability is non-linearly related to WT depth (Price, 1997). Moreover, simple empirical relation between surface moisture and WT are confounded by hysteresis (Kellner and Halldin, 2002). Capillary transport capacity and pore water pressure may be more representative of moss evaporative potential and moisture availability respectively (Thompson and

Waddington, 2008; McCarter and Price, 2012). If the long-term response of peatlands to disturbance is to be assessed, either in terms of their feedback on large scale model simulations or for peatland carbon balances, *Sphagnum* moisture availability must be evaluated in a physically-based manner which accounts for differences in peat moisture retention and hydraulic structure between microforms. While some studies have identified different moisture stress thresholds for characteristic hummock and hollow *Sphagnum* species (Hajek and Beckett, 2008), a generally accepted range for the hydrologic threshold for *Sphagnum* species based on moss physiology is a pore water pressure between -100 mb and -600 mb (Hayward and Clymo, 1982; Lewis, 1988). Field studies examining the link between surface pore water pressure and *Sphagnum* colonization on bare peat suggest the same limit of roughly -100 mb (Price and Whitehead, 2001). Therefore, the ecohydrological response of peatlands to long-term changes in moisture storage will be the result of any competitive advantage between hummocks and hollows that result from desiccation avoidance and tolerance, where *Sphagnum* species which naturally grow further from the WT tend to have a competitive advantage under drying conditions (Robroek *et al.*, 2007). By incorporating the distinct hydrophysical properties of hummock and hollow peat and the moss surface using physically based soil hydrology, the role of moisture retention and hydraulic structure on *Sphagnum* moisture status can be assessed.

1.3 Study objectives

A comparison of three collocated peatlands with different mean depths to WT, microtopographic variation, and abundance of plant functional types provide the basis for

examining the link between moisture status, vegetation community, and resultant energy and water balances. The three sites also provide the opportunity to examine differences in energy partitioning, the relative role of vascular plants under different moisture regimes, and the effect of hydrophysical properties on surface moisture status. Given that the sites are subject to the same local weather conditions, the research site provides a unique opportunity to evaluate ecosystem scale processes under similar atmospheric conditions. Furthermore, given that two of the sites were subject to water table manipulation (both an increase and decrease relative to the reference site) in the 1950s, the long-term impact of WT manipulation on ecohydrological processes can be examined.

Within the context of comparing and contrasting sites along a WT manipulation gradient, the main research objectives were to: (1) quantify and explain differences in the seasonal variability in ecosystem scale energy and water balance components of peatlands with an increasing mean depth to WT; (2) quantify the relative contribution of non-vascular vegetation to peatland water vapour fluxes and the link to surface moisture variability and vascular plant phenology; (3) examine differences in peat hydrophysical properties from contrasting microtopographical elements and across sites with different mean depths to WT; and (4) determine how differences in peat hydrophysical properties feedback into surface moisture availability under current and a future climate change scenario.

1.4 References

- Admiral SW, Lafleur PM. 2007. Modelling of latent heat partitioning at a bog peatland. *Agricultural and Forest Meteorology* **144**: 213-229.
- Admiral SW, Lafleur PM, and Roulet, NT. 2006. Controls on latent heat flux and energy partitioning at a peat bog in eastern Canada. *Agricultural and Forest Meteorology*, **140**: 308-321.
- Andrus RE, Wagner DJ, Titus JE. 1983. Vertical zonation of *Sphagnum* mosses along hummock-hollow gradients. *Canadian Journal of Botany* **61**: 3128-3139.
- Baldocchi DD, Law BE, and Anthoni PM, 2000. On measuring and modeling energy fluxes above the floor of a homogenous and heterogeneous conifer forest. *Agricultural and Forest Meteorology*, **102**: 187-206.
- Baldocchi DD, Vogel CA, and Hall B. 1997. Seasonal variation of energy and water vapour exchange rates above and below a boreal jack pine canopy. *Journal of Geophysical Research*, **102**(D24): 28,939-29,951.
- Baldocchi DD, Xu LK, and Kiang N, 2004. How plant functional-type, weather, seasonal drought, and soil physical properties alter water and energy fluxes of an oak-grass savanna and an annual grassland. *Agricultural and Forest Meteorology*, **123**(1-2): 13-39.
- Belyea LR, Baird AJ. 2006. Beyond “the limits to peat bog growth”: cross-scale feedback in peatland development. *Ecological Monographs*, **76**(3): 299-322.
- Belyea LR, Clymo RS. 2001. Feedback control of the rate of peat formation. *Proceedings of the Royal Society of London. Series B: Biological Sciences*, **268**(1473): 1315-1321.
- Bird MI, Santruckova H, Lloyd J Veenendaal EM. 2001. The Global Soil Organic Carbon Pool. In: Schulze ED, Harrison S, Heimann M, Holland E, eds. *Global Biogeochemical Cycles in the Climate System*. San Diego: Academic Press. pp 185-226.
- Blanken, PD, Black TA, Yang PC, den Hartog G, Neumann HH, Nesic Z, Staebler R, Novak MD, and Lee X. 1997. Energy balance and canopy conductance of a boreal aspen forest: partitioning overstory and understory components. *Journal of Geophysical Research*, **102**: 28,915-28,927.
- Boelter DH. 1969. Physical properties of peats as related to degree of decomposition. *Soil Science Society of America* **33**(4): 606-609.
- Bond-Lamberty B, Gower ST, Amiro B, Ewers BE. 2011. Measurement and modelling of bryophyte evaporation in a boreal forest chronosequence. *Ecohydrology*, **4**(1): 26-35.

- Brown SM, Petrone RM, Mendoza C, Devito KJ. 2010. Surface vegetation controls on evapotranspiration from a sub-humid Western Boreal Plain wetland. *Hydrological Processes*, **24**(8): 1072-1085.
- Bubier JL, Moore TR, Crosby G. 2006. Fine-scale vegetation distribution in a cool temperate peatland. *Botany*, **84**(6): 910-923.
- Cagampan JP, Waddington JM. 2008. Moisture dynamics and hydrophysical properties of a transplanted acrotelm on a cutover peatland. *Hydrological processes*, **22**(12): 1776-1787.
- Campbell D, and Williamson JL. 1997. Evaporation from a raised peat bog. *Journal of Hydrology*, **193**: 142-160.
- Chapin FS, McGuire AD, Randerson J, Pielke R, Baldocchi D, Hobbie SE, Roulet N, Eugster W, Kasischke E, Rastetter EB, Zimov SA, Running SW. 2000. Arctic and boreal ecosystems of western North America as components of the climate system. *Global Change Biol.* **6** (Suppl.1): 211-223.
- Chivers MR, Turetsky MR, Waddington JM, Harden JW, McGuire AD. 2009. Climatic and vegetation controls on peatland CO₂ fluxes in Alaska: Early response to ecosystem-scale manipulations of water table and soil temperature. *Ecosystems* **12**: 1329-1342, doi: 10.1007/s10021-009-9292-y.
- Christensen JH, Hewitson B, Busuioc A, Chen A, Gao X, Held I, Jones R, Kolli RK, Kwon W-T, Laprise R, Magaña Rueda V, Mearns L, Menéndez CG, Räisänen J, Rinke A, Sarr A and Whetton P. 2007. Regional Climate Projections. In: *Climate Change 2007: The Physical Science Basis. Contribution of Working Group I to the Fourth Assessment Report of the Intergovernmental Panel on Climate Change* [Solomon S, Qin D, Manning M, Chen Z, Marquis M, Averyt KB, Tignor M and Miller HL (eds.)]. Cambridge University Press, Cambridge, UK.
- Clymo RS. 1984. The limits to peat bog growth. *Philosophical Transactions of the Royal Society of London. B, Biological Sciences*, **303**(1117): 605-654.
- Comer NT, Lafleur PM, Roulet NT, Letts MG, Skarupa M, and Versegny D. 2000. A test of the Canadian Land Surface Scheme (CLASS) for a variety of wetland types. *Atmosphere-Ocean*, **38**(1): 161-179.
- Devito K, Mendoza C, Qualizza C. 2013. Conceptualizing Water Movement in the Boreal Plains: Implications for Watershed Reconstruction, Synthesis report prepared for the Canadian Oil Sands Network for Research and Development. Environmental and Reclamation Research Group.
- Eugster W, Rouse WR, Pielke RA, McFadden JP, Baldocchi DD, Kittel TGF, Chapin FS, Liston GE, Vidale PL, Vaganov E, Chambers S. 2000. Land-atmosphere energy exchange in Arctic tundra and boreal forest: available data and feedbacks to climate. *Global Change Biol.* **6** (Suppl.1): 84-115.

- Farrick KK, Price JS. 2009. Ericaceous shrubs on abandoned block-cut peatlands: implications for soil water availability and *Sphagnum* restoration. *Ecohydrology*, **2**(4): 530-540.
- Frolking S, Talbot J, Jones MC, Treat CC, Kauffman JB, Tuittila ES, Roulet N. 2011. Peatlands in the Earth's 21st century climate system. *Environmental Reviews*, **19**: 371-396.
- Garratt JR. 1993. Sensitivity of climate simulations to land-surface and atmospheric boundary-layer treatments-A review. *Journal of Climate*, **6**(3): 419-448.
- Gnatowski T, Szatyłowicz J, Brandyk T, Kechavarzi C. 2010. Hydraulic properties of fen peat soils in Poland. *Geoderma*, **154**(3): 188-195.
- Gorham E. 1991. Northern peatlands: role in the carbon cycle and probable responses to climatic warming. *Ecological applications*, **1**(2): 182-195.
- Gunnarsson U, Malmer N, Rydin H. 2002. Dynamics or constancy in *Sphagnum* dominated mires ecosystems? A 40-year study. *Ecography* **25**: 685-704.
- Hajek T, Beckett RP. 2008. Effect of water content components on desiccation and recovery in *Sphagnum* mosses. *Annals of Botany* **101**: 165-173, DOI: 10.1093/aob/mcm287.
- Hayward PM, and Clymo RS. 1982. Profiles of water content and pore size in *Sphagnum* and peat, and their relation to peat bog ecology. *Proceeds of the Royal Society of London, Series B*, **215**: 299-325.
- Hilbert DW, Roulet N, Moore T. 2000. Modelling and analysis of peatlands as dynamical systems. *Journal of Ecology*, **88**(2): 230-242.
- Holden J. 2005. Peatland hydrology and carbon release: why small-scale process matters. *Philosophical Transactions of the Royal Society A: Mathematical, Physical and Engineering Sciences*, **363**(1837): 2891-2913.
- Huemrich KF, Kinoshita G, Gamon JA, Houston S, Kwon H, Oechel WC. 2010. Tundra carbon balance under varying temperature and moisture regimes. *J. Geophys. Res.*, **115**, G000I02
- Humphreys, ER, Lafleur PM, Flanagan LB, Hedstrom N, Syed KH, Glenn AJ, and Granger R. 2006. Summer carbon dioxide and water vapour fluxes across a range of northern peatlands. *Journal of Geophysical Research*, **111**: G04011, doi:10.1029/2005JG000111.
- Ise T, Dunn AL, Wofsy AC, Moorcroft PR. 2008. High sensitivity of peat decomposition to climate change through water-table feedback. *Nature Geoscience*, **1**: 763–766.
- Johnson LC, Damman AWH. 1991. Species-controlled *Sphagnum* decay on a South Swedish raised bog. *Oikos*, **61**: 234-242.

- Kelliher FM, Whitehead D, McAneney KJ, and Judd MJ. 1990. Partitioning evapotranspiration into tree and understory components in two young *Pinus radiata* stands. *Agricultural and Forest Meteorology*, **50**: 211-227.
- Kellner E. 2001. Surface energy fluxes and control of evapotranspiration from a Swedish Sphagnum mire. *Agricultural and Forest Meteorology*, **110**(2): 101-123.
- Kellner E, Halldin S. 2002. Water budget and surface-layer water storage in a Sphagnum bog in central Sweden. *Hydrological Processes*, **16**(1): 87-103.
- Kennedy GW, Price JS. 2005. A conceptual model of volume-change controls on the hydrology of cutover peats. *Journal of Hydrology* **302**: 13-27.
- Kettridge N, Baird A. 2006. A new approach to measuring the aerodynamic resistance to evaporation within a northern peatland using a modified Bellani plate atmometer. *Hydrological processes*, **20**(19): 4249-4258.
- Kettridge N, Waddington JM. 2013. Towards quantifying the negative feedback regulation of peatland evaporation to drought. *Hydrological Processes*, DOI: 10.1002/hyp.9898.
- Kim J, and Verma SB. 1996. Surface exchange of water vapour between an open *Sphagnum* fen and the atmosphere. *Boundary-Layer Meteorology*, **79**: 243-264.
- Korner C, Scheel JA, Bauer H. 1979. Maximum leaf diffusive conductance in vascular plants. *Photosynthetica*, **13**: 45-82.
- Lafleur PM, Hember RA, Admiral SW, and Roulet NT. 2005. Annual and seasonal variability in evapotranspiration and water table at a shrub-covered bog in southern Ontario, Canada. *Hydrological Processes*, **19**: 3533-3550.
- Lafleur PM, McCaughey JH, Joiner DW, Bartlett PA, and Jelinski DE. 1997. Seasonal trends in energy, water and carbon dioxide fluxes at a northern boreal wetland. *Journal of Geophysical Research*. **102**(D4): 29009-29020.
- Laiho R, Minkkinen K, Anttila J, Vávřová P, Penttilä T. 2008. Dynamics of litterfall and decomposition in peatland forests: Towards reliable carbon balance estimation?. In *Wastewater treatment, plant dynamics and management in constructed and natural wetlands* (pp. 53-64). Springer Netherlands.
- Lawrence DM, Oleson KW, Flanner MG, Thornton PE, Swenson SC, Lawrence PJ, Zeng XB, Yang ZL, Levis S, Sakaguchi K, Bonan GB, Slater AG. 2011. Parameterization improvements and functional and structural advances in version 4 of the Community Land Model. *J. Adv. Earth Syst.* **3**, DOI: 10.1029/2011MS000045.
- Lewis AM. 1988. A test of the air-seeding hypothesis using *Sphagnum* hyalocysts. *Plant Physiology* **87**: 577 – 582.

- Liljedahl AK, Hinzman LD, Harazono Y, Zona D, Tweedie CE, Hollister RD, Endstrom R, Oechel WC. 2011. Nonlinear controls on evapotranspiration in arctic coastal wetlands. *Biogeosciences*, **8**: 3375-3389.
- Luken JO, Billings WD, Peterson KM. 1985. Succession and biomass allocation as controlled by *Sphagnum* in an Alaskan peatland. *Canadian journal of botany*, **63**(9): 1500-1507.
- Lund M, Christensen TR, Mastepanov M, Lindroth A, Strom L. 2009. Effects of N and P fertilization on the greenhouse gas exchange in two northern peatlands with contrasting N deposition rates. *Biogeosciences*, **6**: 2135-2144.
- Macrae ML, Devito KJ, Strack M, Waddington JM. 2013. Effect of water table drawdown on peatland nutrient dynamics: implications for climate change. *Biogeochemistry*, **112**(1-3): 661-676.
- McCarter CPR, Price JS. 2012. Ecohydrology of *Sphagnum* moss hummocks: mechanisms of capitula water supply and simulated effects of evaporation. *Ecohydrology*, DOI: 10.1002/eco/1313.
- Miller CA. 2011. The Effect of Long-Term Drainage on Plant Community Composition, Biomass, and Productivity in Boreal Continental Peatlands. (Master's thesis – University of Guelph).
- Moore PD. 2002. The future of cool temperate bogs. *Environmental Conservation* **29**: 3-20.
- Murphy MT, Moore TR. 2010. Linking root production to aboveground plant characteristics and water table in a temperate bog. *Plant and soil*, **336**(1-2): 219-231.
- Naasz R, Michel JC, Charpentier S. 2005. Measuring hysteretic hydraulic properties of peat and pine bark using a transient method. *Soil science society of America Journal*, **69**(1): 13-22.
- Oechel WC, Vourlitis GL, Hastings SJ, Ault RP, Brant P. 1998. The effects of water table manipulation and elevated temperature on the net CO₂ flux components of Alaskan Coastal Plain tundra to shifts in water table. *J. Geophys. Res.*, **115**, G00I05.
- O'Neil KP. 2000. Role of bryophyte-dominated ecosystems in the global carbon budget: In: *Bryophyte Biology*. Eds.: Shaw, AJ, and Goffinet, B. Cambridge University Press, pp. 344-368.
- Päivänen J. 1973. Hydraulic conductivity and water retention in peat soils. *Acta Forestalia Fennica*. **129**: 1-70.
- Pellerin S, Lavoie C. 2003. Recent expansion of jack pine in peatlands of southeastern Quebec: A paleoecological study. *Ecoscience* **10**, 247-257.

- Price, J.S., 1991. Evaporation from a blanket bog in a foggy coastal environment. *Boundary-Layer Meteorology*, **57**: 391–406.
- Price J. 1997. Soil moisture, water tension, and water table relationships in a managed cutover bog. *Journal of hydrology*, **202**(1): 21-32.
- Price JS, Whitehead GS. 2001. Developing hydrologic thresholds for Sphagnum recolonization on an abandoned cutover bog. *Wetlands*, **21**(1): 32-40.
- Price JS, Whittington PN. 2010. Water flow in *Sphagnum* hummocks: Mesocosm measurements and modelling. *Journal of Hydrology*, **381**(3): 333-340.
- Robroek BJM, Limpens J, Breeuwer A, Crushell PH, and Schouten MGC. 2007. Interspecific competition between *Sphagnum* mosses at different water tables. *Functional Ecology*, **21**: 805-812.
- Roulet N, Moore T, Bubier J, Lafleur P. 1992. Northern fens: methane flux and climatic change. *Tellus: Series B*. **44**(2): 100-105.
- Rydin H, Jeglum JK, Hooijer A. 2006. The biology of peatlands. Oxford University Press, Oxford, New York, 343 pp.
- Rydin H. and McDonald AJS. 1985. Photosynthesis in Sphagnum at different water contents. *Journal of Bryology*, **13**: 579–584.
- Schlotzhauer SM, Price JS. 1999. Soil water flow dynamics in a managed cutover peat field, Quebec: Field and laboratory investigations. *Water Resources Research*, **35**(12): 3675-3683.
- Schulze ED, Kelliher FM, Korner C, Lloyd J, Leuning R. 1994. Relationships among maximum stomatal conductance, ecosystem surface conductance, carbon assimilation rate, and plant nitrogen nutrition: a global ecology scaling exercise. *Annual Review of Ecology and Systematics*, **25**: 629-660.
- Schwarzl K, Renger M, Sauerbrey R, Wessolek, G. 2002. Soil physical characteristics of peat soils. *Journal of plant nutrition and soil science*, **165**(4): 479.
- Sellers PJ, Mintz YC, and Dalcher, A. 1986. A simple Biosphere Model (SiB) for use within General Circulation Models. *Journal of Atmospheric Science*, **43**(6): 505–531.
- Sundström E, Magnusson T, Hånell B. 2000. Nutrient conditions in drained peatlands along a north-south climatic gradient in Sweden. *Forest ecology and management*, **126**: 149-161.
- Strack M, Waddington JM. 2007. Response of peatland carbon dioxide and methane fluxes to a water table drawdown experiment. *Global Biogeochemical Cycles*, **21**(1). DOI: 10.1029/2006GB002715.
- Takagi K, Tsuboya T, Takahashi H, and Inoue T. 1999. Effect of the invasion of vascular plants on heat and water balance in the Sarobetsu mire, northern Japan. *Wetlands*, **19**(1): 246-254.

- Talbot J, Richard PJH, Roulet NT, Booth RK. 2010. Assessing long-term hydrological and ecological responses to drainage in a raised bog using paleoecology and a hydrosequence. *Journal of Vegetation Science*, **21**(1): 143-156.
- Teklemariam TA, Lafleur PM, Moore TR, Roulet NT, Humphreys ER. 2010. The direct and indirect effects of inter-annual meteorological variability on ecosystem exchange at a temperate ombrotrophic bog. *Agric. For. Meteorol.* **150**: 1402-1411.
- Thompson DK. 2012. Wildfire impacts on peatland ecohydrology. PhD thesis – McMaster University.
- Thompson DK, Waddington JM. 2008. *Sphagnum* under pressure: towards an ecohydrological approach to examining *Sphagnum* productivity. *Ecohydrology* **1**: 299-308, DOI: 10.1002/eco.31.
- Thompson DK, Waddington JM. 2013. Wildfire effects on vadose zone hydrology in forested boreal peatland microforms. *Journal of Hydrology*. **486**: 48-56. DOI: 10.1016/j.jhydrol.2013.01.014
- Thormann MN, and Bayley SE. 1997. Above-ground net primary productivity along a bog-fen-marsh gradient in southern boreal Alberta, Canada. *Ecoscience*, **4**: 374-384.
- Turetsky MR, Crow SE, Evans RJ, Vitt DH, Wieder K. 2008. Trade-offs in resource allocation among moss species control decomposition in boreal peatlands. *Journal of Ecology* **96**: 1297–1305.
- Vitt DH, Halsey LA, Bauer IE, Campbell C. 2000. Spatial and temporal trends in carbon storage of peatlands of continental western Canada through the Holocene. *Canadian Journal of Earth Sciences*, **37**(5): 683-693.
- Waddington JM, Kellner E, Strack M, Price JS. 2010. Differential peat deformation, compressibility, and water storage between peatland microforms: Implications for ecosystem function and development. *Water Resources Research*, **46**(7), DOI: 10.1029/2009WR008802.
- Waddington JM, Lucchese MC, Duval TP. 2011. *Sphagnum* moss moisture retention following the re-vegetation of degraded peatlands. *Ecohydrology*, **4**(3): 359-366.
- Waddington JM, McNeil P. 2002. Peat oxidation in an abandoned cutover peatland. *Canadian Journal of Soil Science*, **82**(3): 279-286.
- Wells E, Williams B. 1996. Effects of drainage, tilling and PK-fertilization on bulk density, total N, P, K, Ca and Fe and net N-mineralization in two peatland forestry sites in Newfoundland, Canada. *Forest ecology and management*, **84**: 97-108.
- Weltzin JF, Bridgham SD, Pastor J, Chen J, and Harth C. 2003. Potential effects of warming and drying on peatland plant community composition. *Global Change Biology*, **9**: 141-151.

- Weltzin JF, Pastor J, Harth C, Bridgham SD, Updegraff K, Chapin CT. 2000. Response of bog and fen plant communities to warming and water-table manipulations. *Ecology*, **81**(12): 3464-3478.
- Whittington PN, Price JS. 2006. The effects of water table draw-down (as a surrogate for climate change) on the hydrology of a fen peatland, Canada. *Hydrological Processes*, **20**(17), 3589-3600.
- Wu J, Roulet NT, Moore TR, Lafleur P, Humphreys E. 2011. Dealing with microtopography of an ombrotrophic bog for simulating ecosystem-level CO₂ exchanges. *Ecological Modelling*, **222**(4): 1038-1047.
- Yu Z, Beilman DW, Frohking S, MacDonald GM, Roulet NT, Camill P, Charman DJ. 2011. Peatlands and their role in the global carbon cycle. *Eos, Transactions American Geophysical Union*, **92**(12): 97-98.

CHAPTER 2: EFFECT OF LONG-TERM WATER TABLE MANIPULATIONS ON PEATLAND EVAPOTRANSPIRATION

2.1 Abstract

Continuous measurements of ecosystem scale evapotranspiration (ET) were obtained using the eddy covariance method over the 2010 and 2011 growing seasons (May to September) at three adjacent peatlands that have undergone long-term water table manipulation. The three (wet, dry and intermediate) sites represent peatlands along a hydrological gradient, with different average depths to water table (WTD) and different resulting vegetation and microform assemblages. The 2010 growing season was warmer and wetter than normal, while 2011 conditions were near normal. The difference in maximum daily ET values (95th percentiles) between sites were greater in 2010 (3.14 mm d⁻¹ – 4.17 mm d⁻¹) compared to 2011 (3.68 mm d⁻¹ – 3.95 mm d⁻¹), yielding cumulative growing season ET that followed the wet to dry gradient in both 2010 and 2011. Synoptic weather conditions (*i.e.* air temperature, vapour pressure deficit, and incoming solar radiation, *etc.*) could not explain differences in ET between sites due to their proximity to one another. Peat surface wetness was more spatially homogeneous at the wet site due to small average microtopographic variations (0.15 m) compared to the intermediate (0.30 m) and dry (0.41 m) sites. Although average Bowen ratios were less than one at all three sites, greater surface wetness and heating of the near-surface peat at the wettest site lead to differences in energy partitioning, with higher average Bowen ratios at the sites with a deeper average WTD. No significant relation between normalized ET and WTD was

found at any of the sites that were consistent across both study years. In addition, the lack of a relation between ET and near-surface moisture suggests that the unsaturated hydraulic conductivity and the boundary layer resistance created by the vascular canopy combined with low surface roughness limits evaporative losses from the peat surface. This study suggests that the low ET of a dry peatland site compared to a wet site may be due to the impact of a long-term change in WTD on leaf area and the relative distribution of plant functional groups.

2.2 Introduction

While peatland ecosystems cover only approximately 3% of the world's total land surface (Gorham, 1991), peatlands can cover in excess of 50% of the landscape in regions such as northern Alberta, the Hudson/James Bay Lowland (*e.g.* Tarnocai, 1984), Fennoscandinavia, and the West Siberian Plain (*e.g.* Paavalainen and Paivanen, 1995). In areas where peatlands are abundant, these ecosystems can have a significant impact on regional climate through surface-atmosphere exchanges of mass and energy, where evapotranspiration (ET) is a large component of the water balance across peatland types (Price and Maloney, 1994; Kellner and Halldin, 2002).

Peatland ecosystems also represent a potential long-term impact on future climate (Frolking *et al.*, 2011) through their role in the global carbon cycle, where the oxidation and/or combustion of the large carbon pool stored in peatlands (*e.g.* Gorham, 1991; Vasander and Kettunen, 2006; Turetsky *et al.*, 2011) would represent a positive feedback to current climate forcings. Rapid and/or long-term persistent oxidation of peatland carbon stores has been inferred from future climate scenario modelling studies (Ise *et al.*,

2008) and from experimental manipulations of sites that were impacted by multiple disturbances, such as temperature change and drainage (Strack and Waddington, 2007; Chivers *et al.*, 2009; Huemmrich *et al.*, 2010). However, to improve our understanding of the role of peatland surface-atmosphere interactions on regional climate and the potential of peatlands to feedback on global climate change, a greater level understanding on peatland surface energy partitioning and the controls on ET is required (den Hartog *et al.*, 1994; Kellner, 2001; Kettridge and Baird, 2006).

Due to the wet conditions prevalent in many peatlands, past research has sought to characterize simple metrics relating peatland ET to open-water or equilibrium evaporation and water table depth (WTD). Equilibrium evaporation is defined as the evaporation rate from an extensive, well watered surface where the overlying air mass has no saturation deficit (Monteith, 1981), and differs from open-water evaporation since the effect of entrainment of air from above the convective boundary layer (Priestley and Taylor, 1972) is not taken into account. In general, peatlands evaporate at or near the equilibrium level, similar to high productivity broadleaf forests in the boreal region, but less than open-water evaporation (Baldocchi *et al.*, 2000; Humphreys *et al.*, 2006), suggesting a weak but important control of vapour pressure deficit (D) or water limitation. The relation between ET, and WTD for peatlands in general is not straight forward as studies have shown a range of responses including a strong WTD relation (Lafleur and Roulet, 1992), no significant effect of WTD (Paramentier *et al.*, 2009; and Wu *et al.*, 2010), and a moderate or threshold type response (Lafleur *et al.*, 2005). The control of ET by D in peatlands is similarly varied. In peatlands dominated by vascular

vegetation having a relatively high LAI, there is evidence that ET is strongly controlled by surface resistance (Comer *et al.*, 1999), and thus by D . In contrast, clear-day ET was shown to be more strongly controlled by net radiation in a moss-dominated peatland (Price, 1991). In assessing the controls on ET, surface resistance has been shown to be better correlated with D in comparison to water availability (Kellner, 2001). However, the strength of the relation between ET and D can deteriorate under drying conditions (Admiral *et al.*, 2006), where a change in the ET regime may only be detected at relatively large WTD (Lafleur *et al.*, 2005).

These findings suggest that the range of responses in peatland ET are, in part, due to the disparate controls on moss evaporation and vascular plant ET, and their respective links to the spatio-temporal variability in moisture availability. Moreover, the relative abundance of vascular vegetation within a given peatland will dictate whether a peatland can be modelled using a big-leaf model with ET partitioned into soil, vegetation, and interception loss components such as in the ORCHIDEE land surface scheme (Ducoudre *et al.*, 1993), or if a more detailed dual source model is required (Kim and Verma, 1996; Lafleur *et al.*, 2005). The Canadian land surface scheme (CLASS) and Community Land Model have recognized the importance of both organic soils (*e.g.* Letts *et al.*, 2000; Lawrence *et al.*, 2008) as well as the need for a dual source model to better characterize surface evaporation (*e.g.* Verseghy, 1993; Lawrence *et al.*, 2011). Nevertheless, despite having dual source ET and organic soil parameterization, Comer *et al.* (1999) show that CLASS does not simulate ET well for peatlands with a sparse vascular canopy, suggesting a potential need for better parameterization of moss evaporation. Furthermore,

potentially important dynamics which are missing from peatland classifications in land surface schemes include the role of microtopography on the spatial variability in moisture (*e.g.* Wu *et al.*, 2011) and plant functional groups in peatlands (*e.g.* Korner *et al.*, 1979), as well as the ability for microtopography and plant functional groups to change through time as a result of changing environmental conditions.

The response of peatland ET to changes in moisture availability has been characterized using interannual variability at a site (Lafleur *et al.*, 2005; Liljedahl *et al.*, 2011), climatic gradients between sites (Humphreys *et al.*, 2006), and through field or laboratory manipulations (Whittington and Price, 2006). Measurements in years with different synoptic weather conditions can be used to quantify short-term, direct impacts on surface energy partitioning that result from warmer/colder or wetter/drier conditions (Teklemariam *et al.*, 2010), but often both moisture availability, temperature, and other synoptic weather variables vary simultaneously so specific impact attribution can be difficult to elicit. Comparisons between sites along climatic gradients are often used to represent long-term impacts of climate (*e.g.* Chapin *et al.*, 2000; Eugster *et al.*, 2000), where plant community composition is assumed to be in quasi-equilibrium with the local climate. However, attribution of change can be confounded by other overlapping gradients (*e.g.* nitrogen deposition, Lund *et al.*, 2009). Manipulation studies, which are predominantly focused on carbon fluxes (*e.g.* Oechel *et al.*, 1998; Weltzin *et al.*, 2003; Strack and Waddington, 2007; Chivers *et al.*, 2009; and Huemmrich *et al.*, 2010), use warming or draining to control for different anticipated climate change effects, but are often limited to a few years and thus are potentially measuring the response of a system

in disequilibrium. As such, there is a need to characterize peatland ET following a persistent change in moisture availability, where sufficient time has elapsed for both peat hydrophysical properties and the vegetation community to come into a quasi-equilibrium with the new hydrological conditions. In order to be able to constrain the degrees of freedom in a comparative study, the ideal research design would be to examine impacted and control sites in close enough proximity to one another that they can be considered to be subjected to the same synoptic weather conditions. To address this research need we took advantage of a large scale ‘natural experiment’ resulting from the construction of berms perpendicular to water flow in a large peatland complex in northern Michigan *ca.* 75 years ago by measuring growing season ET at three adjacent peatlands along a post-disturbance hydrosequence using the eddy covariance (EC) method. The objectives of this study were to: (i) quantify ET along a hydrosequence under the same synoptic weather conditions; (ii) determine if growing season ET was different between sites; and (iii) determine whether energy partitioning and/or controls on ET differed between sites.

2.3 Methods

2.3.1 Study site

The study area is located in the Seney National Wildlife Refuge (SNWR) in the Upper Peninsula of Michigan (46.20° N, 86.02° W, elev. ~205 m a.s.l.). The region is characterized by relatively flat topography which slopes towards the south-east at 1.1 – 2.3 m km⁻¹ (Heinselman, 1965). Land cover consists primarily of upland forests (67%), and open peatlands (20%), while the remainder of the region is made up of mostly

forested swamps and open water (Casselman, 2009). Wet sand of glacial origin overlies the regional bedrock up to a thickness of 60 m (Albert, 1995). Surface soils throughout SNWR are mostly a complex of poorly drained muck and sand, while the study area itself contains poorly drained peats (Casselman, 2009).

The peatland complex within SNWR is subdivided by a combination of upland sand ridges of lacustrine origin, creeks, old drainage ditches, as well as a network of roads and berms constructed mostly during the late 1930's and early 1940's by the Civilian Conservation Corps (Kowalski and Wilcox, 2003; Wilcox et al., 2006) for the purpose of creating open water habitat for migratory birds. As a result of the construction of berms perpendicular to water flow in the study area *ca.* 75 years ago, a natural experiment was created where an upslope peatland site (hereafter referred to as WET) likely became wetter and a downstream peatland site (hereafter referred to as DRY) likely became drier. Aerial photography of the study area shows a clear increase in ponding at the WET site and a rapid terrestrialization at the DRY site following berm construction. Moreover, contemporary WTD data shows a large difference between the WET and DRY sites, with the latter being up to 50 – 60 cm deeper. A site with an intermediate WTD (hereafter referred to as INT) is located adjacent to the WET site. All three study sites are located in the southern portion of SNWR and have greater than 200 m of continuous fetch in the dominant wind sector, with only 100 m along the lateral wind sectors. All three sites are located directly adjacent to one another along a roughly north-south transect, and separated by sandy upland ridges between 25 – 100 m wide.

The maximum distance between tower-based measurements (see *Instrumentation*) is approximately 750 m.

Dominant vegetation at all three peatland sites consists of a ground cover of *Sphagnum* sp. (*S. angustifolium*, *S. capillifolium*, *S. magellanicum*), with an overstory of vascular species. The dominant vascular vegetation consists of *Carex oligosperma*, *Eriophorum vaginatum*, *Ericaceae* (e.g. *Chamaedaphne calyculata*, *Ledum groenlandicum*, *Kalmia polifolia*, and *Vaccinium oxycoccus*), with trees becoming more abundant at sites with increasing WTD (e.g. *Picea mariana*, *Pinus banksiana*, and *Larix laricina*), particularly towards the margins. The berm and upland area surrounding the research sites is dominated by coniferous species such as red pine (*Pinus resinosa*), eastern white pine (*Pinus strobus*), jack pine (*Pinus banksiana*), and black spruce (*Picea mariana*). Although each peatland site has almost identical species richness, the relative proportion of given species differs between sites (J. Hribljan, personal communication). Generally, shrubs dominate hummocks, and sedges dominate hollows across sites, where the proportion of hummocks, height of hummocks relative to adjacent hollows, and acidity of near-surface water increases from the WET, to INT and DRY sites (Table 2-1). Moreover, both leaf area index (LAI) and plant area index (PAI) are highest at the WET site (Table 2-1).

Based on the 1981-2010 climate normals from the Newberry 3S weather station (46.32° N, 85.50° W, elev. ~260 m a.s.l.) ~45 km from the study sites, the area has an average annual temperature of 5.6°C and receives 784 mm of precipitation, where greater

monthly totals occur during May through October (NOAA NCDC, 2012) compared to other months.

2.3.2 Instrumentation

Standard eddy covariance (EC) equipment was used at all three sites to measure surface energy and mass exchanges based on the method described by Baldocchi *et al.* (1996). Three component wind speed and sonic air temperature were measured using a CSAT3 3D sonic anemometer-thermometer (Campbell Scientific Inc. (CS), Logan, Utah). Water vapour concentrations were measured using an LI-7500A open-path infrared gas analyzer (IRGA) (LI-COR Biosciences, Lincoln, Nebraska). All EC sensors were mounted between 1.7 and 2.1 m above the average hummock surface, had a vertical and lateral separation less than 0.15 and 0.3 m respectively, and were oriented upwind of the tower based on the dominant summertime wind direction. EC data was sampled at 10 Hz, with mean values and fluxes calculated every 30 minutes.

Radiation measurements were made using a combination of CMP3 and LP02 pyranometers (CS), NR-LITE net radiometers (CS), and CNR2 net short and long-wave radiometers (CS). A CNR2 was used at the INT and DRY site mounted at a height of 1.78 and 3.2 m respectively, while a NR-LITE was used at the WET and INT site mounted at a height of 1.7 and 2.3 m respectively. Both types of net radiometers were used at the INT site to provide a continuous cross-comparison of instrument type in order to correct for any systematic bias. In order to calculate albedo for all three sites, a single CMP3 was mounted 1.7 m above the sedge canopy at the WET site to measure incoming short-wave radiation. Outgoing short-wave radiation was measured at the WET site using

a LP02 mounted at 1.7 m above the sedge canopy. Outgoing short-wave radiation was obtained by difference from net shortwave radiation at each of the INT and DRY sites using a CNR2.

Supplementary air temperature and relative humidity (RH) were measured and recorded at 10 Hz using a HMP45C (Vaisala Oyj, Helsinki, Finland) temperature and relative humidity probe mounted in a radiation shield at a height of 1.35 m on all EC towers. Peat temperature profiles were measured in a representative hummock and hollow at each site using T-type thermocouple (Omega Engineering, CT, USA) wire inserted at depths of 0.01, 0.05, 0.1, 0.2, and 0.5 m relative to the local surface.

Measured hydrometric data included rainfall, soil volumetric water content (θ), and WTD. Rainfall was measured using a TE525 tipping bucket rain gauge (Texas Electronics, Dallas, TX, USA) mounted 0.7 m above the surface. Soil moisture profiles were measured using CS-616 water content reflectometers (CS). θ sensors were installed at all three sites in a representative hummock and hollow at depths of 0.05, 0.15, and 0.25 m relative to the surface, with an additional sensor at 0.5 m in hummocks. WTD was measured hourly in 1.5 m deep wells using self-logging Levellogger Junior pressure transducers (Solinst, Georgetown, ON (Solinst)). WTD measurements were corrected for changes in atmospheric pressure using a Barologger Gold barometric logger (Solinst). WTD was recorded at all three sites in two separate groundwater wells with the average local topography used as a datum, where the height of the average local surface was determined from 50 m transects with the groundwater wells at the center.

All high frequency data was recorded on a CR5000 datalogger (CS) at the WET and DRY site, while a CR3000 datalogger (CS) was used at the INT site. Meteorological, peat temperature and θ data were measured every minute and averaged and recorded at 30 minute intervals using a CR1000 (CS) or CR10X (CS) datalogger.

2.3.3 High-frequency data processing and corrections

Prior to calculating half-hour covariances, high-frequency EC measurements were subjected to a spike detection algorithm analogous to that presented in Vickers and Mahrt (1997), where spikes were identified when a measurement exceeded the recursive mean by a standard deviation of 2.6 (also derived recursively). The mean was constructed as a recursive digital filter (Kaimal and Finnigan, 1994):

$$\tilde{c}_t = \left(1 - \frac{\Delta t}{\tau_f}\right) \tilde{c}_{t-1} + \frac{\Delta t}{\tau_f} c_t \quad (2.1)$$

where c_t is the measured value at time t , Δt is the incremental time step between measurements (0.1 s), and τ_f is the RC filter time constant (60 s). The cut-off for spike detection is lower than the typical 3 – 5 SD range reported by others (*e.g.* Baldocchi *et al.*, 1997; Vickers and Mahrt, 1997; Humphreys *et al.*, 2006) because, given the above time constant, the recursive mean is more responsive to coherent transient departures from the long-term mean compared to block averaging.

Sonic anemometer wind vectors were mathematically rotated based on the tilt correction algorithms presented by Wilczak *et al.* (2001), also known as the planar fit method. The planar fit method helps to address the problem of over-rotation in sloping

terrain associated with the more commonly used method of Tanner and Thurtell (1969) as outlined by Lee *et al.* (2004).

Before calculating energy and mass fluxes, a time lag was introduced into the appropriate mass or energy time series in order to maximize the average covariance with the rotated vertical wind speed. In addition to flux loss that results from the asynchrony in the measured time series due to finite instrument processing times, spectral transfer functions were used to correct for high-frequency spectral losses that result from sensor separation, line and volume averaging, and digital filtering. Frequency response corrections were calculated according to the analytical solutions presented in Massman (2000) and applied to despiked, rotated, and lagged covariances.

Errors in EC flux measurements associated with variations in air density due to changing temperature and humidity were corrected based on the method outlined by Webb *et al.* (1980). The sensible heat flux is used in the WPL correction, and is itself dependent on air density fluctuations when measured using a sonic-anemometer. Sonic temperatures were thus corrected using the method of Kaimal and Finnigan (1994).

2.3.4 *Quality assurance and gap filling*

Half-hour flux measurements were rejected based on a number of statistical and physical environmental conditions. Basic statistical criteria for rejection of fluxes were based on second, third, and fourth-moment statistics. The thresholds for skewness and kurtosis were based both on those presented by Vickers and Mahrt (1997) and measured empirical probability distributions. A site dependent friction velocity (u_*) threshold of $\sim 0.08 \text{ m s}^{-1}$ was used as a basic rejection criterion for removing measurements made

under conditions without well developed turbulence. Although data was not explicitly rejected during periods of rainfall, data was rejected for approximately 99% of all half-hours with rainfall as a result of the aforementioned statistical criteria.

A comprehensive data quality flagging system was also used to identify half-hours with high-quality, questionable, and bad data (Foken *et al.*, 2004). Data quality was assessed based on integral turbulence characteristics, stationarity (Foken and Wichura, 1996), and wind direction, where wind-sectors travelling through the tower to the instrumentation were considered inappropriate.

In order to estimate growing season total ET, missing data was filled using an artificial neural network (ANN). ANNs have been shown to be suitable for gap-filling EC flux data (Moffat *et al.*, 2007) where standard meteorological and soil variables were used as driving variables. Day and night time gaps were modelled separately, where the disparity in available data for these two time periods would result in a bias towards daytime conditions during ANN calibration and validation. However, due to the relatively small contribution of nighttime latent heat fluxes, LE ($W\ m^{-2}$), the effect of nighttime bias was assumed to be negligible.

2.3.5 Calculations

A common method to investigate the controls on ET is by using the Penman-Monteith (Monteith, 1973) equation which takes the following form:

$$LE = \frac{s(R_n - G) + \rho_a C_p D r_a^{-1}}{s + \gamma \left(1 + \frac{r_s}{r_a}\right)} \quad (2.2)$$

where s (kPa °C⁻¹) is the slope of the saturation vapour pressure versus temperature curve, γ (kPa °C⁻¹) is the psychrometric constant, R_n (W m⁻²) is the net radiation flux, G (W m⁻²) is the ground heat flux, ρ_a (kg m⁻³) is the air density, C_p is the heat capacity of air (J kg⁻¹ °C⁻¹), D (kPa) is the vapour pressure of the atmosphere, r_a (s m⁻¹) is the aerodynamic resistance, and r_s (s m⁻¹) is the bulk surface resistance.

Aerodynamic resistance to heat and vapour transport was calculated as the sum of the resistance to momentum transfer, r_{am} , and the boundary layer resistance, r_b . r_a was calculated according to Stewart and Thom (1973):

$$r_a = \frac{u_z}{u_*^2} + r_b \quad (2.3)$$

where u_z is the wind speed (m s⁻¹), u_* is the friction velocity (m s⁻¹), and r_b is calculated according to the empirical formula of Kellner (2001):

$$r_b = \frac{a(u_* z_0 / \nu)^{0.25} - b}{k u_*} \quad (2.4)$$

where z_0 is the roughness length (m), ν is the kinematic viscosity of air (m² s⁻¹), k is the von Karman constant, and a and b are empirical parameters. Estimates of 1.58 and 3.4 for a and b from a Swedish bog were used to calculate r_b (Molder and Kellner, 2001). Stability correction factors were omitted from Eq. 2.3 and 2.4 since u_* was calculated based on turbulent measurements of all three Cartesian wind speed components rather than from wind speed profiles.

Surface roughness was estimated using a direct search algorithm (The MathWorks, R2010a) to minimize a least square difference function based on the log wind profile equation for near-neutral stability:

$$f(d, z_0) = \left(\frac{u_*}{k} \ln \left(\frac{z-d}{z_0} \right) - u_z \right)^2 \quad (2.5)$$

where d is the zero-plane displacement (m), subject to the constraint that $d > z_0$.

Bulk surface resistance, r_s ($s \text{ m}^{-1}$), was calculated by rearranging the Penman-Monteith equation (Monteith, 1973) and substituting the Bowen ratio, $\beta = H/LE$, which yields:

$$r_s = r_a \left(\frac{s}{\gamma} \beta - 1 \right) + \frac{\rho C_p D}{R_n - G} (1 + \beta) \quad (2.6)$$

In order to determine whether cumulative differences in ET between sites exceeded measurement uncertainty, a simple error analysis was used where the error in high quality data was assumed to be the result of random error. The calculation of random error was adapted from the method of Moncrieff *et al.* (1996):

$$Err_i = p \cdot DV_{ET,0.95} \cdot n^{-0.5} \quad (2.7)$$

where p is the magnitude of random error proportional to the measured flux, $DV_{ET,0.95}$ is the half-hourly diurnal variation of the 95th percentile of ET using a two week moving window, and n is the i^{th} measurement. In order to ensure that non-overlapping error bounds represented meaningful differences in cumulative ET, p was set equal to one. Assuming the true value of p cannot exceed one for high quality data, then non-

overlapping error bounds also represent a statistically significant difference in cumulative ET.

Unless otherwise stated, the period of analysis corresponds with the 2010 and 2011 growing seasons. Given that there is no universal definition for the climatological growing season (Walther and Linderholm, 2006), the growing season herein corresponds to the time of year when air temperature (T_a) was above 5 °C for over five consecutive days (Frich *et al.*, 2002).

Finally, all data processing, quality assurance, and statistical tests were done using MATLAB 7.8 (The MathWorks, Inc., 2009). Statistical tests were considered significant when the p -value was less than 0.01.

2.4 Results

2.4.1 Meteorological and hydrological conditions

The length and timing of the growing season was similar in both years (Table 2-2). Over the course of the two study years, 2011 was slightly warmer based on a comparison of cumulative GDD (Table 2-2). GDD for 2010 and 2011 were similar to the historical average of 1629 °C based on climate normals from the Newberry weather station (1981 – 2010 US Normals Data – National Climatic Data Center – National Oceanic and Atmospheric Administration). Considering GDD during the period defined by the climatological growing season alone, the difference between years becomes negligible. Moreover, during this period, there were no strong seasonal departures in T_a from the normal in either study year.

Rainfall during the 2010 and 2011 growing season was higher than normal (430 mm) over the same period (Table 2-2). The greater seasonal rainfall total in 2010 was the result of both fewer dry days and greater average rainfall on wet days (Table 2-2). Despite a greater growing season rainfall total, there was an extended dry period in 2010 where there was a 22 day period with only 6.4 mm of rainfall (day of year (DOY) 130 – 151). The maximum period with no rainfall in 2010 and 2011 was 10 and 12 days, respectively.

The difference in the average WTD (Fig. 2-1) between sites was fairly consistent over 2010 (median: $WTD_{WET} - WTD_{INT} = 0.20$ m; and $WTD_{WET} - WTD_{DRY} = 0.35$ m) with the exception of some anomalous values where WTD_{WET} was increasing while WTD_{INT} and WTD_{DRY} were decreasing (DOY 266 - 273). The difference in average WTD was smaller in 2011 (median: $WTD_{WET} - WTD_{INT} = 0.15$ m; and $WTD_{WET} - WTD_{DRY} = 0.28$ m) where the magnitude of the difference between WTD_{WET} and WTD_{DRY} increased as WTD_{DRY} moved into deeper peat late in the growing season. Overall, the average WTD was greater in 2011, which corresponds with a lower seasonal rainfall total. In terms of seasonality, WT was relatively stable in 2010 except early in the growing season during the extended dry period (DOY 130 – 151). Conversely, 2011 was characterized by a shallow WTD early in the growing season with progressive drying due to fewer and smaller rainfall events.

The effect of WTD variation was not apparent in the near-surface (0.05 m) θ of hummocks at two of the study sites (Fig. 2-1). Near-surface $\theta_{INT,hum}$ and $\theta_{DRY,hum}$ remained relatively stable throughout the growing season in both years, varying between 0.10 –

$0.20 \text{ m}^3 \text{ m}^{-3}$. Both $\theta_{WET, hum}$ and all θ_{hol} had much greater ranges of variability in both years, loosely corresponding to periods of large WTD variability. The magnitude of variability in θ_{hol} differs between sites. During the drying phase of both study years, θ_{hol} reached a minimum daily value of 0.21 and 0.22 $\text{m}^3 \text{ m}^{-3}$ at the WET site compared to 0.56 and 0.47 $\text{m}^3 \text{ m}^{-3}$ for the INT site, and 0.73 $\text{m}^3 \text{ m}^{-3}$ (2011 data missing) for the DRY site despite a greater WTD at the INT and DRY sites.

2.4.2 Surface Energy Exchange

2.4.2.1 Evapotranspiration

Daily ET at the WET site had a maximum of 5.0 and 4.8 mm for 2010 and 2011, with typical (25th to 75th percentile) values ranging from 1.9 to 3.4 mm d^{-1} and 1.6 to 3.1 mm d^{-1} in each of the two growing seasons, respectively (Fig. 2-2). In addition to having small differences in typical ET values, seasonality was more pronounced in 2011 compared to 2010, particularly due to lower ET values early in the 2011 growing season. Fig. 2-2 shows that throughout the 2010 growing season daily ET at both the INT and DRY sites was often lower compared to the WET site with a median difference of -0.41 mm d^{-1} for INT and -0.56 mm d^{-1} for DRY. In 2011, the differences between sites were not as pronounced, particularly early and late in the growing season, with values of -0.13 mm d^{-1} and -0.15 mm d^{-1} for INT and DRY respectively. Total ET over the growing season was substantially higher at the WET site in 2010 (Table 2-2), with total ET corresponding to 0.63 (WET), 0.49 (INT), and 0.48 (DRY) of the total rainfall over the same period. In 2011, ET accounted for a greater proportion of total rainfall at all sites, where total ET corresponded to 0.80 (WET), 0.72 (INT), and 0.72 (DRY) of total rainfall.

When only periods of overlapping, high quality, non gap-filled data are considered, the same general trends exist (Fig. 2-3). When simple error analysis was applied to the data set (Eq. 7), we determined that, in 2010, ET at the WET site was significantly greater than the other two sites, whereas ET at the DRY site was less than at the INT site (Fig. 2-3). While ET at both WET and DRY sites was different from INT, the magnitude of the difference was on the order of five times greater at the WET site. In 2011, the relatively large differences in mid growing season ET between the WET and other two sites (Fig. 2-2) resulted in significantly different cumulative totals over that period. However, later in the growing season, where daily ET values were similar, the accumulation of random error resulted in there being no net significant difference in the cumulative total ET. Because the fundamental atmospheric controls on ET (i.e., incoming solar radiation and D) were the same between sites, the differences in surface radiative, thermal, and biophysical properties were examined to explain the differences in ET between sites, where significant.

2.4.2.2 Net radiation

Despite the potential for differences in surface radiative properties between sites, the difference in half-hourly average net radiation at each site was small. In order to investigate the significance of potential differences, a simple residual analysis was carried out for each unique site combination. Based on the Kolmogorov-Smirnov test, all three residual R_n -pairs were non-normally distributed ($p \ll 0.01$; $D = \{0.190, 0.140, 0.215\}$; $n = \{15131, 16320, 16273\}$), where there tended to be a strong clustering of residuals about zero, with relatively infrequent yet large residuals (Fig. 2-4). Due to the non-normality of

the residuals, the Wilcoxon signed rank test was used to determine whether the distributions had a zero median. As a result of a lack of symmetry in the residual distributions, all residual R_n -pairs had medians significantly different from zero ($p < 0.01$). However, in absolute terms, the median residuals were relatively small (-5.0, -3.4, 0.49), with corresponding mean absolute deviations of 30.6 W m^{-2} , 28.9 W m^{-2} , and 29.1 W m^{-2} and root mean square errors of 57.4 W m^{-2} , 44.1 W m^{-2} , and 57.7 W m^{-2} (WET-INT; WET-DRY; and INT-DRY). The results indicate that the median half-hourly $R_{n,\text{wet}}$ was less than the other two sites.

It is important to note that these differences are based on half-hourly measured values which are susceptible to small variations in local apparent cloud cover. Differences in cumulative R_n were tested by assuming only random error in R_n measurements, where the sum of square errors was generated from the estimated random error associated with each measurement (*cf.* Moncrieff *et al.*, 1996). A conservative random error estimate equal to the midday flux value was used. If we treat the cumulative sum as a mean, when summed over the growing season there was no significant difference in cumulative R_n between the INT and DRY sites (Table 2-2), while $R_{n,\text{wet}}$ was only significantly less than the other sites in 2010 (2010: $p = 0.03$, $n = 8303$; 2011: $p = 0.16$, $n = 8039$). Integrated across daily or larger time scales, we can assume the differences in incoming solar radiation and the radiative sky temperature are negligible given the close proximity of the three study sites. As such, the differences in net radiation between sites are most likely attributed to surface albedo and/or the radiative temperature of the surface.

2.4.2.3 Albedo

Due to the strong variation of albedo with the angle of incident solar radiation, average values were calculated based on measurements within 2 hr of solar noon. During the 2011 growing season, daily variability of albedo was relatively small at the WET site, where a significant positive trend ($p < 0.01$, $n = 148$) was evident throughout the year (Fig. 2-5). In contrast, both INT and DRY had greater short-term variability, where a small negative and non significant trend was apparent over the growing season for INT ($p = 0.02$, $n = 140$) and DRY ($p = 0.04$, $n = 148$) respectively. Due to mid-season equipment problems with the downwelling shortwave radiometer in 2010, full growing season albedo was not available. However, average midday albedo at the WET site was 0.21 and 0.15 in the early and late growing season of 2010, compared to 0.13 and 0.17 in 2011. The change in albedo over the same period was small for both the INT (2010: 0.23 and 0.21; 2011: 0.21 and 0.21) and DRY sites (2010: 0.22 and 0.19; 2011: 0.20 and 0.21).

2.4.2.4 Long-wave radiation

All else being equal, a simple radiation balance approach suggests that a lower average albedo, such as that of the WET site, will be balanced by a higher surface temperature, and thus greater outgoing long-wave radiation. The magnitude of the daily average net long-wave radiation (L_{net}) was comparatively high at the WET site, such that the slope of the relation between $L_{net,WET}$ and $L_{net,DRY}$ ($p < 0.01$, slope \pm SE = 1.33 ± 0.034 , $n = 275$) was significantly greater than a 1:1 ratio (Fig. 2-6). The degree of correlation of $L_{net,DRY}$ with $L_{net,WET}$ was only somewhat lower ($R^2 = 0.841$) than with $L_{net,INT}$ ($R^2 = 0.966$). In addition to the strong linear relation between $L_{net,INT}$ and $L_{net,DRY}$

over both growing seasons, the slope of the relation ($p = 0.3034$, slope \pm SE = 1.01 ± 0.006 , $n = 276$) was not significantly different from 1:1. These results lump both day and nighttime measurements, as well as any changes throughout the season. Qualitatively, in both study years there was no strong seasonal trend in the difference in L_{net} between the INT and DRY sites, nor were there frequent large half-hourly differences (RMSE = 7.5 W m^{-2} , MAD = 4.2 W m^{-2}). The magnitude of half-hourly differences between $L_{\text{net,WET}}$ and $L_{\text{net,DRY}}$ were greater (RMSE = 35.1 W m^{-2} , MAD = 25.5 W m^{-2}), but the difference was largely attributable to daytime (RMSE = 50.1 W m^{-2} , MAD = 38.7 W m^{-2}) versus nighttime measurements (RMSE = 23.3 W m^{-2} , MAD = 18.1 W m^{-2}). Based on the Stefan-Boltzman law, differences in L_{net} between sites are related to the surface temperature given their close proximity to one another. Although the surface radiative temperature integrates both the canopy and peat surface temperature, in the absence of canopy temperature measurements, differences in peat temperature measured at a depth of 0.01 m provide a qualitative indirect comparison. For simplicity, we focus here on the differences in near-surface temperature between the WET and DRY sites. Again, the difference in half-hourly values was separated by day ($K_{\text{ex}} > 100 \text{ W m}^{-2}$) and nighttime ($K_{\text{ex}} < 10 \text{ W m}^{-2}$), where K_{ex} is the modeled clear-sky incoming short-wave radiation over the growing season. WET hummock temperatures were higher compared to the DRY site with a mean daytime and nighttime difference (\pm STDV) of $3.0 \pm 2.7^\circ\text{C}$ and $5.3 \pm 2.3^\circ\text{C}$, respectively in 2010, and similarly for 2011: $4.5 \pm 2.1^\circ\text{C}$; and $4.1 \pm 3.1^\circ\text{C}$. In comparison to the mean difference in hummock temperatures, the difference in near-surface hollow temperatures between the WET and DRY sites tended to be smaller during both the day

(2010: 1.9 ± 2.2 °C; and 2011: 0.7 ± 2.1 °C) and night (2010: 0.0 ± 2.0 °C; and 2011: 0.7 ± 1.7 °C).

2.4.2.5 Ground heat flux

Differences in peat thermal properties between sites and microforms associated with θ can have a strong influence on ground heat flux (G) where, for example, higher average near-surface θ at the WET site should lead to higher thermal admittance and a greater partitioning to G . As a result of the relatively small microtopographic variation and WTD, near-surface $G_{WET,hum}$ was consistently greater than $G_{INT,hum}$ and $G_{DRY,hum}$, with values similar to $G_{WET,hol}$. As a result, average midday G_{WET} was higher compared to the other sites (Fig. 2-7). $G_{INT,hum}$ and $G_{DRY,hum}$ were numerically similar since they were consistently dry throughout both study years, yet they were significantly different as a result of near-surface $\theta_{DRY,hum}$ being consistently lower while having similar temperature profiles. Overall, when the proportion of hummocks and hollows was factored in, a greater proportion of R_n was partitioned to G_{INT} than G_{DRY} . Overall, the energy available (R_a) for turbulent fluxes is the remainder of R_n which is not consumed by G (Table 2-2). The resulting cumulative daytime R_a over the growing season was $1.63 \cdot 10^3$ MJ, $1.83 \cdot 10^3$ MJ, and $1.86 \cdot 10^3$ MJ for the WET, INT, and DRY sites over 2010. Similarly, the corresponding values for 2011 were $1.77 \cdot 10^3$ MJ, $1.90 \cdot 10^3$ MJ, and $1.92 \cdot 10^3$ MJ. These results indicate that in both study years, there was less available energy for turbulent fluxes at the WET site. Therefore, in order to have higher ET at the WET site, partitioning to LE must be disproportionately greater than the relative differences in R_a between sites.

2.4.2.6 Energy partitioning

There was a relatively large range of variability in daily energy partitioning across all sites in both study years, where the ratio of H to LE (β) was calculated based on the sum of daytime flux values. Using a 7-day running average, distinct trends emerge from the data (Fig. 2-8). In 2010, β was fairly distinct at all three sites where the WET site tended to have the lowest average β , whereas the DRY site had the highest average β , with the INT site taking on intermediate values. However, in 2011, there was a much closer correspondence between the running average β at the WET and INT sites. While, β ratio values were not available during the early 2011 growing season at the DRY site due to instrument failure, during the mid growing season, β tended to be higher at the DRY site, with average values becoming more similar towards the end of the growing season. Independent of the differences between sites, there was a common seasonal trend in 2010, where β values tended to decrease towards mid growing season and then remained relatively stable. A muted version of the same early season trend occurs in 2011, where average mid to late growing season β values increased progressively, though only by a small amount.

2.4.3 Controls on Evapotranspiration

2.4.3.1 Resistance

Under near-neutral stability, the linear relation (\pm SE) between u^*/k and u_z (Eq. 5) yielded the following estimates of z_0 for 2010: WET_{z0} = 0.052 \pm 0.003; INT_{z0} = 0.065 \pm 0.027; DRY_{z0} = 0.11 \pm 0.01 and 2011: WET_{z0} = 0.062 \pm 0.009; INT_{z0} = 0.078 \pm 0.013; and DRY_{z0} = 0.079 \pm 0.06. In addition to the data on average microtopographical

variation, estimates of z_0 suggest that the WET site was less aerodynamically rough compared to the other sites. All else being equal, this would imply greater aerodynamic resistance to evaporative losses at the WET site. However, when the distributions of measured wind speed are considered, the average wind speed value was ~26% higher at the WET site compared to the other sites in both study years. As a result of the negative correlation between wind speed and r_a , median midday $r_{a,WET}$ was often significantly less than $r_{a,INT}$ and $r_{a,DRY}$ ($p \ll 0.01$) as a result of small standard error estimates, with the exception of $r_{a,WET}$ and $r_{a,INT}$ in 2010 ($p = 0.08$). Nevertheless, median daytime values within sites and between years were fairly similar ($r_{a,WET} - 55.5 \text{ s m}^{-1}$, 54.2 s m^{-1} ; $r_{am,INT} - 56.5 \text{ s m}^{-1}$, 52.2 s m^{-1} ; and $r_{am,DRY} - 57.5 \text{ s m}^{-1}$, 58.2 s m^{-1}).

Despite the differences in r_a being statistically significant, the small absolute difference between sites and years would have a small effect on differences in total ET. The variability in r_s between sites, however, tended to be greater compared to r_a . Overall, if we consider median daytime r_s values between sites and years, $r_{s,WET}$ was 42.3 s m^{-1} and 44.3 s m^{-1} , $r_{s,INT}$ was 55.2 s m^{-1} and 42.3 s m^{-1} , and $r_{s,DRY}$ was 87.3 s m^{-1} and 74.3 s m^{-1} for 2010 and 2011, respectively. Qualitatively, r_s at all sites trended downwards during the 2010 growing season, while only the WET site varied seasonally in 2011, with a slight increase towards the end of the growing season. Using a simple linear regression, all negative trends in 2010 were significantly different from zero ($p \ll 0.01$). In 2011 only $r_{s,WET}$ had a slope significantly different from zero ($p \ll 0.01$), whereas $r_{s,INT}$ and $r_{s,DRY}$ did not ($p_{INT} = 0.449$ and $p_{DRY} = 0.02$). A Jarvis-type phenomenological model for stomatal resistance (r_{st}) is typically written as a function of solar radiation, D , and some metric of

water availability. Given an appropriate scaling factor for LAI, r_s is related to r_{st} and peat surface resistance. Since incoming solar radiation does not vary greatly between sites, the relation between r_s and D was investigated using equation (Eq. 6). Comparing the two growing seasons, the relation between r_s and D only changed appreciably at the WET site where bin-averaged r_s values shifted higher for most D classes in 2011 (Fig. 2-9). In both growing seasons, bin-averaged r_s values were often highest at the DRY site, where based on the standard error estimates, the difference was only significant between the WET and DRY sites in 2010. Overall, the difference between the WET and INT sites was less distinct, where only r_s in low D classes were significantly different in 2010. The D - r_s relation only tends to increase at low D and remains relatively constant over a range of D classes. The relative insensitivity of r_s to D would suggest that the sites are decoupled from atmospheric demand. The Jarvis-McNaughton decoupling coefficient (Ω) can be used to investigate the degree to which ET is linked to D through strong turbulent mixing (low Ω values) or R_a (high Ω values). Broadly, all three sites have high Ω -values in both study years, where median Ω_{WET} was 0.83 and 0.79, Ω_{INT} was 0.76 and 0.80, and Ω_{DRY} was 0.71 and 0.73. The sites exhibit variable seasonal trends in Ω , where at the WET site Ω tended to increase early in the growing season to a mid-summer high. In 2010, Ω remained high until the end of the growing season, while in 2011 Ω followed more of a parabolic trend by decreasing gradually from the mid-summer high. The trend in Ω for both INT and DRY sites in both study years more closely resembled that of the WET site in 2011, with a shallow seasonal parabolic trend.

2.4.3.2 Water table depth

Because WTD integrates the variable behavior of hummocks versus hollows, and *Sphagnum* versus vascular vegetation it was chosen as a simple metric to investigate the effect of moisture availability on ET. ET was first normalized by potential ET (PET) so that the seasonal effect of changing R_a was removed (Fig. 2-10). Overall given the magnitude of standard error estimates, ET/PET did not tend to vary significantly over the range of measured WTD for all sites over both growing seasons. Qualitatively, ET/PET appeared to be more responsive to WTD class in 2010, where values decreased slightly when WTD was below the average peat surface. In 2011, however, there was no apparent trend with WTD. In 2010, each site had a distinct modal peak in the WTD distribution towards the respective high ends on the WTD distributions, whereas the WTD distributions were relatively broad and flat in 2011. In 2010, this limited direct comparison of the ET/PET vs. WTD relation over the same WTD classes. In 2011, comparing the region of overlap between the WET and INT sites, ET/PET tended to be lower for INT. The same relation was investigated but with wet canopy conditions removed, where the vascular canopy was assumed to be wet during and for several hours following rainfall events. The same general patterns exist for dry canopy conditions in both study years.

2.5 Discussion

2.5.1 Evapotranspiration

A direct comparison of peatland ET rates between studies is problematic due to differences in hydrology (*e.g.* fen *v.* bog), vegetation type (*e.g.* sedge *v.* *Sphagnum* dominated or treed *v.* open), growing season R_n associated with latitude, and prevailing synoptic weather conditions. In a mesocosm study, total ET from fen plots was found to be greater compared to bog plots over the snow-free season (Bridgham *et al.*, 1999), where the difference was largely associated with the lack of *Sphagnum* cover in the fen plots and low early-season ET. This is in contrast to our study sites which all have near-total groundcover by *Sphagnum*. Synoptic weather conditions can play an important role where, for example, coastal peatlands tend to have relatively low ET regardless of WTD due to small vapour gradients associated with the low D of offshore winds (Sottocornola and Kiely, 2010; Liljedahl *et al.*, 2011). Thus, comparing *Sphagnum*-dominated peatlands of a similar latitude and general synoptic weather conditions, maximum ET at our sites were similar to a northern Minnesota open fen (4.8 mm d^{-1} – Kim and Verma, 1996) and a southern Ontario bog (4 to 5 mm d^{-1} – Lafleur *et al.*, 2005).

In peatlands, R_n is often the dominant control on ET, however there are physiological limitations to transpiration imposed by vascular vegetation due to the response of r_s to D (Humphreys *et al.*, 2006) particularly as vascular LAI and canopy height increases. A strong positive correlation between ET and R_n has been shown on both a daily (Sottocornola and Kiely, 2010; Wu *et al.*, 2010) and seasonal (Brummer *et al.*, 2012) timescale for peatland sites. Moreover, Sonntag *et al.* (2010) demonstrated

that R_n explained twice the variance in ET compared to D at a minerotrophic fen. Given our high Ω values, the strong control of R_n on ET was also evident at our study sites. However, because the WET site had lower R_n compared to the other two sites, and D was the same across our sites due to their close proximity to one another, these controls on ET cannot explain the differences observed, particularly during the 2010 growing season.

2.5.2 Albedo and Surface Temperature

Although R_n is similar between sites, differences in surface albedo which is linked to surface wetness may affect surface temperature, and thus may help to explain the differences in ET between our study sites. In the absence of disturbance, surface albedo at a northern boreal fen has been shown to vary in response to leaf phenology, ranging between 0.09 and 0.18 during the growing season (Lafleur *et al.*, 1997). A similar growing season trend is reported by Kellner (2001) for a Swedish bog, but with albedo being on average 0.01 lower on wet versus dry days. Moreover, a qualitative relation between albedo and peat wetness was suggested for another bog in Central Sweden where daily albedo was shown to gradually increase over the growing season from 0.12 to 0.17 as the peat progressively dried (Phersson and Pettersson, 1997). Although plant phenology could play a role in the seasonal development of albedo at the WET site, 2010 albedo data suggests WTD is a more important factor. In particular, due to the relatively low albedo of open water (Oke, 1987), ponding in hollows would result in a lower albedo at the WET site; where ponding area for our sites could be estimated from WTD and the proportion of hummocks and hollows. Average early and late 2010 growing season albedo values coincided with a WTD trend that was initially low and remained high

during the mid and late growing season. In 2011, the growing season trend in albedo at the WET site qualitatively corresponds with a decreasing WTD, where early season WTD was above the mean peat surface. Due to the large proportion of the WET site covered by hollows, a high WTD would coincide with significant surface ponding. This is in contrast to the INT and DRY sites where the WTD was consistently below the mean peat surface throughout the study period, and where hollows represent a decreasing proportion of the surface. There was no trend in surface albedo at the INT or DRY site that could be clearly linked to vascular plant phenology or WTD, where the higher average albedo at the INT and DRY sites is consistent with a lack of ponding at these two sites. Despite similar covariance in albedo at the INT and DRY sites, there was no definitive correlation with surface wetness or rainfall events. Although there was no apparent trend in albedo at the INT or DRY sites associated with WTD, the relatively stable $\theta_{-0.05\text{ m}}$ for hummocks suggests that *Sphagnum* was not desiccating, thus there was likely no whitening response as has been observed by other studies (McNeil and Waddington, 2003).

Although a lower albedo does not necessarily lead to greater available energy for turbulent fluxes, all else being equal, a lower albedo will result in a higher surface temperature. If we assume that the difference in average incoming long-wave radiation is negligible between sites when integrated over a daily time step, we can infer that differences in daily net long-wave radiation can be attributed to differences in outgoing long-wave radiation (*i.e.* surface temperature). The lower average daytime net long-wave radiation at the WET site implies a higher integrated surface temperature. Higher near-

surface (0.01 m depth) peat temperatures were also measured in both hummocks and hollows at the WET site which would help contribute to the apparent higher surface radiative temperature at the WET site. The degree and importance of surface heating on energy partitioning depends on the thermal conductivity of the surface and the LAI of the vascular canopy. For a saturated high porosity surface, such as in peatlands, a relatively large portion of additional energy associated with a lower albedo will be used in heating the soil profile due to the high thermal admittance of water versus air, thus increasing potential evaporation due to the effect of temperature on the saturation vapour pressure. Due to the dependence of G on near-surface θ , all else being equal, peatlands with a greater proportion of hummocks, or conversely, peatlands with greater microtopographic variation will tend to have lower average G . At both the INT and DRY sites, the effect of the contrast in surface wetness is apparent in the significant difference in median values ($\alpha = 0.05$) between G_{HUM} and G_{HOL} (Fig. 2-7). Kellner (2001) similarly showed higher G as a proportion of R_n in hollows versus hummocks. In comparison, the small average microtopographic variation between hummocks and hollows at the WET site lead to no significant difference in G due to similar high θ in both microforms. When combined with a slightly lower R_n , the higher average G of the WET site leads to lower available energy for turbulent fluxes at the WET site.

2.5.3 Energy Partitioning

Differences in energy partitioning between the study sites cannot be explained by higher average midday near-surface temperature at the WET site alone using a ‘big-leaf’ model. Assuming the surface vapour pressure is near saturation, all else being equal, a

higher surface temperature would increase β in favour of the sensible heat flux. Despite low values of $\theta_{-0.05\text{ m}}$, the assumption of near-saturated vapour pressure at the surface may not be unreasonable for hummocks at the INT and DRY sites. Over the course of the growing season, daily $\theta_{INT, hum, -0.05}$ and $\theta_{DRY, hum, -0.05}$ did not change substantially at the daily time step in response to evaporative losses. Furthermore, the decrease in $\theta_{INT, hum, -0.05}$ and $\theta_{DRY, hum, -0.05}$ in 2011 with an increasing WTD was only slight. This suggests that either: (i) a negligible amount of water is being lost from the moss surface; (ii) capillary transport is able to replenish evaporative losses at a daily time step; or (iii) an extreme hydrological gradient exists between the moss surface and the $\theta_{-0.05\text{ m}}$ measurement level. Differences in energy partitioning can perhaps be better explained by dual-source models where the lower LAI at the INT and DRY sites limit transpiration in comparison to the WET site, while increasing the relative contribution of moss surface evaporation. Evaporative losses from the *Sphagnum* surface have been shown to be relatively high given an LAI of 0.4 to 0.7 $\text{m}^2\text{ m}^{-2}$ (Kim and Verma, 1996), but the contribution of moss evaporation to total ET is reduced when surrounded by vascular vegetation (Heijmans *et al.*, 2004) where our LAI values are much higher than those reported by Kim and Verma (1996). Moreover, despite the potential small contribution from the moss surface given our relatively high LAI values, land surface schemes such as CLM include a moisture dependent empirical term to limit surface evaporation which is meant to be a surrogate for molecular diffusion in the unsaturated zone (Lawrence *et al.*, 2011). Thus, we would expect that the greater proportion of hummocks and low near-surface θ at the INT and DRY sites would serve to further limit total moss evaporation, and thus measured ET.

2.5.4 Aerodynamic and Surface Resistance

In general, our z_0 values are higher than the range of values of 0.02 – 0.03 reported for a Swedish bog (Kellner, 2001), and are at the higher end of the range reported for a Siberian bog (Shimoyama *et al.*, 2004). In a west Siberian bog, a qualitative relation was shown to exist between vascular development and increasing z_0 which, all else being equal, would enhance ET (Shimoyama *et al.*, 2004). However, because the average microtopographic variation is different between our sites, it is difficult to separate the effect of vascular vegetation and microtopography on z_0 . Nevertheless, the difference in the magnitude of z_0 is proportional to the difference in microtopographic variation. The lower surface roughness of the WET site corresponds with r_a values which are higher across wind speed classes. In the absence of any other resistance term, the higher r_a would lead to lower ET at the WET site. However, in addition to the shading effect of vascular vegetation, a higher LAI would increase resistance to moss evaporation by reducing near-surface turbulent transport (Campbell and Williamson, 1997; Heijmans *et al.*, 2001), thus counteracting increases in transpiration.

Although it has been suggested that the similarity in ET between peatland sites is the result of similarity in r_s - D relations despite differences in vegetation types (Humphreys *et al.*, 2006), our results suggest that the difference in peatland ET between sites is the result of the variable response of r_s to D despite having the same vegetation community composition. Again, the dependence of r_s on D using Eq. 6 should be noted. Since there are no large differences in other components of the combination equation, r_s

is forced to correlate with difference in ET between sites. Nevertheless, a number of peatland studies show a strong response of r_s to D at low D , whereas r_s tends to be less variable at higher D . Our results show a similar pattern where the average r_s only varies significantly below a daily average D of 0.5 kPa. The difference in average r_s may be related to differences in r_{st} , which have been shown to vary between plant functional groups (Korner *et al.*, 1979). While each site has the same basic community composition, the correlation between microtopography and plant functional group results in a greater proportion of graminoids at the WET site, and shrubs at the INT and DRY sites. Admiral and Lafleur (2007) show that shrub species on a raised bog generally have higher stomatal resistance compared to other wetland species. A higher stomatal resistance combined with lower LAI at the INT and DRY sites would have a compound effect in reducing r_s . In addition to the potential effect of variable r_{st} between plant function groups, the $r_s - D$ relation does not account for any temporal relation between WTD, LAI, and D . D has a strong seasonal progression with low average daily values in the winter and high values in mid-summer due to the non-linear positive correlation with temperature. Therefore, if water availability influences r_s , then it is not simply the degree of water availability that will affect r_s , but also the temporal sequence of variability due to the regular seasonal progression of D .

2.5.5 *Evapotranspiration and Water Table Position*

The relation between WTD and ET in peatlands was supported by earlier research (Ingram, 1983), and has been a continuing area of study, in part, due to the relative complexity of modelling physical peat hydrology. However, due in part to the non-linear

relation between WTD and θ (Kellner and Halldin, 2002), and heterogeneity in peat surface dynamics (Waddington *et al.*, 2010), there remains no definitive link between ET and WTD in peatlands. For example, a number of studies have demonstrated that there is no significant relation between ET and WTD when ET is normalized by PET or R_n (Shimoyama *et al.*, 2004; Humphreys *et al.*, 2006; Parmentier *et al.*, 2009; Sottocornola and Kiely, 2010; Wu *et al.*, 2010). However, some of these relations were developed for a relatively shallow WTD (*i.e.* Sottocornola and Kiely, 2010; Wu *et al.*, 2010) while others were in peatlands with near-surface θ retention that was uncharacteristically high (*i.e.* Parmentier *et al.*, 2009) compared to undisturbed *Sphagnum*-dominated peatlands. Other studies, however, have shown a weak to moderate relation between ET and WTD (Kim and Verma, 1996; Lafleur *et al.*, 2005; Sonnentag *et al.*, 2010), where for a deep WTD, a threshold response may exist which corresponds to the rooting depth of woody vegetation.

In general, our results suggest there was no simple univariate relation between ET/PET and WTD. For the WET site, ET/PET was greater when WTD was above the mean peat surface, but only in 2010. This implies that either WTD (as a proxy for water availability) is only a short-term control on ET that depends on when drying occurs within a growing season, or that WTD was simply better correlated with another ET control in 2010. Given the length of time since disturbance, we would expect that the rooting depth at our sites would be adapted to the average or typical range of WTD (*cf.* Mitsch and Grosselink, 2000). Consequently, the threshold response of ET/PET to WTD reported by Lafleur *et al.* (2005) may imply that a threshold response of ET/PET to WTD

is predicated upon large inter-annual differences in WTD, rather than due to longer term persistent dry conditions. Under dry conditions, vascular vegetation will respond with increased fine-root production at depth, and a greater proportion of resources allocated to biomass production in stems versus leaves (Murphy and Moore, 2010). Greater fine root production at depth suggests the mechanism which limits any relation between ET/PET and WTD for peatlands with high LAI. Moreover, the lower LAI at the INT and DRY sites, as well as the relatively high PAI:LAI ratio at the DRY site could be the result of past changes in resource allocation between woody and herbaceous structures in response to drying. Therefore the WTD may have an indirect control on ET at our sites through long-term changes in LAI.

2.6 Conclusions

Overall, despite large differences in WTD, all sites experienced similar energy partitioning with an average β ratio less than one. Significant differences in albedo were likely the result of the timing of shallow WTD (*i.e.* ponding), but where lower albedo at the WET site was balanced by greater long-wave losses due in part to high nighttime surface temperatures, particularly in hollows. Given the similarity in ET between sites, particularly in 2011, and the relative insensitivity of ET/PET to WTD fluctuations, one can infer a degree of resilience in peatland ecosystems to long-term drying under projected future climate change. Despite the relative insensitivity of r_s to the typical midday range in average D and high Ω associated with the relatively low z_0 of peatland microtopography and short vascular plants, higher D will result in greater ET loss from peatlands and lead to an increased WTD (Roulet *et al.*, 1992). This, however, ignores

potential long-term responses of microtopography, shifts in the relative abundance of plant functional groups, or changes in LAI. From the standpoint of vascular vegetation, neither short-term changes in WTD nor near-surface θ are likely to systematically limit transpiration due to the long-term response of rooting depth and fine root growth to average WTD, but where long-term changes in WTD will affect maximum ET through the impact on LAI.

In comparing ET from the WET to INT and DRY sites, our results suggest that the potential long-term effect of WTD on LAI should be incorporated into future land surface schemes since this appears to be one of the primary mechanisms which serves to limit ET. Moreover, microtopography, particularly as it correlates to plant functional groups, needs to be included since, in addition to LAI, differences in r_{st} provides the mechanism for explaining difference in r_s where LAI is relatively high. Despite our relatively large LAI values, the results of our study imply a need for a greater understanding of the limitations on water transport processes in the moss layer, particularly as it relates to moss resistance, where we observed that dry hummocks were able to avoid complete desiccation despite low WTD and high daily ET. Vertically-stratified representations of different peatland vegetation layers in process ecosystem models (*e.g.*, Sonnentag *et al.*, 2008; Lawrence *et al.*, 2011) can help to elicit whether moss evaporation is limited by vascular canopy properties or moisture supply from the underlying peat, where alternative empirical formulations can be used to better understand moss resistance.

2.7 Acknowledgements

This research was funded by a Discovery Grant and Discovery Accelerator Supplement from the Natural Science and Engineering Research Council of Canada to JMW and by the U.S. Department of Agriculture, grant No. 0220341 to TGP. Additional financial support was provided by the U.S. Department of Energy's Office of Science (BER) through the Midwestern Regional Center of the National Institute for Climatic Change Research at Michigan Technological University. We would like to thank the U.S. Fish and Wildlife Service for permitting access to Seney National Wildlife Refuge, and the staff at SNWR for their kind accommodation. We also thank the two anonymous reviewers who provided many useful comments and valuable suggestions which helped to improve the manuscript. Finally, we would like to thank John Hribljan for his invaluable site selection, as well as Jenna Falk and Reyna Peters for their field assistance.

2.8 References

- Admiral, S.W., Lafleur, P.M., Roulet, N.T. 2006. Controls on latent heat flux and energy partitioning at a peat bog in eastern Canada. *Agric. For. Meteorol.* 140, 308-321.
- Admiral, S.W., Lafleur, P.M., Roulet, N.T. 2007. Partitioning of latent heat flux at a northern peatland. *Aquatic Botany.* 86, 107-116.
- Albert, D.A., 1995. Regional landscape ecosystems of Michigan, Minnesota, and Wisconsin: a working classification. U.S. Department of Agriculture technical report NC-178.
- Baldocchi, D., Valentini, R., Running, S., Oechel, W., Dahlman, R., 1996. Strategies for measuring and modeling carbon dioxide and water vapour fluxes over terrestrial ecosystems. *Global Change Biol.* 2, 159-168.
- Baldocchi, D.D., Vogel, C.A., Hall, B., 1997. Seasonal variation of energy and water vapor exchange rates above and below a boreal jack pine forest canopy. *J. Geophys. Res.* 102, 28 939- 28 951.

- Baldocchi, D.D., Kelliher, F.M., Black, T.A., Jarvis, P., 2000. Climate and vegetation controls on boreal zone energy exchange. *Global Change Biol.* 6 (Suppl. 1), 69-83.
- Bridgham, S.D., Pastor, J., Updegraff, K., Malterer, T.J., Johnson, K., Harth, C., Chen, J., 1999. Ecosystem control over temperature and energy flux in northern peatlands. *Ecol. Appl.* 9 (4), 1345-1358.
- Brummer C., Black, T.A., Jassal, R.S., Grant, N.J., Spittlehouse, D.L., Chen, B., Nesic, Z., Amiro, B.D., Arain, M.A., Barr, A.G., Bourque, C.P.-A., Coursolle, C., Dunn, A., Flanagan, L.B., Humphreys, E.R., Lafleur, P.M., Margolis, H.A., McCaughey, J.H., Wofsy, S.C., 2012. How climate and vegetation type influence evapotranspiration and water use efficiency in Canadian forest, peatland and grassland ecosystems. *Agric. For. Meteorol.* 153, 14-30.
- Campbell, D.I., Williamson, J.L., 1997. Evaporation from a raised peat bog. *J. Hydrol.* 193 (1-4), 142-160.
- Casselmann T., 2009. Seney National Wildlife Refuge Comprehensive Conservation Plan. United States Fish and Wildlife Service.
- Chapin, F.S., McGuire, A.D., Randerson, J., Pielke, R., Baldocchi, D., Hobbie, S.E., Roulet, N., Eugster, W., Kasischke, E., Rastetter, E.B., Zimov, S.A., Running, S.W., 2000. Arctic and boreal ecosystems of western North America as components of the climate system. *Global Change Biol.* 6 (Suppl.1), 211-223.
- Chivers, M.R., Turetsky, M.R., Waddington, J.M., Harden, J.W., McGuire, A.D., 2009. Effects of experimental water table and temperature manipulations on ecosystem CO₂ fluxes in an Alaskan Rich Fen. *Ecosystems* 12, 1329-1342.
- Comer, N.T., Lafleur, P.M., Roulet, N.T., Letts, M.G., Skarupa, M., and Verseghy, D.L., 1999. A Test of the Canadian Land Surface Scheme (CLASS) for a Variety of Wetland Types. *Atmos. Environ.* 38, 161-179.
- Den Hartog, G., Neumann, H.H., King, K.M., Chipanshi, A.C., 1994. Energy budget measurements using eddy-correlation and Bowen-ratio techniques at the Kinosheo lake tower site during the northern wetlands study. *J. Geophys. Res. D. Atmos.* 99, 1539-1549.
- Ducoudre, N.I., Laval, K., Perrier, A., 1993. SECHIBA, A new set of parameterizations of the hydrologic exchanges at the land atmosphere interface within the LMD atmospheric general-circulation model. *J. Clim.* 6, 248-273.
- Eaton, A.K., Rouse, W.R., 2001. Controls on evapotranspiration at a subarctic sedge fen. *Hydrol. Processes* 15, 3423-3431.
- Eugster, W., Rouse, W.R., Pielke, R.A., McFadden, J.P., Baldocchi, D.D., Kittel, T.G.F., Chapin, F.S., Liston, G.E., Vidale, P.L., Vaganov, E., Chambers, S., 2000. Land-atmosphere energy exchange in Arctic tundra and boreal forest: available data and feedbacks to climate. *Global Change Biol.* 6 (Suppl.1), 84-115.

- Foken, T., Wichura, B., 1996. Tools for quality assessment of surface-based flux measurements. *Agric. For. Meteorol.* 78, 83-105.
- Foken, T., Gockede, M., Mauder, M., Mahrt, L., Amiro, B.D., Munger, J.W., 2004. Post-field data quality control. In: Lee X, Massman WJ, Law B (eds.), *Handbook of Micrometeorology: A guide for surface flux measurement and analysis*. Kluwer, Dordrecht, pp. 181-208.
- Frich, P., Alexander, L.V., Della-Marta, P., Gleason, B., Haylock, M., Klein Tank, A.M.G., Peterson, T., 2002. Observed coherent changes in climatic extreme during the second half of the twentieth century. *Climate Research* 19, 193-212.
- Frolking, S., Talbot, J., Jones, M.C., Treat, C.C., Kauffman, J.B., Tuittila, E.S., Roulet, N.T. 2011. Peatlands in the Earth's 21st century climate system. *Environ. Rev.* 19, 371-396
- Gorham E., 1991. Northern peatlands: role in the carbon-cycle and probable responses to climatic warming. *Ecol. Appl.* 1, 182-195.
- Hayward, P.M., Clymo, R.S., 1982. Profiles of water content and pore size in *Sphagnum* and peat, and their relation to peat bog ecology. *Proc. R. Soc. London, Ser. B* 215 (1200), 299-325.
- Heijmans, M.M.P.D., Arp, W.J., Berendse, F., 2001. Effects of elevated CO₂ and vascular plants on evapotranspiration in bog vegetation. *Global Change Biol.* 7, 817-827.
- Heijmans, M.M.P.D., Arp, W.J., Chapin III, F.S., 2004. Controls on moss evaporation in a boreal black spruce forest. *Global Biogeochem. Cycles* 18, GB2004, doi: 10.1029/2003GB002128.
- Heinselman M.L., 1965. String Bogs and Other Patterned Organic Terrain Near Seney, Upper Michigan. *Ecology.* 46(1-2), 185-188.
- Huemrich, K.F., Kinoshita, G., Gamon, J.A., Houston, S., Kwon, H., Oechel, W.C., 2010. Tundra carbon balance under varying temperature and moisture regimes. *J. Geophys. Res.* 115, G000I02
- Humphreys, E.R., Lafleur, P.M., Flanagan, L.B., Hedstrom, N., Syed, K.H., Glenn, A.J., Granger, R., 2006. Summer carbon dioxide and water vapour fluxes across a range of northern peatlands. *J. Geophys. Res.* 111, G04011, doi:10.1029/2005JG000111.
- Ise, T., Dunn, A.L., Wofsy, S.C., Moorcroft, P.R., 2008. High sensitivity of peat decomposition to climate change through water-table feedback. *Nat. Geosci.* 1, 763-766.
- Kaimal, J.C., Finnigan, J.J., 1994. *Atmospheric boundary layer flows: Their structure and measurement*. Oxford University Press, New York, 289pp.

- Kellner, E., 2001. Surface energy exchange and hydrology of a poor *Sphagnum* mire. PhD thesis, Uppsala University, Sweden.
- Kellner E., Halldin, S., 2002. Water budget and surface-layer water storage in a *Sphagnum* bog in central Sweden. *Hydrol. Processes* 16, 87-103.
- Kettridge, N., Baird, A., 2006. A new approach to measuring the aerodynamic resistance to evaporation within a northern peatland using a modified Belanni plate atmometer. *Hydrol. Processes* 20, 4249-4258.
- Kim, J., Verma, S.B., 1996. Surface exchange of water vapour between an open *Sphagnum* fen and the atmosphere. *Boundary-Layer Meteorol.* 79, 243-264.
- Korner, C., Scheel, J.A., Bauer, H., 1979. Maximum leaf diffusive conductance in vascular plants. *Photosynthetica* 13, 45-82.
- Kowalski, K.P., and Wilcox, D.A., 2003. Differences in sedge fen vegetation upstream and downstream from a managed impoundment. *The American Midland Naturalist.* 150(2), 199-220.
- Lafleur, P.M., Rouse, W.R., 1988. The influence of surface cover and climate on energy partitioning and evaporation in a subarctic wetland. *Boundary-Layer Meteorol.* 44, 327-347.
- Lafleur, P.M., Roulet, N.T., 1991. A comparison of evaporation rates from two fens of the Hudson Bay Lowland. *Aquatic Botany* 44, 59-69.
- Lafleur, P.M., McCaughey, J.H., Joiner, D.W., Bartlett, P.A., Jelinski, D.E., 1997. Seasonal trends in energy, water, and carbon dioxide fluxes at a northern boreal wetland. *J. Geophys. Res.*, 102 (D24), 29009-29020.
- Lafleur, P.M., Hember, R.A., Admiral, S.W., Roulet, N.T., 2005. Annual and seasonal variability in evapotranspiration and water table at a shrub-covered bog in southern Ontario, Canada. *Hydrol. Processes* 19, 3533-3550.
- Lawrence, D.M., Oleson, K.W., Flanner, M.G., Thornton, P.E., Swenson, S.C., Lawrence, P.J., Zeng, X.B., Yang, Z.L., Levis, S., Sakaguchi, K., Bonan, G.B., Slater, A.G., 2011. Parameterization improvements and functional and structural advances in version 4 of the Community Land Model. *J. Adv. Earth Syst.* 3, DOI: 10.1029/2011MS000045.
- Lawrence, D.M., Slater, A.G., 2008. Incorporating organic soil into a global climate model. *Clim. Dyn.* 30, 145-160. DOI: 10.1007/s00382-007-0278-1.
- Lee, X., Massman, W.J., Law, B., 2004. *Handbook of Micrometeorology: A guide for surface flux measurement and analysis.* Kluwer, Dordrecht, pp. 181-208.
- Letts, M.G., Roulet, N.T., Comer, N.T., Skarupa, M.R., and Verseghy, D.L., 1999. Parametrization of Peatland Hydraulic Properties for the Canadian Land Surface Scheme. *Atmos. Ocean* 38, 141-160.

- Liljedahl, A.K., Hinzman, L.D., Harazono, Y., Zona, D., Tweedie, C.E., Hollister, R.D., Endstrom, R., Oechel, W.C., 2011. Nonlinear controls on evapotranspiration in arctic coastal wetlands. *Biogeosciences* 8, 3375-3389.
- Lund, M., Christensen, T.R., Mastepanov, M., Lindroth, A., Strom, L., 2009. Effects of N and P fertilization on the greenhouse gas exchange in two northern peatlands with contrasting N deposition rates. *Biogeosciences* 6, 2135-2144.
- Massman, W.J., 2000 A simple method for estimating frequency response corrections for eddy covariance systems. *Agric. For. Meteorol.* 104, 185-198.
- McNeil, P., Waddington, J.M., 2003. Moisture controls on *Sphagnum* growth and CO₂ exchange on a cutover bog. *J. Appl. Ecol.* 40, 354-367.
- Mitsch, W.J., Grosselink, J.G., 2000. *Wetlands*, 3rd ed. John Wiley & Sons, New York, NY.
- Moffat, A.M., Papale, D., Reichstein, M., Hollinger, D.Y., Richardson, A.D., Barr, A.G., Beckstein, C., Braswell, B.H., Chukina, G., Desai, A.R., Falge, E., Gove, J.H., Heimann, M., Hui, D., Jarvis, A.J., Kattge, J., Noormets, A., Stauch, V.J., 2007. Comprehensive comparison of gap-filling techniques for eddy covariance net carbon fluxes. *Agric. For. Meteorol.* 147, 209-232.
- Molder, M., Kellner, E., 2001. Excess resistance of bog surfaces in central Sweden. *Agric. For. Meteorol.* 112, 23-30.
- Moncrieff, J.B., Malhi, Y., Leuning, R., 1996. The propagation of errors in long-term measurements of land-atmosphere fluxes of carbon and water. *Global Change Biol.* 2, 231-240.
- Monteith, J.L., 1973. *Principles of environmental physics*. Edward Arnold, London.
- Monteith, J.L., 1981. Evaporation and surface temperature. *Q. J. R. Meteorol. Soc.* 107, 1-27.
- Murphy, M.T., Moore, T.R., 2010. Linking root production to aboveground plant characteristics and water table in a temperate bog. *Plant and Soil* 336 (1-2), 219-231.
- Oechel, W.C., Vourlitis, G.L., Hastings, S.J., Ault, R.P., Brant, P., 1998. The effects of water table manipulation and elevated temperature on the net CO₂ flux components of Alaskan Coastal Plain tundra to shifts in water table. *J. Geophys. Res.* 115, G00I05.
- Oke, T.R., 1987. *Boundary layer climates*. Routledge, New York.
- Paavalainen, E., Paivanen, J., 1995. *Peatland Forestry: Ecology and Principles*. Springer-Verlag: Berlin, pp.248.
- Paramentier, F.J.W., van der Molen, M.K., de Jeu, R.A.M., Hendriks, D.M.D., Dolman, A.J., 2009. CO₂ fluxes and evaporation on a peatland in the Netherlands appear not affected by water table fluctuations. *Agric. For. Meteorol.* 149, 1201-1208.

- Phersson, M., Pattersson, O., 1997. Energy and water balances of a bog in central Sweden. *Nordic Hydrol.* 28, 263-272.
- Priestley, C.H.B., Taylor, R.J., 1972. On the assessment of surface heat flux and evaporation. *Mon. Weather. Rev.* 106, 81-92.
- Price, J.S., 1991. Evaporation from a blanket bog in a foggy coastal environment. *Boundary-Layer Meteorol.* 57 (4), 391-406.
- Price, J.S., Maloney, D.A., 1994. Hydrology of a patterned bog-fen complex in southeastern Labrador, Canada. *Nordic Hydrol.* 25, 313-330.
- Price, J.S., Edwards, T.W.D., Yi, Y., Whittington, P.N., 2009. Physical and isotopic characterization of evaporation from *Sphagnum* moss. *J. Hydrol.* 369, 175-182.
- Roulet, N., Moore, T., Bubier, J., Lafleur, P., 1992. Northern fens: methane flux and climatic change. *Tellus: Series B* 44 (2), 100-105.
- Shimoyama, K., Hiyama, T., Fukushima, Y., Inoue, G., 2004. Controls on evapotranspiration in a west Siberian bog. *J. Geophys. Res.* 109, D08111, doi: 10.1029/2003JD004114.
- Sonnentag, O., Chen, J.M., Roulet, N.T., Ju, W., Govind, A. 2008. Spatially explicit simulation of peatland hydrology and carbon dioxide exchange: Influence of mesoscale topography. *J. Geophys. Res.* 113, G02005, doi: 10.1029/2007JG000605.
- Sonnentag, O., van der Kamp, G., Barr, A.G., Chen, J.M., 2010. On the relationship between water table depth and water vapor and carbon dioxide fluxes in a minerotrophic fen. *Global Change Biol.* 16, 1762-1776, doi: 10.1111/j.1365-2486.2009.02032.x
- Sottocornola M., Kiely, G., 2010. Energy fluxes and evaporation mechanisms in an Atlantic blanket bog in southwestern Ireland. *Water Resour. Res.* 46, W11524, doi: 10.1029/2010WR009078.
- Stewart, J.B., Thom, A.S., 1973. Energy budgets in pine forest. *Quart. J. Roy. Meteorol. Soc.* 99, 154-170.
- Strack, M., Waddington, J.M. 2007. Response of peatland carbon dioxide and methane fluxes to a water table drawdown experiment. *Global Biogeochem. Cycles* 21, GB1007, doi: 10.1029/2006GB002715.
- Tanner, C.B., Thurtell, G.W., 1969. Anemoclinometer measurements of Reynolds stress and heat transport in the atmospheric surface layer. ECOM 66-G22-F, University of Wisconsin, Madison, Wisconsin.
- Tarnocai, C., 1984. Peat resources of Canada. Land Resource Research Institute, Research Branch, Agriculture Canada, Ottawa, Ontario, Canada.
- Teklemariam, T.A., Lafleur, P.M., Moore, T.R., Roulet, N.T., Humphreys, E.R., 2010. The direct and indirect effects of inter-annual meteorological variability on

- ecosystem exchange at a temperate ombrotrophic bog. *Agric. For. Meteorol.* 150, 1402-1411.
- The MathWorks, Inc., 2009. MATLAB, Version 7.8, MathWorks, Natick, Mass.
- Turetsky, M.R., Kane, E.S., Harden, J.W., Ottmar, R.D., Manies, K.L., Hoy, E., Kasischke, E.S., 2011. Recent acceleration of biomass burning and carbon losses in Alaskan forests and peatlands. *Nat. Geosci.* 4 (1), 27-31.
- Vasander, H., Kettunen, A., 2006. Carbon in boreal peatlands. In: *Boreal Peatland Ecosystems*. Wider RK, and Vitt DH (eds.). Springer-Verlag, Heidelberg, Germany, pp.165-194.
- Verseghy, D.L., McFarlane, N.A., Lazare, M., 1993. CLASS – a Canadian land surface scheme for GCMs, II, Vegetation model and coupled runs. *Int. J. Climatol.* 13, 347-370.
- Vickers, D., Mahrt, L., 1997. Quality control and flux sampling problems for tower and aircraft data. *J. Atmos. Ocean. Technol.* 14, 512-526.
- Waddington, J.M., Kellner, E., Strack, M., Price, J.S., 2010. Differential peat deformation, compressibility, and water storage between peatland microforms: Implications for ecosystem function and development. *Water Resour. Res.* 46, W07538, doi: 10.1029/2009WR008802.
- Walther A., Linderholm, H.W., 2006. A comparison of growing season indices for the Greater Baltic Area. *Int. J. of Biometeorol.* 51: 107-118.
- Webb, E.K., Pearman, G.I., Leuning, R., 1980. Correction of flux measurements for density effects due to heat and water vapour transfer. *Quart. J. Roy. Meteorol. Soc.* 106, 85–100.
- Weltzin, J.F., Bridgman, S.D., Pastor, J., Chen, J., Harth, C., 2003. Potential effects of warming and drying on peatland plant community composition. *Global Change Biol.* 9, 141-151.
- Whittington, P.N., Price, J.S., 2006. The effects of water table draw-down (as a surrogate for climate change) on the hydrology of a fen peatland, Canada. *Hydrol. Processes* 20, 3589-3600.
- Wilcox, D.A., Sweat, M.J., Carlson, M.L., and Kowalski, K.P., 2006. A water-budget approach to restoring a sedge fen affected by diking and ditching. *J. Hydrol.* 320, 501-517.
- Wilczak, J.M., Oncley, S.P., Stage, S.A., 2001. Sonic anemometer tilt correction algorithms. *Boundary-Layer Meteorol.* 99, 127-150.
- Wu, J., Kutzbach, L., Jager, D., Wille, C., Wilmking, M., 2010. Evapotranspiration dynamics in a boreal peatland and its impact on the water and energy balance. *J. Geophys. Res.* 115, G04038.

Wu et al., 2011. Dealing with microtopography of an ombrotrophic bog for simulating ecosystem-level CO₂ exchanges. *Ecol. Modell.* 222, 1038-1047. DOI: 10.1016/j.ecolmodel.2010.07.015.

2.9 Tables

Table 2 - 1: Summary of microtopography and vegetation characteristics across study sites.

Variable	WET	INT	DRY
Avg. height (m) of hummocks (\pm SE) ¹	0.15 (0.01)	0.30 (0.02)	0.41 (0.03)
Proportion of hummocks and hollow ²	0.41 / 0.59	0.52 / 0.48	0.63 / 0.37
pH (\pm SE) ³	4.10 (0.06)	3.77 (0.02)	3.69 (0.01)
LAI ⁴ (m ² m ⁻²) – <i>hummocks</i> (\pm SE)	2.7 (0.18)	1.5 (0.06)	1.9 (0.19)
LAI ⁴ (m ² m ⁻²) – <i>hollows</i> (\pm SE)	2.0 (0.32)	1.9 (0.45)	1.3 (0.04)
Plant Area Index ⁵ (m ² m ⁻²)	2.8 (0.52)	1.9 (0.18)	2.6 (0.27)

¹ – Height based on the difference in measured WT depth for adjacent hummock/hollow pairs at each site (n = 20).

² – Proportion based on a transect survey across orthogonal axes of each site; microtopography classified by relative elevation, slope, and vascular community (n = 249 to 386).

³ – pH based on random sampling of near-surface pore water at each site (n = 7).

⁴ – Leaf area index based on destructive sampling of 0.25 m² hummock and hollow plots (n = 4)

⁵ - Plant area index based on gap light photography of hummock and hollow plots (n = 4)

Table 2 - 2: Summary of average climatological and flux variables for the study area.

Variable	2010	2011
Climatological growing season	DOY: 136 - 306	DOY: 130 - 303
GDD* (total / growing season)	1721 °C / 1567 °C	1601 °C / 1558 °C
Rainfall (total/dry days /avg. dpth)	660 mm / 96 days / 8.2 mm	470 mm / 112 days / 7.1 mm
Total ET 10 ³ MJ m ⁻² (& mm)	WET: 1.03 (417) INT: 0.80 (323) DRY: 0.77 (314)	WET: 0.93 (378) INT: 0.84 (340) DRY: 0.82 (336)
Total R _n (\pm std. dev. †) 10 ³ MJ m ⁻²	WET: 1.70 (0.04) INT: 1.86 (0.04) DRY: 1.86 (0.04)	WET: 1.82 (0.05) INT: 1.92 (0.04) DRY: 1.92 (0.05)
Total G (\pm std. dev. †) 10 ³ MJ m ⁻²	WET: 0.076 (0.002) INT: 0.026 (0.002) DRY: 0.007 (0.001)	WET: 0.065 (0.008) INT: 0.021 (0.006) DRY: 0.010 (0.005)

* Cumulative growing degree days (GDD) were calculated using the method established by the Atmospheric Environment Service, Environment Canada, using a base temperature of 5 °C.

† - The sum of square errors is calculated by assuming each half-hourly measurement has no systematic error and a maximum random error equal to the midday flux value.

2.10 Figures

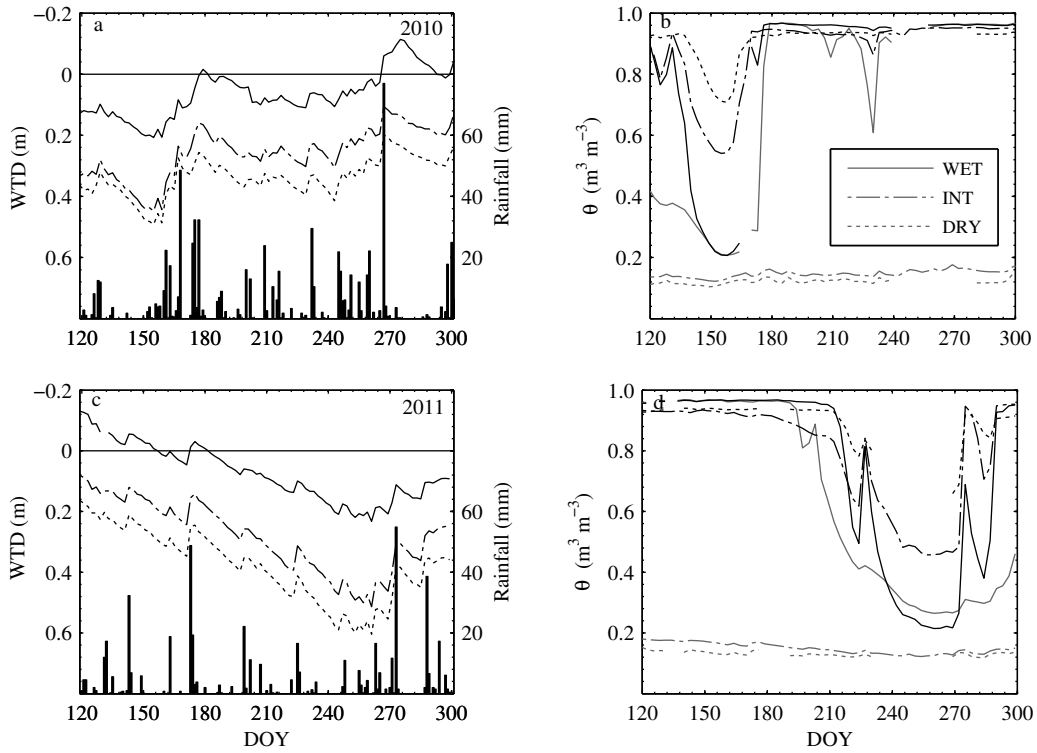


Figure 2 - 1: Daily total rainfall (bars) and water table levels (a and c) for the WET (solid), INT (dash-dot), and DRY (dot) sites. Volumetric water content (three day average shown for clarity) at all three sites (b and d) measured at 0.05 m depth in a representative hummock (grey) and hollow (black) over the 2010 (top) and 2011 (bottom) growing seasons.

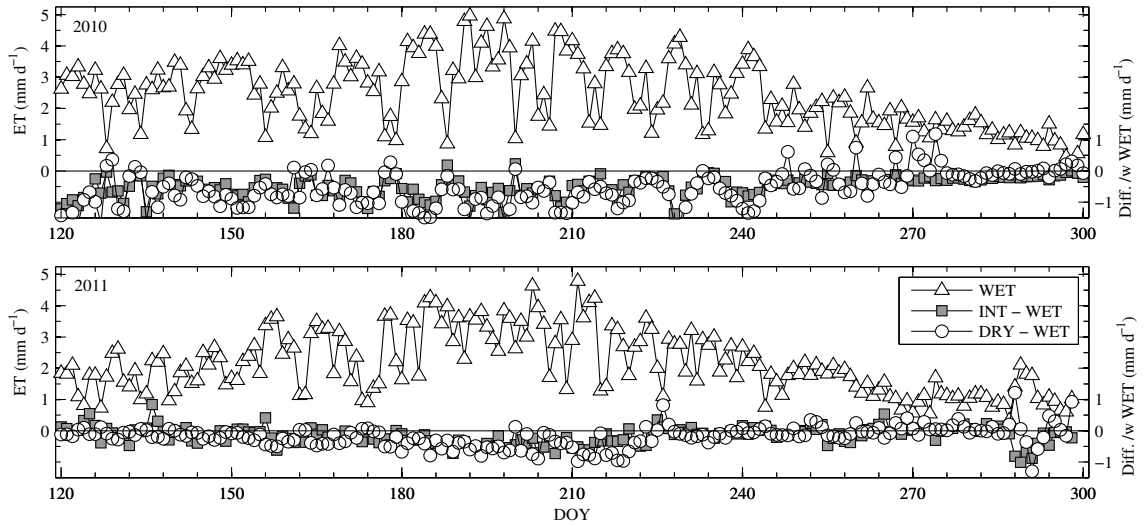


Figure 2 - 2: Daily total gap-filled evapotranspiration at all three study sites over the 2010 and 2011 growing seasons. INT and DRY traces represent the difference in daily evapotranspiration relative to the WET site.

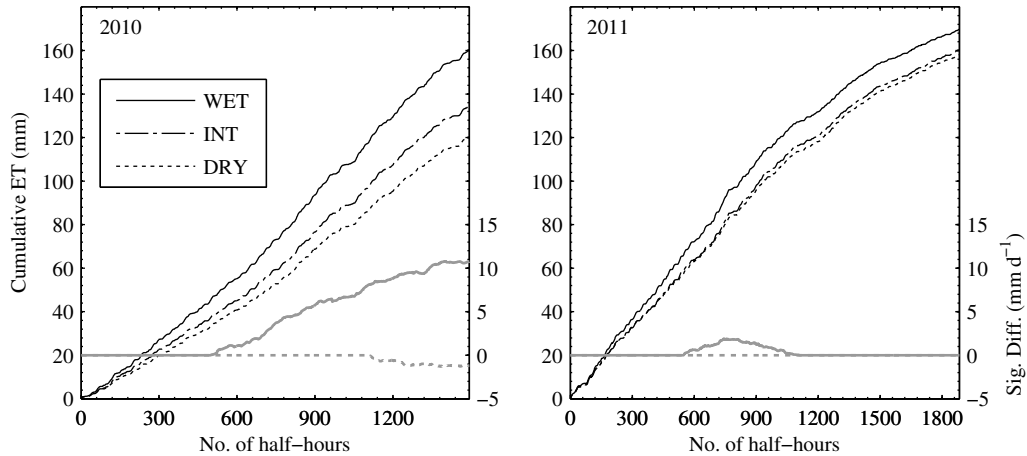


Figure 2 - 3: Cumulative sum of all common half-hourly evapotranspiration measurements (thick black lines) for WET (solid), INT (dash-dot), and WET (dashed) sites where quality control flagging system indicated high quality data based on integral turbulence characteristics, wind direction, stationarity, and a u_* threshold of 0.1 m s^{-1} . Significant differences between sites (thin grey lines) are relative to the INT site and are based on an assumption of purely random error (Moncrieff *et al.*, 1996).

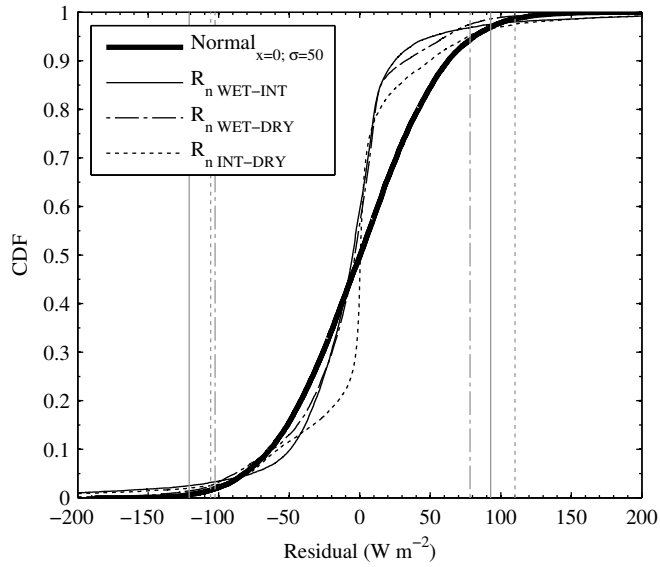


Figure 2 - 4: Empirical cumulative distribution functions of residual half-hourly R_n values between all sites from DOY = 120 – 300, for 2010 and 2011. Vertical bars represent the 2.5th and 97.5th percentiles.

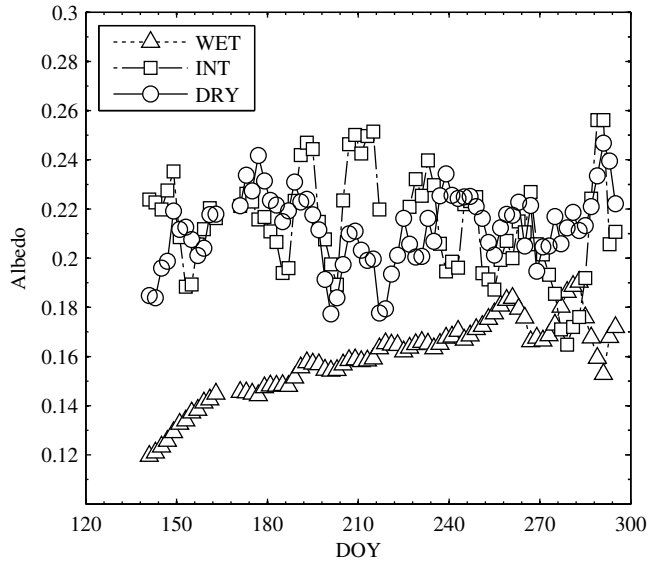


Figure 2 - 5: 7-day running average midday albedo across all study sites during the 2011 growing season.

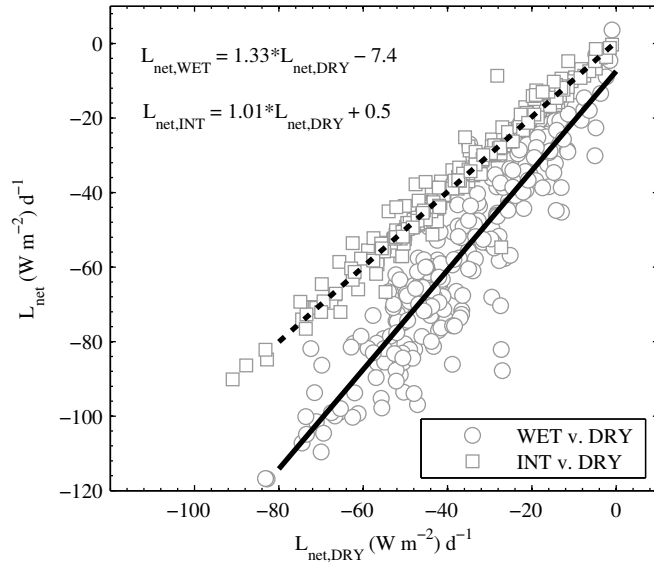


Figure 2 - 6: Correlation of daily average long-wave radiation against the DRY site for 2010 and 2011 growing season data combined. The linear relation between sites is represented by the solid (WET v. DRY) and dashed (INT v. DRY) lines. For clarity, the relation between WET and INT has been omitted due to the close correspondence between INT and DRY.

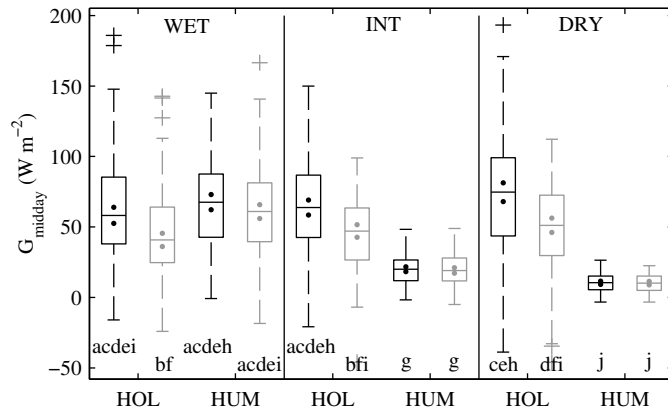


Figure 2 - 7: Boxplots comparing daytime ground heat flux for both 2010 (black) and 2011 (grey). Standard error estimate of the median is represented by the solid dots, and outliers by the crosses. Letters below each boxplot indicate where there are significant differences in the median.

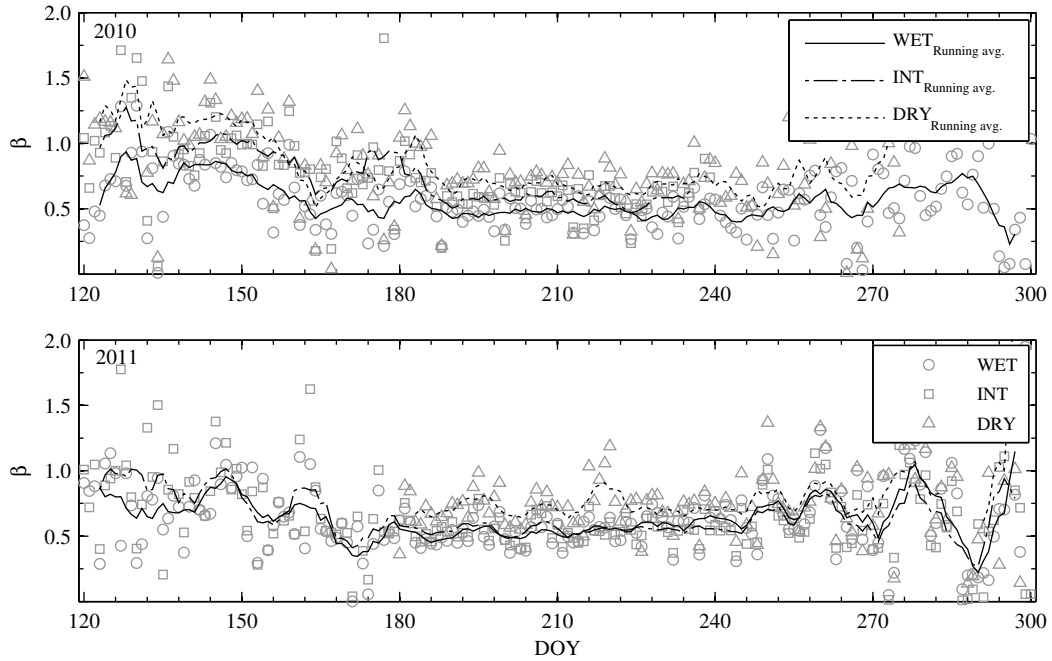


Figure 2 - 8: Daily Bowen ratio for all three sites over the 2010 and 2011 growing seasons. Lines represent the 7-day running average Bowen ratio for WET (solid), INT (dash-dot), and DRY (dashed) sites.

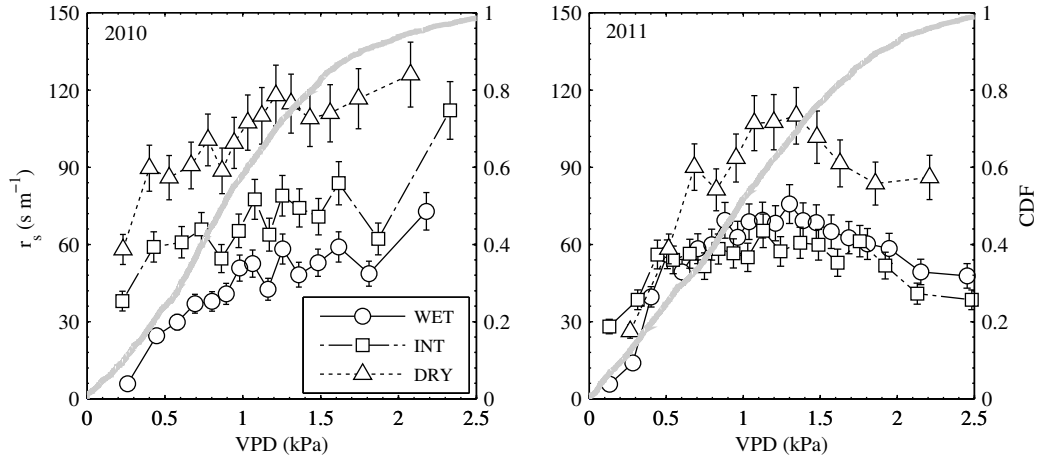


Figure 2 - 9: Median half-hourly daytime ($K_{\text{down}} > 100\ \text{W}\ \text{m}^{-2}$) bulk surface resistance for 2010 (a) and 2011 (b) binned based on vapour pressure deficit with 100 values per bin. Error bars represent the standard error estimate of the median. The grey line represents the cumulative distribution of D .

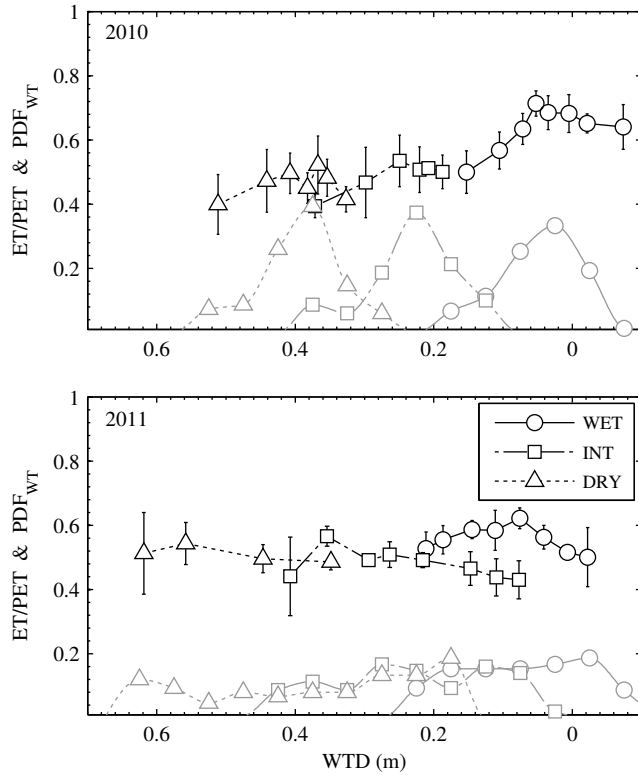


Figure 2 - 10: Relation between normalized ET and bin-averaged WTD for 2010 and 2011 growing seasons. Grey curves represent the relative frequency distribution of WTD.

CHAPTER 3: MICROTOPOGRAPHIC AND VEGETATION CONTROLS ON PEATLAND EVAPOTRANSPIRATION ACROSS A LONG-TERM WATER TABLE MANIPULATION GRADIENT

3.1 Abstract

A peatland complex disturbed by berm construction in the 1950's was used to examine the long-term impact of water table (WT) manipulation on microtopography, vegetation and partitioning of evapotranspiration (ET) at three adjacent sites with increasing depth to WT (WET, INTermediate, and DRY). The relative abundance of the dominant vascular species (*Chamaedaphne calyculata* and *Carex oligosperma*) within microforms were unaffected by WT treatment, but hummocks at progressively dryer sites were taller in relation to hollows and covered a greater proportion of the surface. The difference in microtopographical variation had a significant impact on surface moisture where there were large differences between hummocks and hollows at the WET and INT site, but with no significant difference at the DRY site. Despite the shift to dryer surface conditions, there was no significant change in the relative abundance of the dominant *Sphagnum* species in hummocks (*S. capillifolium*) and hollows (*S. angustifolium*) across the WT treatments.

Averaged across microforms and WT treatments, there was a difference in the median measured leaf resistance (r_{leaf}) between plant functional types ranging from 213 s m⁻¹ for erect dwarf shrubs, 325 s m⁻¹ for sedges, and 520 s m⁻¹ for prostrate dwarf shrubs. Erect dwarf shrubs with a low r_{leaf} dominated hummocks, but sites with a higher

proportion of hummocks had lower total ET due to lower LAI where median scaled canopy resistance (r_v) was 112 s m^{-1} , 172 s m^{-1} , and 168 s m^{-1} at the WET, INT and DRY sites respectively. A three-source model was used to assess the evaporative contribution from the moss surface, with 22 – 45% of total ET estimated to come from the moss surface. LAI and the relative proportion of microforms controlled the overall magnitude of moss evaporation and partitioning between hummocks and hollows, while surface wetness had a greater effect on temporal variability particularly at the WET site and in hummocks. Porometry measurements and functional relations with light and atmospheric moisture demand were used to model canopy transpiration where results correlated well with the three-source model. For moderate persistent changes in WT from land-use or climate change, our results suggest vegetation succession is minimal, but microtopographic development and the concomitant change in leaf area for the various plant functional types is key to understanding changes in total ET and sourcing.

3.2 Introduction

Peatlands store approximately one-third of global soil carbon (Gorham, 1991) and provide valuable ecosystem services (Vitt *et al.*, 2000), including the maintenance of biodiversity (Rydin *et al.*, 2006), and conservation of water resources (Devito *et al.*, 2013). In areas where peatlands are abundant, these ecosystems can have a significant impact on regional climate through surface-atmosphere exchanges of mass and energy, where evapotranspiration (ET) is a large component of the water balance across peatland types (Price and Maloney, 1994; Kellner and Halldin, 2002). Uncertainty exists on how predicted changes in climate will influence peatland ecosystems (Frolking

et al., 2011) where the presence of non-vascular surface cover of *Sphagnum* mosses and a relatively short sparse canopy of vascular plants makes peatlands a particular challenge to energy balance modelling efforts. Moreover, the spatial heterogeneity in the form of microtopography that exists in many peatlands results in distinct differences in moisture and vegetation regimes between relatively low lying wet hollows and raised dry hummocks (Andrus *et al.*, 1983). In general, micrometeorological studies have recognized the importance of the understory contribution to ecosystem scale evapotranspiration (ET) (*e.g.* Kelliher *et al.*, 1990; Baldocchi *et al.*, 1997; Baldocchi *et al.*, 2000; Blanken *et al.*, 1997), where controls on surface evaporation and canopy ET can be out of phase in cases where the plant functional type of the canopy and surface/understory differ (Baldocchi *et al.*, 2004). For peatlands, differences in phenology between vascular and non-vascular vegetation may lead to different sourcing of water vapour throughout the season. A short vascular canopy with a low to moderate leaf area index (LAI), particularly early in the growing season, may allow for considerable contribution of the ground surface in the energy balance (*e.g.* Admiral and Lafleur, 2007). Unlike vascular vegetation, *Sphagnum* lacks internal conductive tissue for accessing water and stomata for restricting water loss (Clymo and Hayward, 1982). Therefore, the physiological mechanisms which control water loss are fundamentally different in *Sphagnum*, where water loss is thought to be limited by the ability of *Sphagnum* and the underlying peat to draw water up from the water table (WT) by capillary action (Hayward and Clymo, 1982), and to a lesser extent, by the diffusion of water vapour through the unsaturated zone (Price *et al.*, 2009). This complicates

modelling of peatland ET since the response of moss evaporation to drying are largely unknown, where both empirical moisture response curves (Sonnentag *et al.*, 2008; Lawrence *et al.*, 2011) and more physically-based controls using surface pore water pressure based on *Sphagnum* and peat moisture-retention properties have been used (Letts *et al.*, 2000; Lawrence and Slater, 2008; McCarter and Price, 2013).

In addition to the uncertainty in moss evaporation, few studies have used field measurements to determine the relative contribution and variation in canopy ET due to vegetation composition or coverage within or between sites (*e.g.* Takagi *et al.*, 1999; Admiral and Lafleur, 2007). The relative abundance of vascular vegetation within a given peatland will dictate whether a peatland can be modelled using a big-leaf model with ET partitioned into soil, vegetation, and interception loss components such as in the ORCHIDEE land surface scheme (Ducoudre *et al.*, 1993), or if a more detailed dual source model is required (Kim and Verma, 1996; Lafleur *et al.*, 2005). The Canadian land surface scheme (CLASS) and Community Land Model have recognized the importance of both organic soils (*e.g.* Letts *et al.*, 2000; Lawrence *et al.*, 2008) as well as the need for a dual source model to better characterize surface evaporation (*e.g.* Verseghy, 1993; Lawrence *et al.*, 2011). Nevertheless, despite having dual source ET and organic soil parameterization, Comer *et al.* (1999) show that CLASS does not simulate ET well for peatlands with a sparse vascular canopy or conversely where spatio-temporal variations in surface wetness are significant, suggesting a potential need for better parameterization of moss evaporation.

Given that climate change is expected to cause large-scale drying in northern peatlands (*e.g.* Roulet et al., 1992) it is likely that hummocks will become more prevalent and there would be concomitant increase in the relative abundance of above-ground shrub biomass (Weltzin *et al.*, 2003). Given that increasing vascular cover has been associated with higher ET in peatlands and a difference in seasonality (Takagi *et al.*, 1999) this suggests a positive feedback to long-term drying effects would occur. However, a lower WT will likely increase fine root production (Weltzin *et al.*, 2000) and nutrient availability (Macrae *et al.*, 2013) which may serve to limit LAI and have a negative impact on leaf conductance (Schulze *et al.*, 1994). Nevertheless, we argue that these studies point to a need for land surface scheme peatland classifications to include both ‘dynamic microforms’ and ‘dynamic vegetation’ that provides the ability for microtopography and plant functional groups to change through time as a result of the changing environmental conditions.

Despite the need for an improved understanding of long-term peatland response to climate change, research is limited on the effects of multi-decadal hydrological alterations on peatland vegetation dynamics (Miller 2011). Moreover, most long-term WT drawdown studies are from peatlands drained for forestry and agriculture by ditching which results in WT drawdowns greater than 0.30 m (Wells and Williams 1996; Sundström et al. 2000; Laiho et al. 2008) and is in excess of the 0.14 cm WT drawdown predicted for northern peatlands under a future climate change scenario (Roulet et al. 1992). Consequently research is lacking on more subtle (*i.e.* ± 0.15 m) long-term (> 50 years) WT alteration effects on vegetation composition, surface morphology, and

associated energy balance dynamics that more realistically reflect the conditions predicted for northern regions in the next century. Within this context, the objectives of this study were to examine ET at multiple peatland sites across a hydrological gradient that were subject to long-term WT manipulation in order to: (i) assess the relative importance of surface evaporation and canopy transpiration to total ET; (ii) assess the effect of microtopography on surface wetness and surface evaporation; and (iii) examine the link between the water table gradient, microtopography, and seasonality on vascular species composition, LAI, and leaf-level conductance. While studies have shown the usefulness of two-source models in analyzing energy balance partitioning, by modifying the two-source energy balance model of Kim and Verma (1996) by considering hummock and hollow surfaces separately, we examine the effect of differences in LAI between microforms as well as the effect of surface wetness on energy partitioning. By linking porometry measurements to ecosystem scale measurements, the relative contributions of vascular plant transpiration and *Sphagnum* evaporation to total ET can be estimated and compared to model results.

3.3 Methods

3.3.1 Study site

The study area is located in the Seney National Wildlife Refuge (SNWR) in the Upper Peninsula of Michigan (46.20° N, 86.02° W, elev. ~205 m a.s.l.). The region is characterized by relatively flat topography which slopes towards the south-east at 1.1 – 2.3 m km⁻¹ (Heinselman, 1965). Land cover consists primarily of upland forests (67%),

and open peatlands (20%), while the remainder of the region is made up of mostly forested swamps and open water (Casselman, 2009). Wet sand of glacial origin overlies the regional bedrock up to a thickness of 60 m (Albert, 1995). Surface soils throughout SNWR are mostly a complex of poorly drained muck and sand, while the study area itself contains poorly drained peats (Casselman, 2009).

The peatland complex within SNWR is subdivided by a combination of upland sand ridges of lacustrine origin, creeks, old drainage ditches, as well as a network of roads and berms constructed mostly during the late 1930's and early 1940's by the Civilian Conservation Corps (Kowalski and Wilcox, 2003; Wilcox et al., 2006) for the purpose of creating open water habitat for migratory birds. Berm construction at our study site resulted in the up-gradient impoundment of water, thus locally reducing down-gradient water inputs by re-routing water surplus through the water-control structure on Marsh Creek. Our measurement locations were chosen to take advantage of this natural experiment, where Fig. 3-1 shows the location of our three sites with different WT regimes in relation to the berm and the general direction of surface and groundwater flow.

All three study sites are located in the southern portion of the SNWR peatland complex. Dominant vegetation at all three peatland sites consists of a ground cover of *Sphagnum* species, an overstory of vascular shrubs and graminoids, and conifers in the surrounding uplands and the margins at the INT and DRY sites (see Moore *et al.*, 2013 or Hribljan, 2012 for details). The WET site is considered a poor fen and the INT and DRY sites both bogs based on pH and vegetation composition (*c.f.* Bedford and Godwin,

2003), but where pH decreases and microtopographical variation increases (Table 3-1) from WET, to INT, to DRY. Height variation between hummocks and hollows was based on the difference in measured WT depth for adjacent hummock-hollow pairs at each site (n = 20). Proportional cover was based on a transect survey across orthogonal axes of each site at 2.5 m intervals (n = 249 to 386). Microtopography was classified as hummock, ridge, or hollow using relative elevation, slope, and vascular community, with ridges aggregated into hummocks and hollows.

Based on the 1981-2010 climate normals from the Newberry 3S weather station (46.32° N, 85.50° W, elev. ~260 m a.s.l.) ~45 km from the study sites, the area has an average annual temperature of 5.6°C and receives 784 mm of precipitation, where greater monthly totals occur during May through October (NOAA NCDC, 2012) compared to other months.

3.3.2 Evapotranspiration and supporting measurements

Site scale evapotranspiration was measured at all three sites using standard eddy covariance (EC) equipment based on the method described by Baldocchi *et al.* (1996). Three component wind speed and sonic air temperature were measured using a CSAT3 3D sonic anemometer-thermometer (Campbell Scientific Inc. (CS), Logan, Utah), and water vapour concentrations were measured using an LI-7500A open-path infrared gas analyzer (IRGA) (LI-COR Biosciences, Lincoln, Nebraska). Details regarding EC sensor placement, measurements, high-frequency data processing, corrections, and quality assurance are presented by Moore *et al.* (2013). Radiation measurements were made using a combination of CMP3 (CS), NR-LITE net radiometers (CS), and CNR2 net short

and long-wave radiometers (CS). A CNR2 was used at the INT and DRY sites, while an NR-LITE was used at the WET and INT sites. Both types of net radiometers were used at the INT site to provide a continuous cross-comparison of instrument type in order to correct for any systematic bias. Supplementary air temperature and relative humidity (RH) were measured using an HMP45C (Vaisala Oyj, Helsinki, Finland) temperature and relative humidity probe. Peat temperature profiles were measured in a representative hummock and hollow at each site using T-type thermocouple (Omega Engineering, CT, USA) wire inserted at depths of 0.01, 0.05, 0.1, 0.2, and 0.5 m relative to the local surface. Soil moisture profiles were measured using CS-616 water content reflectometers (CS). Volumetric moisture content (θ) sensors were installed at all three sites in a representative hummock and hollow at depths of 0.10, 0.20, and 0.30 m relative to the surface, with an additional sensor at 0.45 m in hummocks. The correction of Hansson and Lundin (2006) was first applied to the measured CS-616 period values before calculating θ using the three-phase mixing model for peat (Kellner and Lundin, 2001). All high frequency data was recorded on a CR5000 datalogger (CS) at the WET and DRY site, while a CR3000 datalogger (CS) was used at the INT site. Meteorological, peat temperature and θ data were measured every minute and averaged and recorded at 30 minute intervals using a CR1000 (CS) or CR10X (CS) datalogger.

Plot scale evapotranspiration was measured at eight hummocks and hollows at each of the three sites for a total of 48 permanent sampling locations, with steel collars (0.6 x 0.6 m) imbedded 0.1 m in the peat surface. A sealed Plexiglas chamber (0.6 x 0.6 x 0.6 m) with two small mixing fans and an EGM-4 infrared gas analyzer (PP-systems,

Amesbury, MA) were used to measure the change in water vapour concentration (ρ_v) at 5 s intervals over a two-minute measurement period. A short measurement period was used to minimize temperature changes within the chamber. Measurements were taken between 10:00 and 17:00 h on a bi-weekly basis throughout the growing season, where plot measurement order was quasi-randomized. Instantaneous chamber ET values (LE_{ch}) (mm hr⁻¹) were calculated according to Stannard (1988):

$$LE_{ch} = \frac{MV \cdot cf}{A} \quad (3.1)$$

where M is the rate of change in ρ_v in the chamber, V is the chamber volume (m³), cf is a correction factor to account for vapour adsorption within the chamber (dimensionless), and A is the ground surface area (m²). Due to the non-linear increase in ρ_v over the measurement period, M was calculated using a quadratic fit, where measurement runs with an r^2 less than 0.9 were rejected. In conjunction with ρ_v , photosynthetic photon flux density (PPFD), chamber temperature, and soil temperature were measured inside the chamber using EGM-4 standard probes.

Leaf-level resistance (r_{leaf}) measurements for the dominant vascular species were made using an AP4 dynamic diffusion porometer (Delta-T, Burwell, UK). Measurements were made during the early, mid, and late growing season at each of the chamber plots every other day for a two week period. Measurements took place between 10:00 and 16:00 h, where measurements earlier in the day were unfeasible due to condensation which was prevalent on leaf surfaces. Within each plot r_{leaf} was measured for *Chamaedaphne calyculata*, *Kalmia polifolia*, *Vaccinium oxycoccus*, *Cyperaceae*, and

Vaccinium myrtilloides were present using three to five replicates. The porometer was calibrated at least once each measurement day, with periodic re-calibration occurring with large changes in ambient temperature or RH.

3.3.3 *Supplementary measurements*

One-sided leaf area index (LAI) was determined from the destructive sampling of four random 0.25 m² hummock and lawn plots at each of the three sites (n = 24). LAI was estimated for each species from a scanned subsample and scaling the value based on the dry weight ratio of the sub- to total-sample weight. Samples were further segregated based on leaf, woody, live, and dead tissue in order to assess plant area index (PAI). In order to assess the spatial variability in species abundance, both within and between sites, a vegetation survey was done for eight 1 m² hummock and lawn plots at each of the three sites (n = 48). The vegetation survey was done using the grid-intercept method, with a 10 x 10 grid centered on the chamber measurement collars.

θ in the top 0.07 m was measured using a WET sensor (Delta-T). In order to assess spatial variability, θ measurements were made during the early, mid, and late growing season at each of the chamber plots every other day for a two week period. A θ measurement was taken in each quadrat of the chamber plots. WT levels were measured hourly in 1.5 m deep wells using self-logging Levellogger Junior pressure transducers (Solinst, Georgetown, ON (Solinst)). WT measurements were corrected for changes in atmospheric pressure using a Barologger Gold barometric logger (Solinst). WT level was recorded at all three sites in two separate groundwater wells with the average local

topography used as a datum, where the height of the average local surface was determined from 50 m transects with the groundwater wells at the center.

3.3.4 Modelling and supporting calculations

In order to assess the relative contribution of vascular and *Sphagnum* vegetation to total ET, we used a three-source energy balance equation, omitting heat storage in the vascular canopy:

$$R_n - (LE_v + \sum p_i (LE_{surf,i} - G_i)) - H \approx 0 \quad (3.2)$$

where R_n is the net radiation flux above the vascular canopy (W m^{-2}), LE and H are total latent and sensible heat fluxes (W m^{-2}), G is the ground heat flux (W m^{-2}), p is the relative proportion of hummocks or hollows for the respective sites, the subscripts v and $surf$ are the respective values for the aggregate vascular canopy and *Sphagnum* surface, and i represents values for hummocks or hollows. $LE_{surf,i}$ was calculated according to Kim and Verma (1996):

$$\sum p_i LE_{surf,i} = \sum p_i (R_{n,surf,i} - G_i) / (1 + \beta_{surf,i}) = LE - LE_v \quad (3.3)$$

where $\beta_{surf,i}$ is the Bowen ratio (H/LE) at the *Sphagnum* surface, and $R_{n,surf,i}$ is the estimate of the radiation balance at the *Sphagnum* surface:

$$R_{n,surf,i} = p_i R_n \exp^{-\kappa \cdot LAI_i} \quad (3.4)$$

where κ is the extinction coefficient assumed for simplicity to be 0.5, which corresponds with a spherical leaf angle distribution. G_i is calculated from soil temperature and moisture profiles by calculating heat storage in the top 0.2 m and a flux term at 0.2 m depth as follows:

$$G_i = C_v \Delta z \frac{\Delta \bar{T}|_{0,2m}^{0m}}{dt} + C \frac{\partial T}{\partial z} \Big|_{0,2m} \quad (3.5)$$

where C_v is the volumetric heat capacity ($\text{J m}^{-3} \text{ }^\circ\text{C}^{-1}$), z is depth (m), T is temperature ($^\circ\text{C}$), t is time (s), and C is thermal conductivity ($\text{J s}^{-1} \text{ m}^{-1} \text{ K}^{-1}$). Using Ohm's Law analogy to represent H and LE , through rearrangement of equation 3.3 we obtain an equation with two unknowns, surface resistance ($r_{surf,i}$) (s m^{-1}) and $\beta_{surf,i}$:

$$r_{surf,i} (R_{n,surf,i} - G_i) / (1 + \beta_{surf,i}) + [\rho_a C_p (T_{surf,i} - T_a) - H \cdot r_a] / \beta_{surf,i} = (\lambda \varepsilon \rho_a / P) [e_* (T_{surf,i}) - e_a] - LE \cdot r_a \quad (3.6)$$

where ρ_a is air density (kg m^{-3}), C_p is the specific heat capacity of air ($\text{J kg}^{-1} \text{ }^\circ\text{C}^{-1}$), λ is the latent heat of vapourization (J kg^{-1}), ε is a constant (0.622), P is air pressure (kPa), and e_* and e_a are the saturated and actual vapour pressure (kPa) at the surface and of the air respectively. Aerodynamic resistance (r_a) (s m^{-1}) to heat and vapour transport was calculated as the sum of the resistance to momentum transfer, r_{am} , and the boundary layer resistance, r_b . r_a was calculated according to Stewart and Thom (1973):

$$r_a = \frac{u_z}{u_*^2} + r_b \quad (3.7)$$

where u_z is the wind speed (m s^{-1}), u_* is the friction velocity (m s^{-1}), and r_b is calculated according to the empirical formula of Kellner (2001):

$$r_b = \frac{a(u_* z_0 / \nu)^{0.25} - b}{k u_*} \quad (3.8)$$

where z_0 is the roughness length (m), ν is the kinematic viscosity of air ($\text{m}^2 \text{ s}^{-1}$), k is the von Karman constant, and a and b are empirical parameters. Estimates of 1.58 and 3.4 for

a and b from a Swedish bog were used to calculate r_b (Molder and Kellner, 2001). Stability correction factors were omitted from Eqs. 3.7 and 3.8 since u_* was calculated based on turbulent measurements of all three Cartesian wind speed components rather than from wind speed profiles. We used measured energy balance and turbulence data, air temperature and humidity, and extrapolated measured soil temperature using a quadratic fit to the top three soil temperatures to approximate $T_{surf,i}$ as inputs to Eq. 3.6 and solved for the two unknowns using non-linear least squares regression by using the simplifying assumption that $r_{Sph,i}$ and $\beta_{surf,i}$ don't vary significantly over relatively short periods of time (on the order of several hours). Substituting $\beta_{surf,i}$ into Eq. 3.3, we were able to estimate LE_v as the residual of LE calculated from EC measurements, and the sum of LE_{surf} from hummocks and hollows. An alternate estimate of LE_v was derived from porometry and EC measurements using the Penman-Monteith equation:

$$LE_{v,PM} = \frac{sR_{n,v} + \rho_a C_p D r_a^{-1}}{s + \gamma \left(1 + \frac{r_v}{r_a} \right)} \quad (3.9)$$

where s (kPa °C⁻¹) is the slope of the saturation vapour pressure versus temperature curve, γ (kPa °C⁻¹) is the psychrometric constant, and D (kPa) is the vapour pressure deficit of the atmosphere. $R_{n,v}$ was calculated as:

$$R_{n,v} = \sum p_i R_n \left(1 - \exp^{-\kappa LAI_i} \right) \quad (3.10)$$

r_v was modeled by assuming that the functional response of bulk surface resistance (r_{bulk}) to environmental variables was dominated by the stomatal response of the vascular

vegetation. r_{bulk} was calculated by rearranging the Penman-Monteith equation and substituting in β as follows:

$$r_{bulk} = r_a \left(\frac{s}{\gamma} \beta - 1 \right) + \frac{\rho C_p D}{R_n - \sum p_i G_i} (1 + \beta) \quad (3.11)$$

Different models have been developed to assess the response of r_{bulk} or r_v to various environmental variables, which commonly includes PPFD, D , and some parameterization of water availability. We used an empirical non-linear phenomenological model based on the general form described by Jarvis (1976):

$$r_{bulk}^{-1} = a_1 \prod_{i=1}^n f(x_i) \quad (3.12)$$

where a_1 is the maximum conductance under non-limiting conditions and x_i are the controlling environmental variables. In peatlands, due to the relatively shallow WT, aerenchymous tissue and deep rooting in certain sedge species (Saarinen, 1996), and root growth patterns of erect dwarf shrubs, the effect of WT changes on vascular plant water availability is limited (Malmer *et al.*, 1994). As such, we omit a water availability term in our model, and use PPFD and D as the major controlling variables:

$$f(PPFD) = \frac{a_2 \cdot PPFD}{\sqrt{1 + (a_2 \cdot PPFD)^2}} \quad (3.13)$$

$$f(D) = \frac{a_3}{a_3 + D^{a_4}} \quad (3.14)$$

where a_2 , a_3 , and a_4 are fitted parameters. Since Eqs. 3.13 and 3.14 yield dimensionless values which range from 0 to 1, r_{bulk} was normalized using the 5th percentile ($r_{bulk,5th} = 28 \text{ s m}^{-1}$, 54 s m^{-1} , and 58 s m^{-1}) of half-hourly values calculated from Eq. 3.11. PPFD was

estimated from CMP3 measurements using a fixed ratio of 2.10:1 for PPFD ($\mu\text{mol m}^{-2} \text{s}^{-1}$) to incoming solar radiation (W m^{-2}). Both theoretical and field measurements suggest that the ratio of PPFD to total solar radiation is ~ 0.50 and is relatively constant over a wide range of solar elevation angles and atmospheric conditions (*e.g.* Szeicz, 1974; Weiss and Norman, 1985). We derived the above ratio of 2.10:1, which is consistent with values summarized in Udo and Aro (1999), by dividing 0.50 by the photon energy for the peak wavelength of solar radiation using Wien's displacement law. An estimate for a_l was derived by solving Eq. 3.12 for where the median modelled daytime value equaled the median measured leaf resistance (r_{leaf}), scaled according to LAI and microform ($r_{v,i}$):

$$r_{v,i} = \left(\sum r_{leaf,j}^{-1} LAI_{i,j} \right)^{-1} \quad (3.15)$$

where the subscript j refers to the various vascular species measured using porometry.

Since measurements of LAI and r_{leaf} were temporally limited, a greenness index (I_G) was derived in order to vary LAI seasonally in Eqs. 3.4 and 3.10:

$$LAI = LAI_{\min} + I_G (LAI_{\max} - LAI_{\min}) \quad (3.16)$$

I_G was derived from the red (R), green (Gr), and blue (B) values from daily photos taken at the SNWR fire tower at midday. For a fixed region in the image representing peatland area, the median RGrB intensities were calculated, where I_G was calculated as the ratio of Gr to R+Gr+B, and normalized to vary between 0 and 1.

3.4 Results and Discussion

3.4.1 Microtopography, vegetation, and moisture availability

Differences in site microtopography were pronounced, where the proportion of hummocks and height of hummocks relative to hollows increased from WET, to INT, to DRY (Table 3-1). The difference in the average WT (Fig. 3-1), between sites was fairly consistent over the 2010 and 2011 growing season with a median difference between the WET and INT site of 0.10 m (0.25 m) in hollows (hummocks), and 0.19 m (0.45 m) between the WET and DRY sites when averaged across years. Viewed as a deviation from the INT site, the difference in magnitude of WT depth at the WET and DRY sites are roughly equal and opposite, and of a similar magnitude to the predicted mean WT change under a 2 x CO₂ climate change scenario (Roulet *et al.*, 1992). The differences between sites in relative WT depth in both hummocks and hollows have important implications for the typical range and distinctness of surface θ (θ_{surf} - average of top 0.07 m) between microforms and sites. Although the difference in median θ_{surf} between hummock and hollows is greatest at the WET site, where hollows were considerably wetter than hummocks, the median θ_{surf} in hummocks and hollows is greater than the other two sites (Fig. 3-2c). For both study years the difference between median hummock and hollow θ_{surf} is significant at both the WET and INT sites, but not at the DRY site where both hummocks and hollows were rather dry. These data, which are based on spatial averages, are in contrast to the continuous point measurements of θ at 0.10 m ($\theta_{0.10}$) at an individual hummock and hollow at each site. For $\theta_{0.10}$ at the WET site, we only see relatively small average differences between hummock and hollow measurements (0.10 m³ m³) which are temporally correlated ($r^2 = 0.69$, $p \ll 0.01$), while average differences at both the INT and DRY sites are persistently large (0.76 m³ m³; and

0.81 m³ m³) and uncorrelated ($r^2 = 0.44$, $p = 0.72$; and $r^2 = 0.15$, $p = 0.69$). The disparity between point measurements and spatial averages can be the result of the microforms chosen for θ -profiles not being representative for the respective sites, but where measurements were validated using lab-based peat moisture retention and WT relative to the 0.10 m measurement depth to approximate pore water pressure. Fig. 3-2d shows how the magnitude of spatial variability can be approximated by a Gaussian function, where variability is small at both high and low θ_{surf} . Given the low θ_{surf} in hollows at the DRY site (Fig. 3-2c), spatial variability is unlikely to account for high hollow $\theta_{0.10}$ measured at the DRY site. A similar argument can be made for hollows at the INT site and hummocks at the WET site. Consequently, the disparity between θ_{surf} and $\theta_{0.10}$ is more likely the result of a sharp moisture gradient over the top 0.10 m which may be explained by a disequilibrium between surface pore water pressure and water table depth due to high evaporative loss at the moss surface.

Despite the overall dryer surface conditions in both hummocks and hollows at the INT and DRY site in particular, we don't see a significant difference in the relative abundance of typical hummock/hollow forming *Sphagna* as a result of the WT treatments. While a two-way ANOVA showed a significant difference in the abundance (defined herein as the presence/absence from each point in a 1 m² 10 x 10 grid) of both *Sphagnum capillifolium* and *Sphagnum angustifolium* grouped according to microform ($p < 0.01$), where *S. capillifolium* is more abundant on hummocks and *S. angustifolium* is more abundant in hollows, site and interactive effects were not found to be significant ($0.18 < p < 0.47$). However, when weighted according to the proportion of hummocks and

hollows at each site the total percent cover of *S. capillifolium* does increase, while *S. angustifolium* decreases.

We assessed more generally how differences in moisture availability and WT treatments might affect species richness since higher values would indicate a more varied contribution to ET, particularly if different plant functional types were represented. A two-way ANOVA showed a significant difference in species richness between microforms ($p = 0.017$) where Tukey's honestly significant difference test (hsd) shows richness to be greater in hummocks (9.6 ± 0.35) compared to hollows (8.4 ± 0.35) based on a total of 23 identified species. While there was no significant difference based on site ($p = 0.067$), species richness tended to be higher at the DRY site (9.6 ± 0.43) compared to the INT (9.2 ± 0.43) and WET (8.2 ± 0.43) sites. Although species richness appears to be affected by microform, and to a lesser extent by WT treatment, the difference in species richness does not appear to have a large impact on the relative abundance of the dominant *Sphagnum* or vascular species (Fig. 3-3). While, a Kruskal-Wallis test indicated that there was a significant difference ($p < 0.01$) in the relative abundance of the various species found at each site, a multiple comparison test using Tukey's hsd indicated that the most abundant vascular species at each site were *Chamaedaphne calyculata*, *Carex oligosperma*, *Vaccinium oxycoccus* and *Kalmia polifolia*, and the most abundant *Sphagnum* species were *S. angustifolium*, *S. capillifolium*, and *Sphagnum magellanicum* in their respective orders of abundance.

Because of potential differences in average leaf size for *Ericaceae* (shrubs) and blade length for *Cyperaceae* (sedges), results from the grid intercept method used to

assess species abundance do not necessarily coincide with LAI measurements which are needed for scaling leaf-level transpiration measurements. Based on our destructive sampling, the LAI of live vegetation was highest at the WET site (Table 3-1) for both hummocks and hollows, where in general *C. calyculata* dominated hummocks and *C. oligosperma* dominated hollows (Fig. 3-4). We tested whether the same pattern of species abundance for the two dominant vascular species was reflected in our vegetation survey data since it had a greater number of plots (*i.e.* 8 vs. 4). A two-way ANOVA showed a significant difference in abundance for *C. calyculata* ($p = 0.016$) and *C. oligosperma* ($p < 0.01$) based on microform, where Tukey's hsd showed the abundance of *C. calyculata* to be highest in hummocks and *C. oligosperma* to be highest in hollows.

3.4.2 Evapotranspiration partitioning

Dominant vascular species identified by destructive leaf sampling and the vegetation survey were the focus of porometry measurements, with the intention of identifying whether r_{leaf} differed between species, plant functional type (PFT), microform, or site. The measured r_{leaf} for individual species all followed a log-logistic probability distribution, so non-parametric statistics were used for comparisons (Fig. 3-5). For all species present at all sites and microforms with the exception of *K. polifolia*, a Kruskal-Wallis test showed no significant differences ($p > 0.215$ for all factors and interactions) in median r_{leaf} based on site, microform, and interactive effects. While the median r_{leaf} for *K. polifolia* varied based on both site ($p = 5E-4$) and microform ($p = 0.005$), the overall impact on ecosystem-scale ET is small due to its relatively low abundance (Fig. 3-3) and LAI (Fig. 3-4). Therefore, for scaling purposes, separate values

based on site and microform were not used, though individual species were treated independently with median measured values of 234 s m^{-1} , 192 s m^{-1} , 325 s m^{-1} , and 520 s m^{-1} for *C. calyculata*, *K. polifolia*, *C. oligosperma*, and *V. oxycoccus* (Fig. 3-5). Interestingly, the median and distribution of r_{leaf} qualitatively differs based on PFT, where we classify *C. calyculata* and *K. polifolia* as erect dwarf shrubs, *V. oxycoccus* as a prostrate dwarf shrub, and *C. oligosperma* as a sedge. Using a rank-sum test, significant differences in median r_{leaf} were found between all PFTs ($p = 2.6\text{E-}08$ between erect shrubs and sedges; $p = 2.4\text{E-}08$ between sedges and prostrate shrubs). With respect to site-level controls on ET, the difference in r_{leaf} between the dominant species *C. calyculata* and *C. oligosperma* is important since their LAI varies between microforms (Fig. 3-4), and where the proportion of hummocks and hollows varies between sites (Table 3-1). While the difference in r_{leaf} between *V.oxycoccus* and the other vascular species was large, the overall effect on ET is likely small. Although *V. oxycoccus* represents up to 31% of LAI (Fig. 3-4) depending on the site and microform, the incident radiation on its surface would be comparatively low due to it growing on the *Sphagnum* surface below the canopy of the other vascular species.

Since microforms have different dominant vascular species with distinct r_{leaf} , all else being equal, we would expect to see a difference in ET at the microform-scale. However, due to differences in LAI and θ_{surf} between microforms and sites, chamber measurements were used to assess whether any systematic differences in ET existed between microforms. Owing to the sporadic nature of manual chamber measurements and variability in PPFD and D , direct comparisons between plot ET_{ch} are not valid. In order to

examine site and microform effects on ET_{ch} , the response curve to D was evaluated for high PPF. In general, Fig. 3-6 shows that ET in hollows tends to be greater compared to hummocks, where no clear distinction exists between sites. In hummocks, however, ET tends to be higher at the WET site in comparison to the INT and DRY sites. The distinction between hummocks may be related to differences in surface wetness observed between sites (Fig. 3-2), or the proportion of *C. calyculata* to *C. oligosperma* in hollows. With respect to a possible vegetation control, total LAI cannot explain the difference between hollows at the INT and WET site as they are roughly the same. However, *C. oligosperma* makes up a much greater proportion of hollow vegetation at the INT site. When combined with a lower median r_{leaf} , this would result in lower ET at the INT site.

The three-source model (see section 3.3.4) was used to estimate the contribution of the moss surface to ET in hummocks and hollows at each of the sites. Both the highest daily and seasonal mean value of surface conductance ($g_{surf} = r_{surf}^{-1}$) was at the INT hummock (Fig. 3-7a), with respective values of $7.9E-03 \text{ m s}^{-1}$ (127 s m^{-1}) and $6.1E-03 \text{ m s}^{-1}$ (165 s m^{-1}). While the mean g_{surf} (r_{surf}) was of a similar magnitude at the WET ($4.0E-03 \text{ m s}^{-1}$ or 251 s m^{-1}), INT ($3.9E-03 \text{ m s}^{-1}$ or 259 s m^{-1}) and DRY ($4.1E-03 \text{ m s}^{-1}$ or 242 s m^{-1}) hollows, mean hummock g_{surf} (r_{surf}) was roughly half (double) the magnitude of INT at the WET ($2.3E-03 \text{ m s}^{-1}$ or 444 s m^{-1}) and DRY ($2.4E-03 \text{ m s}^{-1}$ or 421 s m^{-1}) sites. The difference in mean behaviour between hummocks can largely be related to differences in LAI, since the modelled r_{surf} includes the effect of increased aerodynamic resistance within the canopy associated with higher LAI, where Table 3-1 shows LAI at the WET and DRY site hummocks to be higher compared to the INT site. While the mean g_{surf}

(r_{surf}) was similar between hollows, distinct seasonal differences existed which may be related to differences in LAI and surface wetness. Although LAI in WET and INT hollows is similar, with greater θ_{surf} typical of WET hollows, a greater proportion of $R_{n,surf}$ would be partitioned to LE_{surf} assuming small difference in G_{hol} ; which is shown to be the case for all hollows at the site (Moore *et al.*, 2013). Despite having a lower average LAI, and thus higher $R_{n,surf}$, the DRY hollow has a comparable G_{hol} to the other two sites, where a low θ_{surf} results in greater partitioning to H_{surf} . For hummocks (Fig. 3-7a), although the magnitudes are different, the temporal variability in g_{surf} (r_{surf}) is more similar between sites where the sites are moderately to highly correlated ($0.58 \leq r^2 \leq 0.85$, $p < 0.01$). More subtle differences between the WET and DRY hummocks demonstrate the trade-off between LAI and moisture availability, where the higher average θ_{surf} at the WET site (Fig. 3-2) would reduce r_{surf} , counteracting a high total LAI (Fig. 3-4). From the modelled r_{surf} values we calculated LE_{surf} for hummocks and hollows and, by difference, derived an estimate of total LE_v (Table 3-2). Overall, the contribution of the moss surface to total LE ranged from 22% - 45% with greater contributions coming from sites with increasing depth to WT and lower LAI. The reason for the relatively high contribution of hummock surfaces to total ET at the INT and DRY sites is two-fold, owing to higher proportions of the two sites being covered by hummocks as well as moderate to low LAI allowing for more available energy at the surface and boundary layer effects. The results from the WET site follow the same basic pattern where hollows contribute proportionally more than hummocks due to a greater abundance of hollows and lower LAI in hollows.

Results from the three-source model suggest that LE_{surf} is qualitatively linked to water availability, where variation in hummock r_{surf} in particular appears to co-vary with WT depth, and more so at the WET site across microforms. In general, the correlation between WT depth and r_{surf} is moderately low ($r^2 = 0.35$; $p \ll 0.01$) to high ($r^2 = 0.80$; $p \ll 0.01$) for hummocks, but quite poor for INT ($r^2 = 0.22$) and DRY ($r^2 = 0.08$) hollows. In INT and DRY hollows, periodic sensor issues required more extensive gap-filling of G data where small magnitude flux errors may be amplified given the low average midday $R_{n,surf}$ range of 82 – 187 $W\ m^{-2}$ based on LAI estimates across sites and microforms. In order to gain further insight into what might be occurring at the moss surface early in the growing season, we examined how $r_{bulk}\ r_a^{-1}$ responded to $\theta_{0.10}$. We chose to examine the ratio of resistances rather than r_{bulk} itself since there are a number of methods for calculating r_a , particularly when differences between the resistance to momentum and latent heat transfer are taken into consideration. The midday (between 10:00 and 14:00 h) median r_a calculated according to Eq. 3.6 was similar between all three sites, ranging between 75 – 78 $s\ m^{-1}$. Median midday r_{bulk} , on the other hand, was 161 $s\ m^{-1}$, 299 $s\ m^{-1}$, and 317 $s\ m^{-1}$ at the WET, INT, and DRY sites respectively. Since r_a is relatively conservative between sites, the difference in median r_{bulk} between WT treatments is reflected in the relative magnitudes of the optimal $r_{bulk}\ r_a^{-1}$ ratio (Fig. 3-8). Fig. 3-8 shows a greater response of $r_{bulk}\ r_a^{-1}$ to $\theta_{0.10}$ at the WET site, increasing two-fold early in the growing season. Water availability for vascular plants is mediated by rooting depth and fine root production, where all else being equal, water availability to vascular plants is lower in hummocks versus hollows due to a greater depth to WT. However, results from

Hribljan (2012) suggest that WT treatments affect below-ground production and total biomass, where greater below-ground production compensates for lower WT at the INT and DRY sites in hummocks. Consequently, the effect of water availability on vascular vegetation is likely to be limited, where we assume that any response in r_{bulk} to changing moisture conditions is more strongly linked to r_{surf} . This is supported by our measurements of r_{leaf} , where within species, no WT treatment effect was observed between microforms or sites. The greater response in $r_{bulk} r_a^{-1}$ at the WET site is in part related to greater near-surface drying in hollows compared to the other two sites (Fig. 3-2). Furthermore, the covariance between hummock and hollow $\theta_{0.10}$ at the WET site is three to four orders of magnitude greater compared to the INT and DRY sites. This means that, in addition to there being a greater proportion of hollows at the WET site, hummocks tend to behave more like hollows at the WET site. Moreover, no strong response in r_{surf} to θ in hummocks is expected at the INT and DRY sites since the range in near-surface θ over the growing season was roughly $0.10 - 0.20 \text{ m}^3 \text{ m}^{-3}$. Fig. 3-8 also shows that the effect of $\theta_{0.10}$ on r_{bulk} is conditional. Early in the growing season, $r_{bulk} r_a^{-1}$ was increasing and reached a maximum around DOY 148. Over the same period, $\theta_{0.10}$ in the WET hollow decreased from saturation to roughly $0.2 \text{ m}^3 \text{ m}^{-3}$ while I_G was increasing, reaching 50% of its maximum value. Low $\theta_{0.10}$ persisted in the WET hollow until DOY 169 while I_G continued to increase, thus lowering r_{bulk} through increasing LAI. Throughout the remainder of the growing season, WT and $\theta_{0.10}$ remained high. There were, nevertheless, notable changes in $r_{bulk} r_a^{-1}$ during the senescence period following DOY 243, where initially there was a rapid drop. The drop in $r_{bulk} r_a^{-1}$ directly followed a

week-long period without rain and coincided with several days of rain delivering a total of 49 mm. Subsequently, $r_{bulk} r_a^{-1}$ rose steadily in response to vascular senescence. While these results suggest early growing season estimates of r_{surf} from the three-source model are likely overestimated, particularly for wet microforms, the conditional bias does not necessarily refute our basic findings.

In order to validate results from the three-source model, porometry measurements were scaled according to Eq. 3.15 and modelled using the functional relations shown in Fig. 3-9. The three-source model does not treat the vascular canopy of hummocks and hollows separately, where results are segregated by site alone. Fig. 3-9 shows that the PPFD response curves are generally similar at all sites, while for the D response curves, the INT and DRY plot higher than the WET site implying that the WET site is more responsive to changes in D . It is important to note, however, that these values are normalized by the 5th percentile of r_{bulk} which was lowest at the WET site (see section 3.4.2). In order to calculate LE_v using the functional relations in Fig. 3-9, an estimate for a_1 (maximum conductance) was derived by solving Eq. 3.12 for where the median modelled daytime value using measured PPFD and D equaled the median r_v (Table 3-1). Median values of r_v were obtained by scaling median r_{leaf} (Fig. 3-5) according to the LAI of hummocks and hollows separately (Fig. 3-4) and then weighted according to the proportion of hummocks and hollows at each site to get total r_v estimates (Table 3-1). However, since the a_1 parameter is for total canopy estimates of LE, we would expect a_1 to scale with LAI. Since our measurements of LAI were infrequent, we used daily images of the study region to derive an index of plant phenology. Figure 3-10 shows the

transition from a low winter I_G , through rapid leaf out, early-summer peak, and a slow decline through late-summer and early autumn. In order to corroborate our I_G index we used changes in surface roughness derived from EC turbulence measurements. Under self-similar atmospheric stability conditions the relation between friction velocity (u^*) and wind speed (u) is governed by surface roughness (Holton, 1979). While daily variation in u/u^* follows a random normal distribution ($p = 0.40$), seasonal variation may be attributed to changes in surface roughness associated with increasing vegetation height or leaf area. The seasonal variation in u/u^* was used as a basic check on the validity of using I_G to vary LAI, where a simple quadratic fit to the u/u^* time series was used to assess potential seasonality in u/u^* . By evaluating the first derivative of u/u^* at zero, we obtained estimates of minimum seasonal values (*i.e.* highest surface roughness) between day of year (DOY) 193 and 218, which overlaps with the maximum I_G values. Based on the estimated median r_v of 112 s m^{-1} , 172 s m^{-1} , and 168 s m^{-1} at the WET, INT, and DRY sites respectively (Table 3-1), the corresponding a_I^{-1} values were estimated to be 25 s m^{-1} , 51 s m^{-1} , and 53 s m^{-1} which corresponds closely with 5th percentile of r_{bulk} obtained from half-hourly EC measurements. Although there is a degree of auto-correlation between the 5th percentile of r_{bulk} and a_I^{-1} since both use data obtained from EC measurements, the close correspondence in values is more fundamentally controlled by the r_{leaf} and LAI estimates which were obtained independently from porometry measurements and destructive sampling.

A comparison between the three-source estimate of LE_v , and LE_v modelled from functional relations and porometry measurements show reasonable correspondence with

each other (Fig. 3-11). Since there is uncertainty in both methods, an orthogonal least-squares regression was used to compare LE_v , where the best-fit lines were $0.97x - 11.1$ for WET, $1.22x - 6.4$ for INT $1.33x - 13.9$ for DRY, and for all results combined, $0.94x - 2.5$. In general, early growing season estimates of LE_v by residual are outliers for the WET site, but not for the INT and DRY sites. For both hummocks and hollows at the WET site, Fig. 3-7 suggests that r_{surf} may be overestimated which would result in an overestimation of LE_v . Despite a similar potential overestimation of r_{surf} at the INT and DRY site, the greater proportion of hummocks and relatively deep WT means not only that $\theta_{0.10}$ more accurately reflects θ_{surf} at the INT and DRY site hummocks, but also that behaviour of energy balance partitioning in hollows is less important from a site-scale perspective.

3.5 Implications and Conclusions

Although there is no change in the relative abundance of *C. calyculata* and *C. oligosperma* for hummocks and hollows individually when compared between WT treatments, the relative increase in hummocks at sites with increasing depth to WT has important implications for the total abundance of the various PFTs present within peatlands. Furthermore, there is a trade-off between decreasing LAI and the potential contribution from the moss surface, where all else being equal, lower LAI leads to greater available energy at the surface. Evaporative losses from the *Sphagnum* surface have been shown to be relatively high given an LAI of 0.4 to 0.7 $m^2 m^{-2}$ (Kim and Verma, 1996), but where the contribution of moss evaporation to total ET is reduced when surrounded by vascular vegetation (Heijmans *et al.*, 2004). Nevertheless, with total LAI across WT

treatments ranging from 1.7 to 2.3 $\text{m}^2 \text{m}^{-2}$, we observed a relatively high estimated evaporative contribution from the moss surface which is in accordance with partitioning estimates from other peatland studies (Kim and Verma, 1996; Kellner, 2001; Admiral and Lafleur, 2007).

By modelling canopy transpiration losses from leaf-level conductance measurements and EC-measured ET, we were able to corroborate our estimates of total moss evaporative losses. A transpiration model using functional relations derived from r_{bulk} was viewed as advantageous over extensive direct measurements in our study, such as by Admiral and Lafleur (2007), due to the need for simultaneous spatial and temporal coverage of all major vascular species given multiple sites. Moreover, the development of direct biophysical relations from porometry measurements is complicated by evergreen shrubs since, in addition to light, humidity, water status, nutrient content, and interactive effects related to position within the understory (Zeiger *et al.*, 1987), conductance is affected by leaf age (Field and Mooney, 1983). The development of probability distributions of peatland vascular leaf conductances using a pseudo-random sampling strategy across a range of environmental conditions provided the necessary constraint on the biophysical relations developed from EC measurements. Despite there being no significant difference in the distribution of leaf conductance for the dominant vascular species between WT treatments, there was a notable WT treatment effect on the D response of r_{bulk} . Humphreys *et al.* (2006) suggest that there are no large differences in the D - r_{bulk} relations between multiple peatland sites, but where differences in average r_{bulk} can be related to different r_{leaf} between PFTs (Korner *et al.*, 1979). Moreover, results

from Admiral and Lafleur (2007) suggest that the evaporative response to D is stronger from the moss surface compared to the vascular canopy, which suggests that the D - r_{bulk} relation will vary with LAI. Plot-scale measurements of instantaneous ET showed a difference in the D response based on WT treatment for hummocks, but not for hollows. This treatment effect in WET hummocks can be attributed to higher LAI and a greater abundance of relatively high conductance *C. calyculata*, where similar conductance values were shown for an ombrotrophic bog in eastern Canada (Admiral and Lafleur, 2007). In reference to the plot-scale measurements, differences in total ET between WT treatments can functionally be described by the relative proportion of microforms at each site, where the INT and DRY sites are more progressively dominated by hummocks, which have lower ET for a given D compared to WET hummocks and all hollows. Kettridge and Wadington (2013) showed a stronger response of r_{surf} to WT drawdown in hollows but not hummocks due to large differences in pore water pressure related to non-equilibrium pressure profiles, suggesting that greater ET at WET hummocks is not directly related to the shallow WT position. Brown *et al.* (2010) showed no significant difference in ET throughout the growing season between *Sphagnum* hummocks and hollows, but where surface θ was similarly low between microforms, and both had a sparse vascular canopy with less than 15% cover. Our results suggest that differences in ET between WT treatments, particularly for hummocks, are the result of differences in LAI and not strongly influenced by differences in surface moisture. Greater below-ground biomass production and a lower leaf to stem ratio are positively correlated with average WT depth, particularly for shrubs which dominate the hummock microforms

(Murphy and Moore, 2010). Consequently, with greater resource allocation to non-transpiring tissue (*i.e.* woody stems) in hummocks, and a difference in the proportion of microforms across WT treatments, PAI can remain high which serves as a limit on water loss from the moss surface through shading effects while constraining LAI which limits transpiration losses. Luken *et al.* (1985) suggest that the change in leaf to stem ratio of shrubs is the result of overgrowth of the stem of vascular vegetation by *Sphagnum*, causing increased fine-root production in the near surface. The implication herein is that the growth response of hummock forming *Sphagnum*, which are argued to control the direction and rate of microform succession (Luken *et al.*, 1985), to the WT treatments was an increase in increment growth length, thus driving the vascular response. This is supported by contemporary *Sphagnum* productivity and bulk density measurements at the research site, where surface bulk density was similar between microforms and WT treatments. Overall, *Sphagnum* net primary productivity was found to be higher in hummocks, where in particular the greater difference in productivity between *S. capillifolium* in hummocks and *S. angustifolium* in hollows was at the DRY site (Hribljan, 2012).

In the absence of direct canopy measurements, this study also demonstrates the usefulness of using a three-source model to estimate evaporative contributions from hummock and hollow surfaces, where surface wetness and LAI have a strong impact on spatial variability. In general, the model suggests that the sensitivity of r_{surf} to WT or near-surface moisture conditions decreases with increasing average depth to WT, where surface moisture variability is low with a deeper WT. Williams and Flanagan (1996) also

found that both conductance and evaporation from moss decreased as surface moisture decreased. If evaporative losses from the moss surface are in part controlled by the unsaturated hydraulic conductivity of the underlying peat, the highly non-linear nature of its decline with increasing depth to WT would effectively decouple r_{surf} from simple descriptors of moisture availability (Price, 1997). Therefore, for wet sites with relatively small microtopographic variation, the use of empirical relations between r_{surf} and surface moisture (*e.g.* Lawrence *et al.*, 2011) or WT (*e.g.* Sonnentag *et al.*, 2008) may be suitable. However, dryer sites would require a more physically-based approach using pore water pressure so that non-linear negative feedbacks to evaporative water loss could be accounted for (*e.g.* Kettridge and Waddington, 2013).

3.6 Acknowledgements

This research was funded by a Discovery Grant and Discovery Accelerator Supplement from the Natural Science and Engineering Research Council of Canada to JMW and by the U.S. Department of Agriculture, grant No. 0220341 to TGP. Additional financial support was provided by the U.S. Department of Energy's Office of Science (BER) through the Midwestern Regional Center of the National Institute for Climatic Change Research at Michigan Technological University. We would like to thank the U.S. Fish and Wildlife Service for permitting access to Seney National Wildlife Refuge, and the staff at SNWR for their kind accommodation. Finally, we would like to thank Drew Ballantyne and Reyna Peters for their field assistance.

3.7 References

- Admiral SW, Lafleur PM. 2007. Partitioning of latent heat flux at a northern peatland. *Aquatic botany*, **86**(2): 107-116.
- Andrus RE, Wagner DJ, Titus JE. 1983. Vertical zonation of Sphagnum mosses along hummock-hollow gradients. *Canadian Journal of Botany*, **61**(12): 3128-3139.
- Albert DA. 1995. Regional landscape ecosystems of Michigan, Minnesota, and Wisconsin: a working classification. U.S. Department of Agriculture technical report NC-178.
- Baldocchi D, Valentini R, Running S, Oechel W, Dahlman R. 1996. Strategies for measuring and modeling carbon dioxide and water vapour fluxes over terrestrial ecosystems. *Global Change Biology*, **2**: 159-168.
- Baldocchi DD, Law BE, Anthoni PM. 2000. On measuring and modeling energy fluxes above the floor of a homogeneous and heterogeneous conifer forest. *Agricultural and Forest Meteorology*, **102**(2): 187-206.
- Baldocchi DD, Vogel CA, Hall B. 1997. Seasonal variation of energy and water vapor exchange rates above and below a boreal jack pine forest canopy. *Journal of Geophysical Research: Atmospheres*, **102**(D24): 28939-28951.
- Baldocchi DD, Xu L, Kiang N. 2004. How plant functional-type, weather, seasonal drought, and soil physical properties alter water and energy fluxes of an oak-grass savanna and an annual grassland. *Agricultural and Forest Meteorology*, **123**(1): 13-39.
- Bedford BL, Godwin KS. 2003. Fens of the United States: Distribution, characteristics, and scientific connection versus legal isolation. *Wetlands*, **23**(3): 608-629.
- Blanken PD, Black TA, Yang PC, Neumann HH, Nesic Z, Staebler R, Den Hartog G, Novak MD, Lee X. 1997. Energy balance and canopy conductance of a boreal aspen forest: partitioning overstory and understory components. *Journal of Geophysical Research: Atmospheres*, **102**(D24): 28915-28927.
- Brown SM, Petrone RM, Mendoza C, Devito KJ. 2010. Surface vegetation controls on evapotranspiration from a sub-humid Western Boreal Plain wetland. *Hydrological Processes*, **24**(8): 1072-1085.
- Casselman T. 2009. Seney National Wildlife Refuge Comprehensive Conservation Plan. United States Fish and Wildlife Service.
- Clymo RS, Hayward PM. 1982. The ecology of Sphagnum. In *Bryophyte ecology* (pp. 229-289). Springer Netherlands.
- Comer NT, Lafleur PM, Roulet NT, Letts MG, Skarupa M, Verseghy DL. 1999. A Test of the Canadian Land Surface Scheme (CLASS) for a Variety of Wetland Types. *Atmos. Environ.* **38**: 161-179.

- Devito K, Mendoza C, Qualizza C. 2013. Conceptualizing Water Movement in the Boreal Plains: Implications for Watershed Reconstruction, Synthesis report prepared for the Canadian Oil Sands Network for Research and Development. Environmental and Reclamation Research Group.
- Ducoudre NI, Laval K, Perrier A. 1993. SECHIBA, A new set of parameterizations of the hydrologic exchanges at the land atmosphere interface within the LMD atmospheric general-circulation model. *Journal of Climatology*. **6**: 248-273.
- Field C, Mooney HA. 1983. Leaf age and seasonal effects on light, water, and nitrogen use efficiency in a California shrub. *Oecologia*, **56**(2-3): 348-355.
- Frolking S, Talbot J, Jones MC, Treat CC, Kauffman JB, Tuittila ES, Roulet N. 2011. Peatlands in the Earth's 21st century climate system. *Environmental Reviews*, **19**: 371-396.
- Gorham E. 1991. Northern peatlands: role in the carbon cycle and probable responses to climatic warming. *Ecological applications*, **1**(2): 182-195.
- Hayward PM, Clymo RS. 1982. Profiles of water content and pore size in Sphagnum and peat, and their relation to peat bog ecology. *Proceedings of the Royal Society of London. Series B. Biological Sciences*, **71**(3): 299-325.
- Heijmans MMPD, Arp WJ, Chapin III FS. 2004. Controls on moss evaporation in a boreal black spruce forest. *Global Biogeochemical Cycles*. **18**, GB2004, doi: 10.1029/2003GB002128.
- Heinselman ML. 1965. String Bogs and Other Patterned Organic Terrain Near Seney, Upper Michigan. *Ecology*, **46**(1-2): 185-188.
- Hribljan J. 2012. The effect of long-term water table manipulations on vegetation, pore water, substrate quality, and carbon cycling in a northern poor fen peatland. (PhD thesis – Michigan Technological University).
- Humphreys ER, Lafleur PM, Flanagan LB, Hedstrom N, Syed KH, Glenn AJ, Granger R. 2006. Summer carbon dioxide and water vapour fluxes across a range of northern peatlands. *Journal of Geophysical Research*, **111**, G04011, doi:10.1029/2005JG000111.
- Jarvis PG. 1976. The interpretation of the variations in leaf water potential and stomatal conductance found in canopies in the field. *Philosophical Transactions of the Royal Society of London. B, Biological Sciences*, **273**(927): 593-610.
- Kellner E. 2001. Surface energy exchange and hydrology of a poor *Sphagnum* mire. (PhD thesis -- Uppsala University, Sweden).
- Kellner E, Halldin S. 2002. Water budget and surface-layer water storage in a *Sphagnum* bog in central Sweden. *Hydrological Processes*, **16**: 87-103.

- Kettridge N, Waddington JM. 2013. Towards quantifying the negative feedback regulation of peatland evaporation to drought. *Hydrological Processes*, DOI: 10.1002/hyp.9898.
- Kellner E, Lundin L-C. 2001. Calibration of time domain reflectometry for water content in peat soil. *Nordic Hydrology* **32** (4/5): 315-332.
- Kim J, Verma SB. 1996. Surface exchange of water vapour between an open Sphagnum fen and the atmosphere. *Boundary-Layer Meteorol.* **79**: 243-264.
- Korner C, Scheel JA, Bauer H. 1979. Maximum leaf diffusive conductance in vascular plants. *Photosynthetica*, **13**: 45-82.
- Kowalski KP, Wilcox DA. 2003. Differences in sedge fen vegetation upstream and downstream from a managed impoundment. *The American Midland Naturalist*, **150**(2): 199-220.
- Lafleur PM, Hember RA, Admiral SW, Roulet NT. 2005. Annual and seasonal variability in evapotranspiration and water table at a shrub-covered bog in southern Ontario, Canada. *Hydrological Processes*. **19**: 3533-3550.
- Laiho R, Minkinen K, Anttila J, Vávřová P, Penttilä T. 2008. Dynamics of litterfall and decomposition in peatland forests: Towards reliable carbon balance estimation?. In *Wastewater treatment, plant dynamics and management in constructed and natural wetlands* (pp. 53-64). Springer Netherlands.
- Lawrence DM, Oleson KW, Flanner MG, Thornton PE, Swenson SC, Lawrence PJ, Zeng XB, Yang ZL, Levis S, Sakaguchi K, Bonan GB, Slater AG. 2011. Parameterization improvements and functional and structural advances in version 4 of the Community Land Model. *J. Adv. Earth Syst.* **3**, DOI: 10.1029/2011MS000045.
- Lawrence DM, Slater AG. 2008. Incorporating organic soil into a global climate model. *Clim. Dyn.* **30**: 145-160. DOI: 10.1007/s00382-007-0278-1.
- Letts MG, Roulet NT, Comer NT, Skarupa MR, Verseghe DL. 1999. Parametrization of Peatland Hydraulic Properties for the Canadian Land Surface Scheme. *Atmos. Ocean.* **38**: 141-160.
- Luken JO, Billings WD, Peterson KM. 1985. Succession and biomass allocation as controlled by Sphagnum in an Alaskan peatland. *Canadian journal of botany*, **63**(9): 1500-1507.
- Malmer N, Svensson BM, Wallén B. 1994. Interactions between Sphagnum mosses and field layer vascular plants in the development of peat-forming systems. *Folia Geobotanica et Phytotaxonomica*, **29**(4): 483-496.
- McCarter CPR, Price JS. 2012. Ecohydrology of *Sphagnum* moss hummocks: mechanisms of capitula water supply and simulated effects of evaporation. *Ecohydrology*, DOI: 10.1002/eco/1313.

- Macrae ML, Devito KJ, Strack M, Waddington JM. 2013. Effect of water table drawdown on peatland nutrient dynamics: implications for climate change. *Biogeochemistry*, **112**(1-3): 661-676.
- Miller CA. 2011. The Effect of Long-Term Drainage on Plant Community Composition, Biomass, and Productivity in Boreal Continental Peatlands. (Master's thesis – University of Guelph).
- Molder M, Kellner E. 2001. Excess resistance of bog surfaces in central Sweden. *Agricultural and Forest Meteorology*, **112**: 23-30.
- Moore PA, Pypker TG, Waddington JM. 2013. Effect of long-term water table manipulation on peatland evapotranspiration. *Agricultural and Forest Meteorology*, **178-179**: 106-119, DOI: 10.1016/j.agrformet.2013.04.013
- Murphy MT, Moore TR. 2010. Linking root production to aboveground plant characteristics and water table in a temperate bog. *Plant and soil*, **336**(1-2): 219-231.
- Price J. 1997. Soil moisture, water tension, and water table relationships in a managed cutover bog. *Journal of hydrology*, **202**(1): 21-32.
- Price JS, Edwards TW, Yi Y, Whittington PN. 2009. Physical and isotopic characterization of evaporation from *Sphagnum* moss. *Journal of Hydrology*, **369**(1): 175-182.
- Price JS, Maloney DA. 1994. Hydrology of a patterned bog-fen complex in southeastern Labrador, Canada. *Nordic Hydrology*, **25**(5): 313-330. doi:10.2166/nh.1994.020
- Roulet N, Moore T, Bubier J, Lafleur P. 1992. Northern fens: methane flux and climatic change. *Tellus: Series B*. **44**(2): 100-105.
- Rydin H, Jeglum JK, Hooijer A. 2006. The biology of peatlands. Oxford University Press, Oxford, New York, 343 pp.
- Saarinen T. 1996. Biomass and production of two vascular plants in a boreal mesotrophic fen. *Canadian Journal of Botany*, **74**(6): 934-938.
- Schulze ED, Kelliher FM, Korner C, Lloyd J, Leuning R. 1994. Relationships among maximum stomatal conductance, ecosystem surface conductance, carbon assimilation rate, and plant nitrogen nutrition: a global ecology scaling exercise. *Annual Review of Ecology and Systematics*, **25**: 629-660.
- Sonnentag O, Chen JM, Roulet NT, Ju W, Govind A. 2008. Spatially explicit simulation of peatland hydrology and carbon dioxide exchange: Influence of mesoscale topography. *J. Geophys. Res.* **113**, G02005, doi: 10.1029/2007JG000605.
- Stannard DI. 1988. *Use of a hemispherical chamber for measurement of evapotranspiration*. Department of the Interior, US Geological Survey.
- Stewart JB, Thom AS. 1973. Energy budgets in pine forest. *Quarterly Journal of the Royal Meteorological Society*, **99**: 154-170.

- Sundström E, Magnusson T, Hånell B. 2000. Nutrient conditions in drained peatlands along a north-south climatic gradient in Sweden. *Forest ecology and management*, **126**: 149-161.
- Szeicz G. 1974. Solar radiation for plant growth. *Journal of Applied Ecology*, **11**(2): 617-636.
- Takagi K, Tsuboya T, Takahashi H, Inoue T. 1999. Effect of the invasion of vascular plants on heat and water balance in the Sarobetsu mire, northern Japan. *Wetlands*, **19**(1): 246-254.
- Udo SO, Aro TO. 1999. Global PAR related to global solar radiation for central Nigeria. *Agricultural and Forest Meteorology*, **97**(1): 21-31.
- Verseghy DL, McFarlane NA, Lazare M. 1993. CLASS – a Canadian land surface scheme for GCMs, II, Vegetation model and coupled runs. *Int. J. Climatol.* **13**: 347-370.
- Vitt DH, Halsey LA, Bauer IE, Campbell C. 2000. Spatial and temporal trends in carbon storage of peatlands of continental western Canada through the Holocene. *Canadian Journal of Earth Sciences*, **37**(5): 683-693.
- Weiss A, Norman JM. 1985. Partitioning solar radiation into direct and diffuse, visible and near-infrared components. *Agricultural and Forest meteorology*, **34**(2): 205-213.
- Wells E, Williams B. 1996. Effects of drainage, tilling and PK-fertilization on bulk density, total N, P, K, Ca and Fe and net N-mineralization in two peatland forestry sites in Newfoundland, Canada. *Forest ecology and management*, **84**: 97-108.
- Weltzin JF, Pastor J, Harth C, Bridgham SD, Updegraff K, Chapin CT. 2000. Response of bog and fen plant communities to warming and water-table manipulations. *Ecology*, **81**(12): 3464-3478.
- Weltzin JF, Bridgham SD, Pastor J, Chen J, Harth C. 2003. Potential effects of warming and drying on peatland plant community composition. *Global Change Biology*, **9**(2), 141-151.
- Wilcox DA, Sweat MJ, Carlson ML, Kowalski KP. 2006. A water-budget approach to restoring a sedge fen affected by diking and ditching. *Journal of Hydrology*, **320**: 501-517.
- Williams TG, Flanagan LB. 1996. Effect of changes in water content on photosynthesis, transpiration and discrimination against ^{13}C and $\text{C}_{18}\text{O}_{16}\text{O}$ in *Pleurozium* and *Sphagnum*. *Oecologia*, **108**(1): 38-46.
- Zeiger E, Farquhar G, Cowan I. 1987. Stomatal Function. Stanford University Press. pp.520

3.8 Tables

Table 3 - 1: Summary of microtopography and vegetation characteristics across study sites.

Variable	WET	INT	DRY
Avg. height (m) of hummocks (\pm SE)	0.15 (0.01)	0.30 (0.02)	0.41 (0.03)
Proportion of hummocks and hollow	0.41 / 0.59	0.52 / 0.48	0.63 / 0.37
LAI ($\text{m}^2 \text{m}^{-2}$) – <i>hummocks</i> (\pm SE)	2.7 (0.18)	1.5 (0.06)	1.9 (0.19)
LAI ($\text{m}^2 \text{m}^{-2}$) – <i>hollows</i> (\pm SE)	2.0 (0.32)	1.9 (0.45)	1.3 (0.04)
PAI ($\text{m}^2 \text{m}^{-2}$)	2.8 (0.52)	1.9 (0.18)	2.6 (0.27)
r_v^{\S} – <i>hummocks / hollows</i> (s m^{-1})	92 / 133	166 / 178	141 / 248
r_v^{\S} – <i>total</i> (s m^{-1})	112	172	168

[§] - Estimated from LAI, median stomatal resistance (r_{st}) (Fig. 3-5), and proportion of hummocks and hollows at each site

Table 3 - 2: Summary of the ET components from EC and three-source model (Eq. 3.3-8) over the 2010 growing season.

Variable	WET	INT	DRY
LE – <i>total</i> (mm)	434	341	317
LE _v – <i>canopy</i> (mm / %)	337 / 0.78	188 / 0.55	211 / 0.67
LE _{surf} – <i>hummock</i> (mm / %)	21 / 0.05	98 / 0.29	58 / 0.18
LE _{surf} – <i>hollow</i> (mm / %)	76 / 0.17	55 / 0.16	48 / 0.15

3.9 Figures

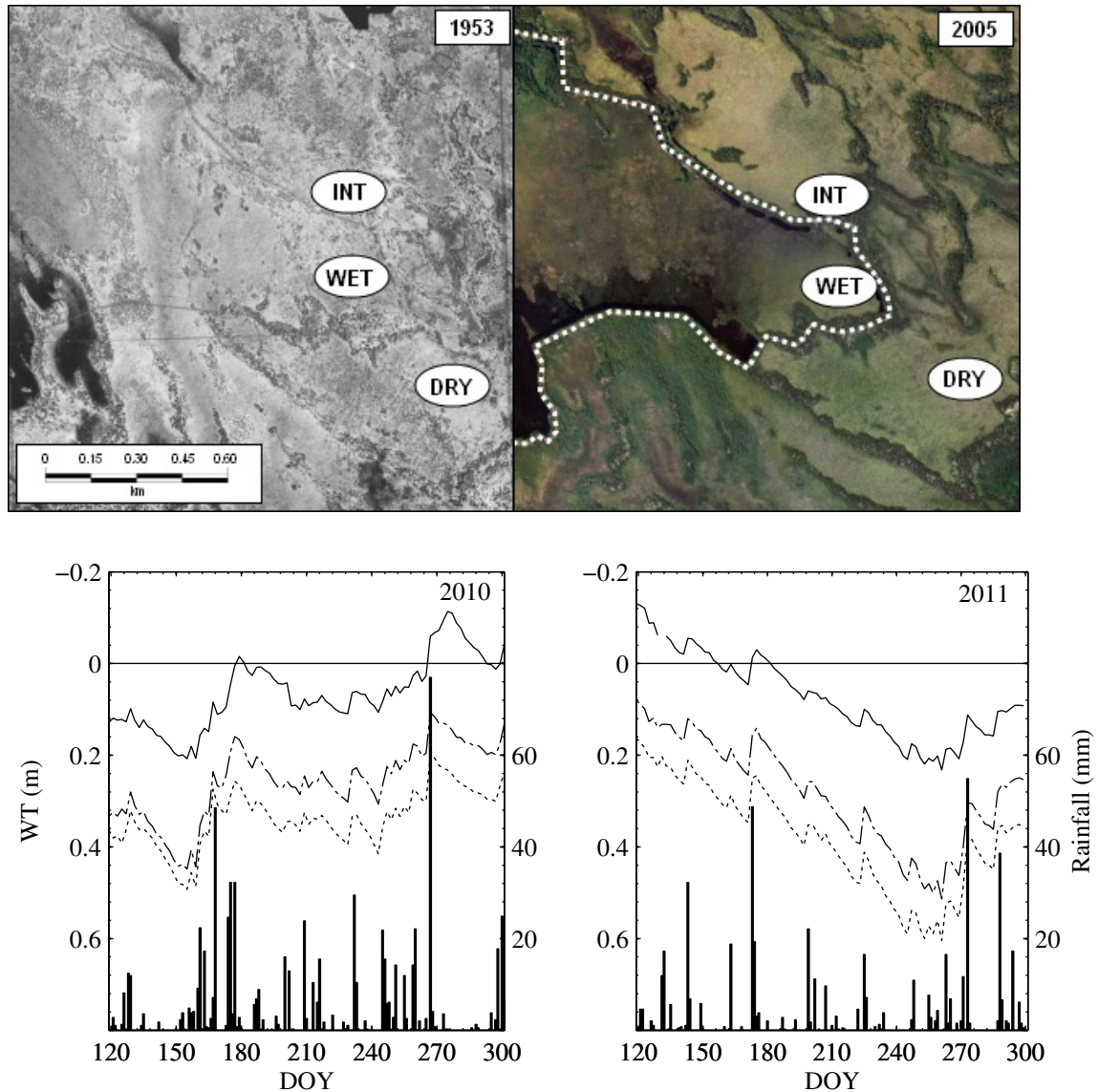


Figure 3 - 1: Seney National Wildlife Refuge (SNWR) study area in the Upper Peninsula of Michigan (46.20° N, 86.02° W, elev. ~205 m a.s.l.) showing the three primary sampling locations. The top-left panel shows the study area prior to berm construction (SNWR airphoto BWD-5K-147) and general flow direction (white arrow), while the top-right panel shows the location of the berm (white dashed line) and impact on surface ponding (Google Earth – imagery date: 31/05/2005 – USDA Farm Service Agency). Daily total rainfall (bars) and water table levels for the WET (solid), INT (dash-dot), and DRY (dot) sites are shown for the 2010 (bottom-left) and 2011 (bottom-right) growing seasons.

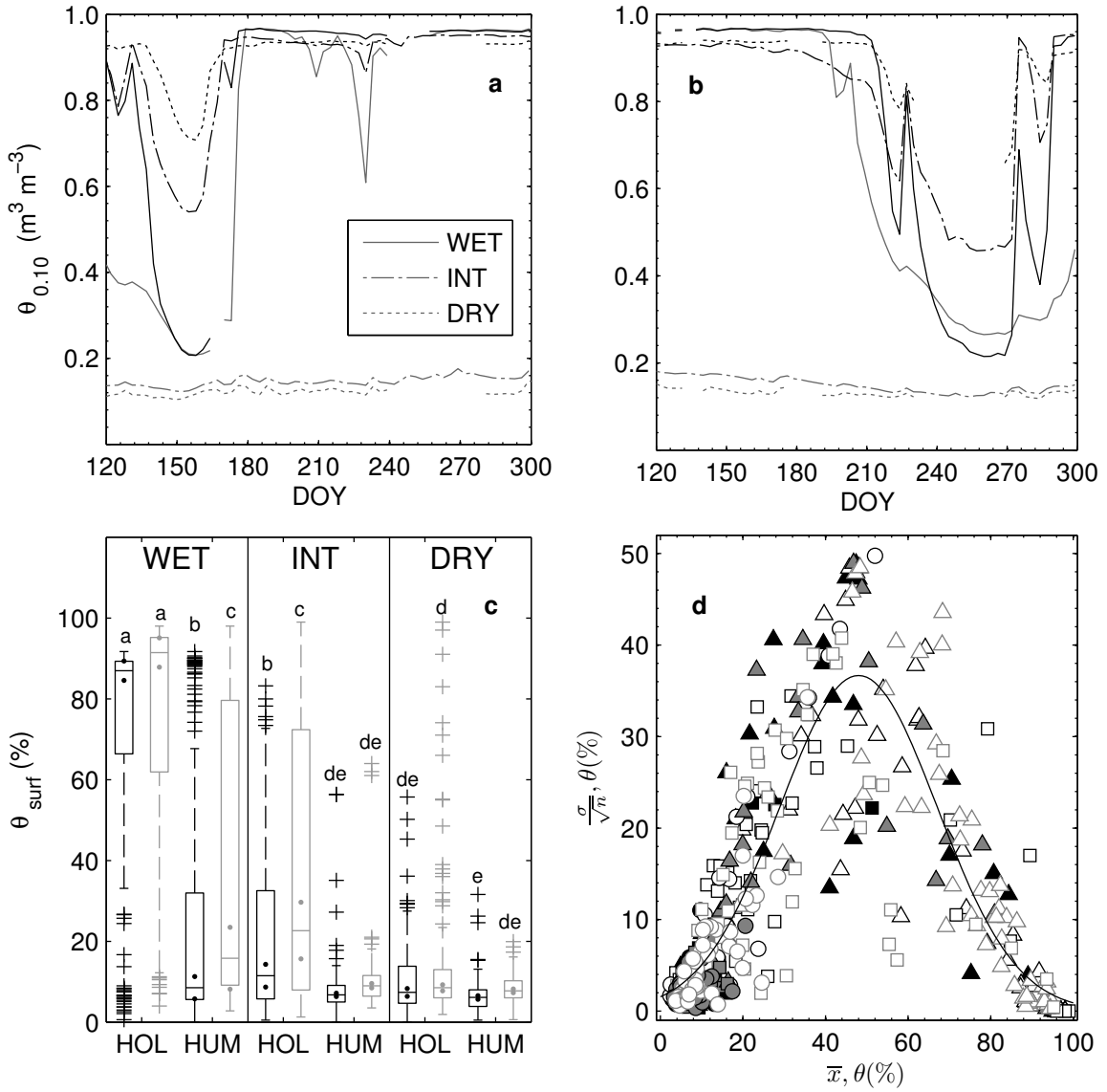


Figure 3 - 2: Temporal variability in near-surface θ ($\theta_{0.10}$) at all three sites in a representative hummock (grey) and hollow (black) over the 2010 (a) and 2011 (b) growing seasons. Boxplot comparison of plot-measured surface θ (θ_{surf}) where dots are the confidence interval on the median, crosses represent outliers, and letters represent significant differences ($\alpha = 0.05$) using Tukey's hsd (c). Spatio-temporal variability in θ_{surf} within 0.6 x 0.6 m plots ($n = 4$) for hummock (solid) and hollows (open) at the WET (Δ), INT (\square), and DRY (\circ) sites (d). Gaussian fit (solid line) parameters: $scale = 36.7$; $mean = 48.0$; and $std = 27.0$.

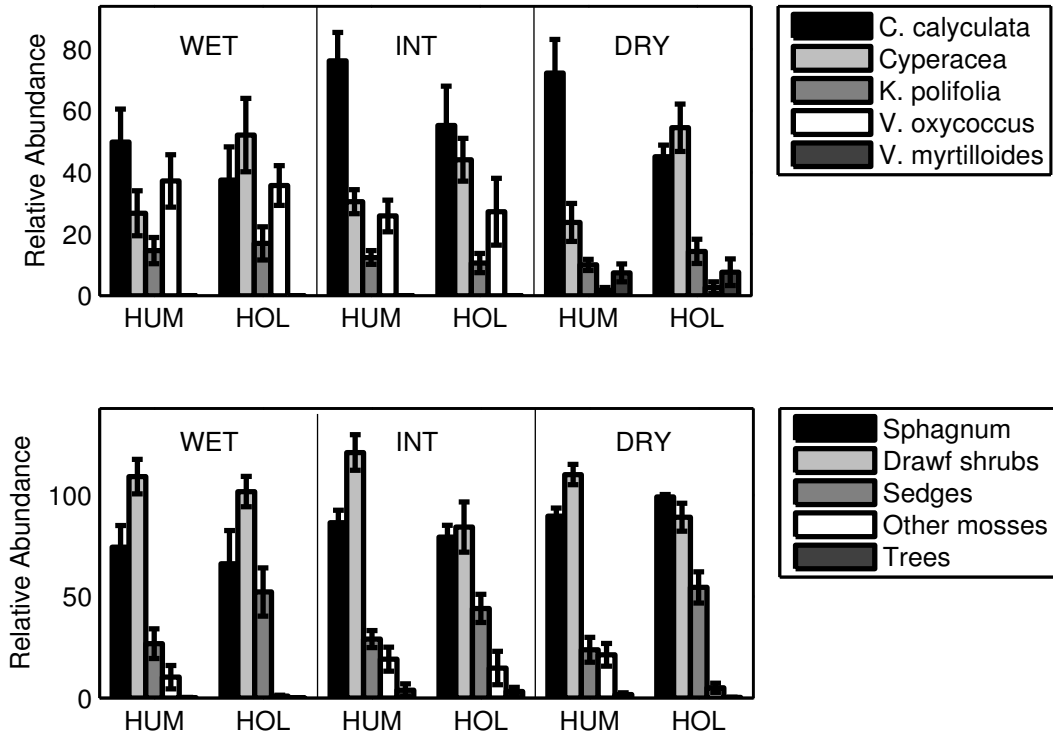


Figure 3 - 3: Relative abundance from vegetation survey using a 10 x 10 grid-intercept method for a 1 m² area centered on each of the chamber collars.

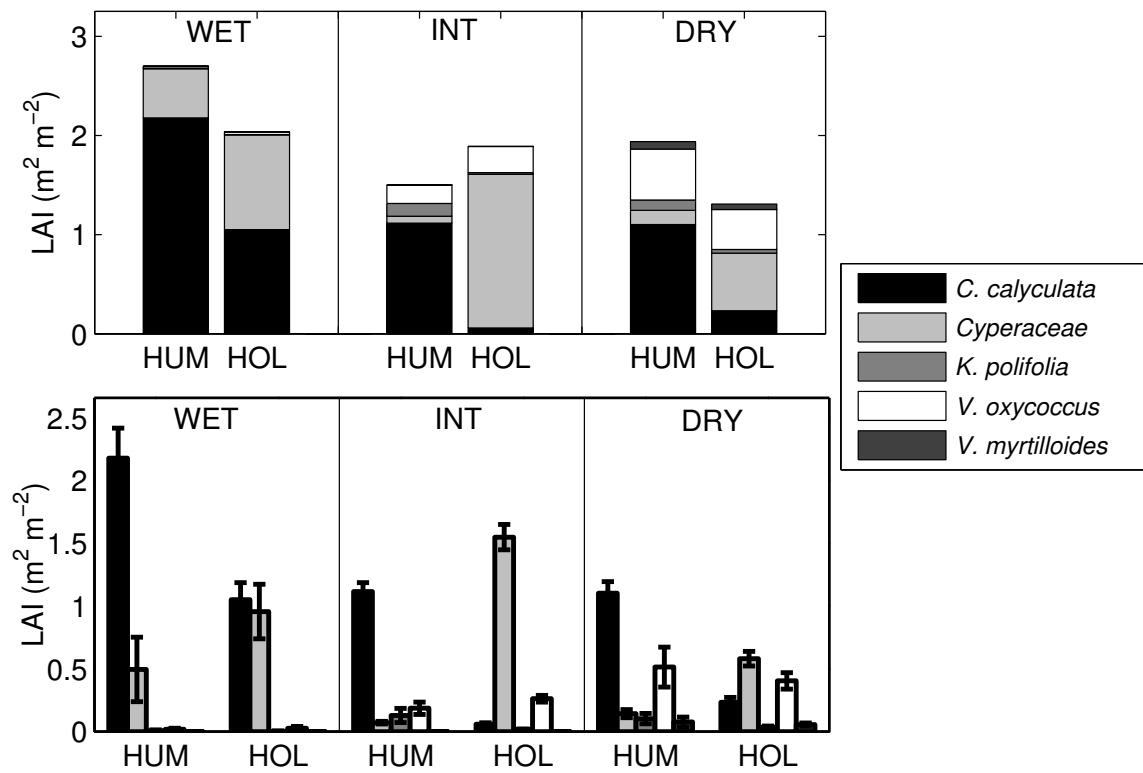


Figure 3 - 4: One-sided leaf area from destructive sampling plots (top) and mean leaf area and standard deviation (error bars) for live vascular vegetation based on four 0.25 m² plots (bottom).

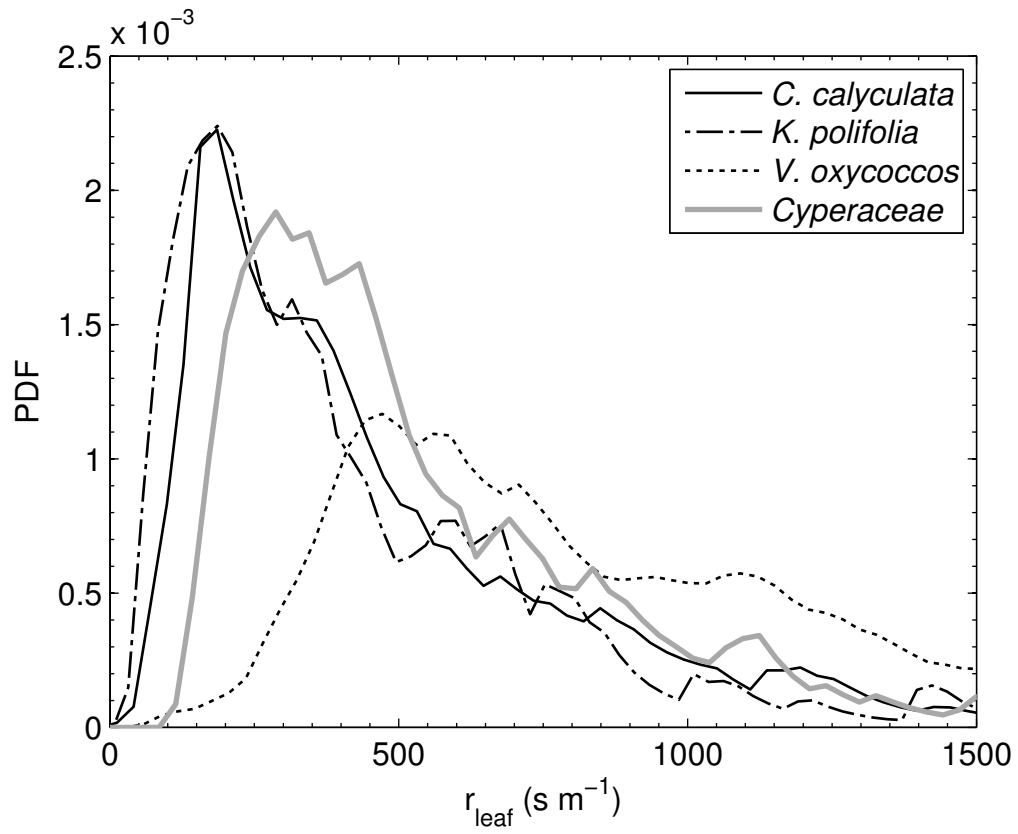


Figure 3 - 5: Distribution of stomatal resistance (r_{leaf}) values from daytime porometry measurements for the dominant vascular species.

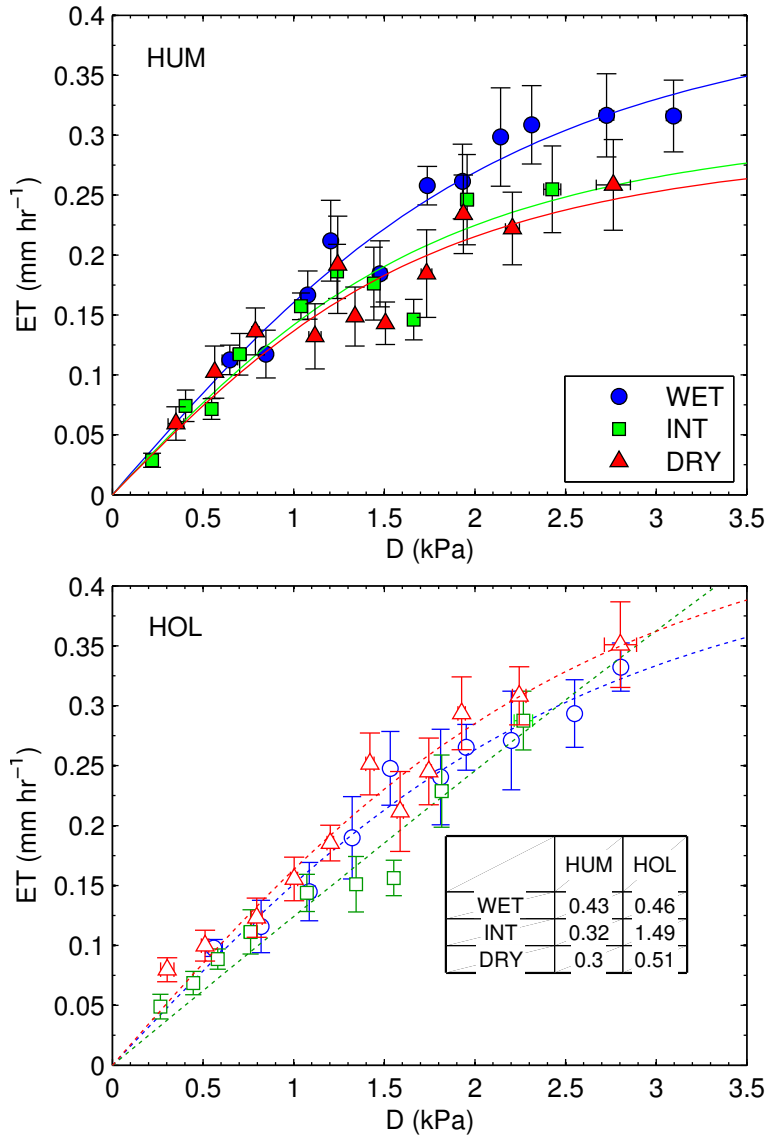


Figure 3 - 6: Chamber ET response (ET_{ch}) to vapour pressure deficit D , for PPFD > 1000 $\mu\text{mol m}^{-2} \text{s}^{-1}$.

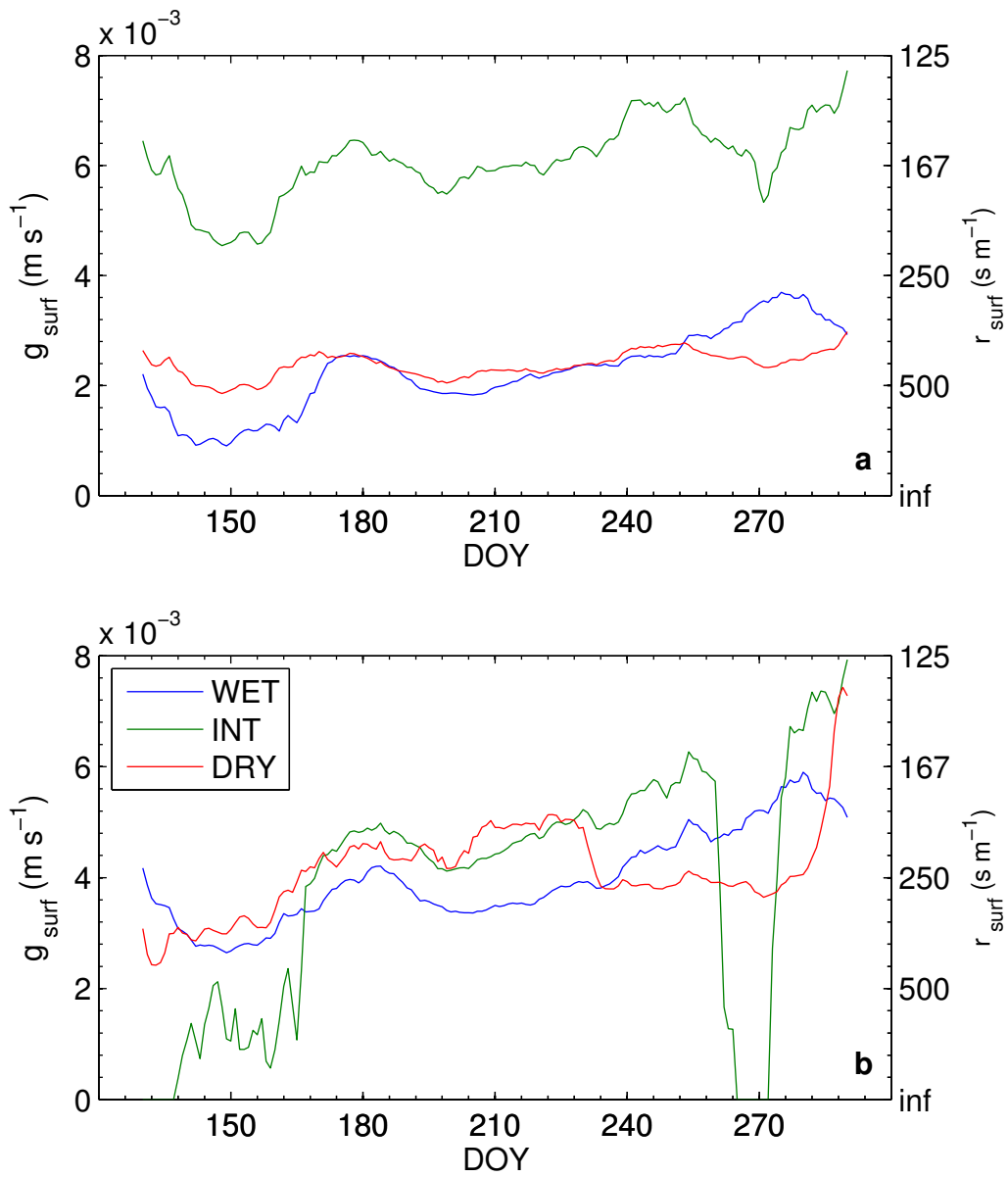


Figure 3 - 7: Daily modeled surface conductance (g_{surf}) / resistance (r_{surf}) for a hummock (a) and hollow (b) at each site, determined using a modified three-source model derived from Kim and Verma (1996).

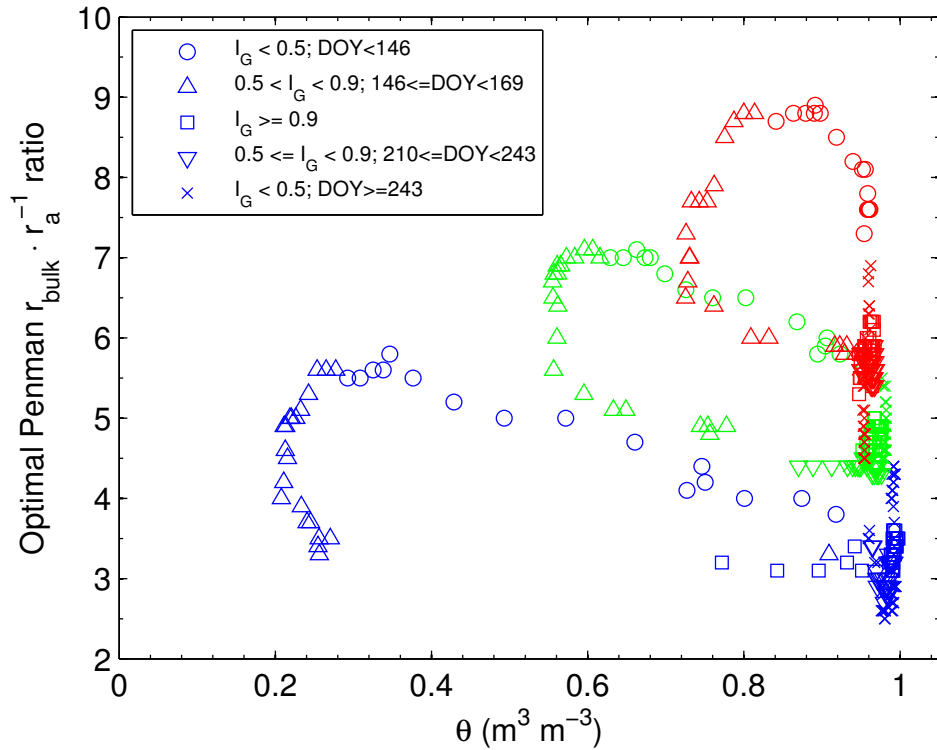


Figure 3 - 8: Response of $r_{bulk} r_a^{-1}$ to $\theta_{0.10}$ at the WET (blue), INT (green), and DRY (red) sites over the 2010 growing season.

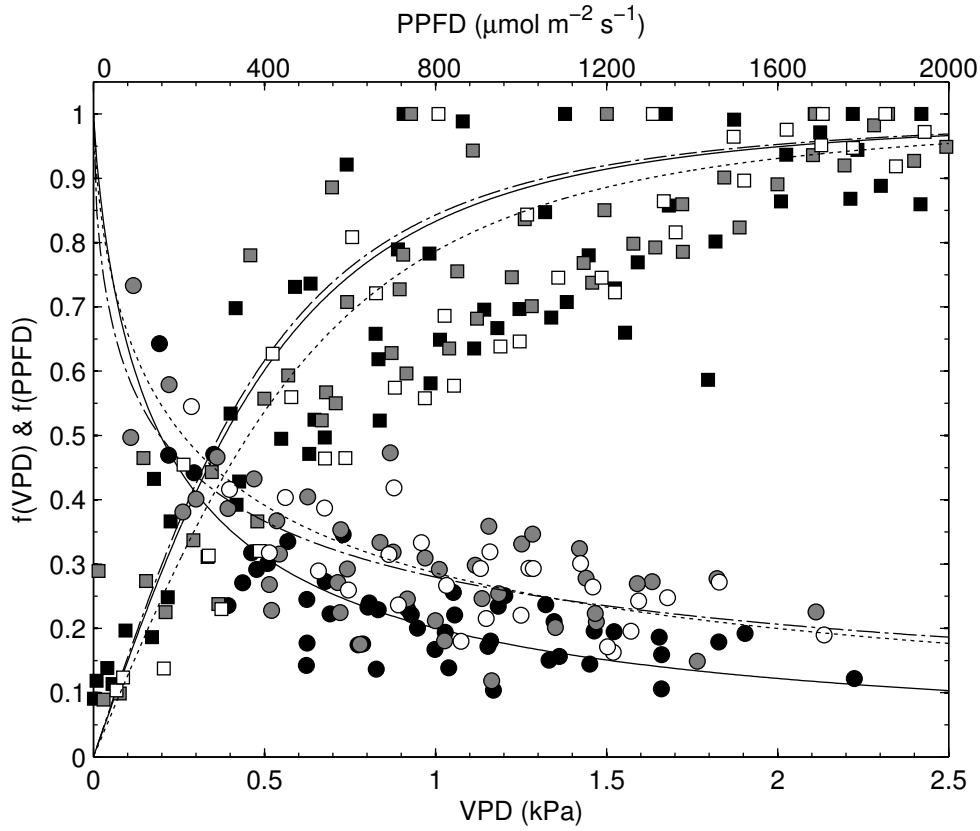


Figure 3 - 9: Jarvis-style component functions describing the relative control of $PPFD$ (squares) and D (circles) on bulk surface conductance (r_b^{-1}) for the WET (black), INT (grey), and DRY (white) sites. $PPFD$ data points are bin averages of 50 daytime half-hour measurements where D is relatively constant, and vice versa for D data points. The best fit parameters for $PPFD$ (see Eq. 2.13) and D (see Eq. 2.14) curves are: $a_2 = 1.9E-03 / 2.0E-03 / 1.6E-03$, $a_3 = 0.25 / 0.39 / 0.40$, and $a_4 = 0.85 / 0.58 / 0.68$ for WET (solid) / INT (dashed) / DRY (dotted) respectively.

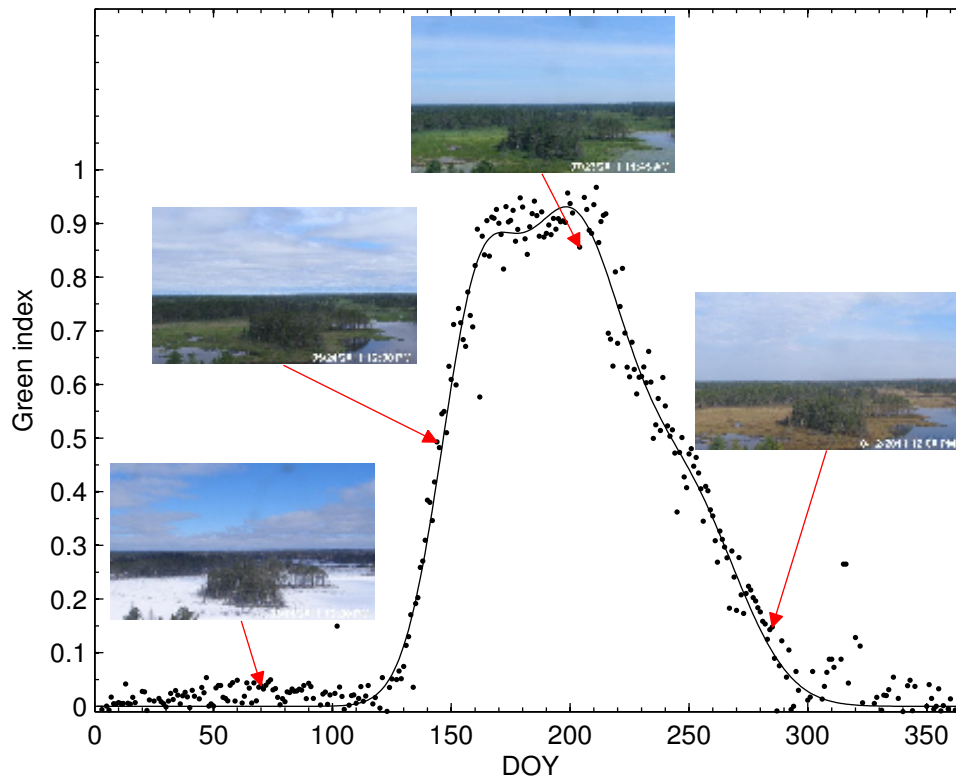


Figure 3 - 10: Green index (dots) during 2010 based on changes in the spectral characteristics of the lower left portion of daily images taken at SNWR at 12:00. A summation of several Gaussian curves was used to fit measured data (black line).

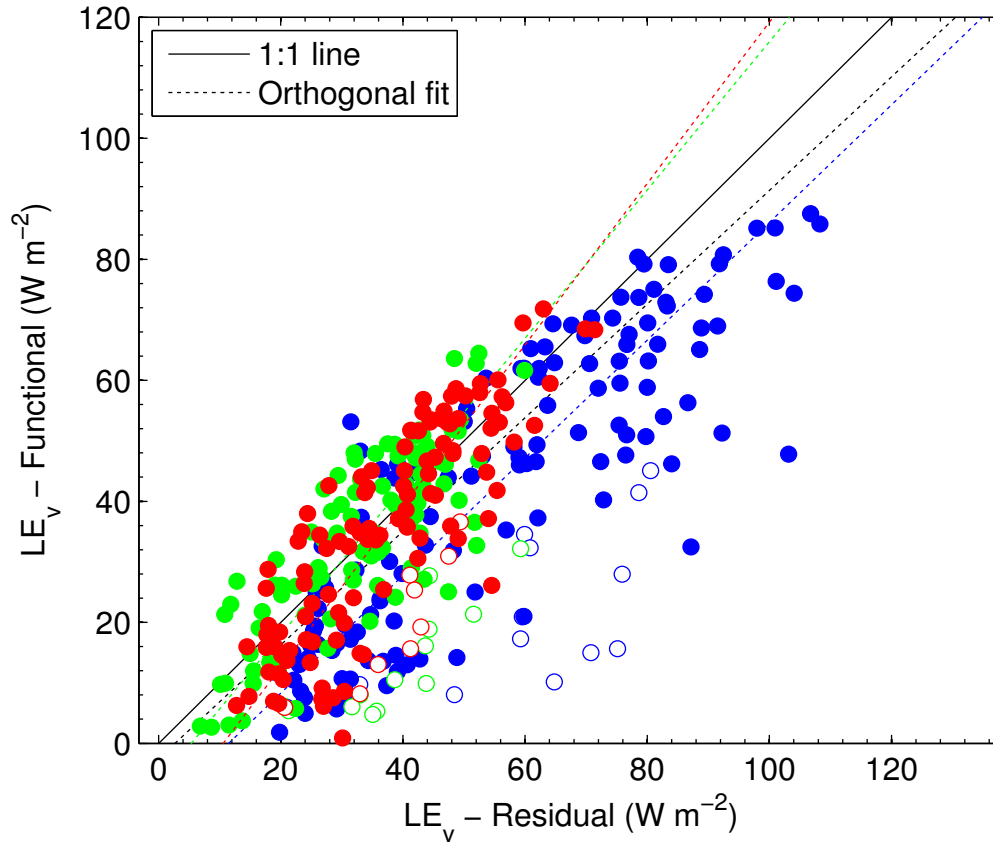


Figure 3 - 11: Comparison of canopy LE estimated from the phenomenological model (x-axis) and the residual of the measured LE and estimated surface LE (y-axis) for the WET (blue), INT (green) and DRY (red) sites. Open circles represent 'early' growing season values up to DOY 141.

CHAPTER 4: MULTI-DECADAL WATER TABLE MANIPULATION ALTERS PEATLAND HYDRAULIC STRUCTURE AND MOISTURE RETENTION

4.1 Abstract

A peatland complex disturbed by berm construction in the 1950's was used to examine the long-term impact of water table (WT) manipulation on peatland hydraulic properties and moisture retention at three adjacent sites with increasing depth to WT (WET, INTermediate, and DRY). By examining long-term differences between sites, it allows for vegetation and microtopographic succession to occur in response to the initial disturbance. Saturated hydraulic conductivity (K_s) was found to decrease with depth by several orders of magnitude over a depth of 1-1.5 m, but where the lowest average measured K_s was at the DRY site at depth. The depth-dependence of WT response to rainfall was broadly similar across WT treatments, where WT response was large (5:1) at a depth of 0.5 m, and near 1:1 at the surface. However, with a greater average depth to WT, the INT and DRY sites experienced greater WT fluctuations compared to the WET site. Differences in specific yield between sites were relatively small in comparison to differences between hummocks and hollows, where surface values were similar, but where the rate of decrease with depth was 0.014 cm^{-1} in hollows and 0.007 cm^{-1} in hummocks. A greater decrease in sample volume with drying was observed for hollows (16%) compared to hummocks (8%) and for the WET site samples (13%) relative to the INT (11%) and DRY (10%) sites.

Bulk density (ρ_b) exhibits a similar depth-dependent pattern, where median surface values for both hummocks and hollows were 21 kg m^{-3} , but respectively increased to 23 and 59 kg m^{-3} by 22.5 cm depth. Based on 5 cm depth increments, there was a significant increase in ρ_b at the WET, INT and DRY site at depth between 7.5 and 12.5 cm in hollows, and between 17.5 and 47.5 cm in hummocks. For pore water pressures (ψ) ranging from -5 to -500 mb, there were greater differences in moisture retention between hummocks and hollows compared to differences between sites, where hollow samples retained more water for samples from 0 to 25 cm. However, the estimated residual water content from the Van Genuchten equation for surface *Sphagnum* samples, while on average lower in hummocks ($0.082 \text{ m}^3 \text{ m}^{-3}$) versus hollows ($0.087 \text{ m}^3 \text{ m}^{-3}$), increased from WET ($0.058 \text{ m}^3 \text{ m}^{-3}$) to INT ($0.088 \text{ m}^3 \text{ m}^{-3}$) to DRY ($0.108 \text{ m}^3 \text{ m}^{-3}$) which has important implications for moisture stress under persistent conditions of WT drawdown. ρ_b alone explains a high amount of variance ($r^2 > 0.69$) in moisture retention across a range of ψ (-15 to -500 mb), where a log-linear equation describes well how ρ_b -dependent retention changes with ψ ($r^2 = 0.967$). Since ρ_b has good explanatory power for describing moisture retention across WT treatments, and the depth-dependence of ρ_b differs between sites and microforms, from a modelling perspective moisture-retention parameterizations which correlate well with ρ_b may be seen as advantageous, where we propose a logistic equation as an alternative to the Van Genuchten equation.

4.2 Introduction

Peatlands store ~10% of the global surface freshwater (Holden, 2005) and account for approximately one-third of the terrestrial soil carbon pool (Gorham, 1991). However,

there is a concern these water and carbon stores may be at risk to due to climate change (e.g., Ise et al., 2007) as vapour pressure deficits, evapotranspiration and summer moisture deficits are expected to increase, leading to greater water table (WT) drawdown (Roulet *et al.*, 1992) in northern continental regions where peatlands are prevalent (Gorham, 1991). In-situ short-term field studies have demonstrated that peatland WT drawdown leads to peat subsidence (Waddington *et al.*, 2010), altered carbon fluxes and vegetation community (Strack and Waddington, 2007; Chivers *et al.*, 2009), increased peat bulk density (ρ_b), decreased specific yield (S_y) and saturated hydraulic conductivity (K_s) (Whittington and Price, 2006), increased above-ground shrub and tree biomass (Pellerin and Lavoie, 2003; Weltzin *et al.*, 2003), and a greater competitive advantage for hummock *Sphagnum* species (Grosvernier *et al.*, 1997; Robroek *et al.*, 2007), but an overall decrease in *Sphagnum* cover (Gunnarsson *et al.*, 2002). Conversely, the long-term ecohydrological response to changes in WT will likely be mediated by continued vegetation succession (Strack and Waddington, 2007) and a different hydrological response between peatland hummock and hollow microforms (Whittington and Price, 2006). However, not only is there a dearth of studies examining the peat hydrophysical properties of peatland microforms, but literature on the long-term impacts of WT manipulation in the absence of other land-use impacts, such as horticultural extraction (e.g. Schwarzel *et al.*, 2002; Gnatowski *et al.*, 2010) or wildfire (e.g. Sherwood *et al.*, 2013) are limited. The aim of this research is to examine the effect of long-term WT manipulation on peatland hydraulic structure and peat moisture retention.

Sphagnum mosses are non-vascular species, and so rely on capillary transport to meet surface evaporative demand and to supply the apical bud (capitula) with the water necessary for physiological processes. Consequently, moisture status is related to WT depth, particularly when capillary flow is able to meet evaporative demand. The ability of hummock forming species (*e.g. Sphagnum fuscum* and *S. capillifolium*) to grow relatively high above the WT is linked not only to the greater moisture retention in capitula (Hayward and Clymo, 1982), but also due to a greater ability to conduct water up from the WT under dry conditions (McCarter and Price, 2012) and greater desiccation avoidance (Schipperges and Rydin, 1998; Hajek and Beckett, 2008). Conversely, hollow species (*e.g. Sphagnum cuspidatum* and *S. angustifolium*) are able to outcompete hummock species due to higher productivity under wet conditions (Gunnarsson, 2005) and a greater ability to minimize depth to WT through deformation of the peat matrix with changing pore water pressure (ψ) (Price, 2003). Moreover, changes in temperature and water supply to hummock-forming *Sphagnum fuscum* moss capitula can lead to changes in bulk density and by extension peat moisture retention (Boelter, 1969) through changing community structure (Dorrepaal *et al.*, 2003). Therefore, with a persistent change in WT level, a systematic difference in the moisture retention properties may develop within hummocks over time.

Strack *et al.* (2009) suggest that resilience of the peatland carbon pool to climate change may be controlled by the contemporary distribution of *Sphagnum* moss species that occupy both hummock and hollow habitats, whereby a change in the moss community, coupled with the associated internal ecohydrological feedbacks (*e.g.*,

Kettridge *et al.*, 2013), may enhance peatland resilience to WT drawdown through the expansion of hummock microforms. While a shift to a greater abundance of hummock forming species may represent a negative feedback to carbon loss due to the inherent recalcitrance of hummock forming *Sphagnum* (Coulson and Butterfield, 1978; Turetsky *et al.*, 2008), the slower decay rates may help limit decomposition and peat subsidence in hummock microforms. Consequently, we argue that in order to evaluate the hydrological response of peatlands to increased moisture deficit under future climate change scenarios, including changes in WT level, storage, surface ψ , and moss evaporation, the hydrophysical properties of peat must be well defined. Here we examine peatland hydrology and peat moisture retention in three adjacent peatlands where natural subsurface water flow was impacted *ca* 60 years ago, resulting in differences in mean WT depth and relative proportion of vascular and non-vascular species at the three sites. The specific objectives of this study were to: (i) assess the depth dependence of hydrophysical properties in peat; (ii) compare and contrast the moisture retention properties of hummock and hollow peat within the unsaturated zone; and (iii) determine if a systematic difference in hydrophysical properties exist between sites with an increasing average depth to WT several decades following disturbance.

4.3 Methods

4.3.1 Study site

The study area is located in the Seney National Wildlife Refuge (SNWR) in the Upper Peninsula of Michigan (Fig. 4-1). The region is characterized by relatively flat

topography which slopes towards the south-east at $1.1 - 2.3 \text{ m km}^{-1}$ (Heinselman, 1965). Land cover consists primarily of upland forests (67%), and open peatlands (20%), while the remainder of the region is made up of mostly forested swamps and open water (Casselman, 2009). Wet sand of glacial origin overlies the regional bedrock up to a thickness of 60 m (Albert, 1995). Surface soils throughout SNWR are mostly a complex of poorly drained muck and sand, while the study area itself contains poorly drained peats (Casselman, 2009) approximately 0.75 – 1.5 m deep.

The peatland complex within SNWR is subdivided by a combination of upland sand ridges of lacustrine origin, creeks, old drainage ditches, as well as a network of roads and berms constructed mostly during the late 1930's and early 1940's by the Civilian Conservation Corps (Kowalski and Wilcox, 2003; Wilcox et al., 2006) for the purpose of creating open water habitat for migratory birds. Berm construction in the southern end of the refuge where our study sites are located was completed in the late 1950's, creating a natural experiment where an upslope peatland site (hereafter referred to as WET) likely became wetter and a downstream peatland site (hereafter referred to as DRY) likely became drier. Aerial photography of the study area shows a clear increase in ponding upslope of the berm and areas of rapid terrestrialization downslope following berm construction (Fig.1). Moreover, contemporary WT data shows a large difference between the WET and DRY sites, with the latter being up to several dm deeper. A site with an intermediate depth to WT variation (hereafter referred to as INT) is located adjacent to the WET site. Although each peatland site has almost identical species richness, the relative proportion of given species differs between sites (Hribljan, 2012).

The WET site is classified as a poor sedge-fen ($\text{pH} = 4.10 \pm 0.06$) with an average microtopographical variation of 0.15 ± 0.05 m. The INT and DRY sites are both classified as bogs, with a pH of 3.77 ± 0.02 and 3.69 ± 0.01 respectively, and have an average microtopographical variation of 0.30 ± 0.08 m and 0.41 ± 0.11 m respectively. In addition to the increase in relative height of hummocks, the proportion of hummocks at each site also increases along the hydrological gradient, with an estimated coverage of 41%, 52% and 63% for the WET, INT, and DRY sites respectively.

4.3.2 Lab measurements

A factorial design was used to obtain peat moisture-retention curves based on site, microtopography, and depth. Peat blocks measuring approximately $0.3 \times 0.3 \times 0.3$ m were cut from each site and placed in a waterproof rigid plastic crate. Surface peat blocks (0 - 0.3 m depth) were taken from 3 randomly chosen hummocks and hollows at all three sites (WET, INT, and DRY), while deeper samples (0.3 – 0.6 m depth) were only obtained for hummocks. Peat blocks were saturated in order to maintain high pore water pressure to help reduce peat compression during transportation. In order to minimize the amount of disturbance to the pore-space geometry, peat blocks were frozen within 24 to 48 hours of removal from the site. While frozen, each peat block was sectioned into 0.05 m thick layers with 3 – 4 samples produced per 0.05 m layer. Each cylindrical sample was cut to 0.098 m diameter to match the inside diameter of a PVC collar used to hold the sample. The bottom of the PVC collar was covered by cheese cloth to hold the sample in place while allowing water to drain freely from the peat samples.

Moisture-retention measurements were carried out using a 0.56 m diameter porous ceramic plate (Soilmoisture Equipment Corp, Santa Barbara, CA) with an air-entry pressure of 1 bar. Pressure was controlled using a pediatric vacuum regulator connected to a large vacuum reservoir, with moisture-retention measurements made at pore-water pressure (ψ) steps of -5, -10, -15, -20, -30, -40, -50, -75, -100, -150, -200, and -500 mb. Samples were first saturated for 24 h using deionized water prior to commencing moisture-retention measurements. At each pressure step, samples were weighed every 24 h until they approached hydrostatic equilibrium, inferred from a weight change equal to or less than 0.1 g. Sample weight was determined using an Acculab EC-411 digital balance, with 0.1 g precision. In order to limit evaporation from the peat samples, the porous plate was placed in an acrylic enclosure with a water bath as a free source of water to ensure a high relative humidity in the enclosure head space. Nevertheless, potential water loss from evaporation was estimated using the daily average change in weight of four 50 mL water samples placed inside the acrylic enclosure. The 50 mL beakers were weighed daily over a 13-day period using an Acculab ALC80 analytical balance with a precision of 0.01g. A daily correction factor equivalent to $0.045 \text{ mm m}^{-2} \text{ d}^{-1}$ was applied to the measured peat sample weights.

Bulk density, ρ_b (kg m^{-3}), was determined from the dry weight of the peat samples following 72 hr in an oven at 65 °C. Porosity, \square ($1 - \rho_b/\rho_s$), was calculated based on an average peat particle density, ρ_s (kg m^{-3}), of 1475 kg m^{-3} (Redding and Devito, 2006). Due to the non-rigid structure of peat, reported ρ_b and \square values are based on initial sample volume measurements. In order to quantify the effect of shrinkage on moisture-

retention, sample height and diameter were measured at each pressure step using a Vernier caliper. Sample weight and volume were also corrected for woody content. Woody content was determined gravimetrically following oven drying. Woody root volume was calculated based on the measured average bulk density of woody roots which was determined based on a volume displacement test in ethanol. Finally, volumetric water content, θ ($\text{m}^3 \text{ m}^{-3}$), was calculated based on the adjusted weight and volume measurements according to the method of Freeze and Cherry (1979).

Laboratory-based saturated hydraulic conductivity, K_s (m s^{-1}), was measured based on the constant-head method using a modified apparatus presented in Price *et al.* (2008). A constant head gradient of 0.03 m was maintained across each 0.05 m peat sample. K_s was determined from the average discharge rate over three measurement cycles, where discharge was determined from the time it took to fill a 250 mL overflow beaker.

4.3.3 Field measurements

Laboratory moisture-retention data was supplemented by field measurements of θ and water table depth (WTD). Field-based θ was measured using CS-616 water content reflectometers (Campbell Scientific (CS), Logan, Utah) installed at depths of 0.05, 0.15, and 0.25 m relative to the surface of a hummock and hollow at each of the three study sites. An additional sensor was installed at depth of 0.50 m in a hummock at the INT and DRY sites due to the greater microtopographic variation at these two sites. The correction of Hansson and Lundin (2006) was first applied to the measured CS-616 period values before calculating θ using the three-phase mixing model for peat (Kellner and Lundin,

2001). Porosity for the three-phase mixing model was estimated from laboratory measurements described above. Hourly θ values were recorded using a CR10X datalogger (CS).

Estimates of field pore water pressure were derived from measured WTD at each of the sites. By assuming a depth-dependent hydraulic head profile that is in hydrostatic equilibrium with the water table, pressure at three measurement depths (0.05, 0.15, and 0.25 m) was estimated as the height above the water table. WTD was measured hourly at all three sites in a 1.5 m deep well using self-logging Levellogger Junior pressure transducers (Solinst, Georgetown, ON (Solinst)) and was corrected for changes in atmospheric pressure using a Barologger Gold barometric logger (Solinst). Periodic measurements of ψ were made in a representative hummock and hollow at each of the three study sites in order to validate WTD-based ψ estimates. Direct measurements of pore water pressure were made at the same depths as θ using ceramic cup tensiometers (Soil Measurement Systems, Tucson, AZ).

Field-based K_s was determined using a head recovery slug test in piezometers with an inside diameter of 0.254 m and screen length of 0.1 m. Only measurements with greater than 90% head recovery were used for our calculations. K_s at depths of 0.15, 0.25, and 0.5 m were measured at two piezometer nests at each of the three sites, with average values based on three trials. Deeper K_s values were based on the average of multiple measurements along two 275 m transects, with measurements taken at intervals of approximately 50 m. Since piezometers were only temporarily installed for the transect-

based K_s measurements, the piezometers were pumped several times to clear debris from the intake screen prior to the slug test.

4.3.4 Calculations and statistics

$\theta - \psi$ relations from laboratory measurements were modelled using the Van Genuchten (VG) equation (1980):

$$\theta = \theta_r + \frac{\phi - \theta_r}{(1 + \alpha\psi^n)^m} \quad (4.1)$$

where the subscript r denotes the residual value, α is the inverse of the air-entry pressure, n is the dimensionless pore-size distribution index, and $m = 1 - 1/n$. θ_r , α , and n were determined iteratively using a Levenberg-Marquardt algorithm for a non-linear least squares fit. The iterative process involved first using a fixed value of θ_r estimated from the linear extrapolation of the final three ψ -steps to a ψ of -1,500 mb, then solving for α and n . Preliminary results suggested n had a narrow range of variability, therefore the second step fixed n and solved for θ_r and α simultaneously. This procedure was repeated using the updated values for θ_r and n in each subsequent iteration and continued until parameter estimates varied by no more than 0.1%. A logistic equation was also used as an alternative empirical fit to θ - ψ data:

$$\theta = \theta_r + \frac{\phi - \theta_r}{1 + \exp[a_{log} \cdot (\psi + b)]} \quad (4.2)$$

where a_{log} is the slope parameters, and b is the horizontal offset.

A sigmoidal curve was used to determine the explanatory power of ρ_b on the variance in moisture-retention. θ at a given ψ (θ_ψ) was first normalized by \square in order to

constrain moisture-retention values between 0 and 1. The following sigmoidal function was used:

$$\frac{\theta_{\psi}}{\phi} = \frac{a_{sig}^{-1} \cdot \rho_b}{\sqrt{1 + (a_{sig}^{-1} \cdot \rho_b)^2}} \quad (4.3)$$

where a_{sig}^{-1} is the slope at the origin, with independent values calculated for each ψ .

4.4 Results

4.4.1 General hydrology

The median WT positions (2010/2011) relative to the hollow surface were 3.8/-0.1 cm, -12.9/-13.7 cm, and -17.9/-14.9 cm for the WET, INT, and DRY sites respectively (Fig. 4-2). There is a close correspondence between the WT positions for the INT and DRY sites in comparison to the WET site. However, taking into account the differences in the height of hummocks relative to the surrounding hollows between sites, the difference in WT position relative to hummocks becomes larger, where the mean relative height (\pm SE) of hummocks are 14.9 (1.0) cm, 29.6 (1.9) cm, and 40.5 (2.7) cm for the WET, INT, and DRY sites respectively. Rainfall during the 2011 measurement period (407 mm) was much lower compared to 2010 (643 mm), leading to greater WT declines in 2011. Combined with wetter early spring conditions in 2011, the WT distribution was much broader in 2011, thus providing better overlap for a comparison of WT response to rainfall events. The maximum WT drawdown in the 2011 growing season increased from WET (36 cm), to INT (41 cm), to DRY (50 cm), where the

magnitude of average WT response to rainfall events was 1.2 cm, 2.0 cm, and 2.0 cm at the WET, INT, and DRY sites respectively.

Nevertheless, depth appears to have a stronger influence on the WT response to rainfall than site, where rainfall as a proportion of WT response is near 1 when WT is near the surface, decreasing to roughly 0.2 when the WT position is -55 cm (Fig. 4-3 – upper panel). Based on a 2-way ANOVA, the depth class is significant ($p < 0.01$, d.f. = 7), while site is not ($p = 0.130$, d.f. = 2). It is important to note that only two depth-classes are common to all three sites, so the above site-effect is skewed by non-overlapping depth classes. Furthermore, WT response to rainfall does not take into consideration potential differences in specific yield (S_y) between hummocks and hollows, where the proportion of each site covered by hummocks increases from WET (0.39), to INT (0.49), to DRY (0.63). Since S_y was not measured directly, we used the difference between \square and the water retained at $\psi = -5$ cm as a surrogate to examine the effects of site, depth, and microform on S_y . Fig. 4-3 (lower panel) shows that, overall, S_y tends to decrease with depth, with average surface values of 0.67 for hummocks and 0.55 for hollows, and values at depth of 0.35 for hummocks and 0.30 for hollows. In hollows, S_y decreases relatively rapidly at an average of -0.013 cm^{-1} ($r^2 = -0.710$, $p = 6.6\text{E-}05$), while in hummocks S_y decreases more gradually at an average of -0.007 cm^{-1} ($r^2 = 0.777$, $p < 0.01$).

A similar depth-dependent trend was observed in the field-based K_s data at the WET and DRY sites. A power function was fit to log-transformed depth-dependent median K_s for the WET and DRY site yielding $\exp(119.1d^{-1} - 9.4)$ for the WET site and

$\exp(100.3d^{0.66} - 17.2)$ for the DRY site, where d is depth. K_s was relatively high at all three sites for the 10 – 20 cm interval, ranging from 0.21 – 0.44 cm s^{-1} with an order of magnitude decrease in K_s at all sites for the 20 – 30 cm interval (Fig. 4-4b). K_s was observed to continue decreasing at the WET and DRY sites to a minimum of 4.87×10^{-5} cm s^{-1} and 7.24×10^{-6} cm s^{-1} respectively. K_s in the top 25 cm was examined across microforms using lab-based measurements. While Fig. 4-4a suggests no strong relation between K_s and ρ_b for samples in the top 25 cm, near-surface K_s was lowest at the WET site (0.05 cm s^{-1}), with higher median values at the INT (0.284 cm s^{-1}) and DRY (0.389 cm s^{-1}) sites. The lower near-surface K_s values at the WET site may be attributable to greater peat compression during the test. Although not observable during the K_s test, the change in volume of peat samples was monitored during the moisture retention measurements. A two-way ANOVA showed that both site ($p = 0.027$) and microform ($p \ll 0.01$) were significant factors for explaining changes in peat volume with decreasing ψ , while interactive effects were not ($p = 0.137$). Overall, the median magnitude of volume change was greater in hollows (-15.7%) compared to hummocks (-8.3%), and decreased from WET (-12.7%) to INT (-11.1%) to DRY (-9.8%).

4.4.2 Bulk density

Near-surface (0 – 25 cm) ρ_b was relatively low across all three study sites, ranging from 6 to 106 kg m^{-3} , with a median value of 23 kg m^{-3} . Porosity ranged from 0.921 to 0.994, with a median value of 0.982 (Table 4-1). An unbalanced two-way ANOVA was used to test for significant effects of site and microtopography, as well as interaction effects on near-surface ρ_b . Only microtopography ($p \ll 0.01$) had a significant effect on

near-surface ρ_b , while both site ($p = 0.05$) and interaction effects were not significant ($p = 0.11$). Lumping all sites together, the near-surface ρ_b for hummocks ($\rho_{b,hum}$) was relatively invariant with depth, while ρ_b in hollows ($\rho_{b,hol}$) tended to increase with depth (Fig. 4-5). Comparison of the marginal means using the Tukey-Kramer method shows that $\rho_{b,hol}$ is significantly greater than $\rho_{b,hum}$ ($\alpha = 0.95$) in the near-surface. Based on Fig. 4-5, the higher average near-surface $\rho_{b,hol}$ is related to its increase with depth. Due to the similarity in ρ_b between sites and apparent depth-dependency in hollows, a two-way ANOVA was used to test for significant effects of microtopography and depth, as well as interaction effects on near-surface ρ_b . Both factors and their interaction were significant ($p < 0.01$). A comparison of the interaction groups showed that there were no significant differences between surface samples between hummocks and hollows as well as amongst all near-surface hummock samples. All $\rho_{b,hol}$ groups from 5 – 25 cm were greater than all hummock groups, while significant increases with depth in hollow groups occurred at depths of 7.5 cm at the DRY site and 12.5 cm at the WET and INT sites (Fig. 4-5). $\rho_{b,hum}$ tended to increase at greater depths at all sites, occurring at 17.5 cm, 27.5 cm, and 47.5 cm at the WET, INT and DRY sites respectively based on the marginal means of microtopography x depth groups ($\alpha = 0.95$).

4.4.3 Lab and field moisture-retention

When grouped according to site and microtopography, there is not a large difference in the moisture retention for samples in the 0 – 10 cm range (Fig. 4-6a). Nevertheless, on average, hollow samples for a given site tend to retain more water at a given ψ in comparison to hummock samples. For samples from the 0 – 10 cm interval,

hollows retain on the order of $0.1 \text{ m}^3 \text{ m}^{-3}$ more than hummock samples over much of the measured ψ range. Furthermore, within both hummocks and hollows, moisture retention for the INT and DRY sites corresponds much more closely to one another than to the WET site. These general trends differ for samples deeper in the peat profile (15 – 25 cm) where moisture retention in hummock samples remains largely unchanged, and where hollow retention has noticeably increased (Fig. 4-6b). For samples from the 15 – 25 cm interval, hollows retain on the order of $0.25 \text{ m}^3 \text{ m}^{-3}$ more than hummock samples over much of the measured ψ range, with diminishing differences at lower (more negative) ψ . Furthermore, the distinction between the WET samples and the other two sites is no longer present.

The summary of VG parameters for all site x microtopography x depth combinations (Table 4-1) shows similar patterns. An ANOVA was used to examine the effect of site, microtopography, depth, and their interactions on θ_r , α , and n . Depth and microtopography, as well as their interaction, were significant ($p < 0.01$) for θ_r . A comparison of the marginal means using the Tukey-Kramer method shows θ_r increases with depth in hollows, but not hummocks. Examining surface values alone, we see that the average θ_r increases from WET ($0.058 \text{ m}^3 \text{ m}^{-3}$) to INT ($0.088 \text{ m}^3 \text{ m}^{-3}$) to DRY ($0.108 \text{ m}^3 \text{ m}^{-3}$). Broadly similar depth-dependent findings apply to $\alpha^{-0.5}$ (transform applied to normalize α), but with decreased significance (e.g. microtopography ($p=0.0002$); depth ($p=0.040$); and their interaction ($p=0.084$)). For n , however, depth is not a significant factor ($p=0.276$), while microtopography ($p=0.003$), site ($p=0.001$), and their interaction ($p=0.0004$) are significant. A comparison of the marginal means using the Tukey-Kramer

method shows the difference in n between hummocks and hollows decreases from DRY, to WET, to INT.

In order to assess whether lab-based measurements broadly corresponded with field-based moisture retention, continuously measured θ and relative WT position were used, where the relative WT position was taken to represent the approximate pore water pressure. Field ψ measurements were sparse, so the assumption of an equilibrium ψ -profile was assessed by combining all sites and microtopography (Fig. 4-7a). Given the relative uncertainty in ψ and relative WT position, an orthogonal linear regression was used. The slope of the regression (\pm SE) is 0.953 (0.027), making it close to a 1:1 relation, but where the difference is statistically significant ($p = 0.085$, $df = 232$), and with only 45% of ψ measurements between the ± 5 cm uncertainty of the tensiometer. Field-based estimates of moisture retention (Fig. 4-7b) show more scatter than lab-based measurements, but provide more data at small ψ values as well as θ during both wetting and drying phases. Estimates of θ_r and θ_s from field data broadly correspond with lab-based data presented in Table 4-1, whereas estimates of α and n do not. The flexibility of the VG curve combined with the non-linear fit method may be partly responsible for the disparity between field and lab-based estimates of α and n .

4.4.4 Van Genuchten vs. logistic

Since the field-based VG parameters are based on an estimate of relative WT position, the effect of the uncertainty in relative WT position on the non-linear fit was examined. Fig. 4-8a shows that the VG fit is sensitive to relatively small uncertainty in the relative WT position, particularly for positive values. Since there is uncertainty of up

to ± 5 mb for the vacuum regulator we used for lab-based θ - ψ measurements, the same sensitivity may apply to lab-based estimates as well. The greater sensitivity in the positive range relates to the rapid loss of water from low density peat at small negative ψ , where positive WT uncertainty moves the recession curve closer to $\psi = 0$. From Fig. 4-8a, each parameter in the VG equation, where \square is taken to be fixed, is dependent on one another. Combined with limitations on the non-linear curve fitting procedure, this produces non-monotonic behaviour in the relation between estimated VG parameters and uncertainty in the relative WT position. Based on Fig. 4-8a, in order for field-based VG parameters to correspond with lab-based measurements would require a systematic error in relative WT position of approximately 4 cm. Conversely, there could be systematic error in the lab measurements of ψ . A systematic error of 4 cm is within the stated uncertainty range (± 5 cm) of the vacuum gauge used to control ψ in the porous ceramic plates. The relatively high sensitivity of the VG parameters not only limits the ability to compare field and lab-based measurements, but also limits comparisons with other studies, particularly if ψ is subject to systematic error.

An alternative approach would be to use a curve with less flexibility while having parameters which have a physical interpretation. The logistic equation shown in Fig. 4-8b is a suitable candidate, where all points are a double reflection about the lines $y = (\square - \theta_r)/2$ and $x = -b$ (or conversely a 180° rotation about the point $(-b, (\square - \theta_r)/2)$). Moreover, the form of the logistic equation used has only one free shape parameter (a), along with scaling/translation parameters \square , θ_r and b , where a and b are analogous to n and α in the VG equation. The benefits of the logistic equation in light of potential systematic error

can be seen in Fig. 4-8b, where only the b parameter is affected and changes are monotonic.

4.4.5 Empirical relations for moisture-retention parameters

The VG n represents the pore size index, yet based on our results there is no apparent relation with ρ_b (Fig. 4-9a). If we consider the distribution of n , it has a near normal distribution ($p = 0.133$), where some skewness has been artificially introduced as a matter of expediency in the non-linear fitting process by limiting n estimates to values equal to or greater than 1.1. Modifying the VG equation so that $n = 2$, creates a sigmoid-like curve with properties similar to the logistic function presented in Fig. 4-8b. However, the mean n (\pm SE) from our samples is 1.72 (0.02), which is close but significantly different ($p < 0.01$) than 2. We assume that the VG α parameter should be related to S_y since it is supposed to represent the air entry pressure. Using the yield of water at $\psi = -5$ cm as a surrogate for S_y , we see that it is a good predictor of α if we assume that large values of α are outliers (Fig. 4-9b). This is not an unreasonable assumption, given that high α values represent an air-entry pressure approaching zero, making the α estimate highly sensitive to the tolerance of the fitting procedure and dependence on other parameter estimates. However, considering that we would expect a low air entry pressure for near-surface peat with high ϕ and low ρ_b which is the case for all WT treatments, the reliability of α estimates and therefore the ability to compare between studies becomes questionable. Finally, we would expect that the true θ_r , or θ at any sufficiently low ψ , to be well correlated with ρ_b . Fig. 4-9c shows only a moderate correlation between the VG θ_r parameter and ρ_b , where a grouping of near-zero θ_r at intermediate ρ_b values appears to

be the result of the interdependence of parameters and the fitting method rather than physically based.

Fig. 4-10 shows equivalent results to Fig. 4-9, but in relation to the logistic fit. While ρ_b only explains a moderate amount of variance in a , this is a vast improvement over the results from Fig. 4-9a, where the slope of the logistic curve at $\psi = -b$ is inversely related to ρ_b (Fig. 4-10a). Although the amount of explained variance in b is similar to that for a , there is no need for assumptions about how to treat outliers, or rather about the behaviour of the fitting procedure as the air-entry pressure approached zero. Similar to a , a simple inverse relation is used to describe the decrease in b with increasing $\square - \theta_{\psi=-5 \text{ cm}}$ (Fig. 4-10b). Unlike the results from Fig. 4-9a, the θ_r estimate using the logistic equation is not interdependent with the other parameters and thus yields estimates that are better correlated with ρ_b . It should be noted that while ρ_b and $\square - \theta_{\psi=-5 \text{ cm}}$ provide more robust parameter estimates for the logistic fit, the VG parameterization yields higher r^2 and RMSE compared to the logistic fit. The median r^2 and RMSE for the VG parameterization is 0.983 and 0.018, and 0.889 and 0.052 for the logistic fit.

Although θ_r using the VG or logistic equation is the limit as ψ approaches $-\infty$, the lower range of ψ applied to our samples provide a close approximation to θ_r due to the low density and high proportion of large pore spaces in our samples. Fig. 4-11a shows that ρ_b explains a high degree of variance in $\theta_{\psi=-200 \text{ cm}}$, where θ has been normalized by \square in order to provide a natural upper limit of one. Given the range in measured ρ_b , Fig. 4-11b shows that ρ_b can be used to predict θ with a relatively high degree of confidence. For ψ less than -10 mb, ρ_b explains over 0.69 of the variance in θ_{ψ}/\square . Consequently,

qualitative variables such as depth interval, microtopography, and site do not have a strong direct effect on moisture-retention (once correlation with ρ_b is removed). An ordinary least-squares regression for the relation between a_{sig} and $\ln(\psi)$ yielded slope and intercept (\pm SE) parameters of 29.6 (1.64) and 5.11 (6.65). Although the log-linear model explains a large amount of variance in $a_{sig}(\psi)$, ρ_b is a poor predictor of θ_{ψ} for $\psi \geq -10$ mb given the moderately low r^2 values.

4.5 Discussion

4.5.1 General hydrology

Short-term WT manipulation experiments, on the order of seasonal to ten years post-drainage, have shown relatively large surface adjustments (Schlotzhauer and Price, 1999), increases in ρ_b and WT variability, and decreases in K_s (Price, 2003; Whittington and Price, 2006) in response to drying. An assessment of the vegetation community across WT treatments in this study shows that, within microform type, there was no significant change in the abundance of the dominant vascular and *Sphagnum* species between WT treatments (Hribljan, 2012), but where we observed a difference in the relative abundance of microforms between sites. This may suggest that the short-term hydrological impact of WT manipulation, when on the order of ± 10 cm, on ρ_b , S_y and K_s may be mediated by long-term shifts in microform distributions due to the greater competitive advantage for hummock *Sphagnum* species under drying (Grosvernier *et al.*, 1997; Robroek *et al.*, 2007), along with the inherent hydrophysical properties associated with different *Sphagnum* species (Hayward and Clymo, 1982; McCarter and Price, 2012)

and recalcitrance of hummock forming species regardless of WT treatment (Turetsky *et al.*, 2008).

The difference in WT variability we observed between WT treatments was the result of the difference in depth-dependence in S_y between hummocks and hollows, and the proportion of hummocks and hollows at each site. Nevertheless, this has important implications for the hydraulic structure and function of each site, where the WT typically resides in lower K_s peat, particularly at the DRY site. The large reduction in K_s with depth, which has been observed in a number of peatlands (*cf.* K_s summary table in Letts *et al.*, 2000), combined with low hydrologic gradients results in slow turnover in peat pore water at depth, limiting decomposition particularly for peatlands with large lateral extent and low annual net rainfall (Morris and Waddington, 2011). The lower average K_s at the DRY site in comparison to the WET site can be viewed as a negative feedback to potential carbon loss which has been observed for *Sphagnum* dominated sites under short-term extreme WT drawdown (Strack *et al.*, 2009). However, subsidence of the peat surface (or lack thereof) in response to short-term drying, which we observed to be greater in hollows, has important implications for changes in carbon exchange (Oechel *et al.*, 2000; Strack and Waddington, 2007). Again, the short-term response would be mediated by long-term changes in the proportion of hummocks and hollows in response to long-term WT drawdown.

4.5.2 Bulk density

Similar to the findings of Boelter (1969), our results highlight the utility of ρ_b as a simple explanatory variable for describing the θ - ψ relations of peat. Moreover, our results

show that, systematic differences in θ - ψ relations between hummocks and hollows or with depth are explained by differences in ρ_b . This strong explanatory power occurs despite differences in botanical origin (*Sphagnum* species and vascular vegetation) dominant in hummock and hollows at each of the respective sites (Hribljan, 2012). The lower ρ_b of near-surface hummock samples is in contrast to other studies that show greater ρ_b and stem density for *Sphagnum* species growing further from the WT (Luken, 1985). While in general higher moisture content in hummock species for a given WT depth can be attributed to the morphology of the capitula (Hayward and Clymo, 1982), and greater branching and tight branch packing on *Sphagnum* stems (Green, 1968; Clymo 1970) which enhances capillary rise, greater retention in the capitula and a larger proportion of small pore space does not necessarily translate to greater retention at larger scales if not accompanied by higher stem densities. The low ρ_b and lack of depth dependence in hummocks over the top few decimeters may be related to the inherent recalcitrance of hummock forming *Sphagnum* (Turetsky *et al.*, 2008), limited dynamic stress associated with WT variation in upper hummocks, and the relatively high abundance of woody shrubs (Hribljan, 2012) providing structure that limits consolidation of the peat matrix. Other studies have shown that, over similar depth intervals, herbaceous peat has a slightly higher ρ_b compared to moss peat (Boelter, 1969; Gnatowski *et al.*, 2010). For our study site, although total vascular belowground biomass is similar between hummocks and hollows, the proportion of graminoids is on the order of two to five times greater in hollows (Hribljan, 2012), potentially contributing to high ρ_b .

4.5.3 Moisture retention

Uncertainty in fixed model parameters, such as α and often θ_r , and differences in experimental design complicates direct comparison of VG parameters between studies. In the case of α , our values are calculated from ρ_b and ρ_s , and thus depend on the ρ_s estimate used. Overall, the range in measured ρ_s for peat is relatively small, where values ranging from 1350 to 1630 kg m⁻³ were obtained over a range of peat types including sedge, *Sphagnum*, and woody peat (Paivanen, 1973), and more generally for bog and fen peat (Silins and Rothwell, 1998; Price, 2003; Redding and Devito, 2006). Values of ρ_s for peat types analogous to our study sites were determined by Redding and Devito (2006), where they found peat ρ_s values of 1440 kg m⁻³, 1500 kg m⁻³, and 1570 kg m⁻³ based on three surface samples from a bog hummock, hollow, and open fen respectively. Given their reported level of uncertainty, there was no significant change in ρ_s with depth ($\alpha = 0.05$). Using the range of ρ_s reported by Redding and Devito (2006), only a small amount of uncertainty is introduced into our α and VG parameters estimates, with maximum relative uncertainties of 0.9%, 3.7%, 2.2%, and 1.9% for α , n , and θ_r .

For moss peat with a similar range of ρ_b , Gnatowski *et al.* (2010) report similar estimates of θ_r , but a lower average n of 1.4 and α of 0.016 cm⁻¹. The lower α , equivalent to an air-entry pressure of 63 cm seems incongruous with the amount of large pore spaces typically present in low density moss peat. We believe their low average α is a result of their methodology, where the first ψ -step used was -100 mb. This limits the ability to adequately characterize the recession curve, where our data shows that even with ψ -steps beginning at -5 mb, much of the water has already been lost from the sample (Fig. 4-5).

Within the literature, our θ - ψ data corresponds closely with data for *Sphagnum magellanicum* presented by McCarter and Price (2012) with a similar ρ_b range of 7 to 140 kg m⁻³ over the top 0.3 m, and α values from 0.07 to 2.66 cm⁻¹. However, similar to other studies (e.g. Thompson and Waddington, 2013), the reported n values are lower, with typical values less than 1.5. While McCarter and Price (2012) only measure θ to $\psi = -25$ mb, most samples appear to be decreasing asymptotically by the lower ψ -step. The systematic difference in n can be attributed to treating θ_r as a fixed rather than free, or conditionally free parameter. If, for example, we take a subsample ($n = 59$) of our results and derive VG parameter estimates using a fixed value for θ_r of 0.01, the average n value drops from 1.91 to 1.34. Furthermore, there is only a weak correlation between normalized n -values using both methods ($r^2 = 0.20$, $p < 0.01$) because of a simultaneous non-linear change in α (analogous to Fig. 4-8a).

4.5.4 VG vs. logistic

Weiss *et al.* (1998) tested several θ - ψ models for both drained and undrained peat, where the VG equation was found to be most suitable if θ_r was set to zero. While arbitrarily setting θ_r to zero (or near zero) may be validated by using a positive pressure pore-water extractor which can achieve much higher pressures than our experimental setup which was limited to 1 bar, we feel that the assumption and use of a zero θ_r is often used as a necessary limit on the number of free parameters in the VG equation in order to achieve rapid, unique solutions for the non-linear fitting procedure rather than being physically based. In fact, θ - ψ data presented by Boelter (1969) for a range of peat ρ_b and botanical origin shows that θ_r (θ at $\psi = -15$ bar) is only near zero for live undecomposed

Sphagnum moss, whereas moderately to well decomposed woody or herbaceous peat can have a θ_r in excess of $0.2 \text{ m}^3 \text{ m}^{-3}$. By allowing θ_r to be a conditionally free parameter by using an iterative method, our results align with those of Boelter (1969) where our θ_r estimates for *Sphagnum* moss peat are roughly in the range of 0.05 to $0.15 \text{ m}^3 \text{ m}^{-3}$. Furthermore, under conditions of persistent WT drawdown such as we observed between WT treatments, differences in θ_r , or conversely θ at low ψ values may have important implications for *Sphagnum* productivity and the abundance of hummock versus hollow-forming *Sphagna* at a particular site. The modification of the VG equation for better convergence in the non-linear fitting method reduces its physical basis and puts it in the same category as the empirical logistic equation we have presented. Similarly to what we have shown (Fig. 4-9 and 10), Weiss *et al.* (1998), demonstrate that empirical θ - ψ equations offer greater robustness compared to the VG model with respect to the explanatory power of peat characteristics on model parameters.

While the logistic curve provides both a good empirical fit to our θ - ψ data and parameters which are well correlated with ρ_b and S_y , it is recognized that the usefulness of the logistic curve is partly dependent on the fact that we lacked deep and/or high density samples. The range of ρ_b (or conversely θ) we report is of a similar magnitude to values reported by a number of studies, including: undisturbed *Sphagnum* peat from the top 30 cm of hummocks (McCarter and Price, 2012); *Sphagnum* moss and herbaceous peat (Boelter, 1969); and a combination of undrained near-surface hummock and hollow, burned and unburned peat (Sherwood *et al.*, 2013; Thompson and Waddington, 2013). We did not observe ρ_b in excess of 100 kg m^{-3} in the unsaturated zone such as has been

observed for peat that has undergone drainage (Schwarzel *et al.*, 2002; Gnatowski *et al.*, 2010; Sherwood *et al.*, 2013). Furthermore, we did not examine ρ_b deeper in the peat profile, where it is subject to permanent saturation. However, we argue that from a modelling standpoint that θ - ψ becomes progressively less important as you move deeper into the peat profile since at depth, saturated conditions prevail and thus K_s dominates. Furthermore, ρ_b data from Minnesota peatlands which occupy a similar hydroclimatic setting as our study area show that for a raised bog, ρ_b is relatively constant with depth, while for fens ρ_b was shown to have a weak positive correlation with depth, but limited to values less than 140 kg m^{-3} over the 2 m depth (Chason and Siegel, 1986).

4.5.5 Empirical relations for moisture-retention parameters

Peatland hydrologic functioning is strongly modified by the deformable nature of the peat matrix (Price and Schlotzhauer, 1999; Price, 2003; Whittington and Price, 2006), where the influence of shrinkage on θ - ψ is not well understood (Kellner and Halldin, 2002). Kennedy and Price (2005) present a conceptual model for the effect of volume-change on peat hydrophysical properties where they distinguish between volume changes as a result of oxidation, compression, and shrinkage. Compression is the result of increasing stress or load of overlying material and WT changes, while shrinkage in the unsaturated zone is related to changes in ψ . Insofar as the role of shrinkage on ρ_b and θ - ψ relations are concerned, our lab results capture the effect of shrinkage by tracking volume changes at each ψ -step, where failure to account for shrinkage at progressively higher ψ can lead to a large underestimate of θ , particularly when the degree of humification is low (Schwarzel *et al.*, 2002). One of the potential benefits of the logistic equation for

modelling θ - ψ relations is a more robust simulation of transient peat properties based on permanent increases in ρ_b over time and/or with depth as a result of oxidation and compression beyond the point of elastic deformation. Furthermore, by linking peat hydrophysical properties to ρ_b , differences in volume change between WT treatments or microforms, as we observed, can be dynamically linked to moisture retention. Our empirical relation for θ - ψ builds on that presented by Kennedy and Price (2004), who modify air-entry pressure based on an empirical equation which accounts for the effect of ρ_b changes on ψ , by also modifying the pore-size distribution index parameter and θ_r .

4.6 Conclusions

With a focus on the unsaturated zone, our study shows that there are significant differences in the hydrophysical properties of peat between microforms, but where no large change in ρ_b was seen as a result of the hydrologic gradient created by the water table manipulations. However, the depth at which ρ_b increased loosely corresponded with the median WT depth observed over the two study growing seasons, where we believe the persistence of *Sphagnum capillifolium* and the recalcitrance of hummock forming *Sphagna* may contribute to the apparent resilience in θ - ψ relations. While we did not observe significant differences between sites, we did observe a greater proportional coverage of hummocks at progressively drier sites. This suggests that, while peatland ecohydrological models may not need to account for changing θ - ψ relations as a result of modest increases in soil moisture deficits under future climate change scenarios, they should account for changing proportional coverage of microforms and their associated θ - ψ relations.

The utility of the VG equation for describing θ - ψ relations is limited, particularly for low density near-surface peat, due to a lack of simple, robust explanatory variables for the VG parameters. However, it is of critical importance to have a good understanding of the near-surface θ - ψ relationship and its controls for near-surface peat and live *Sphagnum* in order to model the stress response of *Sphagnum* to WT drawdown. The survival of *Sphagnum* under conditions of WT drawdown are mechanistically linked to the ψ (Thompson and Waddington, 2008), where water storage cells in the capitula (hyaline cells) will drain at a ψ in the range of approximately -100 to -600 mb based on the average pore size of hyaline cells (Hayward and Clymo, 1982; Lewis, 1988). We suggest that by using the respective θ - ψ relations of hummocks and hollows along with moisture-productivity relations, the competitive advantage of *Sphagnum* from contrasting microforms could be assessed.

Finally, we presented an empirical logistic equation that has several desirable qualities which should be considered for future θ - ψ studies with peat. Similar to the VG equation, the logistic parameters have analogous representations for air-entry pressure and pore-size distribution index while not being sensitive to uncertainty in WT position for field-based measurements, or ψ in lab-based measurements. This is important given the high ϕ of the moss surface across microforms which would confer low air-entry pressures and where ϕ varies only slightly with WT treatment at SNWR. Furthermore, the ability to predict model parameters from simple peat properties such as ρ_b is advantageous for modelling due to its small data requirements and the ability to mechanistically link ρ_b to changes in production, decomposition, and export based on

changes in temperature and precipitation inputs, as well as dynamic θ - ψ properties based on the shrinking and swelling of peat with WT fluctuations which we show to be greater in hollows and vary based on WT treatment.

4.7 References

- Albert DA. 1995. Regional landscape ecosystems of Michigan, Minnesota, and Wisconsin: a working classification. U.S. Department of Agriculture technical report NC-178.
- Boelter DH. 1969. Physical properties of peats as related to degree of decomposition. *Soil Science Society of America* **33**(4): 606-609.
- Casselmann T. 2009. Seney National Wildlife Refuge Comprehensive Conservation Plan. United States Fish and Wildlife Service.
- Chason DB, Siegel DI. 1986. Hydraulic conductivity and related physical properties of peat, Lost River Peatland, northern Minnesota. *Soil Science*, **142**(2), 91-99.
- Chivers MR, Turetsky MR, Waddington JM, Harden JW, McGuire AD. 2009. Effects of experimental water table and temperature manipulations on ecosystem CO₂ fluxes in an Alaskan rich fen. *Ecosystems*, **12**(8): 1329-1342, doi: 10.1007/s10021-009-9292-y.
- Clymo RS. 1970. The growth of Sphagnum: methods of measurement. *The Journal of Ecology*, **58**(1): 13-49.
- Coulson JC, Butterfield J. 1978. An investigation of the biotic factors determining the rates of plant decomposition on blanket bog. *J. Ecol.* **66**: 631-650.
- Dorrepaal E, Aerts R, Cornelissen JH, Callaghan TV, Van Logtestijn RS. 2004. Summer warming and increased winter snow cover affect Sphagnum fuscum growth, structure and production in a sub-arctic bog. *Global Change Biology*, **10**(1), 93-104.
- Freeze RA, Cherry JA. 1979. *Groundwater*. Englewood Cliffs, NJ: Prentice-Hall.
- Gnatowski T, Szatyłowicz J, Brandyk T, Kechavarzi C. 2010. Hydraulic properties of fen peat soils in Poland. *Geoderma*, **154**(3): 188-195.
- Gorham E. 1991. Northern peatlands: Role in the carbon cycle and probable responses to climate warming. *Ecological Applications* **1**: 182–195.
- Green BH. 1968. Factors influencing the spatial and temporal distribution of Sphagnum imbricatum Hornsch. ex Russ. in the British Isles. *The Journal of Ecology*, **56**(1): 47-58.

- Grosvernier P, Matthey Y, Buttler A. 1997. Growth potential of three *Sphagnum* species in relation to water table level and peat properties with implications for their restoration in cut-over bogs. *Journal of Applied Ecology*, **34**(2): 471-483.
- Gunnarsson U. 2005. Global patterns of *Sphagnum* productivity. *Journal of Bryology*, **27**(3): 269-279.
- Gunnarsson U, Malmer N, Rydin H. 2002. Dynamics or constancy in *Sphagnum* dominated mires ecosystems? A 40-year study. *Ecography* **25**: 685-704.
- Hajek T, Beckett RP. 2008. Effect of water content components on desiccation and recovery in *Sphagnum* mosses. *Annals of Botany* **101**: 165-173, DOI: 10.1093/aob/mcm287.
- Hansson K, Lundin L-C. 2006. Water content reflectometer application to construction materials and its relation to time domain reflectometry. *Vadose Zone Journal* **5**: 459-468. DOI: 10.2136/vzj2005.0053
- Hayward PM, Clymo RS. 1982. Profiles of water content and pore size in *Sphagnum* and peat, and their relation to the peat bog ecology. *Proceedings of the Royal Society of London (B)* **215**: 299–325.
- Heinselman ML. 1965. String Bogs and Other Patterned Organic Terrain Near Seney, Upper Michigan. *Ecology*, **46**(1-2): 185-188.
- Holden J. 2005. Peatland hydrology and carbon release: why small-scale process matters. *Philosophical Transactions of the Royal Society A: Mathematical, Physical and Engineering Sciences*, **363**(1837): 2891-2913.
- Hribljan JA. 2012. The effect of long-term water table manipulations on vegetation, pore water, substrate quality, and carbon cycling in a Northern poor fen peatland. *Theses and Dissertations*, pp.132.
- Kellner E, Halldin S. 2002. Water budget and surface-layer water storage in a *Sphagnum* bog in central Sweden. *Hydrological Processes*, **16**(1), 87-103.
- Kellner E, Lundin L-C. 2001. Calibration of time domain reflectometry for water content in peat soil. *Nordic Hydrology* **32** (4/5): 315-332.
- Kennedy GW, Price JS. 2004. Simulating soil water dynamics in a cutover bog. *Water Resources Research*, **40**(12). DOI: 10.1029/2004WR003099.
- Kennedy GW, Price JS. 2005. A conceptual model of volume-change controls on the hydrology of cutover peats. *Journal of Hydrology* **302**: 13-27.
- Kettridge N, Waddington JM. 2013. Towards quantifying the negative feedback regulation of peatland evaporation to drought. *Hydrological Processes*, DOI: 10.1002/hyp.9898.
- Kowalski KP, Wilcox DA. 2003. Differences in sedge fen vegetation upstream and downstream from a managed impoundment. *The American Midland Naturalist*, **150**(2): 199-220.

- Letts MG, Roulet NT, Comer NT, Skarupa MR, Verseghy DL. 2000. Parameterization of peatland hydraulic properties for the Canadian Land Surface Scheme. *Atmosphere-Ocean* **38**: 141-160.
- Lewis AM. 1988. A test of the air-seeding hypothesis using *Sphagnum* hyalocysts. *Plant Physiology* **87**: 577 – 582.
- Luken JO. 1985. Zonation of *Sphagnum* mosses: interactions among shoot growth, growth form, and water balance. *Bryologist*, **88**(4): 374-379.
- McCarter CPR, Price JS. 2012. Ecohydrology of *Sphagnum* moss hummocks: mechanisms of capitula water supply and simulated effects of evaporation. *Ecohydrology*, DOI: 10.1002/eco/1313.
- Moore PA, Pypker TG, Waddington JM. 2013. Effect of long-term water table manipulation on peatland evapotranspiration. *Agricultural and Forest Meteorology*, **178-179**: 106-119, DOI: 10.1016/j.agrformet.2013.04.013
- Morris PJ, Waddington JM. 2011. Groundwater residence time distributions in peatlands: Implications for peat decomposition and accumulation. *Water Resources Research*, **47**(2), DOI: 10.1029/2010WR009492.
- Oechel WC, Vourlitis GL, Hastings SJ, Zulueta RC, Hinzman L, Kane D. 2000. Acclimation of ecosystem CO₂ exchange in the Alaskan Arctic in response to decadal climate warming. *Nature*, **406**: 978-981. DOI:10.1038/35023137
- Päivänen J. 1973. Hydraulic conductivity and water retention in peat soils. *Acta Forestalia Fennica*. **129**: 1-70.
- Pellerin S, Lavoie C. 2003. Recent expansion of jack pine in peatlands of southeastern Quebec: A paleoecological study. *Ecoscience* **10**, 247-257.
- Price JS. 2003. The role and character of seasonal peat soil deformation on the hydrology of undisturbed and cutover peatlands. *Water Resources Research*, **39**(9): W12410, doi:10.1029/2002WR001302.
- Price, JS, Schlotzhauer SM. 1999. Importance of shrinkage and compression in determining water storage changes in peat: the case of a mined peatland. *Hydrological Processes*, **13**(16): 2591-2601.
- Redding, TE, Devito KJ. 2006. Particle densities of wetland soils in northern Alberta, Canada. *Canadian journal of soil science*, **86**(1), 57-60.
- Robroek BJ, Limpens J, Breeuwer A, Schouten MG. 2007. Effects of water level and temperature on performance of four *Sphagnum* mosses. *Plant Ecology*, **190**(1), 97-107.
- Roulet N, Moore T, Bubier J, Lafleur P. 1992. Northern fens: Methane flux and climatic change. *Tellus B* **44**: 100–105.

- Schlotzhauer SM, Price JS. 1999. Soil water flow dynamics in a managed cutover peat field, Quebec: Field and laboratory investigations. *Water Resources Research*, **35**(12): 3675-3683.
- Schwarzl K, Renger M, Sauerbrey R, Wessolek, G. 2002. Soil physical characteristics of peat soils. *Journal of plant nutrition and soil science*, **165**(4): 479.
- Sherwood JH, Kettridge N, Thompson DK, Morris PJ, Silins U, Waddington JM. 2013. Effect of drainage and wildfire on peat hydrophysical properties. *Hydrological Processes* **27**(13): 1866-1874.
- Shipperges B, Rydin H. 1998. Response of photosynthesis of *Sphagnum* species from contrasting microhabitats to tissue water content and repeated desiccation. *New Phytologist* **140**: 677-684. DOI: 10.1046/j.1469-8137.1998.00311.x.
- Silins U, Rothwell RL. 1998. Forest peatland drainage and subsidence affect soil water retention and transport properties in an Alberta peatland. *Soil Science Society of America Journal*, **62**(4): 1048-1056.
- Strack M, Waddington JM. 2007. Response of peatland carbon dioxide and methane fluxes to a water table drawdown experiment. *Global Biogeochemical Cycles*, **21**(1). DOI: 10.1029/2006GB002715.
- Strack M, Waddington JM, Lucchese MC, Cagampan JP. 2009. Moisture controls on CO₂ exchange in a *Sphagnum*-dominated peatland: Results from an extreme drought field experiment. *Ecohydrology* **2**: 454-461, doi: 10.1002/eco.68.
- Thompson DK, Waddington JM. 2008. *Sphagnum* under pressure: towards an ecohydrological approach to examining *Sphagnum* productivity. *Ecohydrology* **1**: 299-308, DOI: 10.1002/eco.31.
- Thompson DK, Waddington JM. 2013. Wildfire effects on vadose zone hydrology in forested boreal peatland microforms. *Journal of Hydrology*. **486**: 48-56. DOI: 10.1016/j.jhydrol.2013.01.014
- Turetsky MR, Crow SE, Evans RJ, Vitt DH, Wieder K. 2008. Trade-offs in resource allocation among moss species control decomposition in boreal peatlands. *Journal of Ecology* **96**: 1297-1305.
- van Genuchten MTh. 1980. A closed form equation for predicting the hydraulic conductivity of saturated soils. *Soil Science Society of America Journal* **44**: 892-898.
- Waddington JM, Kellner E, Strack M, Price JS. 2010. Differential peat deformation, compressibility, and water storage between peatland microforms: Implications for ecosystem function and development. *Water Resources Research*, **46**(7), DOI: 10.1029/2009WR008802.
- Weiss R, Alm J, Laiho R, Laine J. 1998. Modeling moisture retention in peat soils. *Soil Science Society of America Journal*, **62**(2): 305-313.

- Weltzin JF, Bridgham SD, Pastor J, Chen J, Harth C. 2003. Potential effects of warming and drying on peatland plant community composition. *Global Change Biology*, **9**(2), 141-151.
- Whittington PN, Price JS. 2006. The effects of water table draw-down (as a surrogate for climate change) on the hydrology of a fen peatland, Canada. *Hydrological Processes*, **20**(17), 3589-3600.
- Wilcox DA, Sweat MJ, Carlson ML, Kowalski KP. 2006. A water-budget approach to restoring a sedge fen affected by diking and ditching. *Journal of Hydrology*, **320**: 501-517.

4.8 Tables

Table 4 - 1: Summary of mean hummock (HUM) and hollow (HOL) Van Genuchten parameters (std) for moisture-tension relations for the WET, INT, and DRY sites at SNWR. (* - Reported values are medians)

Site	Depth (cm)	WET		INT		DRY	
		HUM	HOL	HUM	HOL	HUM	HOL
□	2.5	0.991 (0.003)	0.986 (0.005)	0.981 (0.004)	0.983 (0.005)	0.979 (0.004)	0.982 (0.005)
	7.5	0.989 (0.003)	0.976 (0.012)	0.982 (0.003)	0.976 (0.012)	0.980 (0.003)	0.975 (0.005)
	12.5	0.988 (0.003)	0.956 (0.020)	0.984 (0.001)	0.961 (0.007)	0.983 (0.004)	0.964 (0.004)
	17.5	0.984 (0.007)	0.937 (0.014)	0.984 (0.003)	0.951 (0.004)	0.984 (0.002)	0.961 (0.004)
	22.5	0.978 (0.007)	0.938 (0.014)	0.981 (0.003)	0.952 (0.005)	0.982 (0.003)	0.955 (0.007)
θ_r	2.5	0.048 (0.040)	0.068 (0.071)	0.092 (0.077)	0.083 (0.069)	0.105 (0.046)	0.110 (0.053)
	7.5	0.080 (0.048)	0.084 (0.073)	0.107 (0.084)	0.113 (0.061)	0.128 (0.044)	0.156 (0.051)
	12.5	0.068 (0.043)	0.075 (0.089)	0.054 (0.056)	0.130 (0.107)	0.062 (0.050)	0.126 (0.119)
	17.5	0.069 (0.042)	0.095 (0.125)	0.031 (0.047)	0.149 (0.135)	0.058 (0.045)	0.135 (0.116)
	22.5	0.078 (0.059)	0.099 (0.125)	0.033 (0.061)	0.101 (0.149)	0.073 (0.056)	0.153 (0.122)
α^* (cm^{-1}) l)	2.5	0.74	0.42	1.38	1.01	0.69	0.69
	7.5	0.85	5.45	1.20	0.84	0.78	0.54
	12.5	0.65	1.07	2.12	0.37	0.81	0.66
	17.5	0.49	0.34	2.89	0.44	0.89	0.43
	22.5	0.52	0.16	141.5	0.10	0.77	0.31
n	2.5	1.89 (0.25)	2.11 (0.73)	1.53 (0.37)	1.83 (0.52)	1.95 (0.25)	1.59 (0.23)
	7.5	1.95 (0.39)	1.84 (0.91)	1.62 (0.38)	1.81 (0.52)	2.01 (0.27)	1.65 (0.33)
	12.5	1.99 (0.24)	1.50 (0.21)	1.55 (0.32)	1.58 (0.23)	1.99 (0.22)	1.54 (0.24)
	17.5	1.99 (0.26)	1.55 (0.28)	1.48 (0.20)	1.49 (0.27)	1.90 (0.10)	1.55 (0.22)
	22.5	1.97 (0.33)	1.62 (0.22)	1.52 (0.40)	1.51 (0.36)	1.89 (0.21)	1.63 (0.15)
r^2	2.5	0.97 (0.03)	0.98 (0.01)	0.97 (0.03)	0.97 (0.02)	0.97 (0.03)	0.98 (0.02)
	7.5	0.98 (0.02)	0.98 (0.01)	0.98 (0.02)	0.97 (0.02)	0.97 (0.03)	0.96 (0.02)
	12.5	0.97 (0.03)	0.97 (0.02)	0.99 (0.01)	0.98 (0.01)	0.97 (0.04)	0.97 (0.01)
	17.5	0.97 (0.03)	0.98 (0.01)	0.99 (0.01)	0.98 (0.01)	0.98 (0.03)	0.98 (0.01)
	22.5	0.98 (0.02)	0.97 (0.01)	0.97 (0.02)	0.98 (0.01)	0.98 (0.03)	0.97 (0.01)
#	2.5	10	6	9	6	8	9
	7.5	15	7	9	9	9	9
	12.5	12	5	7	6	6	6
	17.5	12	5	4	6	6	6
	22.5	11	4	4	4	6	6

4.9 Figures

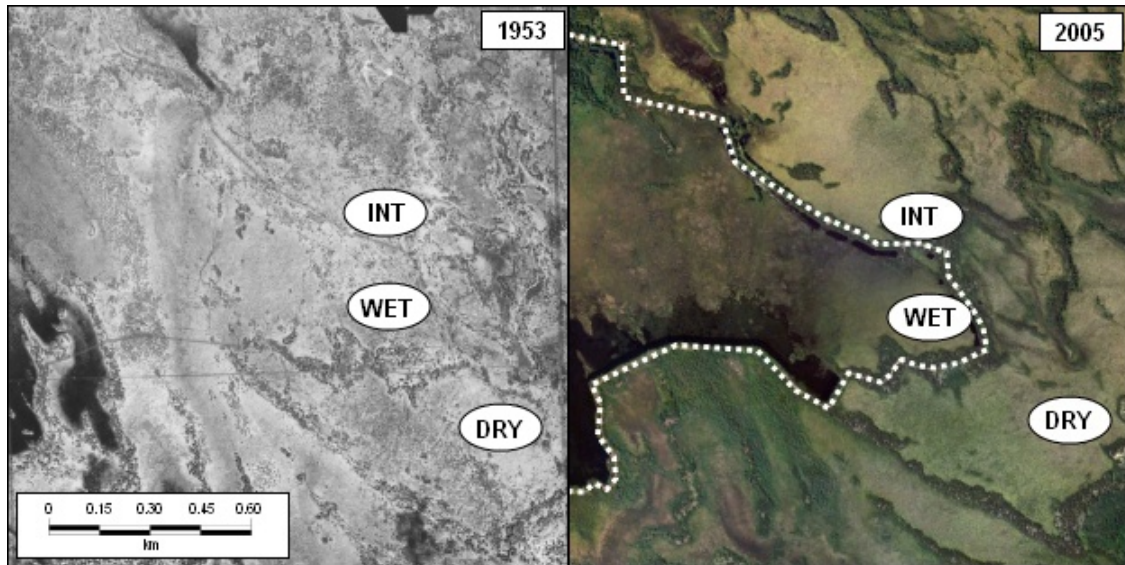


Figure 4 - 1: Seney National Wildlife Refuge (SNWR) study area in the Upper Peninsula of Michigan (46.20° N, 86.02° W, elev. ~205 m a.s.l.) showing the three primary sampling locations. The left panel shows the study area prior to berm construction (SNWR airphoto BWD-5K-147), while the right panel shows the location of the berm (white dashed line) and impact on surface ponding (Google Earth – imagery date: 31/05/2005 – USDA Farm Service Agency).

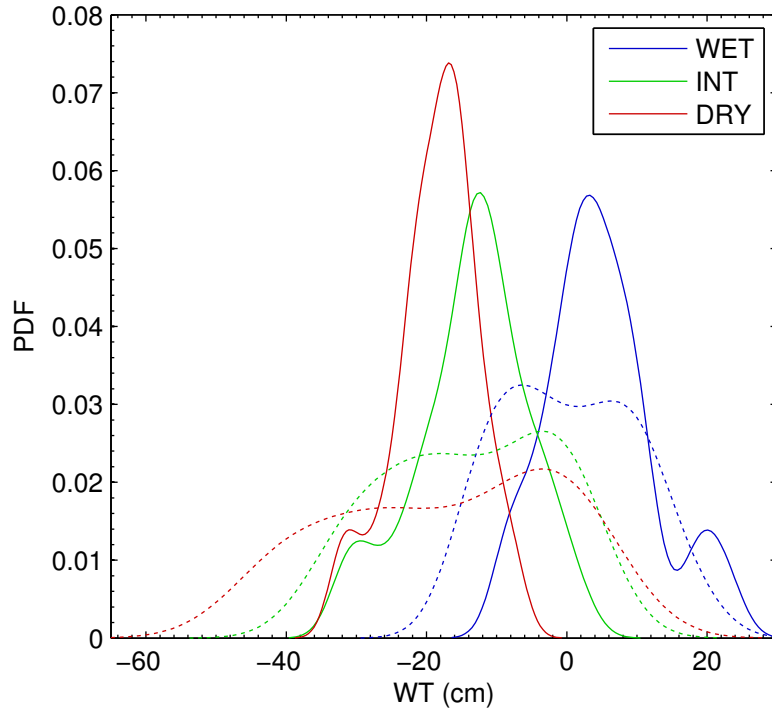


Figure 4 - 2: Estimated WT probability distribution from early May to mid-Oct. using a normal kernel function. Reported WT is relative to the local hollow surface at all three sites for the 2010 (solid lines) and 2011 (dashed lines) growing seasons.

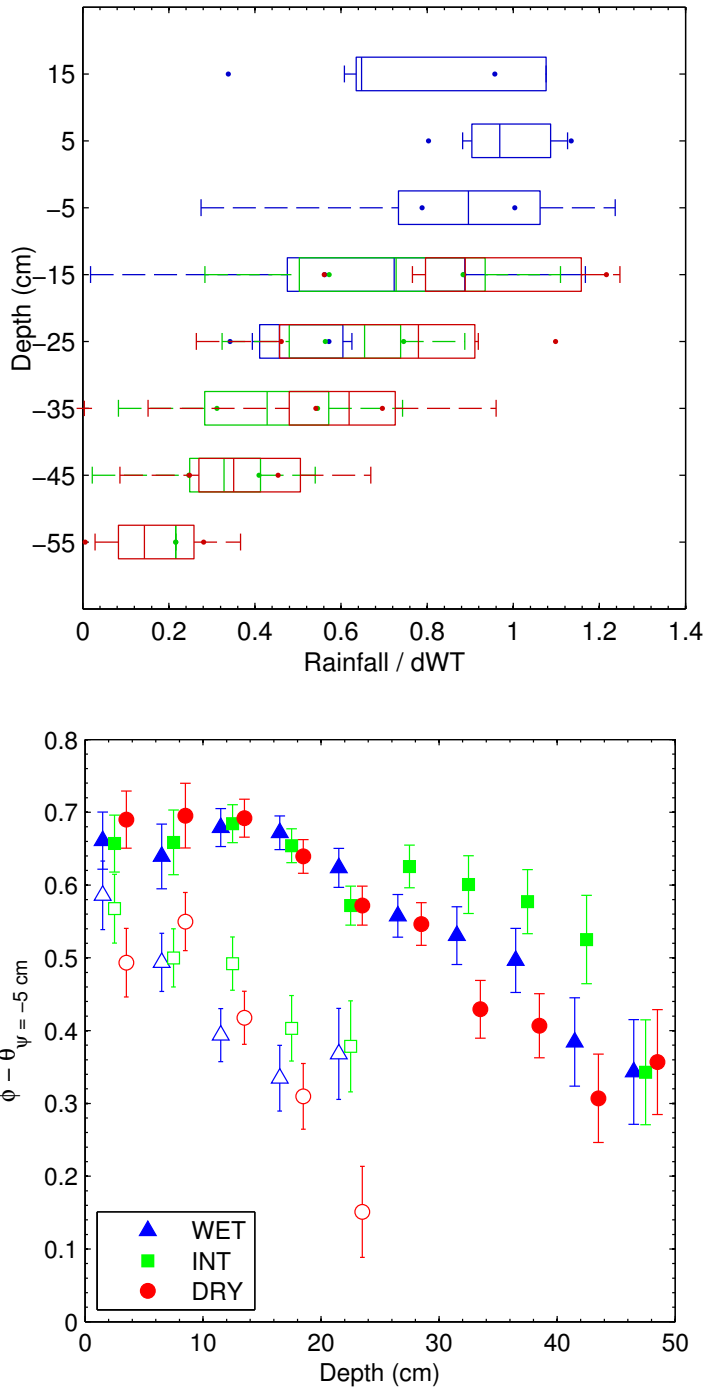


Figure 4 - 3: Boxplots of the depth dependence of the rainfall-water table response (top panel) for the WET (blue), INT (green), and DRY (red) sites. Dots represent the 95% confidence interval on the median. Lower panel shows estimated differences in mean (symbols) specific yield by site, separated into hummocks (solid symbols) and hollows (empty symbols). Error bars show standard error.

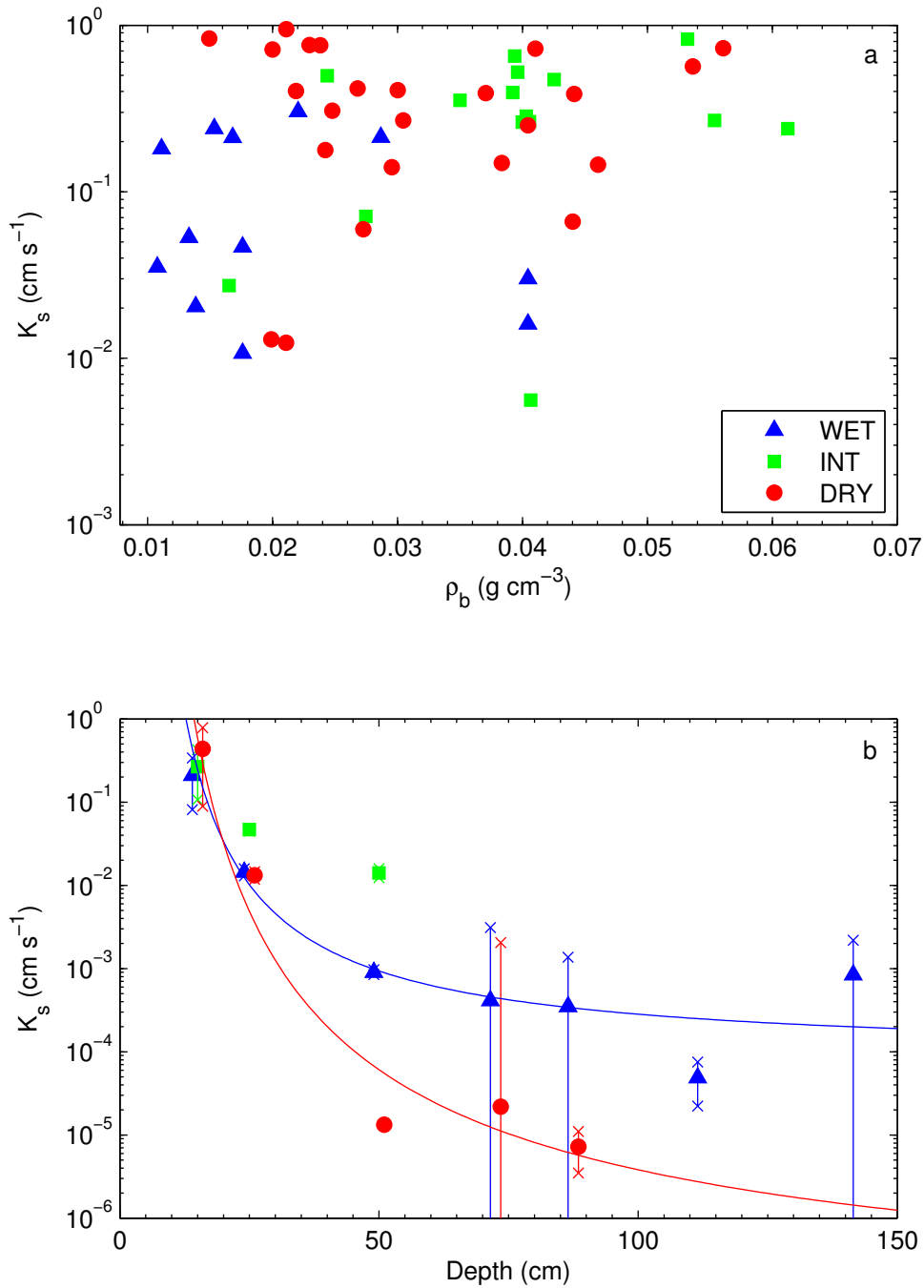


Figure 4 - 4: Relation between lab-measured saturated hydraulic conductivity (K_s) and bulk density for samples from the top 25 cm of the peat profile (a). Depth-dependence of the geometric mean (symbols) and standard deviation (error bars) of K_s in the saturated zone (b).

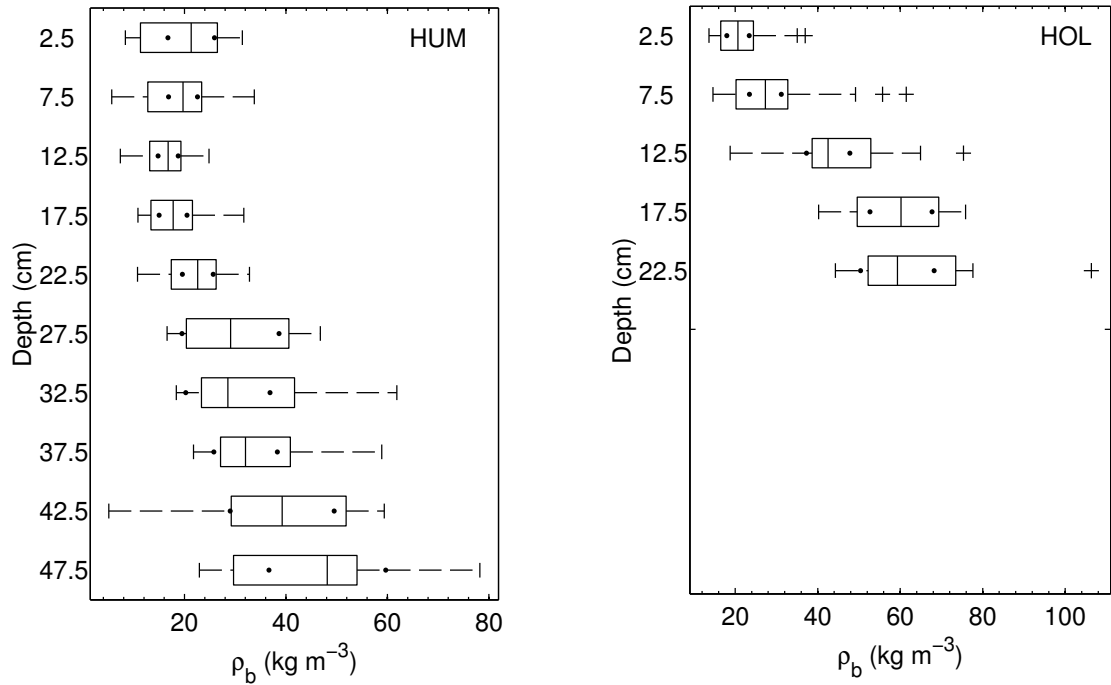


Figure 4 - 5: Boxplots of the depth dependence of peat sample bulk density with all sites lumped together. Black dots represent the 95% confidence interval on the median.

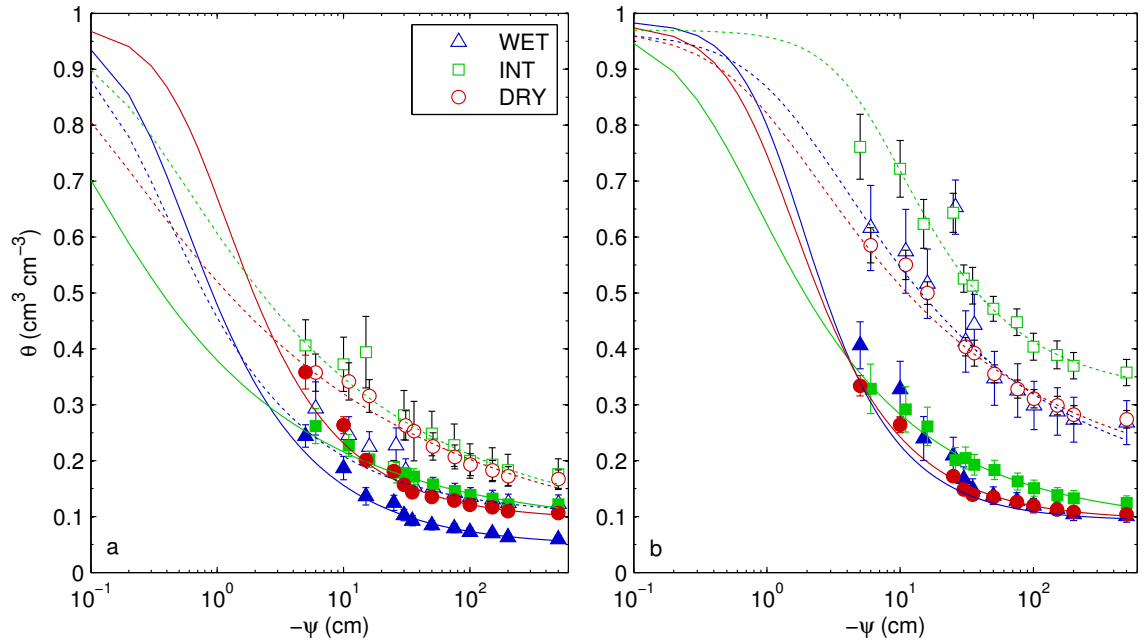


Figure 4 - 6: Comparison of lab-based moisture retention for 0.05 m thick peat samples lumped over 0 – 0.1 m (a) and 0.15 – 0.25 m (b) depth intervals. The mean (symbols) and standard error (bars) are reported for both hummocks (filled symbols) and hollows (open symbols). Lines represent the non-linear least-square fit of the Van Genuchten equation.

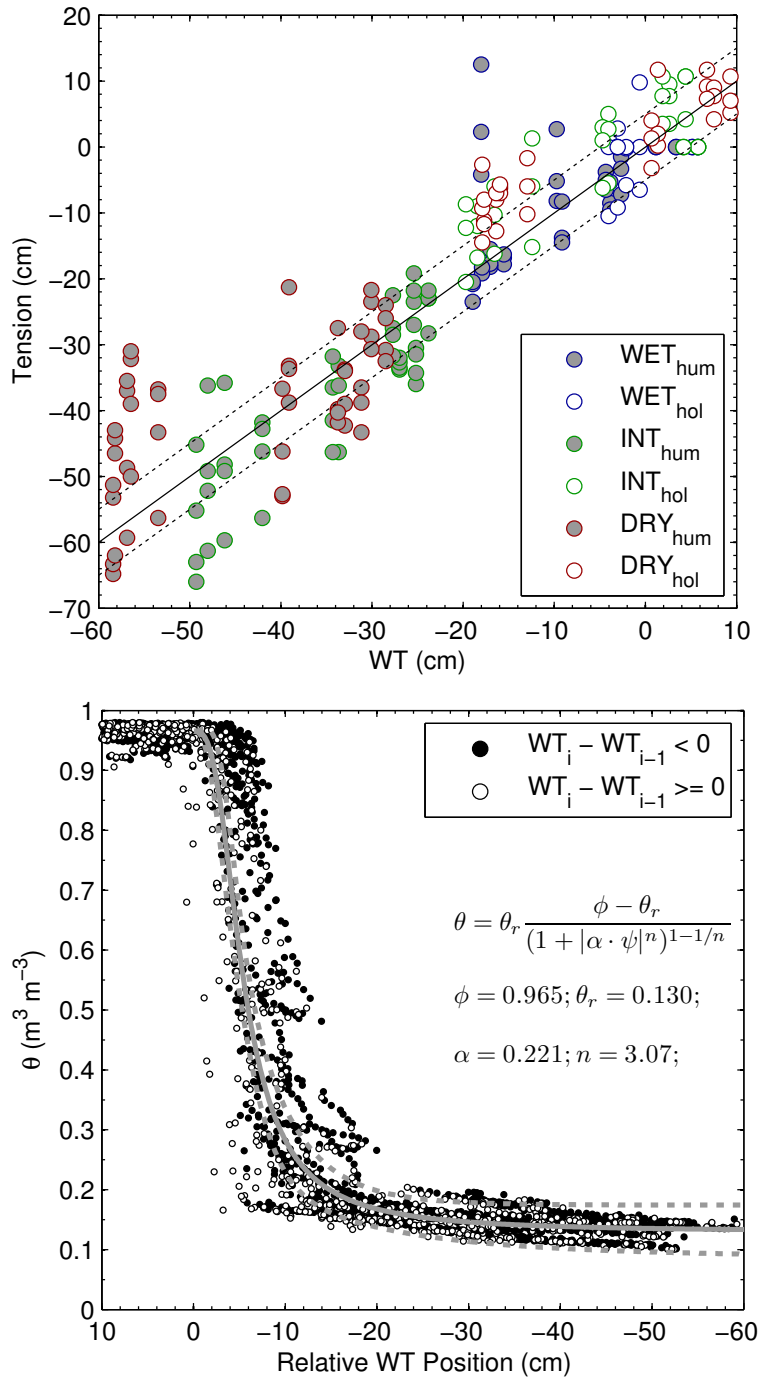


Figure 4 - 7: Field-measured pore water pressure versus relative water table position (top panel). Solid 1:1 line represents an equilibrium ψ profile, with dashed lines representing tensiometer measurement error (± 5 cm). Field-based moisture content as a function of relative water table position (bottom panel). Van Genuchten fit (solid grey) and 95% confidence interval on the curve shown (dashed grey).

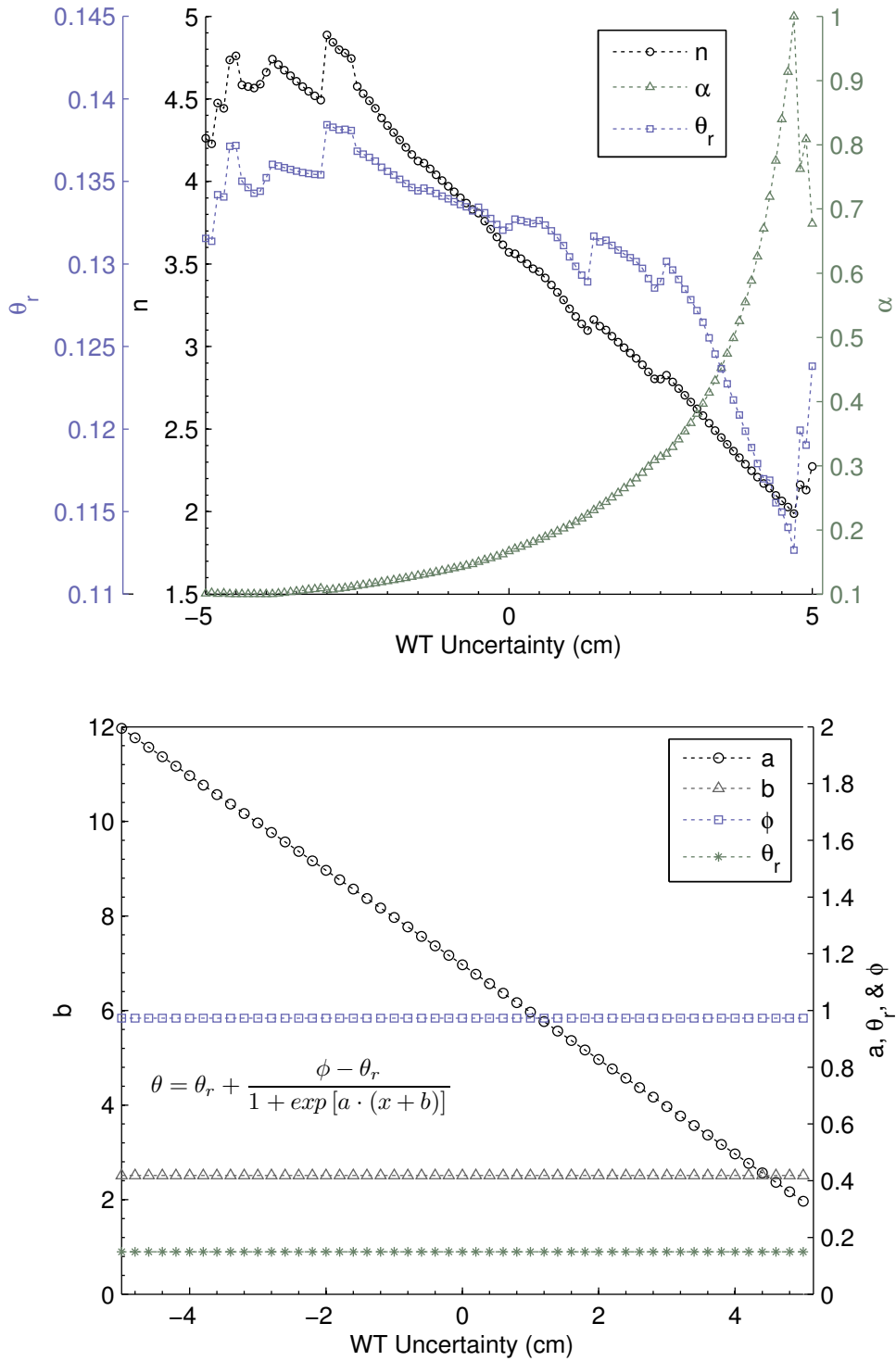


Figure 4 - 8: Uncertainty analysis of Van Genuchten (a) and logistic (b) parameters using a non-linear least squares fit for field-based moisture-retention data.

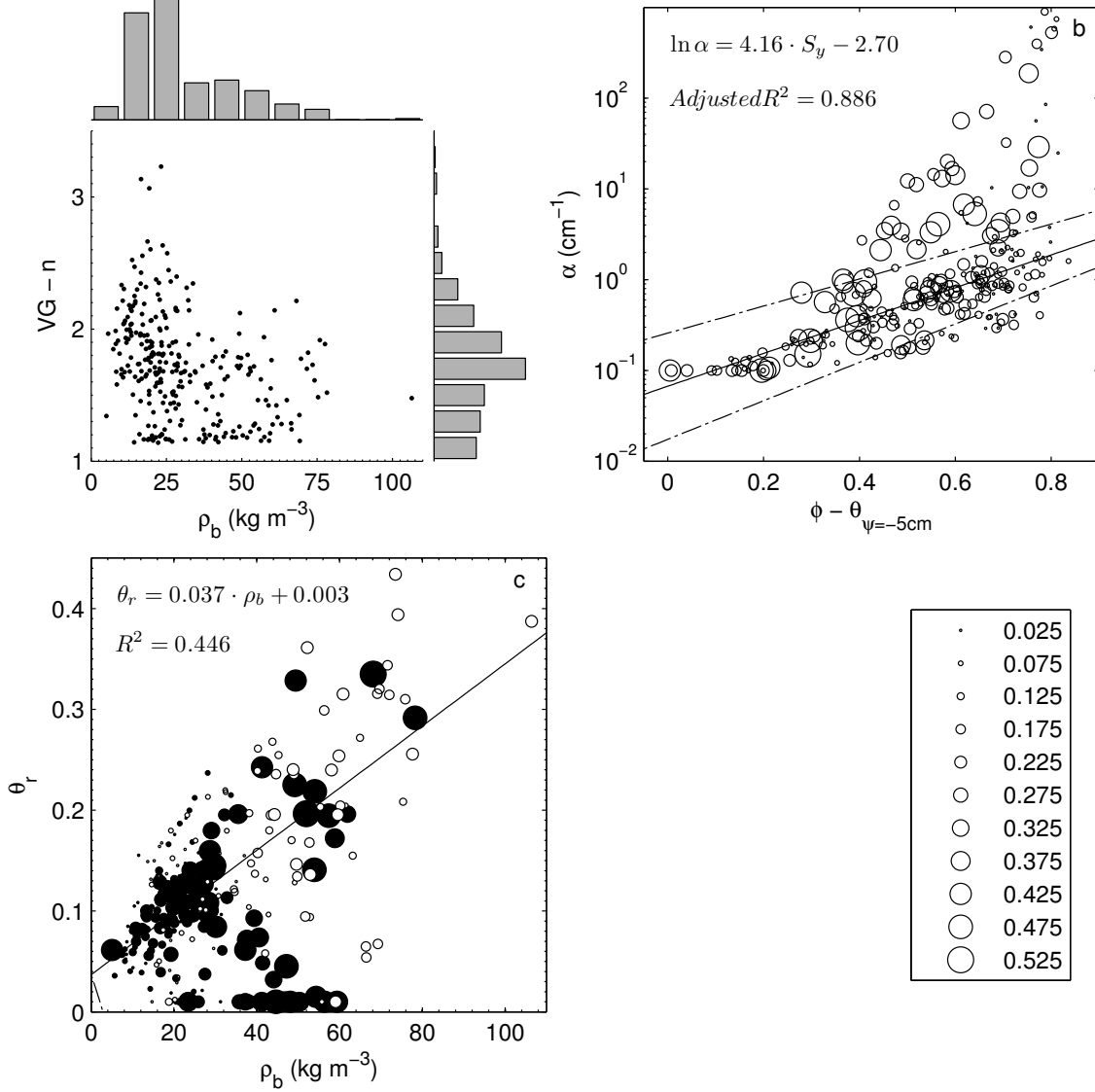


Figure 4 - 9: Empirical relations for moisture retention parameters using the Van Genuchten equation. The grey bars in (a) represent the empirical probability distributions of the Van Genuchten n (VG- n) parameter and bulk density (ρ_b). The log-linear robust fit using a Cauchy weight function (solid line) and 95% confidence interval on the curve (dashed lines) are shown for the relation between α and $\phi - \theta_{\psi=-5 \text{ cm}}$ (b). A robust linear fit (solid line) is shown for the relation between the Van Genuchten residual water content (θ_r) and bulk density (ρ_b) (c).

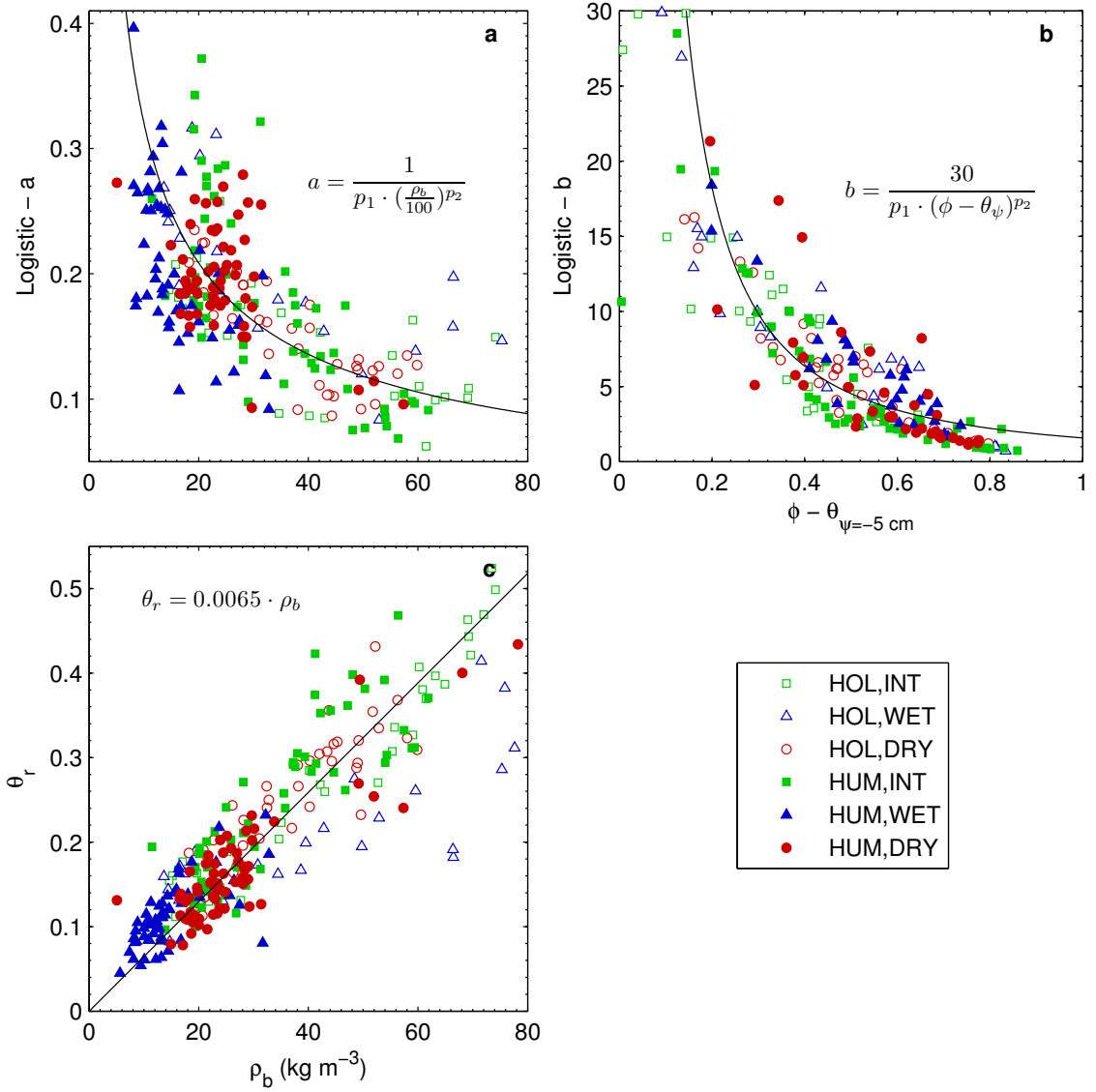


Figure 4 - 10: Empirical relations for moisture retention parameters using a logistic fit. The coefficients for the power functions used in (a) and (b) are $p_1=13$, $p_2=0.62$, and $p_1=19$, $p_2=1.52$ respectively. The coefficients of determination are 0.59, 0.83, and 0.84 based on a robust fit (outliers down-weighted).

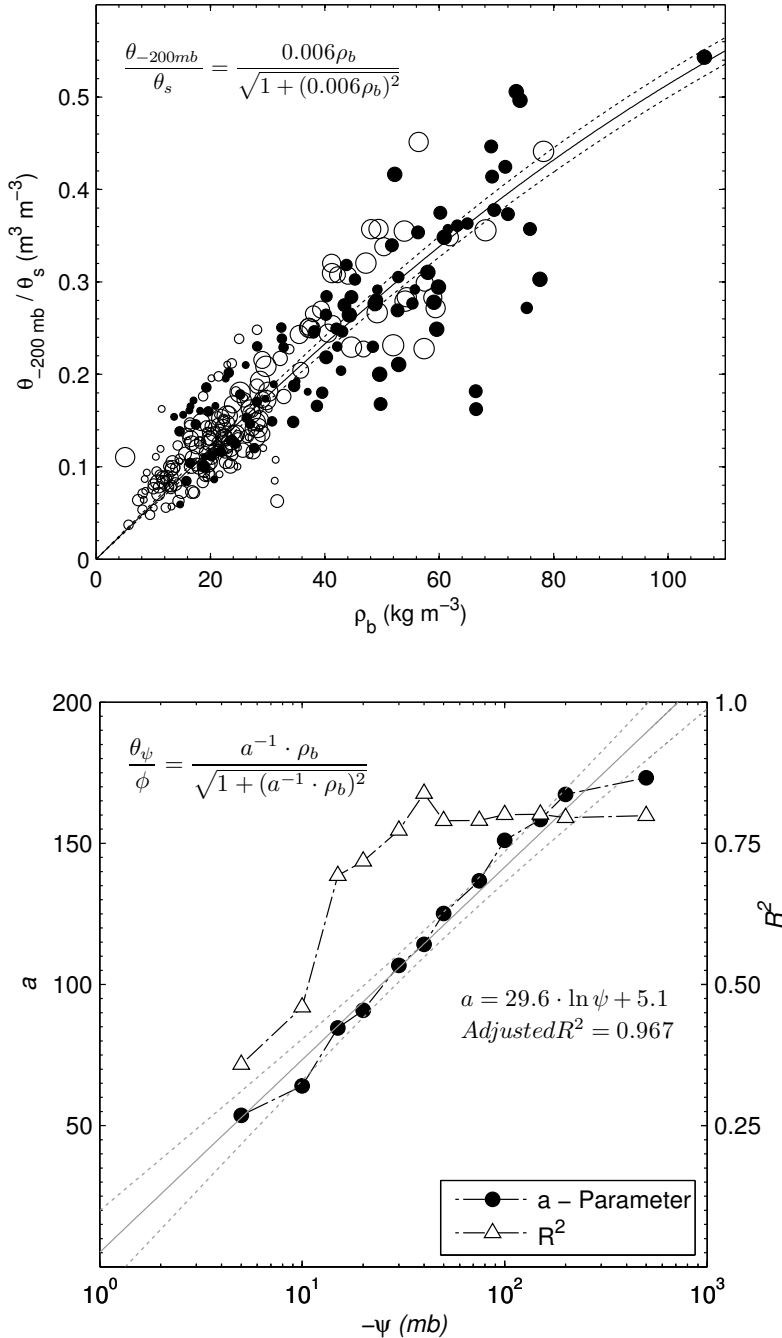


Figure 4 - 11: Sample relation between moisture content at a pore water pressure of -200 mb normalized by porosity ($\theta_{\psi=-200 \text{ cm}}/\square$), and bulk density (ρ_b) for hummock (open) and hollow (filled) samples (a). A sigmoid fit (solid line) and the 95% confidence interval on the curve (dashed line) are shown. The relation between the initial slope of the sigmoid curve (a_{sig}) and pore water pressure (ψ) are shown with the explained variance of the relation over the range of measured ψ (b). A log-linear fit (solid line) and the 95% confidence interval on the curve (dashed line) are shown.

CHAPTER 5: MODELLING *SPHAGNUM* MOISTURE STRESS IN RESPONSE TO 21st CENTURY CLIMATE CHANGE

5.1 Abstract

Sphagnum moss is associated with wet habitats such as northern peatlands, which may be vulnerable to enhanced summer moisture deficits due to climate change. We adapted a physically based, 1-dimensional (vertical) water-balance model to investigate the role of topographic position and depth-dependence of hydrophysical properties on *Sphagnum* moisture stress response to current and projected climate conditions in a northern Michigan peatland. Water table (WT) level was shown to have a strong control on soil water pressure (ψ), and thus on *Sphagnum* moisture stress. As a result of the close correspondence between laboratory measured surface peat hydrophysical properties for hummocks and hollows used to parameterize our model, microtopographic position was shown to have a greater impact on *Sphagnum* moisture stress. Model behaviour suggests that, while ψ maintains equilibrium-profile values relative to the WT level for relatively shallow values, surface ψ becomes non-linearly related to WT level below a value of approximately -0.4 m, thus greatly increasing the likelihood of desiccation under future climate scenarios where growing season soil moisture deficits are projected to increase. The results from our simulations demonstrate the need for a better understanding of *Sphagnum* moisture-stress dynamics. The simulated range of instantaneous and cumulative moisture-stress for hollows under future climate conditions closely corresponds to the range exhibited by hummocks contemporarily. Therefore, in order to

assess the competitive advantage of various *Sphagnum* species to future climate conditions, more data is needed to better inform a physiological ψ -based moisture-stress threshold, the evolution of the stress response to increasing levels of desiccation, and its subsequent recovery dynamics.

5.2 Introduction

Northern peatlands (i.e., those north of 45°N) represent a globally-important long-term sink of soil carbon (C) (~ 220 – 550 Pg C) (Gorham, 1991; Turunen *et al.*, 2002; Yu, 2011) due to cool, wet soil conditions, and the inherent biochemical recalcitrance of peat-forming plants. Under projected future climate change (IPCC, 2007), water table (WT) levels in northern continental peatlands are likely to fall (Roulet *et al.*, 1992). *Sphagnum* moss, which is a dominant peat-forming species (Hayward and Clymo, 1982), has a non-vascular structure and so relies on passive capillary transport from the WT to avoid desiccation. Since the water content in the apical bud of *Sphagnum* (capitula) is related to WT depth up to several dm (Rydin, 1985; Strack and Price, 2009), and capitula net productivity is non-linearly related to water content (Titus *et al.*, 1983; Rydin and McDonald, 1985; Schipperges and Rydin, 1998; Strack and Price, 2009), WT position is commonly used to model long-term peatland ecohydrological and carbon flux responses to climate change (*e.g.*, Roulet *et al.* 1992, Frolking *et al.* 2002). For example, Ise *et al.* (2008), who non-linearly link peatland carbon dynamics with WT level, suggest that the combined effects of drying and increasing peat temperatures will result in future catastrophic peatland degradation, which represents a positive feedback to climate forcing through enhanced peat decomposition and associated greenhouse gas emissions.

However, short-term in-situ field experiments (*e.g.*, Chivers *et al.*, 2009; Strack and Waddington, 2007) have demonstrated that changes in the moss community occur in response to a sustained WT drawdown. A decrease in *Sphagnum* cover (Gunnarsson *et al.*, 2002) and an increase shrub and tree cover (Pellerin and Lavoie, 2003) has also been associated with long-term drying. Strack *et al.* (2009) suggest that resilience of the peatland carbon pool to climate change may be controlled by the contemporary distribution of *Sphagnum* moss species that occupy both wet (hollows) and dry (hummocks) habitats, whereby a change in the moss community, coupled with the associated internal ecohydrological feedbacks (*e.g.*, Kettridge *et al.*, 2013), may enhance peatland resilience to prolonged drought.

Sphagnum species distribution is strongly controlled by ψ and the ability of different *Sphagnum* species to withstand low (more negative) capitula ψ without undergoing severe desiccation (Thompson and Waddington, 2008). For example, hummock-forming species such as *Sphagnum fuscum* are raised above both the surrounding hollows and WT, and therefore must withstand lower ψ than hollow species. Regardless of species specific thresholds, below a moisture-dependent optimal productivity, a lower WT leads to greater moisture stress. However, both hummock and hollow-forming species are generally desiccation intolerant as *Sphagnum* generally recovers poorly from severe desiccation (McNeil and Waddington, 2003; Shipperges and Rydin, 1998). The competitive advantage of hummock species under dry conditions is therefore at least partly attributable to their greater moisture retention properties (*cf.* McCarter and Price, 2012) and their ability to avoid desiccation, thus leading to greater

productivity under dry conditions (Strack and Price, 2009). As such, a prolonged decrease (increase) in soil moisture could cause a shift towards more drought-tolerant (intolerant) hummock (hollow) species. This in turn could cause a shift in ecosystem function due to the relatively lower (higher) decomposition rates (Johnson and Damman, 1991; Turetsky *et al.*, 2008) in hummock- (hollow-) forming *Sphagnum* species.

Therefore, models which simulate peatland carbon dynamics over long timescales which do not incorporate vegetation dynamics are likely to overestimate the sensitivity of peatlands to climate change. In order to be able to predict the likelihood of shifts in the relative abundance of *Sphagnum* species within peatlands, a better understanding of the response of *Sphagnum* moisture-stress to fluctuations in peat moisture storage is required, where species morphology and the hydrological impact of topographical position must be taken into account. Since the stress response of *Sphagnum* is directly related to capitula ψ , in order to accurately model surface moisture dynamics of *Sphagnum*, both *Sphagnum* moisture retention and unsaturated hydraulic conductivity must be well defined. While peat moisture retention data has been published based on degree of humification (e.g. Boelter and Verry, 1977; Grover and Baldock, 2012), botanical origin (e.g. Gnatowski *et al.*, 2010), and most recently for surface and near-surface sample for several hummock species (McCarter and Price, 2012), limited data exists which distinguishes between the moisture retention of hummock and hollow forming species (e.g. Thompson and Waddington, 2013). Similarly, a variety of literature exists for peat saturated hydraulic conductivity (e.g. Boelter, 1969; Hogan *et al.*, 2006; Lewis *et al.*, 2012), and to a lesser degree for measured unsaturated hydraulic conductivity (e.g. Schwarzel *et al.*, 2002;

Naasz *et al.*, 2005; Price and Whittington, 2010; McCarter and Price, 2012), but a specific distinction between hummocks and hollows/hollows is often lacking.

Given the importance of non-linear and temporally-transient *Sphagnum* ecohydrological response to moisture status, and the uncertainty in *Sphagnum* moisture-stress thresholds, we adopted a probabilistic approach to simulating peatland moisture dynamics, plant water stress, and water balance (*e.g.* Rodriguez-Iturbe and Poporato, 2005) as an alternative framework for examining the effects of climate change on peatland and *Sphagnum* ecohydrology. The aim of this research was to compare the independent and combined effects of: i) habitat type; ii) depth-changes in peat hydraulic properties; and iii) uncertainty in *Sphagnum* moisture stress thresholds upon the stress response of *Sphagnum* moss under likely future climate change scenarios. In order to address this aim we adopted a numerical modeling approach to simulate growing season *Sphagnum* hummock and hollow water stress for an idealized southern boreal peatland parameterized with field and lab measurements, using downscaled 21st century general circulation model (GCM) data.

5.3 Methods

5.3.1 Model overview and study area

We adapted elements from the Rodriguez-Iturbe and Poporato (2005) semi-arid soil moisture model (stochastic rainfall and vegetation stress) and HYDRUS 1-D (Simunek *et al.*, 2008) (soil hydrology) and coded them in MATLAB (v.R2009a, The MathWorks) in order to examine *Sphagnum* hummock and hollow moisture stress in

response to summer water deficit conditions in a hypothetical raised bog. We chose a continental study region at the southern limit for boreal peatlands (Upper Peninsula of Michigan) where the contemporary mean annual air temperature ranges from approximately 4-5°C and precipitation and snowfall range from approximately 810 - 890 mm and 2 – 4 m, respectively, over the study area based on climate normals for weather stations within the study region (Environment Canada, 2012; NOAA, 2012).

Field data for model parameterization and validation were obtained from the Seney National Wildlife Refuge (SNWR) in the Upper Peninsula of Michigan (46.20° N, 86.02° W, elev. ~205 m a.s.l.) over the 2010 and 2011 growing seasons. The region is characterized by relatively flat topography which slopes towards the south-east at 1.1 – 2.3 m km⁻¹ (Heinselman, 1965). Land cover consists primarily of upland forests (67%), and open peatlands (20%), while the remainder of the region is made up of mostly forested swamps and open water (Casselman, 2009). Wet sand of glacial origin overlies the regional bedrock up to a thickness of 60 m (Albert, 1995). Surface soils throughout SNWR are mostly a complex of poorly drained muck and sand, while the study area itself contains poorly drained peats (Casselman, 2009).

While future changes in precipitation for this region have less certainty than projected changes in temperature, ensemble atmosphere-ocean GCM simulations over the 21st century predict relatively small to moderate (~5 - 10%) average increases in precipitation in central and eastern North America in all seasons except mid-summer, where no significant changes in precipitation are predicted (Christensen and Hewitson,

2007). However, this is a regional generalization and results from specific GCM grid cells are variable (see Section 5.3.8).

5.3.2 Model description

A simple vertical water balance approach was used to model soil moisture dynamics for a peat profile at an hourly time step, where changes in storage within the peat profile are the result of net infiltration from rainfall (\square), losses from evaporation (E), and fluxes across the upper and lower boundaries of each soil layer.

Laio *et al.* (2001) expressed \square as the balance of rainfall (P), canopy interception (I), and surface runoff (Q). For our model simulations, both I and Q were assumed to be negligible due to the lack of a vascular plant canopy within our modeling framework and a combination of high porosity and small elevation gradients in bogs. P was modelled as a stochastic process based on the following equation:

$$P_{t_{i-1}+r_{r,i}} = r_{d,i} \quad (5.1)$$

using separate continuous distributions to generate a sequence of rainfall return intervals (r_r) and rainfall event depths (r_d).

E was varied seasonally, daily and hourly according to both physical and stochastic functions. In order to account for strong seasonal variability in potential incoming solar radiation (K_{ex}) at northern latitudes, a maximum daily value of E (E_{max}) was varied according to the relative difference in potential daily K_{ex} from that at summer solstice to produce $E_{seas,i}$ (Fig. 5-1a). K_{ex} values were estimated using the radiation model parameterization of Burridge and Gadd (1974). In order to statistically represent the

effect of variable cloudiness on E , daily potential E ($E_{\text{daily},i}$) was modified by a scaling factor ($E_{\text{daily},i} = c_i E_{\text{seas},i}$). A separate scaling factor was used for days with and without rain, where the scaling factors were derived from the probability distribution of the ratio of measured incoming shortwave radiation (K_d) to K_{ex} (Fig. 5-1b). Finally, hourly potential values for E ($E_{\text{hourly},j}$) were calculated based on the product of $E_{\text{daily},i}$ and the ratio of hourly to daily maximum K_{ex} , where negative values were assigned a value of zero (Fig. 5-1c). E was assumed to occur at a maximum potential value of $E_{\text{hourly},i}$ when surface ψ was above a critical threshold (ψ_{crit}) of $\psi_{\text{crit}} = -4$ m (McCarter and Price, 2012). Below ψ_{crit} , E was limited by the unsaturated hydraulic conductivity ($K(\psi)$) and the ψ gradient across the top soil layer. $K(\psi)$ was calculated as follows:

$$K(\psi) = K_{\text{sat}} \sqrt{s} \left(1 - (1 - s^{-m})^m \right)^2 \quad (5.2)$$

where K_{sat} is the saturated hydraulic conductivity, $m = 1 - (1/n)$, n is the dimensionless pore size distribution index, and s is the effective soil moisture content. We used the ψ -based formulation of s (Brooks and Corey, 1964):

$$s = |\alpha\psi|^{-n} \quad (5.3)$$

where α is the inverse of the air-entry pressure, and where $s = 1$ when the magnitude of ψ is less than α^{-1} . The ψ formulation of s was used since it provides a direct mechanistic link to capitula water status (Thompson and Waddington, 2008), and therefore *Sphagnum* moisture stress.

A simple one dimensional finite difference model was used to numerically approximate vertical unsaturated water flow described by the following formulation of the Richards equation (Richards, 1931):

$$C(\psi, z) \frac{\partial \psi}{\partial t} = \frac{\partial}{\partial z} \left[K(\psi, z) \left(\frac{\partial \psi}{\partial z} + 1 \right) \right] \quad (5.4)$$

where z is depth, t is time, and C is the soil water capacity which is equal to the tangent of the volumetric water content (θ) versus ψ curve. The van Genuchten equation (van Genuchten, 1980) was used to describe the relation between ψ and θ when ψ was negative:

$$\theta = \theta_r + \frac{\theta_s - \theta_r}{\left(1 + |\alpha \psi|^n \right)^m} \quad (5.5)$$

where the subscripts r and s denote residual and saturated values.

A standard fully implicit finite difference scheme was used to linearly discretize and simplify Richards equation. ψ values for successive time steps were obtained iteratively by solving the system of linear equations produced from the finite difference scheme using Gaussian elimination. The convergence criteria for the iterative process was met once the maximum absolute difference in ψ estimates between successive iterations was less than 1×10^{-4} m. Spatial and temporal discretization were done using a constant time step of 5 s, and a node spacing of 0.025 m over the top 0.1 m, 0.05 m down to 1 m, and 0.1 m for greater depths. It was found that a short time step was required in order to ensure model stability given high K_s values when the WT was near the peat surface.

Moisture dynamics due to P and E_{max} were incorporated into the finite difference scheme using a constant flux (Neumann) boundary condition for the surface node. In the case of P , daily values were evenly distributed over all time steps for a given day. Under conditions where the surface layer was saturated, excess rainfall was added to the following time step to simulate ponding.

The following initial and boundary conditions were used for all model simulations. After defining an initial WT depth of 0.2 and 0 m for hummocks and hollows respectively, $\psi(z,t)$ at $t = 0$ was set to an equilibrium-profile value corresponding to the position relative to the WT (negative downwards). For $t > 0$, a zero-flux condition was imposed for the lower boundary node, where ψ was set to be in hydrostatic equilibrium with the adjacent node.

5.3.4 Moisture stress

Static vegetation water stress (ξ) is a unitless metric whose value represents the relative degree of *Sphagnum* stress based on s in the surface soil layer. Porporato *et al.* (2002) formulates ξ as follows:

$$\xi(t) = \left[\frac{s^* - s(t)}{s^* - s_w} \right]^q \quad (5.6)$$

where q represents the potential non-linear effects of a soil moisture deficit on plant condition, and s^* and s_w are moisture-stress thresholds. In vascular vegetation, s^* corresponds to an equivalent soil moisture content below which plants start to close their stomata to prevent internal water loss. However, being non-vascular plants, *Sphagnum* mosses do not have stomata. As such, s^* here represents the equivalent soil moisture

progresses slowly at first (*cf.* McNeil and Waddington, 2003). Therefore, all else being equal, with greater n_{s^*} the effect of the lag in recovery becomes more important.

5.3.5 Soil parameterization

Simulations for the *Sphagnum* hummock and hollow were run using a peat profile depth (Z) of 2.00 and 2.20 m respectively. Table 5-1 lists the values used to parameterize the peat hydrophysical properties and stress thresholds for our *Sphagnum* hummock and hollow. Few studies report on a number of the hydrophysical parameters required to model *Sphagnum* water stress, such as species specific stress threshold values. Estimates of the relative soil water content, or conversely ψ , where productivity declines and severe desiccation occurs (s^* and s_w , respectively), are more commonly reported as a gravimetric water content (GWC). Conversion to relative water content requires an estimate of surface bulk density (ρ_b), where uncertainty in stress thresholds were assessed using a range of both GWC thresholds and surface ρ_b . A wide range of K_s values based on both field and laboratory measurements have been reported, where a high degree of variability in K_s exists due to differences in methodology (Beckwith *et al.*, 2003; Kettridge and Binley, 2010), anisotropy (Rycroft *et al.*, 1975), spatial heterogeneity (*e.g.* central *v.* margin) (Baird *et al.*, 2008; Lewis *et al.*, 2012), degree of humification (*cf.* Letts *et al.*, 2000), and botanical origin. Appendix 2 shows a range of reported near-surface K_s values, where we used the values of McCarter and Price (2012) since this represents one of the few studies to differentiate between surface values for different *Sphagnum* species. Parameter values for θ_s (Appendix 3) and E_{max} (Appendix 1) were better constrained, where general agreement was found between multiple sources.

Potentially significant changes in peat hydrophysical properties can exist within a vertical peat profile (*cf.* Letts *et al.*, 2000) which depend partly on changes in pore size distribution and therefore, indirectly on bulk density (ρ_b). However, the presence of a depth-dependent relation for ρ_b is not ubiquitous. Both Clymo (2004) and Lewis *et al.* (2012) show no overall depth-dependence in ρ_b over several meters in a Scottish and Irish bog respectively, but show increases near the bottom of the peat profile. Novak *et al.* (2008) showed an overall increase in ρ_b with depth for several European peatlands, but primarily in the top 0.25 m. Finally, Chason and Siegel (1986) showed increasing ρ_b with depth in two Minnesota fens, but not in a raised bog. If peat compaction and mass loss through decomposition occur at equal rates, then a shift towards a smaller pore size distribution need not be accompanied by an increase in ρ_b . Therefore, despite ambiguity in the depth dependence of ρ_b , a decrease in K_s with depth is more universal (*cf.* K_s summary table in Letts *et al.*, 2000) which is associated with increasing peat humification with depth (Boelter, 1969). The depth-dependence of K_s has, for example, been modeled using an exponential relation (Baird *et al.*, 2012) and where experimental results have shown a linear depth-dependence for log-transformed data. As such, we used an exponential (EXP) depth profile based on the literature, as well as a linear (LIN) and constant (CONST) depth profile as arbitrary alternatives to the EXP profile in order to examine the effect of depth-dependence on model output. Both EXP and LIN used the values in Table 5-1 for the hydrophysical properties at the surface and the bottom of the peat profile, while CONST used the average of surface and deep values. Similarly, depth-

dependent profiles were used for the remaining hydrophysical properties (θ_s , θ_r , α , and n) using values listed in Table 5-1.

5.3.6 Model validation

Model performance was validated against field measurements of WT from the 2010 and 2011 growing seasons (Fig. 5-2). The model was run with measured rainfall and E (see Moore *et al.*, 2013), the soil parameters listed in Table 5-1, and an EXP soil profile. No parameter optimizations were used to generate modelled outputs. Statistical analysis of measured and modelled WT followed that of Willmott *et al.* (1985), which includes the mean, standard deviation, root mean square error (RMSE), and index of agreement (d). 2010 measured and modelled mean (\pm std) WT were -5.56 ± 5.82 cm and -2.38 ± 7.74 cm respectively, while in 2011 they were -7.57 ± 7.96 cm and -7.51 ± 8.45 cm. RMSE was higher in 2010 (5.24 cm) compared to 2011 (2.17 cm), yet in both years systematic error, $RMSE_s$ (2010: 3.26 cm; 2011: 0.22 cm), was smaller than unsystematic error, $RMSE_u$ (2010: 4.11 cm; 2011: 2.16 cm), where $RMSE = (RMSE_u^2 + RMSE_s^2)^{0.5}$. Finally, d for 2010 and 2011 were 0.85 and 0.98. Overall, model performance was strong for 2011, having relatively small error and a good index agreement. By comparison, the relatively poor performance in 2010 can be attributed to the last 40 days of the simulation. Following day 74, measured WT drops several cm, while modelled WT does not. The transition between ponding and sub-surface WT represents a step-wise change in the specific storage which results in a divergent WT response to $P-E$. The lack of a runoff routine may also contribute to greater estimates of surface ponding for the 2010 growing season.

5.3.7 Rainfall simulations

Inherent in modelling the temporal variability of P are specific assumptions regarding the statistical properties of the variables r_r and r_d . The two primary assumptions are that the variables are both random and independent. The run test for randomness and the Kendall rank correlation test for independence were evaluated using 50 consecutive growing seasons of average r_r and r_d values. Our results indicate that r_r and r_d can be considered both random (r_r : $p = 0.53$ and r_d : $p = 0.88$) and independent ($\tau = -0.004$; $p = 0.97$).

An exponential function for the probability distribution of r_r and r_d has been used previously (Laio *et al.*, 2001), in part due to its analytical tractability. Since our model simulations are numerically based, alternative distributions were compared to the exponential model using the likelihood ratio test, where a chi-squared distribution was used for the rejection criteria. A Weibull distribution was chosen for both r_r and r_d (Fig. 5-3), where both were found to have a significantly better fit compared to the exponential distribution ($p \ll 0.01$). Synthetic rainfall data equivalent to 100 growing seasons (MJJAS) was produced using the Weibull distributions to assess overall performance. The modelled average growing season total rainfall was 398.9 ± 90.3 mm compared to the 399.5 mm for the 1971-2000 climate normal. The modelled average number of days with rainfall was 57.6 ± 7.2 days, compared to the growing season normal of 60.2 days. Finally, the largest modelled extreme rainfall event was 108 mm, while the largest measured growing season rainfall event between 1971 and 2000 was 116.6 mm.

In general, the Weibull parameters a and b used to generate the distribution of r_r and r_d can be either constant or variable between simulated growing seasons based on whether climate is considered stationary over the period being simulated. For both r_r and r_d , a had a small but significant negative trend over the period of record (r_r : $t = 3.41$; $p < 0.001$; $df = 49$ and r_d : $t = 2.92$; $p = 0.003$; $df = 49$), and b had a variably significant trend (r_r : $t = 0.10$; $p = 0.461$; $df = 49$ and r_d : $t = 2.44$; $p = 0.009$; $df = 49$) (Fig. 5-3). Using the Kolmogorov-Smirnov normality test, all parameters appeared to be normally distributed (p-values of $a(r_r)$ 0.86, $b(r_r)$ 0.66, $a(r_d)$ 0.52, and $b(r_d)$ 0.83). As such, a and b were kept constant within each simulation period.

5.3.8 Climate change scenario

In order to simulate the evaporative response of peatlands to changing temperatures and the corresponding changes in stress within our modelling framework, E_{max} (which is notionally equivalent to Penman's potential evaporation (PET)) was increased proportionally with PET based on projected increases in temperature (T) and vapour pressure deficit (D) for three future simulation periods (P1: 2011-2040; P2: 2041-2070; and P3: 2071-2100). It was assumed that radiative and aerodynamic components of PET could be treated as constants. Average changes in T , D , and P for the study region were derived from simulated daily near-surface atmospheric variables from the third generation Canadian coupled general circulation model (CGCM3.1/T63) using $2.81^\circ \times 2.81^\circ$ grid spacing (Canadian Centre for Climate Modelling and Analysis). For our projection periods, P1 – P3, we used the ensemble results of five runs of the CGCM3.1/T63, where CGCM3 model runs were initialized from the end of the 20C3M

experiment (20th century) using the A2 (growing population and regional economic growth) emission scenario described in the IPCC fourth assessment report (IPCC, 2007).

Based on these simulated climate data, the average change in P and E_{max} were determined for each of P1, P2, and P3. Downscaling results from the CGCM3 A2 scenario for our study site suggest that growing season P will decrease, while E_{max} will progressively increase over the 21st century. Relative to the 1961–2000 average, projected changes in P are: -3.3% (P1); -5.6% (P2); and -8.7% (P3). Similarly for E_{max} , projected increases are: 4.2% (P1); 6.9% (P2); and 11.3% (P3).

5.3.9 Model simulations

We ran a Monte-Carlo simulation for each of the six model parameterizations (2 microforms x 3 peat profile types) under both contemporary and future climate conditions (4 periods) for a total of 24 model simulations. Each model simulation consisted of 100 iterations, with each iteration representing independent 150 day growing seasons.

5.4 Results

5.4.1 Model sensitivity analysis & non-equilibrium behaviour

Sensitivity analyses were conducted on model input parameters to assess the uncertainty in overall model performance as a result of uncertainty in parameter estimation. Since the aim of the study was to model *Sphagnum* moisture stress, ψ was used for the objective function for the sensitivity analysis since it is a hydrological indicator of water status but does not include the uncertainty in the stress response of *Sphagnum* species. A comparison of the sensitivity analyses showed relatively small

variations between peat profile types, so only the results from the EXP model are shown in Table 5-2. Given the likely range of uncertainty in model parameters (see Appendices), our results indicate that the median model behaviour is most sensitive to increases in E_{max} and a lowering of the initial WT (WT_{ini}) level. Increasing E_{max} by 1 mm d⁻¹ lowers the median ψ_{surf} by ~54%, and a decrease in the WT_{ini} level by 0.1 m lowers the median ψ_{surf} by 47%. The median modelled ψ_{surf} is considerably less responsive to changes in other parameters, where despite the high uncertainty associated with values of K_s , both relative and absolute effects are comparatively small. As we are concerned with differences in moisture stress response for the various model simulations, particularly under dry conditions, the sensitivity of the lower-range (*i.e.* 5th percentile) of ψ_{surf} to model parameters was also evaluated. Similar to the median model response of ψ_{surf} , the $\psi_{surf,p0.05}$ was sensitive to both E_{max} and WT_{ini} . However, the $\psi_{surf,p0.05}$ was also sensitive to K_s , where a low K_s value (based on its general range of uncertainty for surface peat – see Appendices) caused the greatest reduction in $\psi_{surf,p0.05}$ of any parameter.

The nature of the sensitivity of ψ_{surf} to WT level can be seen in Fig.4, which shows that virtually all ψ_{surf} lies on the equilibrium profile line when the WT level is greater than -0.3 m for both hummock and hollow simulations. Furthermore, the median ψ_{surf} corresponds with an equilibrium profile while the WT level is above -0.4 m. Below a WT level of -0.3 m, $\psi_{surf,p0.05}$ becomes non-linearly related to WT level, where values lower (more negative) than the ψ_{crit} are achieved for the hummock simulations once the WT level is below -0.55 m. $\psi_{surf,p0.05}$ for the hollow simulations are similarly non-linearly related to WT level, but where given 100 simulated growing seasons, $\psi_{surf,p0.05}$

approaches but never becomes less than ψ_{crit} . Small infrequent or short-duration positive departures from an equilibrium ψ -profile (as represented by the 95th percentile) are the result of temporary surface storage following a rain event.

5.4.2 Stochastic rainfall and evaporation

Using probability distributions described in the model parameterization for rainfall simulations produced a relatively wide range of growing season total P of approximately 185 – 595 mm. Similarly, there was a large range of variation in total E between growing seasons for both the hummock and hollow simulations, having respective ranges of 394–524 mm and 406–561 mm for the EXP models. Based on a Wilcoxon rank sum test, seasonal total E was significantly different between hummock and hollow simulations ($T = 7248$; $p < 0.01$) where a two-sample Kolmogorov-Smirnov test indicated that seasonal total E for hummock and hollow simulations came from separate distributions ($KS = 0.45$; $p < 0.01$). Overall, there was no significant correlation between P and E for hummock simulations, where the Spearman correlation coefficient (r_s) ranged from -0.046 to 0.172 ($0.087 \leq p \leq 0.648$) depending on the peat profile type, but a moderate correlation existed between P and E for hollow simulations ($0.492 \leq r_s \leq 0.546$; $p < 0.01$). Regardless of microform type, the growing seasons with the highest E corresponded to the years with the highest P for all profile types. For example, using the EXP profile for hummock simulations, there was no significant linear relation (slope \pm st.err. = 0.003 ± 0.020 ; $p = 0.450$; d.f. = 85) between P and E when total P was less than 460 mm, but increased significantly for greater total P (slope \pm st.err. = 0.563 ± 0.177 ; $p < 0.01$; d.f. = 13). The threshold of 460 mm was chosen based on approximately where

Lowess-smoothed E steadily increased with P . The same approximate threshold existed between profile types, but where the value for hollow simulations was 400 mm.

The average growing season moisture deficit (P-E) was relatively small under current climate conditions, with an average (\pm st.dev) P-E of -34 (72) mm compared to -70 (53) mm for P1, -86 (60) mm for P2, and -120 (62) for P3. This means that over the course of a ‘typical’ growing season under current climate conditions, changes in total storage tended to be small given the relatively frequent nature of rainfall in the study region (i.e. mean rainfall return period of 2.1 days). Similarly, since the average rainfall depth was roughly 6 mm, and due to the relatively rapid transmission of water in peat to due relatively large pore space, the temporal variability in θ_{surf} was relatively small and of short duration. The larger moisture deficit for the hollow simulations compared to the hummocks has important implications for WT depth and thus on equilibrium ψ .

5.4.3 Simulations of peatland moisture status and stress

Comparisons of model outputs for both *Sphagnum* hummocks and hollows are presented through a sample of single-growing-season near-surface θ (θ_{surf}) traces (Fig. 5-5), and through all-years cumulative density plots of θ_{surf} and ψ_{surf} (Fig. 5-6). In general, both Fig. 5-5 and 6 show that there are only small differences in model output between the EXP and LIN peat-profile types particularly for hummock simulations. The contrast between the EXP and LIN profiles with the CONST profile is more apparent in Fig. 5-6 (left panel) for both the hummock and hollow simulations, where the CONST simulations tend to have higher θ_{surf} . Due to the stochastic nature of the P and E simulations, there is considerable inter-annual variability in the temporal dynamics of θ_{surf} . For a median P -

total year (Fig.5-5 – middle panel), the range of variability in θ_{surf} for the hummock simulations is fairly small due to a WT_{ini} of -0.2 m, and relatively high porosity and low retention properties of surface peat (Table 5-1). Under dry years (Fig. 5-5 – lower panel), the general behaviour of θ_{surf} is similar to a median P -year, but where the differences in θ_{surf} between the hummock and hollow simulations are less pronounced and where θ_{surf} more frequently approaches residual water content. Overall, the model simulations tend to show a seasonal high θ_{surf} at the beginning of the growing season, with a gradual recession over the first 20 – 30 days of simulation, after which there is a pseudo-dynamic equilibrium reached, where the θ_{surf} maintains a low value with frequent short duration departures associated with rainfall events. High total- P years (Fig. 5-5 – top panel) are characteristically different from median and low total- P years, where a growing season $P-E$ surplus exists, causing the average WT level to be at or near the peat surface.

In general, hollow simulations are more heavily weighted towards higher moisture content, independent of depth-profile where approximately 15% of the total simulation period is spent with some degree of surface ponding compared with 1-3% of the time for the hummock simulations (Fig. 5-6). Not surprisingly, hummocks spend a greater proportion of the simulation period in a stressed state in comparison to hollows. Using a GWC-based moisture-stress threshold we can see the effect of the range of measured surface ρ_b has on the predicted probability of being in a stressed state (Fig. 5-6 – right panel). Given the shape of the distributions in Fig.6, the uncertainty in ρ_b has a comparatively small effect on the probability of *Sphagnum* being in a stressed state for hollows compared to hummocks. For the EXP and LIN profiles, the probability (Pr) of

Sphagnum being in a stressed state based on a high θ^* (θ^*_{high}) was $0.40 \leq \Pr(\theta < \theta^*_{high}) \leq 0.47$ for hummocks compared to $0.08 < \Pr(\theta < \theta^*_{high}) < 0.16$ for hollows. The high moisture retention properties of the CONST profile for the hummock and hollow simulations greatly reduced $\Pr(\theta < \theta^*_{high})$ to 0.03 and 0.01 respectively. The above direct comparison between hummock and hollow simulations is, however, based on the two having the same ρ_b .

Using a general optimal GWC-threshold for *Sphagnum* of 10 g g^{-1} for both the hummock and hollow simulations, and a median measured surface ρ_b of 10.3 kg m^{-3} for hummocks and 15.6 kg m^{-3} (unpublished SNWR data) for hollows yielded a ψ^*_{hum} estimate of -2.0 m and a ψ^*_{hol} of -0.82 m . Comparing ψ^*_{hum} to θ^* places it close to θ^*_{low} . Consequently, these ψ^* estimates would suggest that both hummocks and hollows are similarly infrequently in a stressed state. Moreover, Fig. 5-6 (right panel) shows that the distinctness of the CONST simulation, be it for the hummock or hollow simulation, is less apparent when moisture status is viewed as ψ . This points to the first order control of WT level on ψ_{surf} as seen in Fig. 5-4.

The probability distribution of WT level under current climatic condition tended to be unimodal (Fig. 5-7 – top panels) where the median WT level for the hummock simulations was -0.275 m regardless of the type of peat profile used. WT level for the hollow simulations was higher than hummock simulations, where the median WT level was -0.15 , -0.15 , and -0.175 m for the EXP, LIN, and CONST profiles respectively. Under future projected climatic conditions, where E_{max} becomes progressively higher and P lower, the median WT shifts to a lower position, where the WT PDFs begin to exhibit a

more bimodal character, particularly for the hummock simulations (Fig. 5-7 – lower panels). Median WT level, given an EXP profile for hummock simulations, was -0.35 m for 2011-40 and 2041-70, and -0.425 m for 2071-2100. Similarly for hollow simulations, the WT level was -0.20 for 2011-40 and 2041-70, and -0.275 m for 2071-2100

Considering the link between WT level and ψ_{surf} (Fig. 5-4), the transition from a median WT level higher than -0.3 m to lower than -0.4 m over the course of future climate simulations points to a progressive non-linear increase in ψ_{surf} . This leads to a small but potentially important shift in ψ_{surf} where the current likelihood of desiccation ($\psi < -4$ m) increases from near zero to ~3% and ~1% for hummock and hollow simulations respectively under future climate conditions (Fig. 5-8). Moreover, given their respective ψ^* , the probability of being in a stressed state increases to roughly 9% and 7% of the time, respectively. The shift in ψ_{surf} to lower values is qualitatively significant, where the magnitude of change is greater than that associated with profile type under current climate conditions and is similar in magnitude to the contemporary difference associated with microtopographic position. Specifically, the behaviour of hollow simulations under the 2071-2100 climate scenario becomes similar to the current hummock simulation despite having a WT_{ini} of 0 m. However, in addition to differences in the probability of being in a stressed state, differences in moisture-stress sensitivity and recovery may have important implications for future moss competition.

The nature of the relation between moisture status and *Sphagnum* moisture stress, as expressed by q , has a strong influence on the average static stress (Fig.5-9 – top left) *Sphagnum* experiences while in a stressed state (ζ). Fig. 5-9 (top left) suggests that

regardless of whether the dependence of the average ζ on moisture status has a concave ($q < 1$) or convex ($q > 1$) shape, that the value for s^* has only a small effect, except when s^* is low (e.g. less than 0.1). There is a rapid increase in the average ζ as q transitions from convex to concave because the probability of s approaching s_w is low given our definition of s_w and the limitation of ψ_{crit} on water storage loss from the surface layer. If s_w is in fact higher than the value we have ascribed, the uncertainty in the parameter q would become less important. Similarly, if constraints on surface storage water loss were relaxed, then the effect q on average ζ would be reduced. It is important to note that while the average ζ represents the relative magnitude of stress while in a stressed state, average ζ is more representative of cumulative stress. In contrast to ζ , Fig. 5-9 (top right) shows that average ζ is more sensitive to s^* . The response of average ζ to s^* and k are, however, based on a $q = 1$. If we ignore very low values of k for which meaningful recovery is precluded, average ζ is only sensitive to k over a relatively narrow range s^* . The difference in sensitivity of ζ and ζ to s^* is, in part, due to the increased time spent in a stressed state as s^* increases (Fig. 5-9 – lower left). However, ζ does not increase monotonically with s^* due to the decrease in the number of stress periods at high s^* (Fig. 5-9 – lower right) despite being of longer duration. All else being equal, with an increasing number of stress states the effect of any lag in recovery becomes more important.

Overall, for all depth-profiles in both the hummock and hollow simulations, the average ζ tends to increase with increasing s^* (Fig. 5-10a). However, there exists a local minimum for all model runs at intermediate values of s^* . This behaviour results from the

tendency of θ (or s) to reach a low dynamic equilibrium relatively early in the growing season (Fig. 5-4 – middle panel). As θ^* (or s^*) approaches the dynamic equilibrium value of θ (or s), the number of stress periods increases, with each stress period being of relatively short duration, thus weighting the average ζ to lower values. Fig. 5-10a shows that while there are only small difference in average ζ between hummock and hollow simulations for the EXP and CONST profiles, as a result of large differences in the proportion of the simulation spent in a stressed state (*e.g.* roughly 90% vs. 45%) there is a much clearer distinction in average ζ between profile types (Fig. 5-10b). As a result of climate change, our simulations indicate that there is a relatively large increase in both the average ζ and ζ over the majority of the range of s^* for both hummock and hollow simulations based on an EXP profile (Fig. 5-10c-d). Taking the integrated area under the ζ and ζ curves over the range of s^* examined, there was a relative increase in simulated hummock static and dynamic stress of 39% and 9%, and correspondingly hollow stress increased by 37% and 23% respectively.

5.5 Discussion

5.5.1 Peat hydrology and moisture-retention

Although there are small differences in the moisture retention parameters used in our simulations (Table 5-1), in a practical sense, both hummock and hollow simulations have low near-surface moisture retention, commensurate with surface retention data presented in the literature (Letts *et al.*, 2000; McCarter and Price, 2012). Therefore, given the sensitivity of our simulations to WT_{ini} and the relation between WT level and ψ_{surf} , the

small differences in moisture retention suggest that differences in ψ_{surf} between hummock and hollow simulations are more greatly influenced by microtopographic position. The differences observed between model simulations, therefore, highlight the importance of the WT as a source of water to the replenish soil layers above it through hydraulic redistribution.

Although unimodal, we see the beginning of a shift to a bimodal PDF in the EXP profile in comparison to the LIN and CONST profile under current climate conditions. This is the result of a more rapid transition in peat properties with depth to greater moisture-retention, and thus lower specific yield. Similarly, this is why the absolute depth of the WT reached in the simulations is greatest for the EXP profile for both hummock and hollow simulations, although, if only by a few centimetres. Despite there being no simple analytical solution for the WT distribution in our model, the median WT depth is related to the integral of $K(\psi)$ as well as the magnitude of the summer moisture deficit ($P-E$) since the model hydrology is governed by 1-D fluxes and discharge from the lower boundary is set to zero. For our study region, the magnitude of the median summer moisture deficit is not large enough under current climate conditions to see large differences in WT response between the peat profile types (particularly EXP and LIN), which may lead to the erroneous conclusion that the specific shape of the depth-dependence is unimportant.

If we consider the ascribed peat property profiles, we can surmise that with a larger summer moisture deficit that the median WT level for the EXP profile would decrease relative to the CONST profile. Similarly, the EXP profile will always be less

than the LIN profile, while the LIN profile would approach the CONST profile with progressively larger summer moisture deficits. This is supported by the relative shift in median WT level for hummock versus hollow simulations in our future climate simulations where the *P-E* deficit increases. In comparing the EXP and LIN depth-profiles, the greatest difference in peat properties is at a depth of 0.5 and 0.45 m for the hummock and hollow profiles respectively. While the median WT level in hummocks approaches -0.5 m under future climate projections, and thus should result in a greater relative difference, the median WT level in the hollow simulations does not.

5.5.2 *Sphagnum* stress

If sufficient external water exists on *Sphagnum* capitula, then cell water status should be optimal and thus moisture stress cannot exist. We generally consider a ψ of -1 to -3 m (Hayward and Clymo, 1982) and down to -6 m (Lewis, 1988) to be an important hydrological threshold for *Sphagnum* since this represents the ψ at which hyaline cells will drain based on their pore diameter, and thus is the point where rapid desiccation of *Sphagnum* capitula in response to ambient relative humidity (RH) becomes more likely. Although the above hydrological threshold represents a theoretical limit on the maximum height of capillary rise supportable by a pore radius equivalent to that of hyaline cell pores, this does not guarantee connectivity between *Sphagnum* capitula and the WT via continuous capillary films. The emptying of hyaline cells represents a fairly large loss of water but will not necessarily induce water stress unless accompanied by water loss from chlorophyllous cells, which according to Hajek and Beckett (2008) occurs at a ψ of -1 to -2 MPa depending on species. Moreover, Hajek and Beckett (2008) suggest that

Sphagnum moisture stress coincides with a near-total loss of turgor in the chlorophyllous cells at a GWC of $\sim 1 \text{ g g}^{-1}$ and a ψ of -2 to -3 MPa depending on the species.

A moisture-stress threshold of 1 g g^{-1} is in contrast to data from the gas-exchange literature which suggests maximum net photosynthesis (NP_{max}) begins to decrease over a GWC range of 8 to 13 g g^{-1} (Murray *et al.* 1989; Williams and Flanagan, 1996; Shipperges and Rydin, 1998; summary by Nungesser, 2003). A threshold of 1 g g^{-1} from the gas exchange literature is more commonly associated with the approximate compensation point of *Sphagnum* (Murray *et al.*, 1989; Schipperges and Rydin, 1998) and where the likelihood of *Sphagnum* recovery/survival from desiccation declines (Clymo, 1973; Wagner and Titus, 1984). The large difference in the threshold value between studies may be due to differences in sample preparation or in the characterization of stress via gas-exchange versus chlorophyll fluorescence. Hajek and Beckett (2008), for example, blotted their samples to try and remove all external water prior to measurement of chlorophyll fluorescence. In the absence of this step, water may be lost in response to ambient RH from hyaline and chlorophyllous cells while external water exists in small capillary spaces, resulting in moisture-stress at higher measured water contents. Our simulations show that the choice of *Sphagnum* moisture-stress parameters, over a given range, will lead to widely different conclusions regarding the relative competitive advantage of hummock and hollow species as a result of microtopographic position and future climate conditions.

Although we show a lower ψ^* threshold for hummock versus hollow species (Fig.6 - right panel), our values are based on NP_{max} vs. GWC relations, and measured ρ_b

and ψ - θ characteristics for our study site. From a hydrological perspective, the use of a GWC-based threshold creates uncertainty in accurately representing ψ^* since, in addition to any uncertainty in the ψ - θ relation, conversion from GWC to ψ requires an assumption of surface ρ_b which may vary significantly between sites. While there does not appear to be an unequivocal difference in the photosynthetic response of different *Sphagnum* species to water content (summary in Nungesser, 2003), and desiccation tolerance does not seem to be related to microhabitat (Wagner and Titus, 1984; Sagot and Rochefort, 1996), Schipperges and Rydin (1998) demonstrate the potential importance of the cumulative effects of repeated desiccation (which is what dynamic stress presented herein begins to incorporate). Rydin (1985), for example, suggest that there is no significant difference in desiccation tolerance between hummock and hollow species, where a lack of recovery of net photosynthesis from desiccation has been linked to drying samples below their compensation point (Schipperges and Rydin, 1998). This is in contrast to Hajek and Beckett (2008) who show a variable recovery response between hummock and hollow species depending on the level of desiccation, where at -20 MPa there was no significant difference between species, but at -40 MPa hummock species recovered better. It is argued that the different conclusions regarding desiccation tolerance of hummock versus hollow species may be due to the degree (0.2 g g⁻¹ or -50 MPa of Wagner and Titus, 1984) and rate of desiccation (*e.g.* Sagot and Rochefort, 1996), or the nature of the ‘relaxation’ period (or lack thereof) between field collection and laboratory measurements (Schipperges and Rydin, 1998). This suggests that a recovery parameter

(i.e. k) should, in fact, be dynamic since it depends not only on species but also on the degree of desiccation below a given moisture stress threshold (e.g. ψ^*).

5.5.3 Model limitations and sensitivity

Since WT level can be considered an important first-order control on *Sphagnum* moisture stress in our model, model simplifications which affect WT dynamics introduce uncertainty into modelled hummock-hollow stress relations. For example, we have not included the negative feedback between WT level and peat volume-changes (e.g., Kennedy and Price, 2005). As a result of compression in the near-surface peat layers, there would be a simultaneous decrease the depth to *WT* and increase water retention due to the shift to a smaller pore size distribution. Incorporating a WT-compression feedback into our model would require only modest modifications, where a simple scheme relating ψ and effective stress to changes in the void ratio would result in dynamic layer depths (Kennedy and Price, 2005). However, parameterizing the concomitant changes in peat hydrophysical properties would be challenging. While K_s has been shown to be linearly related to peat compression (Kennedy and Price, 2005), changes in the Van Genuchten parameters associated with a change in pore-size distribution have greater uncertainty. Moreover, because near-surface peat compressibility tends to differ between hummocks and hollows (Waddington *et al.* 2010) due to their difference in void ratio (Lefebvre *et al.* 1984) and bulk density (von Ow *et al.*, 1996), the overall impact of subsidence would likely be of less importance for hummocks.

Since ψ_{surf} becomes non-linearly related to WT level below a value of approximately -0.4 m, this suggests ψ_{surf} becomes increasingly sensitive to progressively

deeper WT_{ini} . Moreover, median modelled ψ_{surf} should also exhibit increasing sensitivity to progressively higher E_{max} since, all else being equal, a higher value of E_{max} will result in greater depletion of soil moisture storage and thus lower WT level. The sensitivity to E_{max} has important implications for the response to climate change, where we have linked changes in temperature and humidity under future climate conditions to E using the Penman equation. The comparative lack of sensitivity to other model parameters lends confidence in the potential effect of climate change on *Sphagnum* moisture stress. However, the sensitivity of the model to WT_{ini} also has important implications for our results under future climate conditions since we continue to assume that WT_{ini} remains at the surface of hollows. While winter precipitation is projected to increase for the study region (Christensen and Hewitson, 2007), depending on the concomitant changes in winter temperatures, the average winter snowpack may be affected.

In addition to potential changes in WT_{ini} with climate change, the effect of changes in growing season length on the water balance should be considered. A fixed 150 day growing season was used, in part, to constrain the number of degrees of freedom in our simulations. However, there is natural inter-annual variability in the length of the growing season which will affect the amount of water lost from storage. Without knowing the probability distribution of growing season length, it is uncertain whether there would be any systematic change in soil moisture storage, and consequently on *Sphagnum* stress. Furthermore, potential E at the beginning and end of the growing season is relatively low, thus the impact would likely be small. With increasing temperatures as a result of climate change, however, the length of the growing season

should systematically increase, further depleting soil moisture storage in regions where a summer moisture deficit is the norm.

5.6 Conclusions

We adapted elements from two hydrological models in order to examine *Sphagnum* hummock and hollow moisture stress in response to summer water deficit conditions in a southern boreal peatland parameterized with field and lab measurements. The distribution of simulated WT level was largely controlled by the distribution in growing season net rainfall, the hydrophysical properties of the given peat profile, and the WT_{ini} . Since the surface θ - ψ parameters were similar between our hummock and hollow simulations, and given typical values of ψ_{surf} in equilibrium with WT level, our model suggests microtopographic position has a strong control on ψ_{surf} and thus potentially on *Sphagnum* stress. Differences between simulations that were the result of the depth-dependence of peat hydrophysical properties were greatest for the CONST profile. The similarity between the EXP and LIN profiles under current climate conditions was related to a small growing season P-E deficit with a corresponding small variation in WT level. The distinct character of the CONST profile was the result of high moisture retention of the surface and near-surface in comparison to the other two profiles. This can be considered analogous to a disturbed peatland in which the surface layer has either been removed (*e.g.* fire or peat extraction), exposing deeper more dense peat layers, or where the surface layer has undergone significant consolidation (*e.g.* drainage). Since *Sphagnum* stress responds to ψ , a GWC-based moisture threshold may be inappropriate where *Sphagnum* properties vary significantly. Fundamentally, we would

expect that *Sphagnum* stress would respond directly to ψ , since it represents a physical constraint on the ability of *Sphagnum* capitula to access water necessary for photosynthesis. Our simulations demonstrate that a better understanding of *Sphagnum* response to desiccation and its recovery dynamics is needed if specific conclusions regarding future competitive advantage of various *Sphagnum* species are to be evaluated.

Our model represents a considerable simplification of the complex water-vegetation dynamics in peatlands. Nevertheless, the use of 1-D physically-based hydrology allowed for a simple application to the wetland system of interest and the statistical evaluation of moisture dynamics and *Sphagnum* stress. However, despite the reasonably good simulation of WT level for our study site, many important vegetation and hydrological processes may need to be included to produce a model that more accurately represents field conditions. Such challenges that must be considered when improving models for wetland systems include those stated in Rodriguez-Iturbe *et al.* (2007), which may be summarized in the context of our model as a need for:

1. Inclusion of vascular plant water uptake dynamics. This requires the use of a sink term in Richards equation, and has taken the form of a simple depth-dependent quadratic function (*e.g.* Schouwenaars and Gosen, 2007).
2. More data characterizing the stress-response of *Sphagnum* to external water deficits, and the relation between external water content and internal (apoplastic) water.
3. Inclusion of lateral flows between hummocks and hollows as well as boundary conditions representing regional flow because of their importance on WT level.

Weiss *et al.* (2006), for example, use a simple groundwater mound equation to estimate runoff, where transmissivity can be related to changing peat properties with depth. Moreover, incorporating our model into a spatially explicit model, such as DigiBog (Baird *et al.*, 2012), with WT interactions between cells would provide the ability to exam different flow regimes (*i.e.* fens) as well as patterning effects and spatial variability on *Sphagnum* stress.

4. Further understanding of the relationship between water and substrate parameters in peatland soils, to include changes in porosity, hydraulic conductivity, *etc.*, with dynamics associated with WT-mediated compression.

5.7 Acknowledgements

We thank Jason Brodeur, Kathryn Prescott, Lana Willhelm, Suo Huang, Bin Chen, Samantha MacKay, Dan Thompson and Tim Duval for many useful discussions. We also are grateful for feedback from Tom Pypker on an earlier version of this manuscript. This research was funded by a NSERC Discovery Accelerator Supplement to JMW.

5.8 References

- Albert, D.A., 1995. Regional landscape ecosystems of Michigan, Minnesota, and Wisconsin: a working classification. U.S. Department of Agriculture technical report NC-178.
- Baird AJ, Morris PJ, Belyea LR. 2012. The DigiBog peatland development model 1: rationale, conceptual model, and hydrological basis. *Ecohydrology* **5**: 242-255, DOI: 10.1002/eco.230.
- Baird AJ, Eades PA, Surridge BWJ. 2008. The hydraulic structure of a raised bog and its implications for ecohydrological modeling of bog development. *Ecohydrology* **1**: 289-298. DOI: 10.1002/eco.33.

- Beckwith CW, Baird AJ, Heathwaite AL. 2003. Anisotropy and depth-related heterogeneity of hydraulic conductivity in a bog peat. I: laboratory measurements. *Hydrological Processes* **17**: 89-101, DOI: 10.1002/hyp.1116.
- Boelter DH. 1969. Physical properties of peats as related to degree of decomposition. *Proceedings of the Soil Science Society of America* **33**: 606-609.
- Boelter DH, Verry ES. 1977. Peatland and water in the northern Lake States. North Central Forest Experiment Station, Forest Service, US Department of Agriculture.
- Brooks RH, Corey AT. 1964. Hydraulic properties of porous media. *Hydrology Papers, Colorado State University*
- Burridge DM, Gadd AJ. 1974. The Meteorological Office operational 10 level numerical weather prediction model. U.K. Met. Office Tech. Notes 12 and 48, 57 pp.
- Casselmann T., 2009. Seney National Wildlife Refuge Comprehensive Conservation Plan. United States Fish and Wildlife Service.
- Cagampan JP, Waddington JM. 2008. Net ecosystem CO₂ exchange of a cutover peatland rehabilitated with a transplanted acrotelm. *Ecoscience* **15**(2): 258-267.
- Chason DB, Siegel DI. 1986. Hydraulic conductivity and related physical properties of peat, Lost River peatland, northern Minnesota. *Soil Science* **142**: 91-99.
- Chivers MR, Turetsky MR, Waddington JM, Harden JW, McGuire AD. 2009. Climatic and vegetation controls on peatland CO₂ fluxes in Alaska: Early response to ecosystem-scale manipulations of water table and soil temperature. *Ecosystems* **12**: 1329-1342, doi: 10.1007/s10021-009-9292-y.
- Christensen JH, Hewitson B, Busuioc A, Chen A, Gao X, Held I, Jones R, Kolli RK, Kwon W-T, Laprise R, Magaña Rueda V, Mearns L, Menéndez CG, Räisänen J, Rinke A, Sarr A and Whetton P. 2007. Regional Climate Projections. In: Climate Change 2007: The Physical Science Basis. Contribution of Working Group I to the Fourth Assessment Report of the Intergovernmental Panel on Climate Change [Solomon S, Qin D, Manning M, Chen Z, Marquis M, Averyt KB, Tignor M and Miller HL (eds.)]. Cambridge University Press, Cambridge, UK.
- Clymo RS. 1973. The growth of *Sphagnum*: some effects of surroundings. *Journal of Ecology* **61**: 849–869.
- Clymo RS. 2004. Hydraulic conductivity of peat at Ellergower Moss, Scotland. *Hydrological Processes* **18**: 261-274, DOI: 10.1002/hyp.1374.
- Frolking S, Roulet NT, Moore TR, Lafleur PM, Bubier JL, Crill PM. 2002. Modeling seasonal to annual carbon balance of Mer Bleue Bog, Ontario, Canada. *Global Biogeochemical Cycles* **16**: 1030, DOI: 10.1029/2001GB001457.
- Gorham E. 1991. Northern peatlands: Role in the carbon cycle and probable responses to climate warming. *Ecological Applications* **1**: 182–195.

- Government of Canada. Environment Canada: National climate data and information archive. online, accessed Jan. 2009.
- Gnatowski T, Szatylowicz J, Brandyk T, Kechavarzi C. 2010. Hydraulic properties of fen peat soils in Poland. *Geoderma* **154**: 188-195, DOI: 10.1016/j.geoderma.2009.02.021.
- Grover SPP, Baldock JA. 2012. Carbon chemistry and mineralization of peat soils from the Australian Alps. *European Journal of Soil Science* **63**: 129-140, DOI: 10.1111/j/1365-2389.2011.01424.x.
- Gunnarsson U, Malmer N, Rydin H. 2002. Dynamics or constancy in *Sphagnum* dominated mires ecosystems? A 40-year study. *Ecography* **25**: 685-704.
- Hajek T, Beckett RP. 2008. Effect of water content components on desiccation and recovery in *Sphagnum* mosses. *Annals of Botany* **101**: 165-173, DOI: 10.1093/aob/mcm287.
- Hayward PM, Clymo RS. 1982. Profiles of water content and pore size in *Sphagnum* and peat, and their relation to the peat bog ecology. *Proceedings of the Royal Society of London (B)* **215**: 299–325.
- Heinselman M.L., 1965. String Bogs and Other Patterned Organic Terrain Near Seney, Upper Michigan. *Ecology*. 46(1-2): 185-188.
- Hoag RS, Price JS. 1995. A field-scale, natural gradient solute transport experiment in peat at a Newfoundland blanket bog. *Journal of Hydrology* **172**(1): 171-184.
- Hogan, JM, Van der Kamp G, Barbour SL, Schmidt R. 2006. Field methods for measuring hydraulic properties of peat deposits. *Hydrological processes* **20**(17): 3635-3649.
- Intergovernmental Panel on Climate Change Fourth Assessment Report: Climate Change. 2007. The Physical Science Basis. Contribution of Working Group I to the Fourth Assessment Report of the Intergovernmental Panel on Climate Change [Solomon S, Qin D, Manning M, Chen Z, Marquis M, Averyt KB, Tignor M and Miller HL (eds.)]. Cambridge University Press, Cambridge, UK.
- Ise T, Dunn AL, Wofsy AC, Moorcroft PR. 2008. High sensitivity of peat decomposition to climate change through water-table feedback. *Nature Geoscience* **1**: 763–766.
- Johnson LV, Damman AWH. 1991. Species-controlled *Sphagnum* decay on a south swedish raised bog. *Oikos* **61**: 234–242.
- Kellner, E., 2001. Surface energy exchange and hydrology of a poor *Sphagnum* mire. PhD thesis, Uppsala University, Sweden.
- Kennedy GW, Price JS. 2005. A conceptual model of volume-change controls on the hydrology of cutover peats. *Journal of Hydrology* **302**: 13-27.

- Kettridge N, Binley A. 2010. Evaluating the effect of using artificial pore water on the quality of laboratory hydraulic conductivity measurements of peat. *Hydrological Processes* **24**: 2629-2640. DOI:10.1002/hyp.7693.
- Kettridge N, Thompson DK, Waddington JM. 2012. Impact of wildfire on the thermal behavior of northern peatlands: Observations and model simulations. *Journal of Geophysical Research: Biogeosciences* **117**(G2). DOI: 10.1029/2011JG001910
- Kettridge N, Thompson DK, Bombonato L, Turetsky MR, Benscoter BW, Waddington JM. 2013. The ecohydrology of forested peatlands: Simulating the effects of tree shading on moss evaporation and species composition. *Journal of Geophysical Research* **118**: 1-14, doi: 10.1002/jgrg.20043.
- Kim J, Verma SB. 1996. Surface exchange of water vapour between an open Sphagnum fen and the atmosphere. *Boundary-Layer Meteorol.* **79**: 243-264.
- Kurbatova J, Arneeth A, Vygodskaya NN, Kolle O, Varlargin AV, Milyukova IM, ... & Lloyd J. 2002. Comparative ecosystem-atmosphere exchange of energy and mass in a European Russian and a central Siberian bog I. Interseasonal and interannual variability of energy and latent heat fluxes during the snowfree period. *Tellus B*, **54**(5): 497-513.
- Lafleur PM, Hember RA, Admiral SW, Roulet NT. 2005. Annual and seasonal variability in evapotranspiration and water table at a shrub-covered bog in southern Ontario, Canada. *Hydrological Processes* **19**: 3533-3550.
- Laio F, Porporato A, Ridolfi L, Rodriguez-Iturbe I. 2001. Plants in water-controlled ecosystems: active role in hydrologic processes and response to water stress II. Probabilistic soil moisture dynamics. *Advances in Water Resources* **24**: 707-723.
- Lefebvre G, Langlois P, Lupien C, Lavalee JG. 1984. Laboratory testing and in-situ behaviour of peat as embankment foundation. *Canadian Geotechnical Journal* **21**: 322-337.
- Letts MG, Roulet NT, Comer NT, Skarupa MR, Versegny DL. 2000. Parameterization of peatland hydraulic properties for the Canadian Land Surface Scheme. *Atmosphere-Ocean* **38**: 141-160.
- Lewis AM. 1988. A test of the air-seeding hypothesis using *Sphagnum* hyalocysts. *Plant Physiology* **87**: 577 – 582.
- Lewis C, Albertson J, Xu X, Kiely G. 2012. Spatial variability of hydraulic conductivity and bulk density along a blanket peatland hillslope. *Hydrological Processes* **26**: 1527-1537, DOI: 10.1002/hyp.8252.
- MathWorks, Inc. 2009. MATLAB, Version 7.8.0, MathWorks, Natick, Mass.
- McCarter CPR, Price JS. 2012. Ecohydrology of *Sphagnum* moss hummocks: mechanisms of capitula water supply and simulated effects of evaporation. *Ecohydrology*, DOI: 10.1002/eco/1313.

- McNeil P, Waddington JM. 2003. Moisture controls on *Sphagnum* growth and CO₂ exchange on a cutover bog. *Journal of Applied Ecology* **40**: 354-367, DOI: 10.1046/j.1365-2664.2003.00790.x.
- Moore PA, Pypker TG, Waddington JM. 2013. Effect of long-term water table manipulation on peatland evapotranspiration. *Agricultural and Forest Meteorology*. DOI: 10.1016/j.agrformet.2013.04.013.
- Murray KJ, Harley PC, Beyers J, Walz H, Tenhunen JD. 1989. Water content effects on photosynthetic response of *Sphagnum* mosses from the foothills of the Philip Smith Mountains, Alaska. *Oecologia* **79**: 244-250.
- Nichols DS, Brown JM. 1980. Evaporation from a sphagnum moss surface. *Journal of Hydrology* **48**(3): 289-302.
- Novak M, Brizova E, Adamova M, Erbanova L, Bottrell SH. 2008. Accumulation of organic carbon over the past 150 years in five freshwater peatlands in western and central Europe. *Science of the Total Environment* **390**: 425-436, DOI: 10.1016/j.scitotenv.2007.10.011.
- Nungesser MK. 2003. Modelling microtopography in boreal peatlands: hummocks and hollows. *Ecological Modelling* **165**: 175-207, DOI: 10.1016/S0304-3800(03)00067-X.
- Pellerin S, Lavoie C. 2003. Recent expansion of jack pine in peatlands of southeastern Quebec: A paleoecological study. *Ecoscience* **10**, 247-257.
- Porporato A, D'Odorico P, Laio F, Ridolfi L, Rodriguez-Iturbe I. 2002. Ecohydrology of water-controlled ecosystems. *Advances in Water Resources* **25**: 1335-1348.
- Price JS, Edwards TWD, Yi Y, Whittington PN. 2009. Physical and isotopic characterization of evaporation from *Sphagnum* moss. *J. Hydrol.* **369**: 175-182.
- Price JS, Maloney DA. 1994. Hydrology of a patterned bog-fen complex in southeastern Labrador, Canada. *Nordic Hydrol.* **25**: 313-330.
- Price JS, Whittington PN. 2010. Water flow in *Sphagnum* hummocks: Mesocosm measurements and modeling. *Journal of Hydrology* **381**: 333-340. DOI: 10.1016/j.hydrol.2009.12.006.
- Richards LA. 1931. Capillary conduction of liquids through porous mediums. *Physics* **1**: 318-333.
- Rodriguez-Iturbe I, Porporato A. 2005. *Ecohydrology of Water-Controlled Ecosystems: Soil moisture and plant dynamics*. Cambridge University Press, UK.
- Rodriguez-Iturbe I, D'Odorico P, Laio F, Ridolfi L, Tamea S. 2007. Challenges in humid land ecohydrology: Interactions of water table and unsaturated zone with climate, soil, and vegetation. *Water Resources Research* **43**: 1–5.
- Roulet N, Moore T, Bubier J, Lafleur P. 1992. Northern fens: Methane flux and climatic change. *Tellus B* **44**: 100–105.

- Rycroft DW, Williams DJA, Ingram HAP. 1975. The transmission of water through peat I. Review. *Journal of Ecology* **63**: 535-556.
- Rydin H. 1985. Effect of water level on desiccation of *Sphagnum* in relation to surrounding *Sphagna*. *Oikos* **45**: 374-379, DOI: 10.2307/3565573
- Rydin H, McDonald AJS. 1985. Photosynthesis in *Sphagnum* at different water contents. *Journal of Bryology* **13**: 579-584.
- Sagot C, Rochefort L. 1996. *Sphagnum* desiccation tolerance. *Cryptogamie Bryologie Lichenologie* **17**: 171-183.
- Schouwenaars JM, Gosen AM. 2007. The sensitivity of *Sphagnum* to surface layer conditions in a re-wetted bog: a simulation study of water stress. *Mires and Peat* **2**(2): 1-19.
- Shimoyama K, Hiyama T, Fukushima Y, Inoue G. 2004. Controls on evapotranspiration in a west Siberian bog. *J. Geophys. Res.* **109**, D08111, doi: 10.1029/2003JD004114.
- Shipperges B, Rydin H. 1998. Response of photosynthesis of *Sphagnum* species from contrasting microhabitats to tissue water content and repeated desiccation. *New Phytologist* **140**: 677-684. DOI: 10.1046/j.1469-8137.1998.00311.x.
- Šimůnek J, Šejna M, Saito H, van Genuchten MTh. 1998. The HYDRUS-1D software package for simulating the one-dimensional movement of water, heat, and multiple solutes in variably- saturated media. Version 4.08. *HYDRUS Software Series 3*, Department of Environmental Sciences, University of California Riverside, Riverside, California, 330pp.
- Sottocornola M, Kiely G. 2010. Energy fluxes and evaporation mechanisms in an Atlantic blanket bog in southwestern Ireland. *Water Resour. Res.* **46**: W11524, doi: 10.1029/2010WR009078.
- Strack M, Price JS. 2009. Moisture controls on carbon dioxide dynamics of peat-*Sphagnum* monoliths. *Ecohydrology* **2**: 34-41. DOI: 10.1002/eco.36.
- Strack M, Waddington JM. 2007. Response of peatland carbon dioxide and methane fluxes to a water table drawdown experiment. *Global Biogeochemical Cycles* **21**: (GB1007), DOI 10.1029/2006GB002715.
- Strack M, Waddington JM, Lucchese MC, Cagampan JP. 2009. Moisture controls on CO₂ exchange in a *Sphagnum*-dominated peatland: Results from an extreme drought field experiment. *Ecohydrology* **2**: 454-461, doi: 10.1002/eco.68.
- Thompson DK, Waddington JM. 2008. *Sphagnum* under pressure: towards an ecohydrological approach to examining *Sphagnum* productivity. *Ecohydrology* **1**: 299-308, DOI: 10.1002/eco.31.
- Titus JE, Wagner DJ, Stephens MD. 1983. Contrasting water relations of photosynthesis for two *Sphagnum* mosses. *Ecology* **64**: 1109-1115. DOI: 10.2307/1937821.

- Turetsky MR, Crow SE, Evans RJ, Vitt DH, Wieder K. 2008. Trade-offs in resource allocation among moss species control decomposition in boreal peatlands. *Journal of Ecology* **96**: 1297–1305.
- Turunen J, Tomppo E, Tolonen K, Reinikainen A. 2002. Estimating carbon accumulation rates of undrained mires in Finland - Application to boreal and subarctic regions. *The Holocene* **12**: 69-80.
- van Genuchten MTh. 1980. A closed form equation for predicting the hydraulic conductivity of saturated soils. *Soil Science Society of America Journal* **44**: 892-898.
- Von Ow C, Ward SM, Lynch J. 1996. Peat compressibility: a parameter for automatic depth control of milling machines. *Journal of Agricultural and Engineering Research* **63**: 295-300.
- Waddington JM, Kellner E, Strack M, Price JS. 2010. Differential peat deformation, compressibility and water storage between peatland microforms: Implications for peatland development. *Water Resources Research* **46**: W07538, doi:10.1029/2009WR008802.
- Wagner DJ, Titus JE. 1984. Comparative desiccation tolerance of two *Sphagnum* mosses. *Oecologia* **62**: 182-187.
- Weiss R, Shurpali NJ, Sallantausta T, Laiho R, Laine J, Alm J. 2006. Simulation of water level and peat temperatures in boreal peatlands. *Ecological Modelling* **192**: 441-456, DOI: 10.1016/j.ecolmodel.2005.07.016.
- Williams TG, Flanagan LB. 1996. Effect of changes in water content on photosynthesis, transpiration and discrimination against (CO₂)-C-13 and (COO)-O-18-O-16 in *Pleurozium* and *Sphagnum*. *Oecologia* **108**: 38-46. DOI: 10.1007/BF00333212.
- Willmott CJ. 1985. Statistics for the evaluation and comparison of models. *Journal of Geophysical Research*. **90**(C5): 8995-9005.
- Wu J, Kutzbach L, Jager D, Wille C, Wilmking M. 2010. Evapotranspiration dynamics in a boreal peatland and its impact on the water and energy balance. *J. Geophys. Res.* **115**: G04038.
- Yu, Z. 2011. Holocene carbon flux histories of the world's peatlands: Global carbon-cycle implications. *The Holocene* **21**: 761-774.

5.9 Tables

Table 5 - 1: Key parameters used in the model for the *Sphagnum* hummock and hollow, and at depth for all profile types.

Parameter	Units	Hummock	Hollow	Deep – Sapric*
K_s	m s^{-1}	4E-04 ^a	4E-04 ^a	1.0E-07
θ_s	$\text{m}^3 \text{m}^{-3}$	0.990 ^b	0.986 ^b	0.83
θ_r^\dagger	$\text{m}^3 \text{m}^{-3}$	0.037 ^b	0.062 ^b	0.22
N	N/A	1.69 ^b	1.86 ^b	1.6
A	cm^{-1}	1.86 ^b	0.85 ^b	0.003
θ^{*c}	--	0.2 ^b	0.2 ^b	--
E_{max}	m d^{-1}	4.5E-03 ^d	4.5E-03 ^d	--

* - Values from Letts *et al.*, 2000; [†] - Residual estimated at $\psi = -15$ m; ^a - See Appendix 2; ^b - SNWR unpublished data; ^c - Based on relation between maximum photosynthetic rate for *Sphagnum* based on gravimetric water content (Nungesser, 2003) and estimated surface ρ_b ; ^d - Estimate from multiple literature sources (see Appendix 1).

Table 5 - 2: Sensitivity analysis of peat surface ψ using hummock parameters (Table 1) and an EXP soil profile.

	Value	Ψ			Parameter Change (%)	$\Psi_{50\text{th pct Change}} (%)$	$\Psi_{5\text{th pct Change}} (%)$
		Median	5 th Percentile	95 th Percentile			
HUM	Standard	-0.276	-1.01	-0.086	--	--	--
E_{high}	5.5 mm d^{-1}	-0.425	-3.33	-0.158	22.2	54.2	228.5
E_{low}	3.5 mm d^{-1}	-0.183	-0.438	0	-22.2	-33.6	-56.8
Fibric ^{a,1}	<i>see below</i>	-0.282	-0.493	0	--	18.7	
Hemic ^{a,2}	<i>see below</i>	-0.281	-0.492	-0.04	--	18.2	
$K_{s,\text{high}}$	4E-03 m s^{-1}	-0.276	-0.566	-0.090	900	0.2	-44.1
$K_{s,\text{low}}$	4E-05 m s^{-1}	-0.284	-3.54	-0.070	-90	2.9	250.1
$WT_{\text{ini,high}}$	-0.1 m	-0.189	-0.538	0	--	-31.4	-46.8
$WT_{\text{ini,low}}$	-0.3 m	-0.404	-2.26	-0.171	--	46.5	123.7
$\Psi_{\text{Crit,high}}$	-1.0 m	-0.278	-0.793	-0.094	-75	0.8	-21.6
$\Psi_{\text{Crit,low}}$	-7.0 m	-0.278	-0.997	-0.087	75	0.8	-1.6

^a – Parameters from Letts *et al.* (2000); ¹ – $K_s=2.8\text{E-}04$; $\theta_s=0.93$; $\theta_r=0.04$; $\alpha=0.08$; $n=1.9$; applied to top node; ² – $K_s=2.0\text{E-}06$; $\theta_s=0.88$; $\theta_r=0.15$; $\alpha=0.02$; $n=1.7$; applied to bottom node.

5.10 Figures

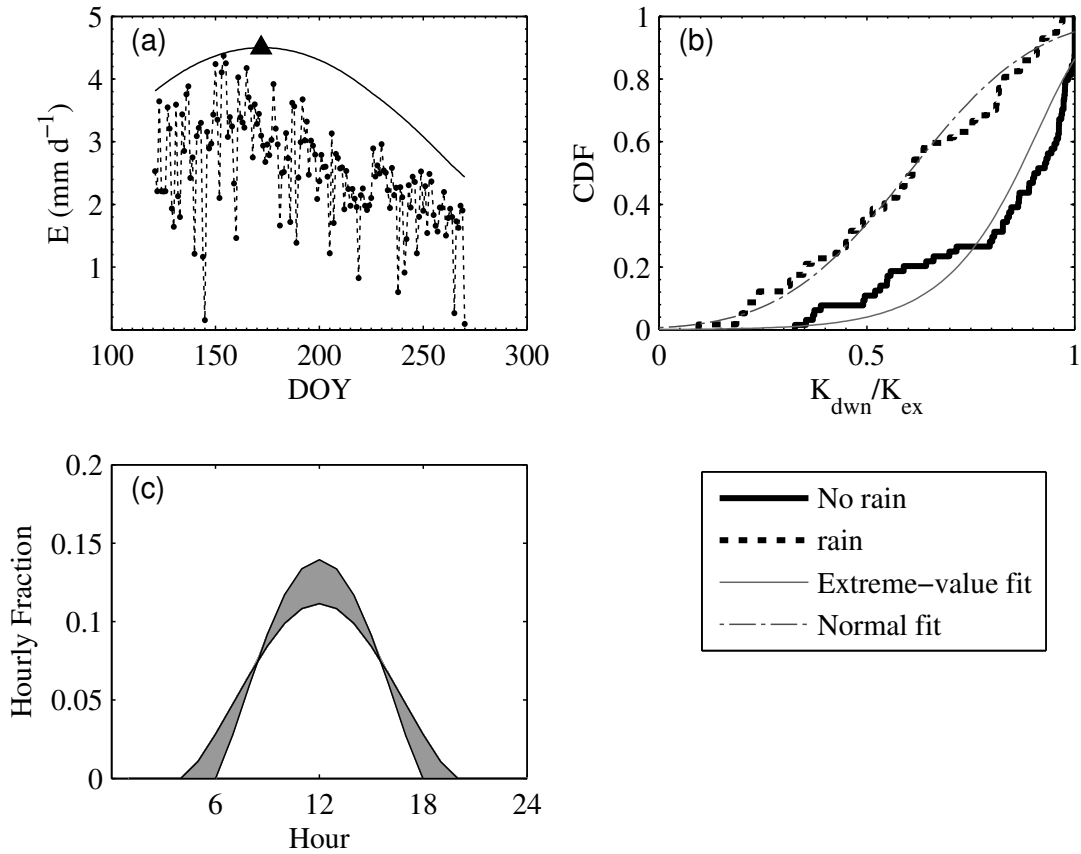


Figure 5 - 1: (a) E_{max} (triangle), $E_{seas,i}$ (solid line), and sample $E_{daily,i}$ (circles with dashed line) based on the occurrence of rainfall and random c_i values from the distributions in (b); (b) empirical cumulative distributions of the ratio of measured daily K_d to modelled K_{ex} for the 2010 growing season at SNWR during days with (dashed black line) and without (solid black line) rain; and (c) hourly fraction of $E_{daily,i}$ based on DOY, where black lines represent the summer solstice and the end of the growing season.

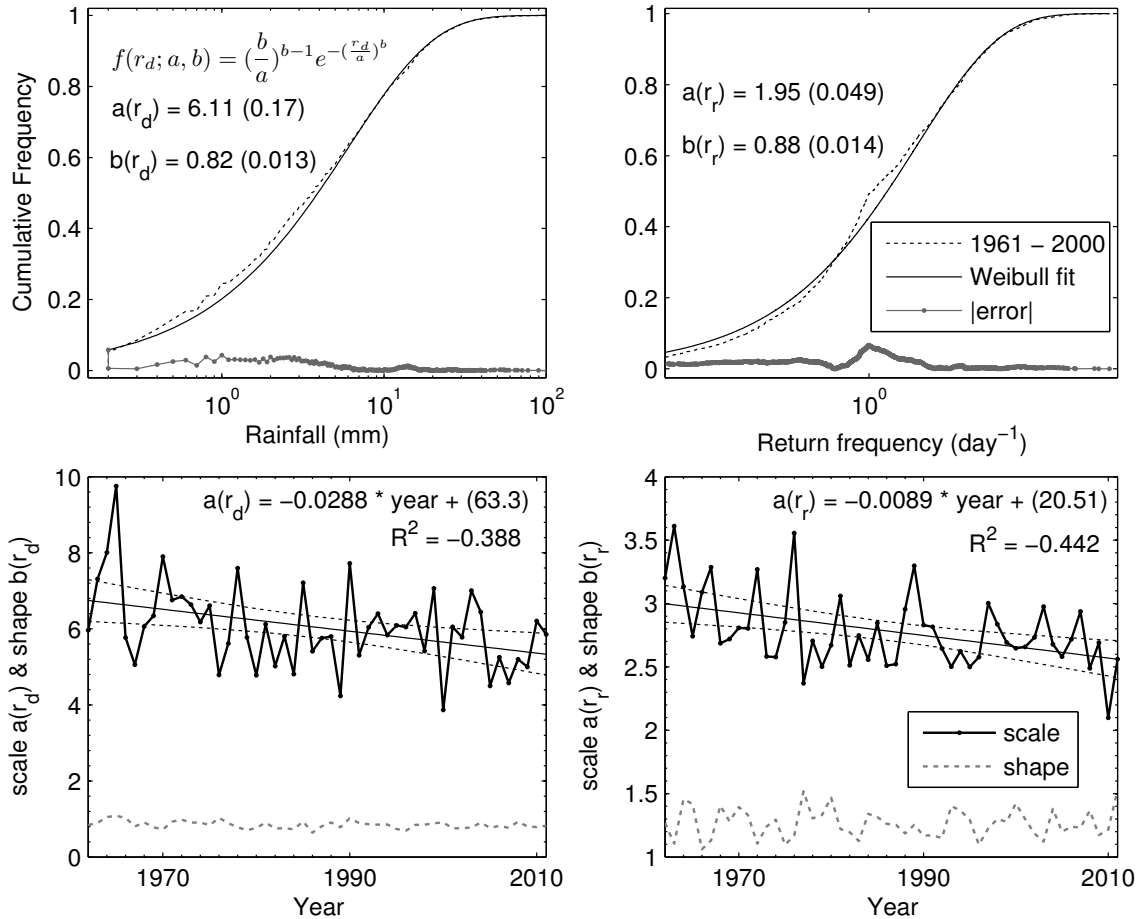


Figure 5 - 2: Cumulative frequency distribution of rainfall depths (a) and return period (b) based on 50 years of MJJAS daily rainfall data. Growing season (MJJAS) stochastic rainfall parameters (rainfall depth – top; return period – bottom) using a Weibull fit based on daily rainfall data from the Sault Ste. Marie, ON weather station (Environment Canada).

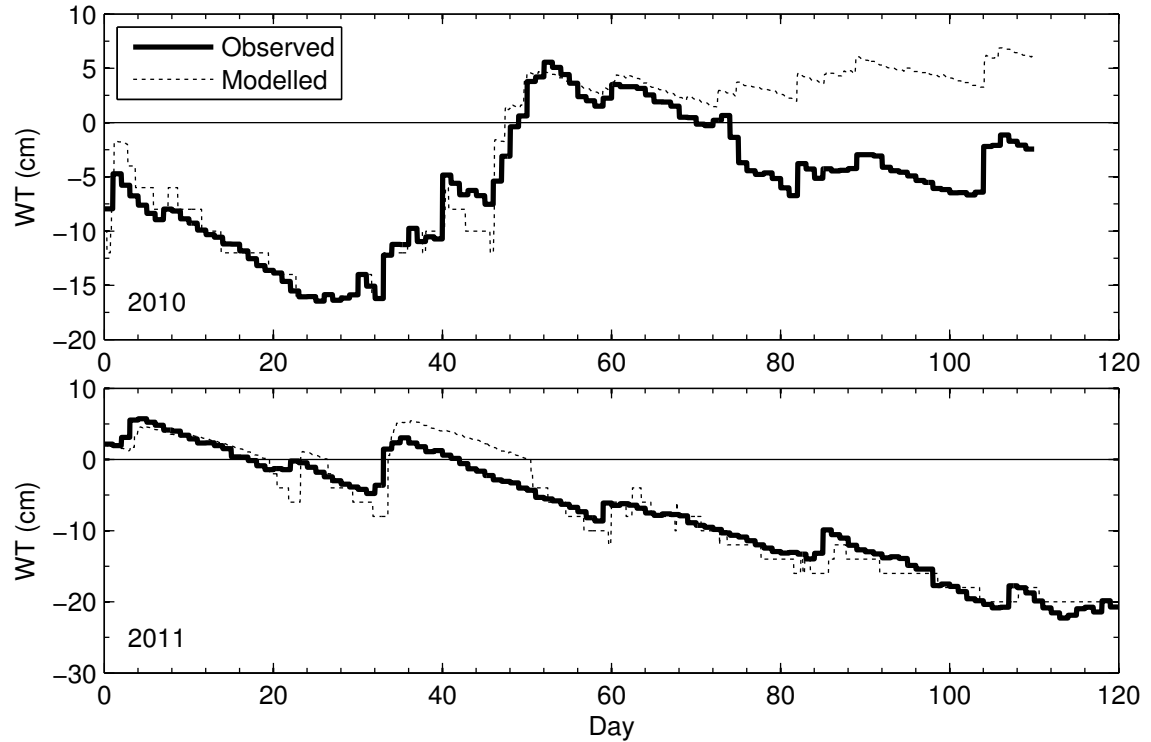


Figure 5 - 3: Comparison between modelled and observed WT position at Seney National Wildlife Refuge for two consecutive growing seasons. The model used the hollow hydrophysical properties listed in Table 1, an EXP profile, and initial WT level equal to the measured value.

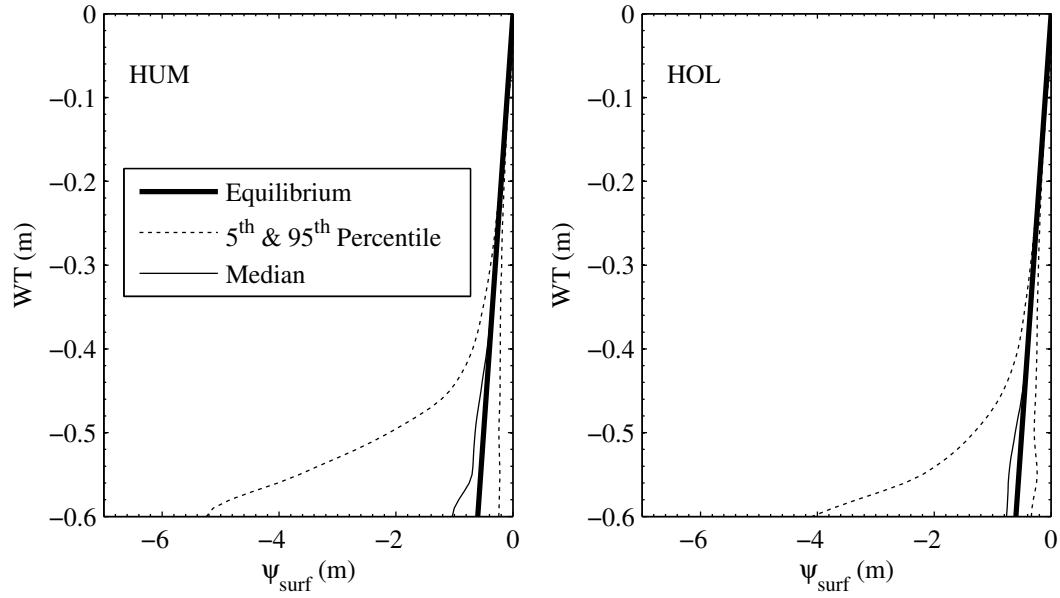


Figure 5 - 4: Deviation of the surface soil water pressure for a hummock and hollow over 100 simulated growing seasons using an EXP soil profile, relative to a soil water pressure profile in equilibrium with the water table level.

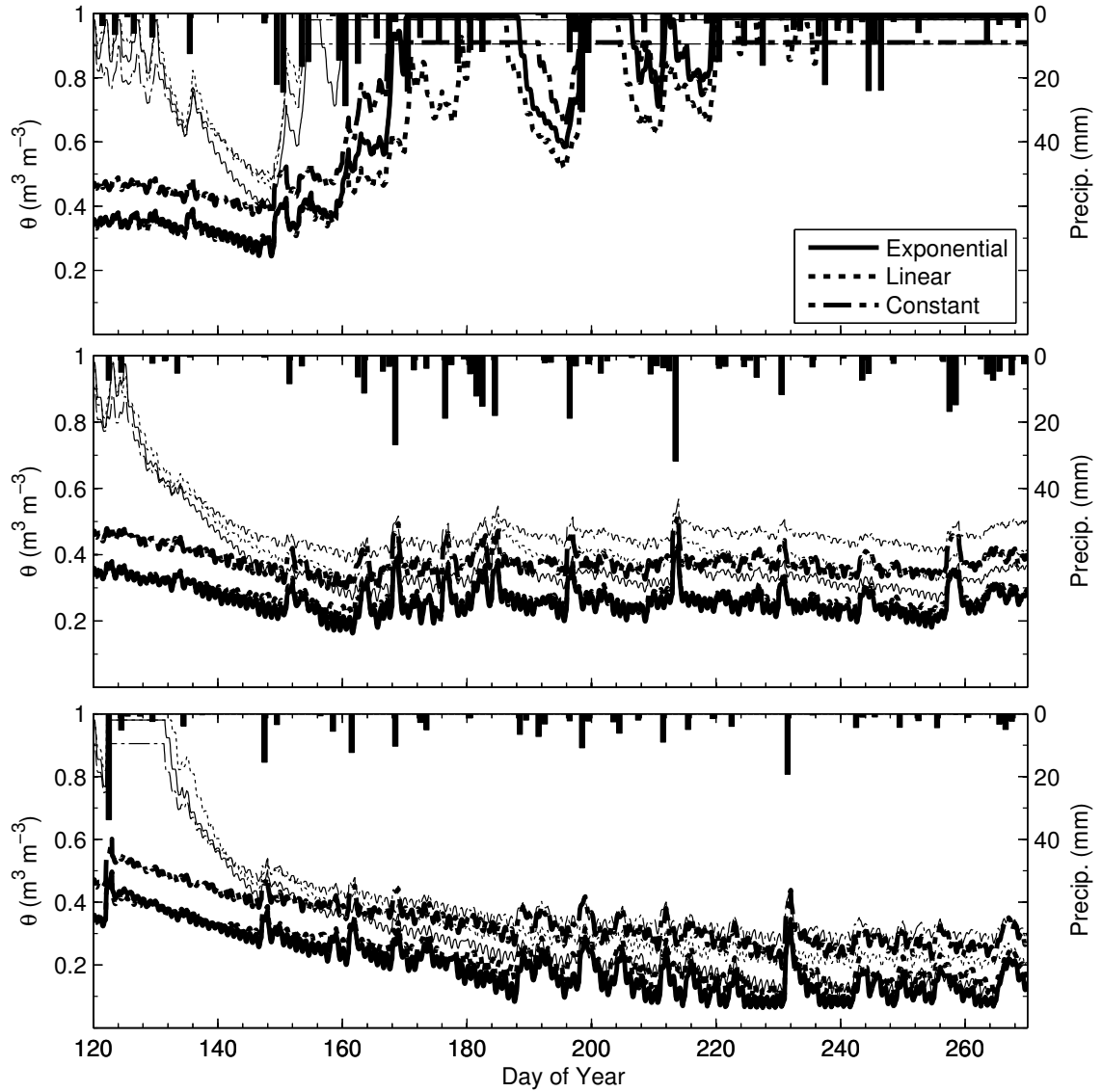


Figure 5 - 5: Sample traces of θ in the surface layer for a simulated growing season with high (top), average (middle) and low (bottom) precipitation.

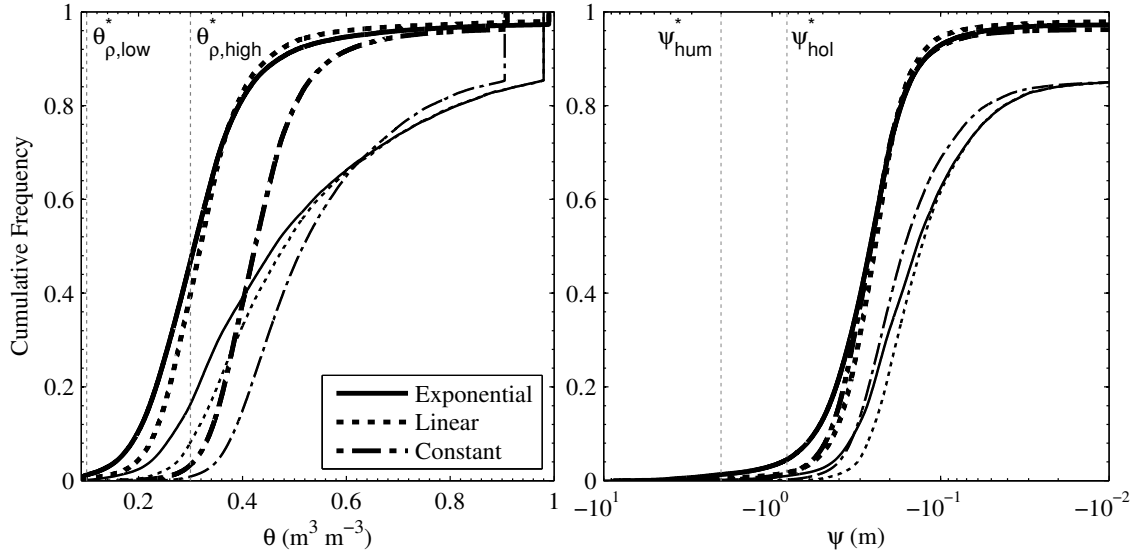


Figure 5 - 6: Cumulative distribution of volumetric water content (left) and soil-water pressure (left) for hummock (heavy lines) and hollow (thin lines) simulations under current climate conditions based on 100 growing seasons. θ^* thresholds are based on an optimal GWC of 10 g g^{-1} and high, mid and low measured ρ_b for surface samples from SNWR where 90% of all surface (0 – 0.05 m) samples fell between 10 and 30 kg m^{-3} . ψ^* thresholds are based on $\theta^*_{\rho_b,med}$ using hummock and hollow surface moisture retention parameters.

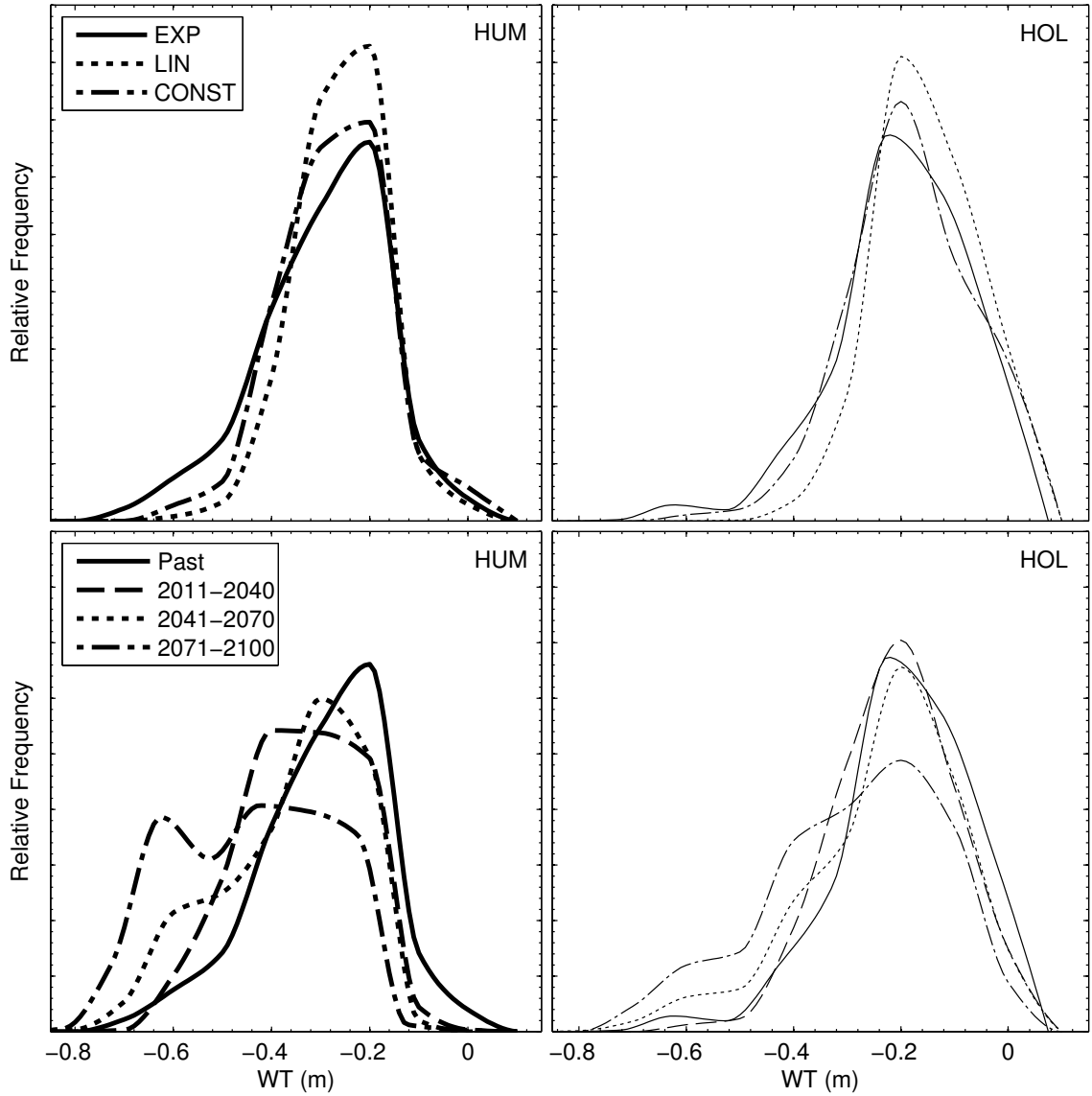


Figure 5 - 7: Empirical probability distributions of water table level based on 100 simulated growing seasons. WT simulations under future climate scenario are based solely on EXP soil profiles.

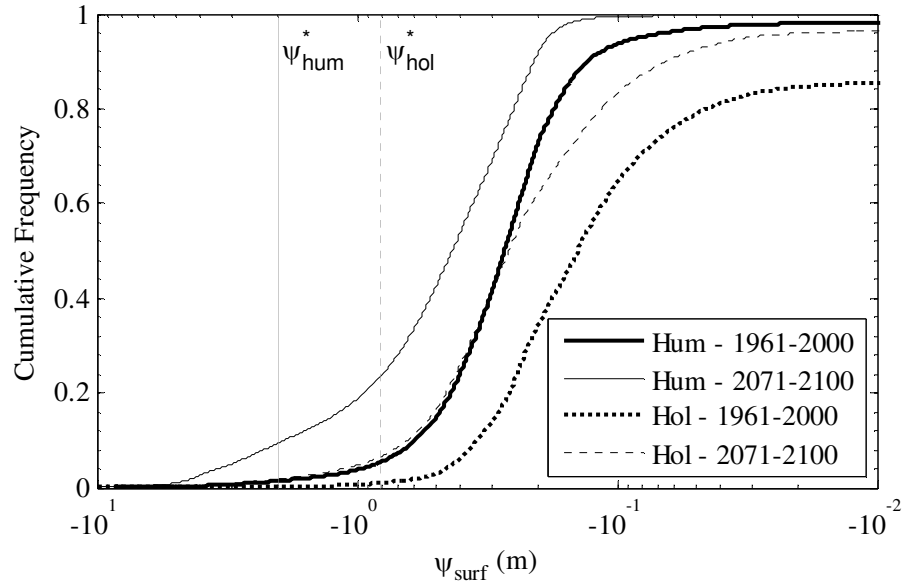


Figure 5 - 8: Comparison of cumulative frequency distribution of surface soil water pressure based on an EXP soil profile.

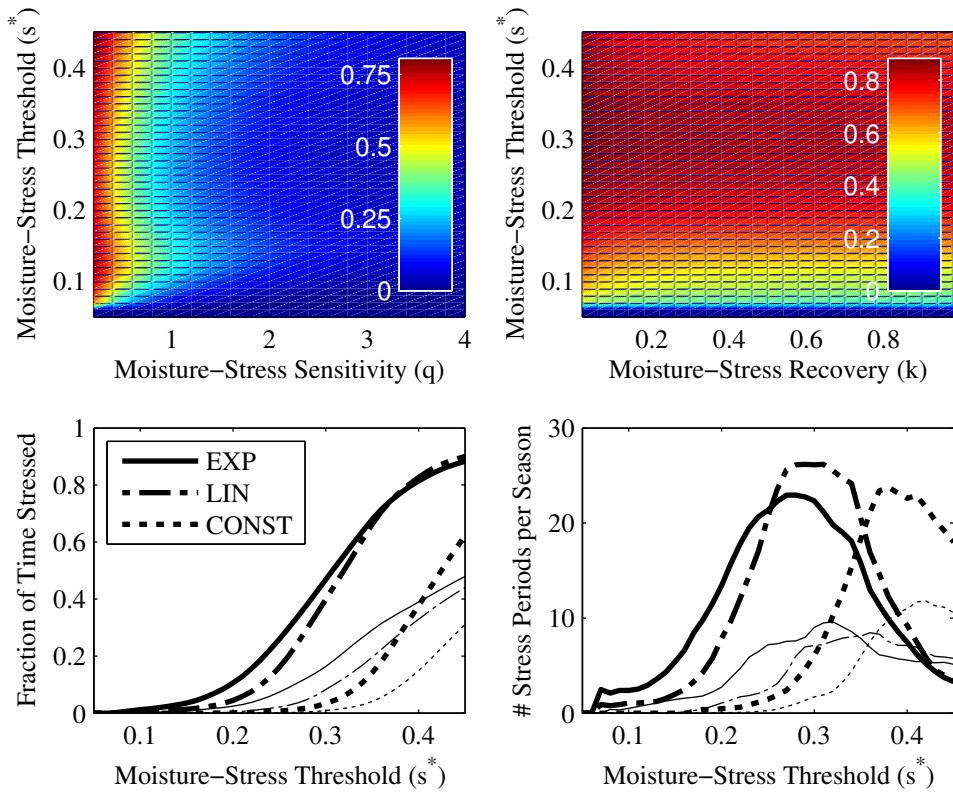


Figure 5 - 9: Average static (top - left panel) and dynamic (top - right panel) stress over a range of stress parameters for the hummock simulations given an EXP profile. Comparisons of time of simulated stress (lower – left panel) and seasonal stress periods (lower – right panel) between hummock (thick lines) and hollow (thin lines) simulations for all three profile types.

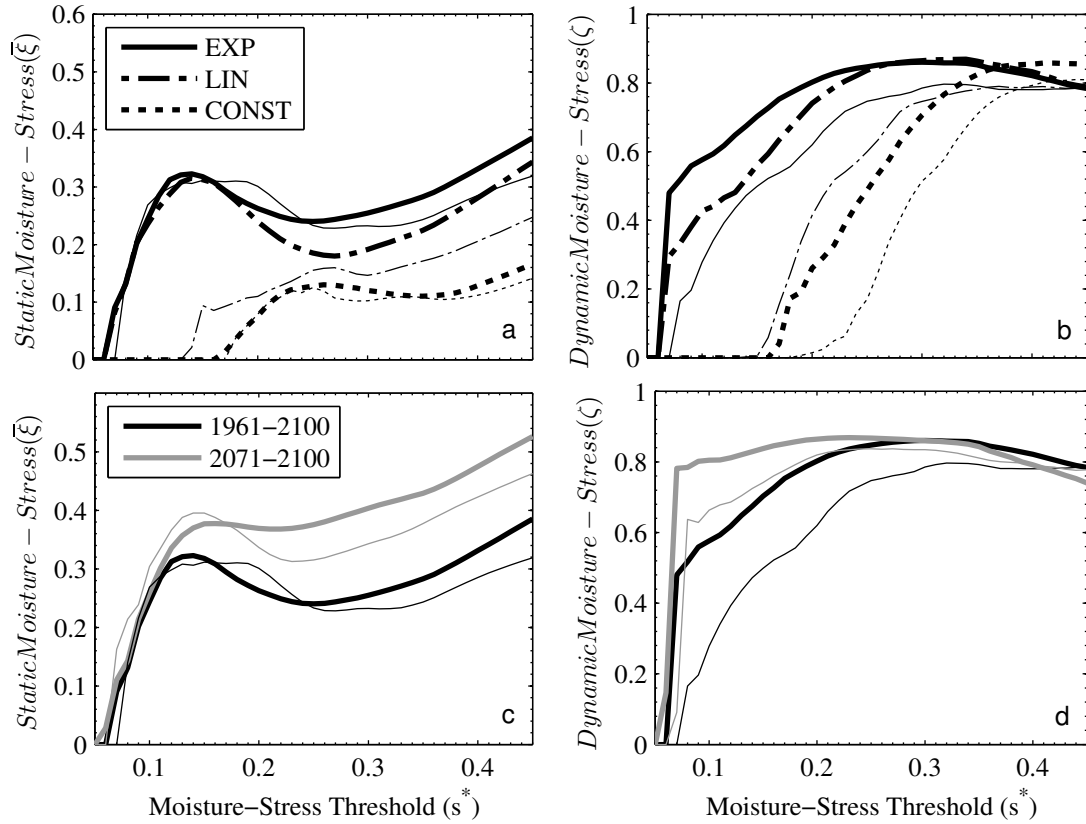


Figure 5 - 10: Comparison of average static and dynamic stress between hummocks (thick lines) and hollows (thin lines) across profile types (a & b) and between EXP-profile simulations under contemporary (black) and future (grey) climate conditions (c & d). Stress values are shown for $q = 1$ and $k = 0.2$.

CHAPTER 6: SUMMARY AND CONCLUSIONS

6.1 Summary and conclusions

The impacts of long-term water table manipulations on peatland energy balances, flux partitioning, and hydraulic structure were examined with an emphasis on microtopographic variation and the relative abundance of plant functional types. Important differences in albedo, surface temperature, wetness, and surface roughness existed between sites. Albedo was systematically lower at the WET site, despite a greater proportion of hollows which contain bright green *Sphagnum angustifolium* versus green-brown to red *Sphagnum capillifolium* which dominated hummocks. The prevalence of surface ponding at the WET site, and perhaps greater radiation trapping as a result of higher LAI, are thought to be the cause of a lower albedo. Despite a lower albedo, the radiation balance and available energy at the bulk surface were similar across WT treatments due to differences in longwave loss and high ground heat flux in saturated hollows. Despite differences in surface aerodynamic, thermal and radiative properties, their net effect could not explain the difference in total ET loss across the WT manipulation gradient. These results are significant in the context of understanding the major controls on peatland ET, and the response to long-term WT manipulations since it appears that changes in site-scale variables which do not take into account differences in the response between microforms are unable to fully explain differences in total ET given the same weather conditions. Because of the variable difference in total ET across WT treatments between growing seasons, there is a need to examine a wider range of natural

climate variability. In particular, inter-annual differences in the growing season water deficit ($P - ET$) would highlight the degree of (dis)similarity between sites following long term WT manipulation. Furthermore, despite differences in the average WT depth and proportion of hummocks, little difference in total ET exists between the INT and DRY sites, which may suggest a potential loss of self-regulation of water loss by the DRY site. By examining past WT levels through testate amoeba, and dating of tree establishment along the periphery of these disturbed peatlands, we could further assess whether these or other similarly disturbed systems represent a dynamic equilibrium or if they are still undergoing microform and vegetation succession.

There is a link between surface moisture availability and evaporative loss at the moss surface, but the overall control on ecosystem scale ET is limited by vascular leaf development. At the ecosystem-scale, we observed higher ET rates as a function of their potential value as predicted by the Penman Monteith equation during the periods of high WT in 2010, but this broadly coincided with full-leaf out. In the subsequent growing season, the period of high-WT occurred early in the growing season while LAI was relatively low, and no relation between WT and ecosystem-scale ET was observed across WT treatments. This finding is significant because it shows that short-term WT variability is important for capturing the seasonal dynamics of peatland ET, where the strength of the ET response to WT partly depends on the synchrony/asynchrony of dry periods and vascular phenology. This points to a need to further examine the phenology of major plant functional groups in peatlands. In particular, differences in the timing of leaf growth, senescence, and seasonal variability in LAI are likely to vary between sedges

and evergreen shrubs. Furthermore, due to potential differences in nutrient availability associated with long-term WT manipulation, the proportion of old versus new evergreen leaf area and their transpiration capacity could have important impacts on the relative strength of seasonal variation in transpiration potential.

At the ecosystem scale, despite large differences in WT depth between sites and the relative height of microtopographical elements, energy partitioning was greatest to latent heat across WT treatments. This suggests that despite a greater proportion of hummocks at progressively dryer sites and greater microtopographic variation, that water availability is not systematically reduced for vascular vegetation which was shown to dominate total ET losses across WT treatments. Although not directly observed from our measurements, other studies suggest that preferential partitioning of energy to sensible heat at dry hummock surfaces can enhance canopy transpiration or surface evaporation from adjacent hollows through micro-advection (Kim and Verma, 1996; Kellner and Halldin, 2002; Admiral and Lafleur, 2007). The importance of micro-advection could be examined using the spatio-temporal variability in moss surface and canopy temperatures through semi-continuous infrared imagery. This would further allow separation of the vascular canopy into hummock and hollows contributions within a four-source ET model, providing better validation of scaled porometry measurements. Furthermore, by investigating whether spatial variability in moss surface and canopy thermal response to surface moisture and WT level is well represented by a random-field for hummocks and hollows separately, the utility of the hummock-hollow concept within a land surface scheme may be evaluated.

Contrary to the potential normalizing effect imposed by micro-advection, our results suggest that the vegetation response to WT drawdown offers two negative feedbacks which increases water availability and limits transpiration loss, namely increased below-ground biomass production and a shift in above-ground resource allocation towards greater proportion of woody tissue. The effect of LAI and surface wetness on ET was observed at the scale of microtopographical elements across WT treatments. ET from all hollows and WET hummocks were observed to be similarly high, owing in part to perennially wet surfaces, a thus a more balanced trade-off between canopy transpiration and surface evaporation. Low moss surface resistance at the INT site, which incorporates the additional boundary layer resistance imposed by the vascular canopy, showed how relatively dry microtopographical elements could contribute a large amount to total ET losses on a per unit area basis. Even for higher LAI, hummocks as a whole at the DRY site were shown to contribute appreciably to total ET losses as a result of the dominance of hummocks. Despite dry conditions, evaporative losses from hummocks can be high, in part, due to the thermal properties of dry peat which limit transfer of energy down into the peat profile, enhancing available energy at the moss surface. It is likely that vapour fluxes become proportionally greater in hummocks versus hollows, but in general vapour fluxes have been shown to be negligible over a range of WT depths (Price *et al.*, 2009). Nevertheless, a continual supply of moisture from the WT is needed in order for hummocks to meet evaporative demand without undergoing severe desiccation. While surface moisture conditions were observed to be low in hummocks, particularly at the INT and DRY sites, there was no strong correlation with WT

variability owing to relatively constant values throughout the growing season, and moisture content was greater than residual value estimated from laboratory experiments. This suggests that moisture retention properties of *Sphagnum* and the capillary transport capacity of peat is sufficient to avoid complete desiccation and thus contribute to total ET losses.

Therefore, differences in peat hydraulic structure and moisture retention between microforms and across WT treatments could have important implications for water balances through moss surface evaporation and the trajectory of future microform succession in response to WT drawdown. With a focus on the unsaturated zone, our study shows that there are significant differences in the hydrophysical properties of peat between microforms, but where no large change in ρ_b was seen as a result of the hydrologic gradient created by the water table manipulations. This is significant since our results show that moisture-retention properties of the moss surface and peat in the unsaturated zone are strongly correlated with ρ_b . While short-term WT drawdown will alter peat hydraulic structure, if followed by microform succession, the properties of the newly forming *Sphagnum* and peat will dictate the long-term impact on hydraulic structure and moisture-retention. In particular, despite a difference in the relative abundance of hummocks and hollows across WT treatments, there was no difference in the relative abundance of dominant *Sphagnum* within the respective microforms across WT treatments, where hummock species have been shown to be inherently recalcitrant and supported by woody roots, and hollow peat has greater volume change in response to change in water storage. This suggests that, while peatland ecohydrological models may

not need to account for changing θ - ψ relations as a result of modest increases in soil moisture deficits under future climate change scenarios, they should account for changing proportional coverage of microforms and their associated θ - ψ relations. Furthermore, we observed a large difference in K_s at depth between WT treatments, where lower K_s at the DRY site would serve to enhance the water storage function of the peatland. In spite of this negative feedback to water loss, greater WT variability was observed with increasing depth to WT as a result of the depth-dependence of S_y and smaller peat volume changes in response to water storage, which could drive greater variability in surface ψ , and limit evaporative losses under conditions where the hydrologic threshold for capillary rise is met.

Fundamentally, it is the ability of the peat profile to conduct water up from the WT along with the hydraulic gradient which are going to both limit evaporative losses from the moss surface and prevent desiccation. By examining differences in the depth-dependence of peat hydrologic structure which may be analogous to differences associated with WT drawdown or other forms of disturbance, the effect of different moisture retention properties between hummocks and hollows on surface moisture availability was evaluated. As a result of the similarity in peat hydraulic structure and moisture-retention in the near-surface, the difference in relative WT position between microforms was shown to have the greatest control on surface ψ and thus on *Sphagnum* moisture stress. However, differences in mean evaporative losses were small, with hollows losing slightly more water from storage compared to hummocks. Model behaviour suggests that, while ψ maintained equilibrium-profile values relative to the WT level for relatively shallow

values, surface ψ became non-linearly related to WT level below a value of approximately -0.4 m, thus greatly increasing the likelihood of desiccation under future climate scenarios where growing season soil moisture deficits are projected to increase. It is under conditions where surface ψ is in disequilibrium with the WT level where hydraulic conductivity is sufficiently reduced to limit evaporative loss from the surface. However, our results also suggest that crossing the ψ threshold either from a stress or evaporative perspective is temporally transient. Overnight recharge at the surface, when evaporative demand is negligible, is often sufficient to return the moss to an unstressed state. Since our model results suggest that microtopographic position has the greatest impact on *Sphagnum* moisture availability, expanding our model to a semi-distributed scheme through WT interactions would allow for the evaluation of varying proportions and sizes of microforms on the water balance and surface moisture availability.

To further evaluate changes that result from long-term WT manipulations, modelling analysis should be extended by incorporating effects of vascular vegetation on water storage, interception losses, and the surface energy balance. In comparing ET from the WET to INT and DRY sites, our results suggest that the potential long-term effect of WT drawdown on LAI should be incorporated since this appears to be one of the primary mechanisms which serve to limit transpiration and affect canopy-surface sourcing. Moreover, microtopography, particularly as it correlates to plant functional groups, needs to be included since, in addition to LAI, differences in transpiration capacity provides the mechanism for driving spatial variability in ET losses. Despite our relatively large LAI values, the results of our study imply a need for a greater understanding of the limitations

on water transport processes in the moss layer, where both field observations and model simulations showed that dry hummocks were able to avoid complete desiccation despite low WT depths and high daily ET. Despite modelling results showing overnight recharge as a likely mechanism for desiccation avoidance, other important process may include direct interception, vapour distillation (Price *et al.*, 2009), and dew fall (Price, 1991). A vertically-stratified representation of different peatland vegetation layers in stochastically-driven process ecosystem models can help to elicit under what conditions moss evaporation is limited by vascular canopy properties versus moisture supply from the underlying peat, where alternative empirical formulations can be used to better understand moss resistance to water vapour loss.

6.2 References

- Admiral SW, Lafleur PM. 2007. Partitioning of latent heat flux at a northern peatland. *Aquatic botany*, **86**(2): 107-116.
- Kellner E, Halldin S. 2002. Water budget and surface-layer water storage in a *Sphagnum* bog in central Sweden. *Hydrological Processes*, **16**: 87-103.
- Kim J, Verma SB. 1996. Surface exchange of water vapour between an open *Sphagnum* fen and the atmosphere. *Boundary-Layer Meteorol.* **79**: 243-264.
- Price JS. 1991. Evaporation from a blanket bog in a foggy coastal environment. *Boundary-Layer Meteorology*, **57**: 391-406.
- Price JS, Edwards TW, Yi Y, Whittington PN. 2009. Physical and isotopic characterization of evaporation from *Sphagnum* moss. *Journal of Hydrology*, **369**(1): 175-182.